SYNTHESISING NUCLEOSIDE ANALOGUES FOR IMAGING PROLIFERATION IN CANCER AND OTHER BIOMEDICAL APPLICATIONS

A Thesis Submitted By

Andreas M. Doepner

In partial fulfilment of the requirements for the degree of

Doctor of Philosophy

Department of Surgery and Cancer
Imperial College London
South Kensington Campus
London SW7 2AZ
United Kingdom

September 2013

Declaration of Originality

This thesis is submitted in partial fulfilment of the requirements for the degree of Doctor of Philosophy. It describes the work carried out in the Department of Surgery and Cancer, Imperial College London, under the joint supervision of Professors Anthony G. M. Barrett and Eric O. Aboagye. Unless stated otherwise, the research is my own work and not the product of collaboration.

Andreas Doepner
London, 30th September 2013

Copyright Declaration

Synthesising nucleoside analogues for imaging proliferation in cancer and other biomedical applications

Andreas M. Doepner

Abstract

Rapidly proliferating cells, such as cancerous cells, show increased reliance on deoxyribonucleic acid (DNA) salvage pathways for producing nucleotides required for DNA synthesis. As such targeting these salvage pathways using radiolabelled nucleosides can provide a means of imaging the extent of proliferation within a tissue using positron emission tomography (PET). This permits the detection of malignant growths. Thiothymidine and 2'-deoxy-2',2'-difluoro nucleoside analogues are currently being evaluated for theoretically superior properties in comparison to 3'-deoxy-3'-[^{18}F]-fluorothymidine (FLT), the current standard PET proliferation marker. Investigations towards the design and synthesis of radiolabelled analogues of these nucleosides for evaluation as PET tracers were carried out.

Synthesis and radiosynthesis of the 2',2'-difluoro nucleoside analogue **i** was completed using a Stille coupling to introduce the carbon-11 radiolabel. The synthesis of **ii**, a precursor to a carbon-11 methylated gemcitabine analogue and **iii**, an intermediate in the synthesis of thiothymidine nucleosides are also reported.

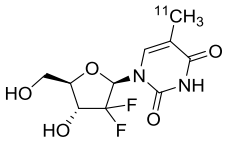

i

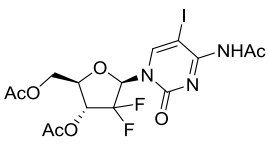

ii

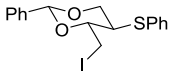

iii

Based on the synthetic route developed for accessing **iv** an analogue of **ii** suitable for radiolabelling with fluorine-18, a series of difluoro nucleoside analogues with potential uses in PET, HIV therapy and fluorescent imaging were also synthesised **v**-**viii**.

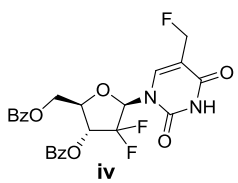

iv

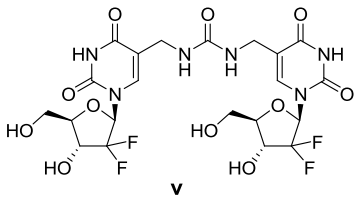

v

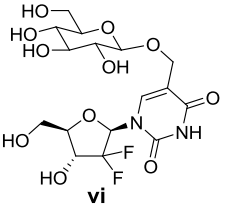

vi

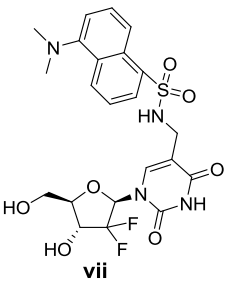

vii

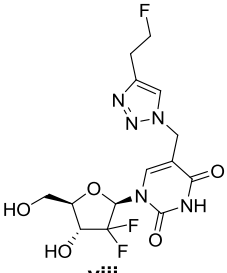

viii

Acknowledgements

I would firstly like to thank my supervisors, Professors Anthony Barrett and Eric Aboagye, for giving me the opportunity to undertake such an interesting and challenging project and for being at hand to provide advice, guidance and encouragement whenever it was needed.

I would also like to extend my gratitude to all members of the Aboagye and Barrett groups for being at hand to discuss chemistry/radiochemistry/biology and for their friendship during my time at Imperial. Of particular mention are: Jullien, Matty Baud, Jensy, Rob Pace, Etienne, Sylvain, Rosa, Angela and Cath, thanks for making the Owen Lab an awesome place to work in. Likewise, I must thank: Paul, Okanya, Kevin, Laurence, Brian, Alex Bandle, Marianne, Claire, Jez, Pete, Liz Stevens, Liz Jones, Roberta, Guillaume, Sheena, Laurianne, Malte, Jenny, Paolo, Jean-Noël, Fred, Matty Penny, Stef, Kate, Katie, Dil, Fanny, Florian, Tim, Bhavesh and Hideki, it has been a pleasure working with all of you. Special thanks to Rob Davidson and Aniello for being good eggs.

Additional thanks to my collaborators on this project: Dr Franklin Aigbirhio for allowing me to make use of his radiochemistry facilities at the WBIC, Dr Patrick Riss for supervising my radiochemical experiments and Robert Sala for biology assistance.

Many thanks to the analytical and administrative staff at Imperial College for their assistance during my PhD.

Further thanks go to Rob Davidson, Aniello Palma, Cath Fletcher, Rosa Cookson, Laurence Carroll and Tim Barrett for proof reading my thesis.

A special mention must go to Sally Cohen. A friend remarked that ‘they have never seen me as happy’ since getting to know you. I can’t help but agree with them. Thank you for your kindness and affection and for bringing a smile to my face.

Most importantly, I would like to thank the Doepner family: Mum, Dad, Apple, Anneka and Granny. Without your encouragement, support and love none of this would have been possible. This thesis is dedicated to you.

Finally I would like to thank Cancer Research UK, the Engineering and Physical Sciences Research Council, the Medical Research Council and the Department of Health for funding my research.

Abbreviations

^{1}H	Hydrogen-1
^{11}C	Carbon-11
^{13}C	Carbon-13
^{13}N	Nitrogen-13
^{15}O	Oxygen-15
^{18}F	Fluorine-18
^{19}F	Fluorine-19
^{64}Cu	Copper-64
^{68}Ga	Gallium-68
^{124}I	Iodine-124
Å	Angstrom
Ac	Acetyl
AIDs	Acquired immunodeficiency syndrome
ATP	Adenosine triphosphate
app	Apparent
aq	Aqueous
Ar	Unspecified aromatic group
ATP	Adenosine triphosphate
AZT	Azidothymidine
Bq	Becquerel
Bn	Benzyl
br	Broad
Bu	Butyl
Bz	Benzoyl
°C	Degree celsius
CAMs	Cell adhesion molecules
CDI	1,1'-carbonyldiimidazole
CI	Chemical ionization
Ci	Curie
COSY	Homonuclear correlation spectroscopy
CT	Computed tomography

D	Distribution coefficient
d	Doublet
d	Deuterated
d	Deuteron
DAST	*N,N*-Diethylaminosulfur trifluoride
DBU	1,8-Diazabicyclo[5.4.0]undec-7-ene
DCE	1,2-Dichloroethane
dCK	Deoxycytidine kinase
DEPT	Distortionless enhancement by polarisation transfer
DIAD	Diisopropyl azodicarboxylate
DIPEA	Diisopropylethylamine
DMAP	4-(Dimethylamino)pyridine
DMDO	Dimethyldioxirane
DMF	*N,N*-Dimethylformamide
DMSO	Dimethylsulfoxide
DNA	Deoxyribonucleic acid
Ds	Dansyl
e-	Electron
EI	Electron ionization
eq	Equivalent
E1cB	Elimination unimolecular conjugate base
Et	Ethyl
ESI	Electrospray ionization
eV	Electronvolt
g	Gram
Glut	Glucose transporter
h	Hour
ID/g	Injected dose per gram tissue
HIF	Hypoxia inducing factor
HIV	Human immunodeficiency virus
HMBC	Heteronuclear multiple-bond correlation spectroscopy
HMDS	Hexamethyldisilizane
HPLC	High performance liquid chromatography
HRMS	High resolution mass spectrometry

HSQC	Heteronuclear single-quantum correlation spectroscopy
HTS	High-throughput screening
Hünig's base	Diisopropylethylamine
Hz	Hertz
IC50	Half maximal inhibitory concentration
^{i}Pr	Isopropyl
IR	Infra-red
J	^{1}H-^{1}H Coupling constant
$J_{C\text{-}F}$	^{13}C-^{19}F Coupling constant
$J_{C\text{-}^{117}Sn}$	^{13}C-^{117}Sn Coupling constant
$J_{C\text{-}^{119}Sn}$	^{13}C-^{119}Sn Coupling constant
$J_{H\text{-}F}$	^{1}H-^{19}F Coupling constant
$J_{H\text{-}^{117}Sn}$	^{1}H-^{117}Sn Coupling constant
$J_{H\text{-}^{119}Sn}$	^{1}H-^{119}Sn Coupling constant
k	Kilo
Kd	Dissociation constant
LDA	Lithium diisopropylamide
log	Logarithm
LTBA	Lithium tri-*tert*-butoxyaluminum hydride
m	Multiplet
M	Molar
Me	Methyl
mg	Milligram
MHz	Megahertz
min	Minute
mL	Millilitre
mmol	Millimole
mol	Mole
MOM	Methoxymethyl
mp	Melting point
MRI	Magnetic resonance imaging
Ms	Methanesulfonyl
MS	Mass spectrometry
MW	Molecular weight

m/z	Mass to charge ratio
n	Nano
n	Neutron
NDPK	Nucleoside diphosphate kinase
NIS	*N*-Iodosuccinimide
NMPK	Nucleoside monophosphate kinase
NMR	Nuclear magnetic resonance
NOESY	Nuclear Overhauser effect spectroscopy
P	Partition coefficient
p	Pico
p	Proton
PET	Positron emission tomography
Ph	Phenyl
PG	Protecting group
pK_a	Acid dissociation constant
PMP	*para*-Methoxyphenyl
ppm	Parts per million
pRB	Retinoblastoma associated protein
q	Quartet
R	Unspecified alkyl group
RNA	Ribonucleic acid
ROI	Region of interest
rt	Room temperature
s	Singlet
SAR	Structure activity relationship
SM	Starting material
S_N2	Biomolecular nucleophilc substitution
S_NAr	Nucleophilic aromatic substitution
SPE	Solid phase extraction
SPECT	Single photon emission computed tomography
SUV	Standard uptake value
t	Triplet
^{t}Bu	*tert*-Butyl
TBAB	Tetra-*n*-butylammonium bromide

TBAF	Tetra-*n*-butylammonium fluoride
TBS	*tert*-Butyldimethylsilyl
TBDPS	*tert*-Butyldiphenylsilyl
Tf	Trifluoromethanesulfonyl
TFA	Trifluoroacetic acid
TGF	Transforming growth factor
THF	Tetrahydrofuran
TK	Thymidine kinase
TLC	Thin layer chromatography
TMS	Trimethylsilyl
TNF	Tumour necrosis factor
Ts	*para*-Toluenesulfonyl
VEGF	Vascular endothelial growth factor
W	Watt
α	Alpha particle
β+	Positron
γ	Gamma radiation
$[\alpha]_D^{25}$	Specific rotation
δ_H	^1H chemical shift in ppm downfield from tetramethylsilane
δ_C	^{13}C chemical shift in ppm downfield from tetramethylsilane
ν_e	Neutrino
μ	Micro

Table of Contents

INTRODUCTION

1.0 Background

Cancer, or malignant neoplasm, is a set of mammalian diseases in which groups of affected cells show uncontrolled growth and proliferation causing damage to nearby tissues. [1] In later stages of the disease cells gain the ability to spread to other areas of the body (metastasize), creating multiple tumours which can ultimately lead to death.[1] The disease occurs as the result of genetic mutations which can be caused by a number of factors including: exposure to chemical pollutants, radiation, specific infections, lifestyle choices and hereditary factors, or indeed, a combination of many of these.[2]

Cancer is a leading cause of death in the world, and was responsible for approximately 7.6 million deaths in 2008, contributing to 13% of all deaths worldwide.[3] The incidence of cancer has been shown to increase with age.[4] Therefore, as the result of a growing, aging population the occurrence of cancer is projected to increase dramatically within the next 20 years with an estimated 22.2 million new cases predicted for 2030 in comparison to 12.7 million cases reported in 2008.[5]

Due to the enormous number of people affected by cancer and subsequent mortality rates, it is imperative to continue research into discovering new treatments for this set of diseases and improved methods for its detection.

1.0.1 The Hallmarks of Cancer

In 2000 Hanahan and Weinberg published their seminal paper proposing six specific cellular traits or "Hallmarks" common to cancerous cells that differentiate them from normal healthy cells. These were: self-production of growth signals, indefinite division, insensitivity to anti-growth signals, avoidance of cell death (apoptosis), metastasis and the acquisition of sustained angiogenesis (*Figure 1*).[6] More recently the authors have published an updated review outlining the emergence of two new hallmarks: reprogramming of cellular energetics and avoiding immune destruction.[7]

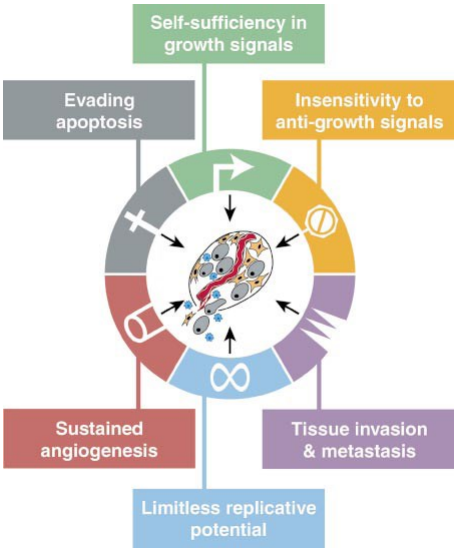

Figure 1- The hallmarks of cancer.[6]

Self-Production of Growth Signals

In general, a cell can only enter a state of proliferation when activated by exogenous growth factors. Growth factors are proteins and hormones which bind to specific trans-membrane receptors. These receptors then relay signals into the cell, and the cell nucleus, inducing growth and cellular division.[8] Cancerous cells have the ability to synthesise their own growth factors as well as expressing the corresponding receptors for binding them. As such, they show a decreased dependence on external growth signals.[9]

Insensitivity to Anti-Growth Signals

In normal cells tumour suppressor genes act in conjunction with anti-proliferative signals (for example transforming growth factor-β (TGF-β)) to regulate cell growth and division within a tissue. However, when these genes mutate causing disruption to the pathways governing cell growth, it can lead to insensitivity to anti-growth signals. For example, in certain human cancers mutation of the tumour suppressor gene coding for the retinoblastoma associated protein (pRB) causes a down-regulation in the production of cell surface receptors for TGF-β. The result is a loss of response to this anti-growth signal, allowing the cell to continue proliferation.[6, 8]

Indefinite Division

It has been demonstrated that normal, healthy cells have a limited potential for replication. Generally a non-proliferative state, known as senescence, is attained after a certain number of cell divisions.[10] Following each division DNA protecting the end of the chromosomes (the telomere) is shortened. When the telomere is eroded to a critical point, fusion of chromosomes can occur. This leads to the formation of dimeric chromosomes and unviable cells, resulting in mass cell death in a state known as crisis. In malignant cells, up-regulation of the DNA polymerase enzyme, telomerase, prevents shortening of the telomere. Found in around 90% of tumour cells, telomerase counteracts the effects of cell division by extending the end of telomeric DNA, granting limitless replicative ability.[11]

Avoidance of Apoptosis

Apoptosis, or programmed cell death, can be induced by detection of both intracellular (for example from DNA damage and hypoxia) and extracellular signals, such as the cytokine tumour necrosis factor (TNF).[12] When these signals are detected, a cascade is initiated which ultimately leads to destruction of the affected cell at the hands of effector caspases. In order for cancerous cells to avoid apoptosis they must either: disable receptors for apoptotic signals or disable their corresponding effectors. A prime example, occurring in approximately 50% of human cancers, is mutation of the gene coding for the protein p53.[13] The p53 protein is a key sensor for detecting abnormalities in DNA. As a result of its inactivation malignant cells are able to ignore apoptotic signals.[7]

Metastasis

The arrangements of cells and maintenance of their quiescent state within tissues is governed by several classes of proteins, particularly cell-cell adhesion molecules (CAMs). These proteins are deregulated as part of the invasion-metastasis cascade. Malignant cells can then detach from the surrounding tissue and travel to other areas of the body, *via* the bloodstream and lymph, to create secondary tumours.[14] Perhaps the most well studied example involves mutations to the epithelial cell protein E-cadherin. E-cadherin transmits signals to maintain specific cellular assemblies and limit growth by forming cell to cell bridges; alterations to this protein prevent these interactions, leading to metastatic behaviour.[15]

Sustained Angiogenesis

In order for a cell to function, it must be provided with oxygen and other specific nutrients which are delivered *via* blood vessels. When a tissue is fully developed the ability to encourage growth of new blood vessels (angiogenesis) is carefully controlled by angiogenic inducing and inhibiting signals. In tumours the balance of these signals is altered. For example, by increasing the expression of the initiator vascular endothelial growth factor (VEGF), and decreasing the expression of the inhibitor β-interferon, the growth of new blood vessels to provide additional resources for the tumour is promoted.[16]

Reprogramming Cellular Energetics and Avoiding Immune Destruction

Reprogramming of cellular energetics is the adjustment of energy metabolism to support increased cell growth and proliferation.[7] Cancerous cells alter the machinery of a cell so that anaerobic respiration is carried out even in the presence of oxygen, an effect first observed by Warburg.[17] The mechanisms behind this process are examined in greater detail in *Section 1.3.1.1*.

It is well known that immunocompromised humans show greater susceptibility to certain opportunistic cancers although these generally arise as a result of viral infection.[18] However, it has been shown in murine models that tumour cells from immunodeficient mice are generally unsuccessfully transplanted into immunocompetent mice whereas cancerous cells originating from healthy mice can effectively cause further tumours when transplanted.[19, 20] This evidence suggests that only cancerous cells which have developed the ability to avoid destruction at the hands of the immune system develop into tumours.[7]

It should be noted that both of these capabilities have yet to be completely validated. They are therefore classified as emerging hallmarks and required further investigation before they can be accepted alongside the other established hallmarks.[7]

In these reviews Hanahan and Weinberg highlight the progress made in understanding the nature of cancer and the causes behind it. However, there is still much to be learned and it is important to continue research into understanding this set of diseases. In terms of therapeutic uses, these

characteristic differences between healthy and malignant cells provide targets for the development of new chemotherapeutic drugs and methods of detection.

1.0.2 Detecting Cancer

There are various methods available for detecting cancer including: endoscopies, biopsies, molecular diagnostics and imaging techniques. Imaging techniques are not only useful in detecting cancer, but can be used in all aspects of treatment including: screening, evaluation of the success of therapy, planning for future therapies and providing guidance for palliation. These modalities also have the advantage of being non-invasive and, in certain cases, are able to provide real time monitoring of a patient.[21] There are a variety of imaging methods, including: magnetic resonance (MRI), single photon emission computed tomography (SPECT), positron emission tomography (PET), ultrasound, X-ray computerised tomography (CT) and optical imaging.[22]

MRI takes advantage of the inherent magnetic moment of hydrogen atoms within the body which will produce a signal known as free induction decay (FID), when placed in an applied magnetic field. The FID produced by these protons can be detected and analysed to give anatomical information on the area of the body being examined (*Figure 2*).[23, 24]

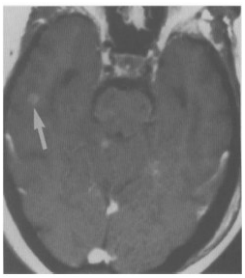

Figure 2- MRI of the brain, showing a metastatic tumour.[25]

MRI is a powerful technique for providing high resolution (up to 10 μm) images of the body and detecting cancers. However, it is a relatively costly modality and has fairly long scanning times (minutes to hours).[22]

Ultrasound is defined as sound with a frequency greater than 20 kHz. However, for medical imaging purposes sound between the frequencies of 2-10 MHz are generally used.[26] Diagnostic ultrasound imaging involves directing a pulse of ultrasound into the body, detecting its reflections/echoes and converting these signals into an image *(Figure 3*). [27]

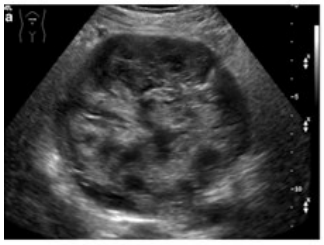

Figure 3- A pancreatic tumour visualised using ultrasound.[27]

Compared to other imaging modalities, ultrasound is cheap and portable and can also offer high resolutions (50 μm) and real time imaging. However, it does require a skilled operator in order to achieve the best images and is unsuitable for imaging certain areas of the body such as the lungs.[22, 26]

X-Ray CT uses similar principles to conventional x-ray imaging i.e. an x-ray will be differentially absorbed and reflected in different tissues of the body. As such the transmitted radiation can be detected and used to form an image. However, CT imaging uses multiple x-ray tubes and detectors which are rotated around the patient. Multiple cross sections are taken to give a three dimensional insight into the body (*Figure 4*).[28]

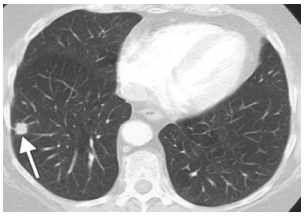

Figure 4- X-ray CT scan of the lungs with a tumour highlighted.[29]

CT scans offer high resolution imaging (50 μm) in a very short time space (50-100 ms) and have excellent specialist usage e.g. for imaging lungs.[22, 28] However, unlike the other

modalities discussed thus far CT scans involve a relatively high dose of ionising radiation and therefore has extra safety considerations.[28]

Optical imaging techniques such as bioluminescence and fluorescence, in general, have minimal uses in directly imaging patients since light in the ultraviolet-visible wavelength (100-650 nm) is absorbed by chromophores in the body. They can however be used as an aid for analysing pathology of biopsied tissues.[21] One exception involves the use of molecules labelled with fluorescent tags (fluorochromes) emitting near infrared (NIR) light (650-900 nm) detected using Fluorescence Molecular Tomography (FMT).[30] In this method, energy from an external light source is used to illuminate tissue causing excitation of the fluorochrome. This subsequently de-excites emitting NIR radiation which is detected (*Figure 5*).[22]

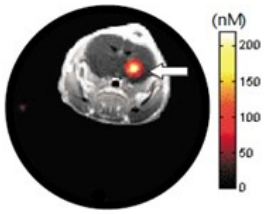

Figure 5- FMT imaging of a murine tumour using a fluorochrome activated by the protease Cathepsin B.[30]

Although this modality is still under development it is an attractive proposition due to its relative low cost, rapid imaging times (seconds to minutes) and use of targeted reporters.[22]

SPECT involves the detection of photons emitted from radiopharmaceuticals by a gamma camera which is rotated around a patient allowing construction of three dimensional images.[31] Radiopharmaceuticals in SPECT generally consist of a gamma emitting radionuclide such as technetium-99 combined with a ligand which targets a disease specific biomarker.[21] Although SPECT has a particularly low resolution (1 cm) and involves the use of ionising radiation it allows imaging of physiological processes (for example blood flow in the brain) at a lower cost than comparable techniques like PET.[22, 31]

1.1 Positron Emission Tomography (PET)

1.1.1 The Principles of PET

The majority of the aforementioned techniques (excluding SPECT and FMT) provide anatomical images of the body and are used to identify cancers based on structural changes within a tissue. PET on the other hand, provides a highly sensitive method of cancer detection by imaging physiological processes (e.g. glucose metabolism and cellular proliferation) occurring in the body. This is performed through the use of imaging agents, or molecular probes, which are molecules labelled with positron (an antimatter electron) emitting radionuclides. Frequently used radionuclides include: fluorine-18 [^{18}F], carbon-11 [^{11}C], oxygen-15 [^{15}O] or nitrogen-13 [^{13}N] and less commonly used radionuclides are: copper-64 [^{64}Cu], iodine-124 [^{124}I], and gallium-68 [^{68}Ga].[32] For the most part these are produced in a particle accelerator known as a cyclotron, a notable exception being [^{68}Ga] which is produced in a specific generator.[32, 33]

Positron emission is a form of radioactive decay occurring in proton-rich nuclei, whereby a proton is converted into a neutron releasing a positron and a neutrino in the process. This results in the formation of a more stable nucleus. Carbon-11 for example, will decay to form elemental boron and in the same way fluorine-18 will produce oxygen-18 (*Figure 6*).[32]

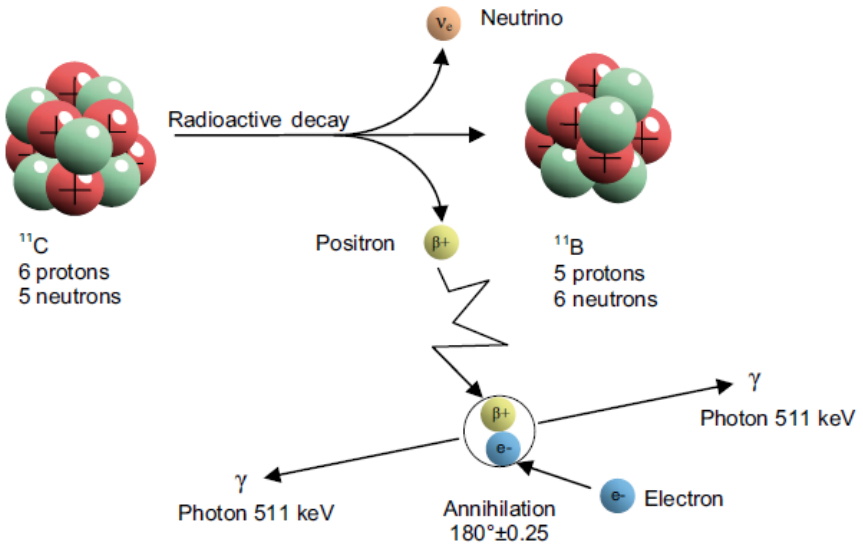

Figure 6- Positron emission by decay of carbon-11 to boron, followed by positron-electron annihilation to produce two gamma photons.[34]

Once synthesised, a radiolabelled probe is either injected intravenously or inhaled by a patient and it then localises within specific areas of the body. Positrons emitted by the radionuclide travel a short distance within a tissue (typically 2 mm) before colliding with an electron; this collision causes an annihilation resulting in the release of two 511 keV gamma photons at 180 degrees to each other (*Figure 6*). These photons are observed by arrays of detectors in PET scanners in a process known as coincident detection: only photons created in the same positron-electron annihilation event arriving at opposite detectors within a few nanoseconds of each other are counted.[32] Within the detector, these gamma photons interact with the crystalline material of a scintillator generating a pulse of light, which is amplified by photomultipliers creating an electrical impulse. This is then further processed and corrected for errors such as attenuation and accidental coincidences giving rise to usable data. The detector array forms a ring around the patient, therefore detection of photons by scintillators in the scanner arrays gives information on the concentration and location of the molecular probe within the patient allowing a 3-D image of the body to be generated (*Figure 7*).[35]

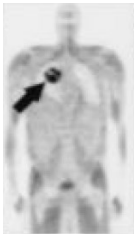

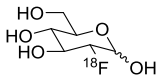

[^{18}F]-FDG

1

Figure 7- PET image of a lung tumour using fluorine-18 labelled glucose ([^{18}F]-fluorodeoxyglucose or [^{18}F]-FDG) [36]

The example depicted in *Figure 7* shows a PET image of glucose metabolism in the body using the glucose analogue [^{18}F]-FDG. The darker areas represent higher concentrations of the labelled glucose probe and hence areas of higher metabolic rate, corresponding to a carcinoma of the lung. Other darkened areas denote clearance of the probe in the bladder.[36] For further information on the uptake of [^{18}F]-FDG see *Section 1.3.1.1*.

PET images are commonly analysed semi-quantitatively to gain further information on a malignancy using a parameter known as the standardised uptake value (SUV). In cancer the SUV provides an index of the radioactivity concentration of the tumour compared to the initial injected radioactivity, divided by the body mass. Areas of abnormal molecular probe uptake are

firstly identified, followed by calculation of the SUV in these regions of interest (ROI).[37] Quantification of the intensity of probe uptake in the ROI yields data which can be analysed to give information on a variety of aspects of the malignancy. For example, SUVs allow differentiation between aggressive and indolent tumours, prediction of prognosis and can give early assessments of a patient's response to therapy.[21, 37, 38]

This highlights the major advantage of PET over other imaging modalities: its ability to provide physiological information on the area of the body being studied. Apart from the aforementioned information gained from SUVs, further beneficial data gained from PET studies include: highlighting biological changes that occur in cancer before anatomical abnormalities can be detected and providing entire body imaging of a primary tumour and its metastases. It is not only in cancer therapy where PET can provide additional insights into diseases; for example [^{18}F]-FDG can also be used as early indicator of Alzheimer's disease.[36] Moreover, the scanning time required to generate a PET image is relatively short (minutes), meaning less inconvenience for patients.[22]

However, PET does have various limitations. For example, in comparison to ultrasound, CT and particularly MRI it offers images with a particularly poor resolution of 1-2 mm, compared to 10-100 μm in MRI. This is a result of the distance travelled by the positron within a tissue prior to annihilation. Furthermore, PET offers little anatomical imaging, to the extent that it becomes difficult to estimate tumour invasion of neighbouring tissues.[22] One solution to this problem involves the use of joint PET/CT and PET/MRI systems. These hybrid techniques allow the combination of the high resolution anatomical imaging of CT and MRI with the functional information gained from PET (*Figure 8*).[39]

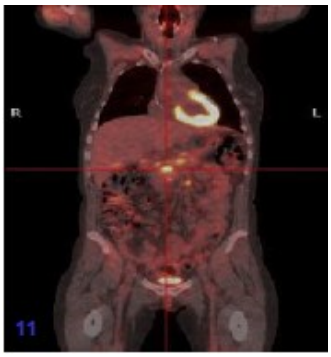

Figure 8- Combined PET/CT image showing multiple malignant tumours using [^{18}F]-FDG.[21]

Other problems associated with PET stem from the radionuclides themselves which have short half-lives (*Table 1*). As a result they have to be synthesised on site by cyclotrons or generators and must be quickly incorporated into their respective molecular probes to prevent significant loss of activity by radioactive decay. This has cost implications and, as will be discussed in following sections, it can present synthetic challenges for probe generation.[22, 36]

Radionuclide	*Half Life*
^{15}O	2 min
^{13}N	10 min
^{11}C	20 min
^{18}F	109 min

Table 1- Half-lives of commonly use radionuclides.[36]

1.1.2 Development of PET Molecular Probes

The development of new PET molecular probes for use in clinical settings is a complex and multidisciplinary process, consisting of a number of steps: selection of a suitable target, organic synthesis, radiolabelling, *in vitro* and *in vivo* evaluation and finally kinetic modelling of data.

Development begins with identification of a suitable target (e.g. an enzyme, receptor or transporter) for imaging the desired process. After selection of a target an appropriate compound to bind this target must be discovered. This is normally performed using high throughput screens or by rational design based on crystal structures. The properties of the compound can then be tailored based on *in vitro* and *in vivo* assays in a lead optimisation process.[40]

With a suitable ligand identified an appropriate radionuclide must be chosen for labelling. The choice of radionuclide is dependent on the biological process being studied: ideally the half-life of the radionuclide and that of the biological process should match. Additionally, the half-life should be sufficient to allow radiolabelling, purification and formulation of the molecular probe.[41] Techniques for introducing different radiolabels are discussed in further detail in *Section 1.2*.

The formulated molecular probe can then be subjected to *in vitro* testing for plasma stability and affinity studies carried out. Finally, *in vivo* testing for can be carried out to evaluate pharmacokinetic properties of the PET probe. For example, biodistribution studies can be used to determine the percentage of injected dose per gram tissue, (% ID/g) which in turn can be used to calculate the SUV.[40]

1.1.3 Desirable Properties of PET Molecular Probes

As alluded to in the previous section there are a number of desirable properties for PET probes to have. These are defined by both the physical characteristics of the radionuclide and the chemical structure of the probe and include: specificity, selectivity, lipophilicity, affinity, specific activity, metabolic stability, clearance and radiochemical yield.

Specificity and Selectivity

A molecular probe should selectively bind to its target to ensure only the desired process is being measured. Additionally, the probe should be designed to reduce the amount of non-specific binding to plasma proteins, cell membranes and other non-target tissues. Excessive non-specific binding gives rise to a high background signal (noise), which reduces the contrast of the enzyme or receptor being targeted. Non-specific binding has been shown to be related to the lipophilicity of a compound.[41, 42]

Lipophilicity

Lipophilicity is the affinity of a molecule for lipophilic environments and is expressed as a logarithm of the partition coefficient 'P'. The partition coefficient is measured as a ratio between the concentration of a compound in octanol versus water (*Equation 1*).[43]

$$P = \frac{[\text{compound}]_{\text{octanol}}}{[\text{compound}]_{\text{water}}} \qquad D = \frac{\sum [\text{compound ionised + unionised}]_{\text{octanol}}}{\sum [\text{compound ionised + unionised}]_{\text{water}}}$$

Equation 1- Partition coefficient and distribution coefficient.

More accurately this value may be measured using the pH dependent distribution coefficient 'D'. This value takes into account the degree of ionisation occurring at a specific pH and is the ratio of the concentration of unionised and ionised compound in both phases. In PET, typical logD values are measured at physiological pH. In general a probe needs to be sufficiently lipophilic to pass through cell membranes but not so lipophilic as to show significant non-specific binding to fatty tissues; ideal logD values will be less than three.[43, 44] It should be noted, that non-specific binding cannot be attributed to lipophilicity alone and that a molecules ability to hydrolyse phospholipid bilayers can also play a role.[45]

Clearance

Ideally the probe should be rapidly cleared from plasma to reduce the blood pool background signal at the target tissue. Similarly the probe should also be rapidly cleared from non-specific areas again to improve the signal to noise ratio.[32, 44]

Affinity

Affinity is the ability of a molecular probe to bind to its target. Useful molecular probes generally have affinities in the range of 0.01−1.00 nM and in principle higher affinity should give rise to a higher signal to noise ratio. However, as increased affinity is often associated with increased lipophilicity this is not always the case. Additionally the density of the target must be taken into account, with lower target densities requiring probes with higher affinity.[42, 43]

Specific Activity

Specific activity (SA) is defined as the activity (A) of a radiolabelled probe per unit mass (GBq or mCi per μmol) (*Equation 2*).[46]

$$SA = A/m$$

Equation 2- Specific activity.[46]

High specific activities are desirable as they allow effective imaging of a target using small amounts of material (typical probes are administered in nano-molar quantities) without perturbing the system being studied by fully saturating the target. Furthermore, using such low amounts of tracer means toxicity is less of an issue.[41] It should be noted that although theoretical specific activity values for radionuclides are very high (e.g.carbon-11 ~ 341,000 GBq/μmol), due to isotopic dilution, unwanted side reactions during labelling and activity loss by decay the specific activity for administered probes tends to be much lower (e.g. carbon-11 ~3,000 GBq/μmol).[44]

Metabolism and Labelling Position

Ideally, a PET probe will be stable to metabolism during the timeframe of scanning. However, in many cases metabolism is unavoidable and therefore the position of the molecular probe subjected to radiolabelling must be carefully chosen. The production of radiolabelled metabolites that show binding affinity for the target or accumulate within the target tissue must be avoided.[47] In certain cases labelling of a molecule can be advantageous, increasing its metabolically stability, therefore simplifying kinetic modelling. For an example of such a situation see *Section 1.3.2.1*.

Radiolabelling and Radiochemical Yield

While more of a synthetic concern, it is nonetheless a desirable property that a molecular probe be rapidly radiolabelled and in good radiochemical yields (RCY, the yield after radiochemical purification expressed as a percentage of the activity originally present).[46] This number is often quoted as the decay-corrected radiochemical yield which takes into account the naturally occurring decay of the isotope.[41] Unless specified RCY shall henceforth refer to decay correct radiochemical yields.

These properties are desirable for all molecular probes, however one can further divide radiopharmaceuticals into three classes defined by their specific target: those based on enzyme–mediated metabolic transformations (often analogues of endogenous compounds), probes based on stoichiometric binding interactions with receptors and those which measure perfusion.[32] The first class of probe will be the focus of much of the work contained in this thesis.

1.2 Introduction to PET Radiochemistry

The production of a PET probe involves numerous steps. Initially, the radionuclide is prepared in a cyclotron by bombarding a target system with a beam of protons or deuterons. The target system is a vessel containing a target material required for the production of a specific radionuclide. The radionuclide is trapped in such a form that it can be directly reacted or further functionalised and then reacted with a 'cold' non-radioactive precursor with a compatible reactive functionality.[41] The cold compound is generally more chemically complex and is reacted with the radioactive synthon in the final stages of the synthesis (*Figure 9*).

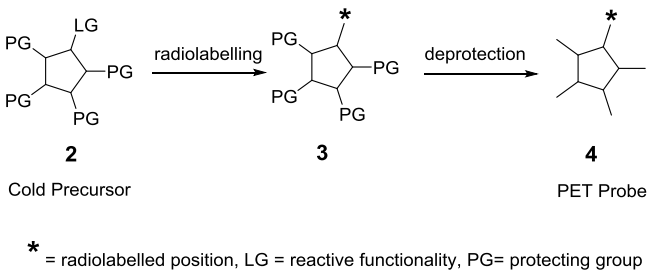

Figure 9- Simple schematic showing the synthesis of a positron emitting molecular probe.

In some cases, removal of protecting groups (PG) is required after radiolabelling although it is desirable to have as few steps as possible after labelling in order to minimise loss of activity by radioactive decay. Finally, the PET probe must be purified, usually by (high performance liquid chromatography) HPLC, and then formulated for use.[48] This entire process should ideally be completed within three half-lives from the end of bombardment (EOB) of the target material.[49] As such each step must be carried out in a time efficient manner. Lengthy purification in particular can have drastic effects on yield and specific activity. Purification time by HPLC can be minimised by increasing the solvent flow rate, reducing the column length and increasing the temperature of the column itself. This however is dependent on the degree of separation between the product and by-products.[49] An alternative is the use of solid phase extraction (SPE): pre-packed chromatographic cartridges which allow the removal of specific contaminants. Using this method can allow rapid purification but is often limited for use with a specific product.[48]

As shown in *Table 1* there are many common radionuclides available for synthesising molecular probes. However, the short half-lives of [^{15}O] and [^{13}N] mean there is relatively little complex

radiochemistry that can be performed with these emitters. On the other hand, [^{11}C] and particularly [^{18}F] have sufficiently long half-lives to allow some flexibility in their synthetic use.

1.2.1 Fluorine-18 Radiochemistry

Fluorine-18 is currently the most widely used radionuclide in PET radiochemistry. Attractive properties of [^{18}F] include its long half-life when compared to [^{11}C], [^{13}N] and [^{15}O] and the fact that it produces the highest resolution PET images due to its low positron energy and hence short linear positron trajectory in tissues. The emergence of [^{18}F]-FDG as an important tool in the detection and staging of cancer has driven interest in [^{18}F] radiochemistry research as well as the use of PET in clinical and research institutions as a whole.[41] Radiochemistry with [^{18}F] can be broadly divided into two categories: electrophilic and nucleophilic fluorination reactions.

1.2.1.1 Nucleophilic Fluorination Reactions with [^{18}F] Fluoride

Nucleophilic fluorination reactions make use of [^{18}F] fluoride [$^{18}F^-$] generated using the $^{18}O(p,n)^{18}F$ nuclear reaction. In this case the target material is [^{18}O] enriched H_2O, which undergoes proton bombardment releasing a neutron and forming a solution of [$^{18}F^-$]. Fluoride in this form ([^{18}F] HF) requires additional modification in order to increase its nucleophilicity. The obtained solution is therefore trapped on an ion-exchange resin and eluted with a K_2CO_3 solution. It is then treated with the phase transfer agent kryptofix-222 (K_{222}) in order to complex the potassium cation, further increasing the reactivity of fluoride anion. Reactions are generally carried out in polar aprotic solvents again with increasing reactivity in mind.[50, 51]

An important consideration when carrying out nucleophilic fluorinations is the functionality of the cold precursor *i.e.* the requirement of a suitable leaving group. For simple aliphatic substitutions triflates, tosylates, mesylates, bromides and iodides are all acceptable (*Scheme 1*).[41]

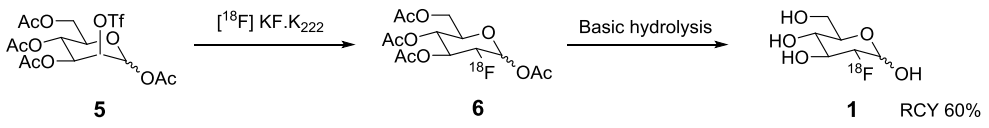

5 **6** **1** RCY 60%

Scheme 1- Synthesis of [^{18}F]-FDG **3** by nucleophilic fluorination.[51]

The reaction of protected pyranose **5** with [^{18}F] KF.K_{222} is the most utilised radiochemical reaction today and provides a highly relevant demonstration of this type of reaction. The requirement of protecting groups to prevent competing nucleophilic attack by other reactive functionalities is a major issue with these procedures. Deprotection and purification increase the synthesis time, limiting the amount of useful steps that can be carried out beforehand.[41, 51]

When attempting nucleophilic fluorinations of aromatic compounds the situation becomes more complex. In order for successful reaction, not only is a suitable leaving group necessitated but in addition, the presence of electron withdrawing groups *ortho* or *para* to the leaving group are required for activation of the aromatic ring. Despite these constraining factors these nucleophilic aromatic substitutions (S_NAr) have become widely used (*Scheme 2*).[52]

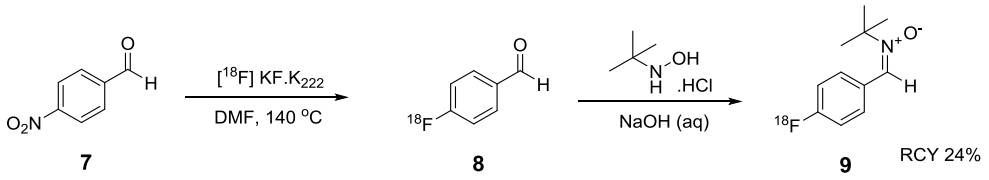

Scheme 2- Synthesis of 4-[^{18}F]-fluorobenzaldehyde.[52]

Reacting *para*-nitrobenzaldehyde with [^{18}F] KF.K_{222} is an excellent method for generating [^{18}F]-fluorobenzaldehyde **8**, which in itself is a highly versatile intermediate. [^{18}F]-fluorobenzaldehyde and analogues of this molecule can be further reacted in a number of different ways to generate more complex molecular probes. For example reacting *N*-(*tert*-butyl)hydroxylamine with **8** yields **9** designed for use in *in vivo* visualisation of free radicals.[53] This is an example of indirect labelling strategy using [$^{18}F^-$].

Another common indirect fluorination strategy involves reacting [^{18}F] labelled alkyl azides with alkynes using the copper catalysed Huisgen cycloaddition. This reaction is particularly amenable to PET chemistry as a result of the fast reaction times, high yields and mild conditions (*Scheme 3*).[54]

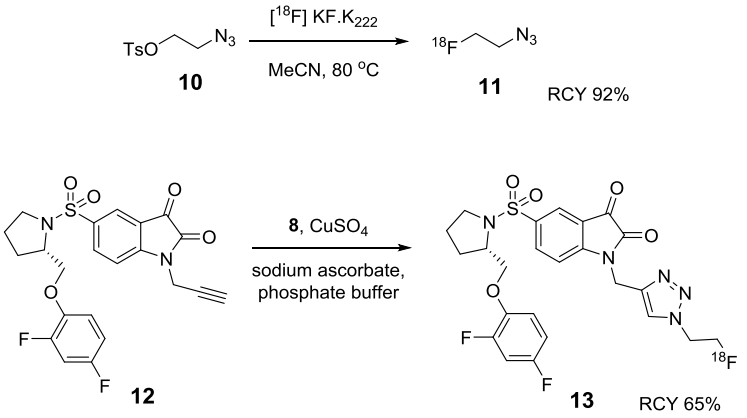

Scheme 3- Labelling of an isatin-sulfonamide with [^{18}F]-fluoroethylazide by Huisgen cycloaddition.[55]

[^{18}F]-Fluoroethylazide for example, is synthesised by reacting a precursor tosylate **10** with nucleophilic fluoride. This can be then be reacted with various different alkynes, an appropriate illustration being the synthesis of radiolabelled isatin-sulfonamide **13**, which binds caspases 3 and 7 and hence can be used for imaging apoptosis.[55] Using these indirect labelling strategies permits access to complex molecular probes that are not viable targets for direct labelling due to the harsh conditions employed in the initial radiolabelling step. However, this also results in an increased number of steps in the radiosynthesis which must also be taken into consideration.

1.2.1.2 Electrophilic Fluorination Reactions with [^{18}F] Fluorine

Electrophilic fluorination reactions traditionally make use of [^{18}F] fluorine gas ([^{18}F] F_2) available from the $^{18}O(p,n)^{18}F$ and $^{20}Ne(d,\alpha)^{18}F$ nuclear reactions. Proton bombardment of [^{18}O] O_2 is the preferred method of [^{18}F] F_2 synthesis as a result of its higher efficiency.[56] This is an example of a carrier added synthesis whereby a small amount of [^{19}F] F_2 (0.2%) is added to the target gas. In the absence of stable fluorine, the radiolabelled gas can adsorb to the walls of the vessel containing the target gas reducing the amount of radioactive material isolated.[57] Compared to reactions with [$^{18}F^-$], the use of [^{18}F] F_2 suffers from a number of drawbacks, including: being more difficult to handle and use therefore requiring specialist equipment, lower specific activity as a result of carrier added fluorine and the high probability of producing unwanted fluorinated by-products due to reactivity of gaseous fluorine.[58]

Nevertheless, [^{18}F] F_2 has been applied in the successful radiolabelling of a variety of compounds including [^{18}F]-5-fluorouracil **15**. Reacting uracil **14** with [^{18}F] F_2 in acetic anhydride furnishes **15**, which can be used as a prognostic agent in cancer therapy (*Scheme 4*).[59, 60]

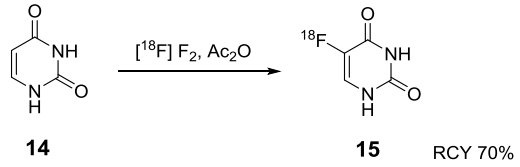

Scheme 4- Synthesis of [^{18}F]-5-fluorouracil using [^{18}F] F_2.[59]

Another example is the synthesis of [^{18}F]-fluoro-L-DOPA **17**. Fluoro-destannylation of precursor **16** with [^{18}F] F_2 is followed by acidic deprotection yielding **17**, a molecular probe used in the study of Parkinson's disease (*Scheme 5*).[61]

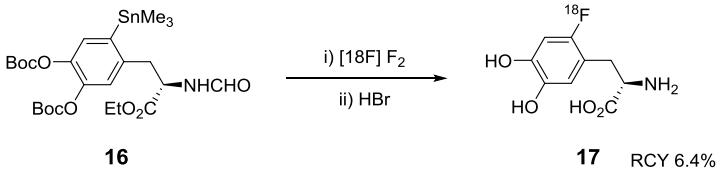

Scheme 5- Synthesis of [^{18}F]-fluoro-L-DOPA using [^{18}F] F_2.[61]

Other less reactive and more selective reagents have emerged in the latest literature. A recent report by Gouverneur *et al.* for example, describes the synthesis of a highly selective electrophilic fluorinating reagent [^{18}F]-Selectfluor *bis*-triflate ([^{18}F]-TEDA) **19** (*Scheme 6*).[58]

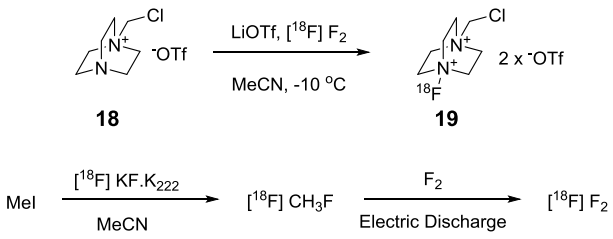

Scheme 6- [^{18}F]-TEDA synthesised using high specific activity [^{18}F] F_2.[58]

This protocol takes advantage of Solin's methodology for the synthesis of high specific activity [^{18}F] F_2. By reacting methyl iodide with [^{18}F] KF.K_{222} [^{18}F]-fluoromethane is produced. The fluoromethane is then mixed with a small amount of carrier [^{19}F] F_2 and subjected to an electrical discharge, resulting in the exchange of [^{18}F] and [^{19}F] in plasma, producing [^{18}F] F_2 with specific activity up to 50 times greater than that available by traditional proton bombardment.[62] 1-Chloromethyl-4-aza-1-azoniabicyclo[2.2.2]octane triflate **18** was then fluorinated with the high specific activity fluorine to yield **19** and this in turn was reacted with silyl-enol ether **20** in a proof of concept reaction (*Scheme 7*).[58]

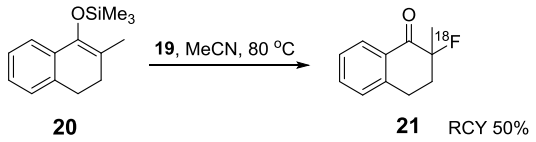

Scheme 7- Fluorination using **19**.[58]

The reaction proceeded successfully with a radiochemical yield of 50%. Owing to its selectivity and mild reaction conditions in comparison to directly using [^{18}F] F_2, [^{18}F] selectfluor bis-triflate **19** presents an exciting development for [^{18}F] fluorinations.[58]

Perhaps even more remarkable is the reported synthesis of an electrophilic fluorine source available directly from nucleophilic [^{18}F] fluoride (*Scheme 8*).

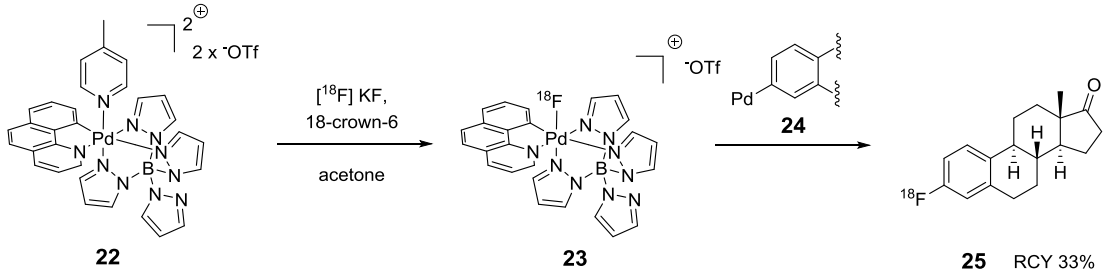

Scheme 8- Electrophilic fluorination of aryl palladium complexes with **23**.[63]

By controlling the properties of palladium (IV) complexes **22** and **23** through careful ligand selection Ritter *et al.* have developed complexes which can react with [$^{18}F^-$] and transform it into an electrophilic source. The cold precursor **22** is specifically tailored for capturing nucleophilic

fluoride; once trapped the nature of complex **23** causes a reversal in the reactivity of the fluorine, thus furnishing an electrophilic [^{18}F] fluorine source. This complex can be used to oxidatively transfer fluorine to palladium (II) aryl complexes, before reductive elimination yields the desired product. The utility of this reaction was demonstration through the fluorination of several aryl palladium precursors, generating [^{18}F]-fluorodeoxyestrone **25** amongst others.[63] Although the applications of complex **23** are potentially very exciting, it should be noted that both this and complex **24** are chemically complex, requiring glove box manipulations for their synthesis. Furthermore, the use of metals such as palladium requires careful purification to avoid toxicity.[64] While this is suitable for research settings it makes transfer to the clinic difficult.

To summarise, while there are a number of challenges in using [^{18}F] for radiolabelling including: a relatively small pool of biologically relevant molecules containing a carbon-fluorine bond, limited synthetic flexibility and the unknown effects of replacing functionality with [^{18}F] (see *Section 1.3.2.1*). It remains an attractive proposition for radiochemists due to its comparatively long half-life. Moreover, recent developments, particularly in the area of electrophilic [^{18}F] sources, are helping to further expand the usefulness of [^{18}F] as a radiolabel.

1.2.2 Carbon-11 Radiochemistry

The most common synthesis of [^{11}C] is *via* the ^{14}N(p,α)^{11}C nuclear reaction. In this case nitrogen gas is bombarded by a high-energy beam of protons, resulting in the formation of [^{11}C] and an α-particle (helium nucleus). In the presence of trace amounts of oxygen or hydrogen gas the [^{11}C] reacts to form either [^{11}C]-carbon dioxide ([^{11}C] CO_2) or [^{11}C]-methane ([^{11}C] CH_4), which can then be trapped and used directly or manipulated to form other precursors (*Scheme 9*).[41]

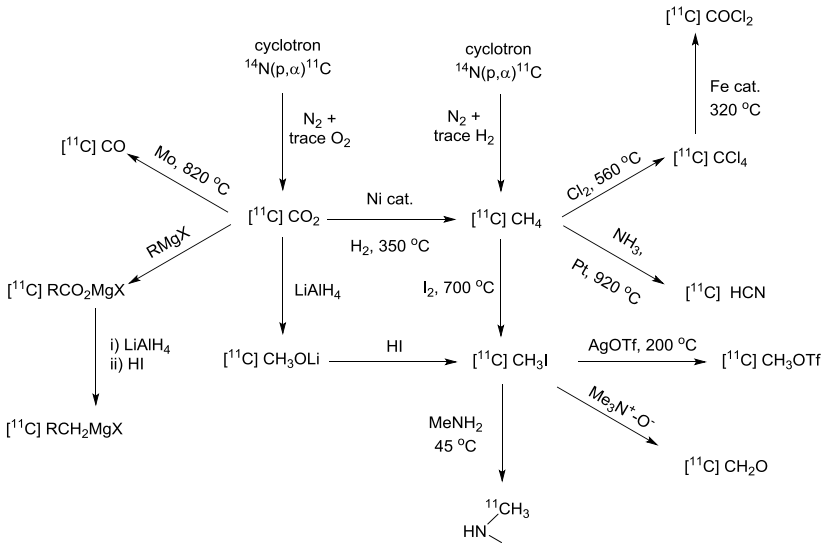

Scheme 9- A selection of ^{11}C precursors used in synthesis, adapted from Scott.[65]

1.2.2.1 [^{11}C] Methyl Iodide

The most frequently used [^{11}C] precursor is undoubtedly [^{11}C] methyl iodide ([^{11}C] CH_3I). [^{11}C] Methyl iodide can be generated using two methods: the reduction of [^{11}C] CO_2 by lithium aluminium hydride, followed by reaction with hydroiodic acid; or radical iodination reaction of [^{11}C] CH_4 with iodine at high temperatures.[66, 67] [^{11}C] methyl iodide has found the majority of its use in simple nucleophilic substitution reactions with nitrogen, oxygen and sulfur heteroatoms. In cases where [^{11}C] CH_3I is insufficiently reactive, further conversion using a hot column of silver triflate can generate the more reactive [^{11}C] CH_3OTf species.[65] Due to their simple nature (a typical methylation involves trapping [^{11}C] CH_3I/[^{11}C] CH_3OTf in solvent with the cold precursor and heating) and rapid reaction times these reactions have become the most widespread way of synthesising [^{11}C] labelled molecular probes.[41]

There are a number of interesting modifications and additions to basic methyl iodide methodology. Jacobsen and Mishani, for example, have demonstrated an appealing approach for introducing radiolabelled [^{11}C]-dimethylamine moieties (common to many drug molecules) into PET probes. [^{11}C] CH_3I can be reacted with methylamine to yield [^{11}C]-dimethylamine **27**, which can then be used in the synthesis of numerous analogues (*Scheme 10*).[68]

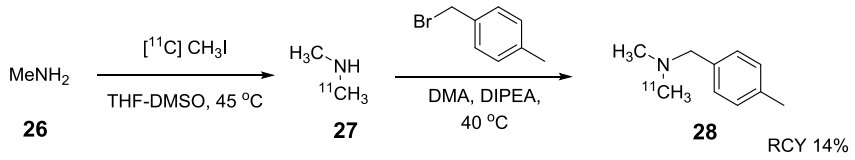

Scheme 10- [^{11}C]-dimethylamine as a precursor.[68]

The principal advantage of this method is the reversal in reactivity profile: using [^{11}C] CH_3I as a radiolabel in a nucleophilic form expands the number of labelling strategies available as well as demonstrating differing functional group tolerance to [^{11}C] CH_3I.[65]

Hooker *et al.* have developed a novel approach for the generation of [^{11}C]-formaldehyde by the oxidation of [^{11}C] CH_3I (*Scheme 11*).[69]

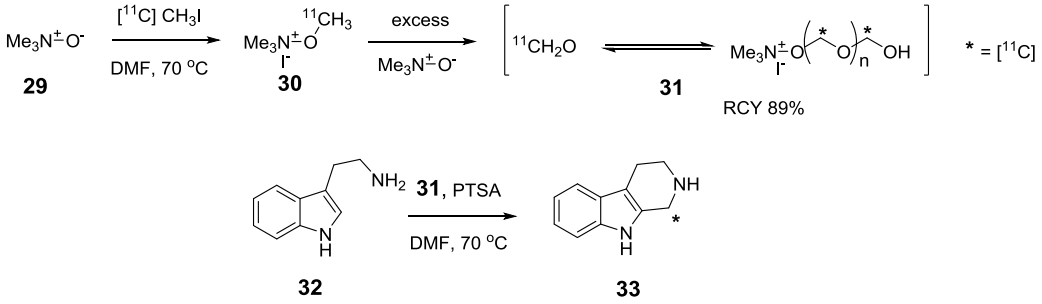

Scheme 11- Synthesis and reaction of [^{11}C]-formaldehyde.[69]

Treatment of trimethylamine *N*-oxide (TMAO) **29** with [^{11}C] CH_3I results in the formation of intermediate **30** which decomposes upon heating resulting in the formation of [^{11}C]-formaldehyde **31**. The usefulness of this intermediate was demonstrated with the synthesis of **33** from tryptamine **32** using the Pictet-Spengler reaction (*Scheme 11*). Oxidation of [^{11}C] CH_3I using TMAO provides a rapid and efficient synthesis of [^{11}C]-formaldehyde in comparison to previous methods involving reduction and oxidation of [^{11}C] CO_2.[69]

[^{11}C] CH_3I has also found use in palladium-catalysed coupling reactions (*Scheme 12*).[41]

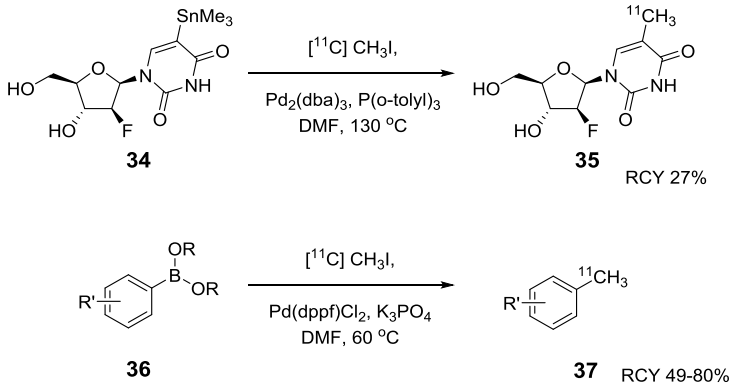

Scheme 12- Palladium cross couplings using [^{11}C] CH_3I.[64, 70]

Due to their tolerance to a wide variety of functional groups Stille couplings have become the most widely used cross couplings in PET radiochemistry. An important example is in the synthesis of the nucleoside 1-(2'-deoxy-2'-fluoro-β-D-arabinofuranosyl)-[methyl-^{11}C]-thymine or [^{11}C]-FMAU **35** a potential marker for proliferation in cancer.[64] However, a major disadvantage of these reactions is the use of organo-stannanes. These compounds and the subsequent by-products produced are highly toxic and require careful removal during purification. Suzuki couplings represent a viable solution to this problem. Hostetler *et al.* for example, reported the successful coupling of aryl boronic esters and acids **36** with [^{11}C] CH_3I. Although these reactions have a more restricted functional group tolerance in comparison to Stille couplings, they report high radiochemical yields and purity and avoid the toxicity issues associated with the use of stannanes.[70]

Also worthy of mention are polymer-supported [^{11}C] methylations. In these reactions the cold precursor **37** is attached to a solid support and then treated with [^{11}C] CH_3I. After completion of the reaction only the successfully labelled precursor can be washed from the polymer-support. This ensures high purity avoiding the need for HPLC purification reducing loss of activity by decay during chromatography (*Scheme 13*).[71]

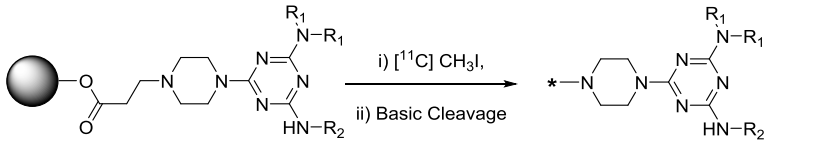

Scheme 13- Polymer-supported methylation and release of labelled product.[71]

Due to their ease of use, high radiochemical yields and versatility so-called microfluidic 'loop' methods have found growing use in the methylation of simple precursors. These methods involve coating the inside surface of a plastic or stainless steel HPLC loop with a solution of the cold precursor and then passing a stream of gaseous [^{11}C] CH_3I through the system. With the loop itself acting as a reaction vessel, the crude mixture can be directly injected onto the HPLC column for purification following reaction. This avoids the loss of material due to transfer from reaction vessels (*Scheme 14*).

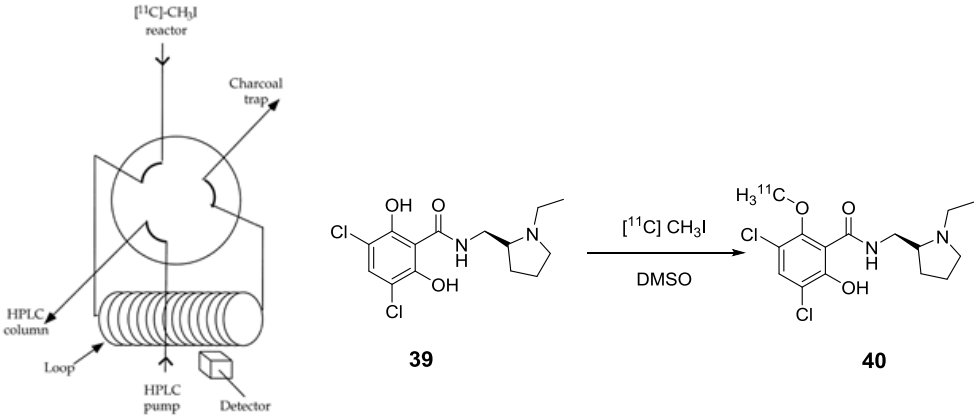

Scheme 14- Schematic of a loop system used for [^{11}C] methylation reactions e.g. methylation to form [^{11}C]-raclopride **40**.[72]

Other advantages of this methodology include its efficiency: using smaller volumes of solvent not requiring any temperature control for trapping or reaction, and rapid reaction rates.[72] See section *3.2.2* for further discussions of microfluidic reactions.

1.2.2.2 [^{11}C] Carbon Monoxide

The carbonyl group is one of the most widely abundant functionalities found in biologically relevant molecules. The ability to introduce [^{11}C] carbon monoxide ([^{11}C] CO) to molecular probes is therefore highly desirable. [^{11}C] CO is produced by the reduction of [^{11}C] CO_2 over molybdenum and zinc catalysts at high temperatures and has found its greatest application in palladium-catalysed carbonylation reactions.[41]

These reactions involve four components: the transition metal catalyst, an aryl or vinyl halide, a nucleophile and [^{11}C] CO. They proceed *via* a typical catalytic cycle: oxidative addition of the halide species, insertion of [^{11}C] CO to form an acyl-palladium complex, followed by nucleophilic attack and reductive elimination to the product (*Scheme 15*).[73]

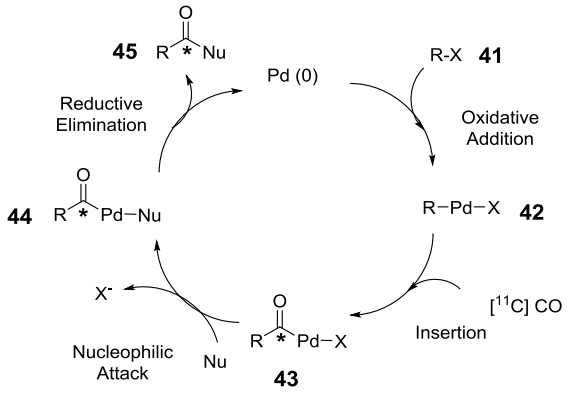

Scheme 15- General mechanism for carbonylative palladium cross couplings.[73]

Initial investigations of this chemistry suffered from low radiochemical yields as a result of the poor solvent solubility of carbon monoxide, thus limiting the rate of the insertion step.[73] Recent developments using high pressure micro-autoclaves have overcome these issues, allowing reactions to be performed at pressures in excess of 350 atm enhancing the solubility of [^{11}C] CO.[74]

Such advances have allowed the synthesis of a variety of ketones and amides using Suzuki, Stille and Buchwald-Hartwig carbonylative coupling procedures (*Scheme 16*).[75, 76, 77]

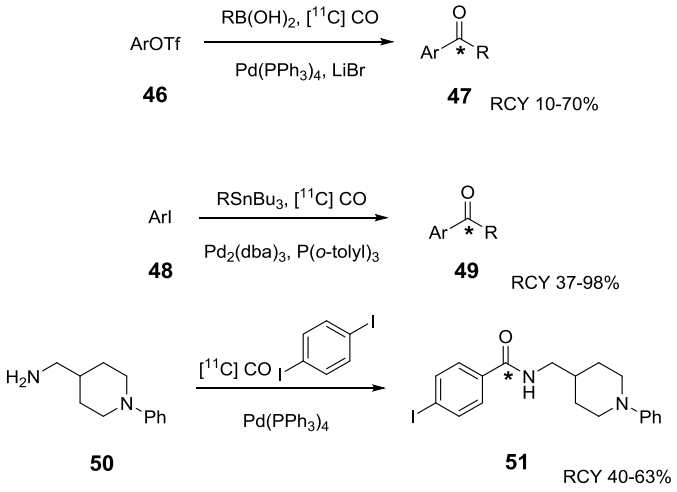

Scheme 16- Palladium catalysed carbonylative cross couplings.[73]

Free-radical carbonylations of alkyl iodides have also been used to synthesise radiolabelled esters, amides and carboxylic acids from [^{11}C] CO (*Scheme 17*).[78, 79]

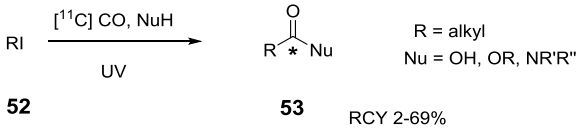

Scheme 17- Free radical carbonylations of alkyl iodides.[73]

Although seemingly analogous to palladium catalysed carbonylations, these reactions provide several distinct advantages. For example, without the risk of β-hydride elimination radical carbonylations can make use of alkyl halides and triflates as well as aryl and vinyl halides. Additionally this method is tolerant to functional groups such as carboxylic acids and alcohols, which are normally protected in syntheses using [^{11}C] CO_2 and Grignard reagents.[79]

1.2.2.3 [^{11}C] Carbon Dioxide

In contrast to [^{11}C] CO and [^{11}C] CH_3I, there are relatively few examples using [^{11}C] carbon dioxide ([^{11}C] CO_2) as the labelling species. A notable exception is in the formation of radiolabelled carboxylic acids and acid chlorides by the reaction of [^{11}C] CO_2 with Grignard reagents (*Scheme 18*).

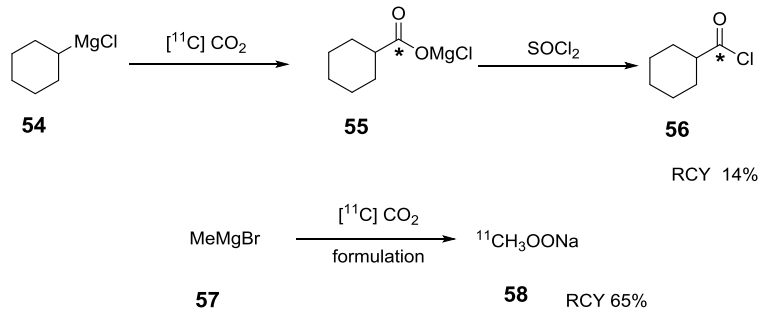

Scheme 18- Reactions of [^{11}C] CO_2 with Grignard reagents.[80, 81]

In both these examples, the [^{11}C] CO_2 is first of all reacted to form the Grignard salt **55** and **58** and then further functionalised as required. The synthesis of [^{11}C] labelled sodium acetate **58**, used for the diagnosis of prostate cancer is an important demonstration of this strategy.[80, 81] However, as previously mentioned the functional group tolerance of these methods can limit their usefulness.

1.2.2.4 [^{11}C] Hydrogen Cyanide and other Reactions

There are numerous biologically relevant molecules containing the nitrile functionality, making it an ideal target for radiolabelling. [^{11}C] Hydrogen cyanide ([^{11}C] HCN), produced by the reaction of [^{11}C] CH_4 with NH_3 at high temperatures using a platinum catalyst, provides a suitable reagent for the introduction of this group (*Scheme 19*).[82]

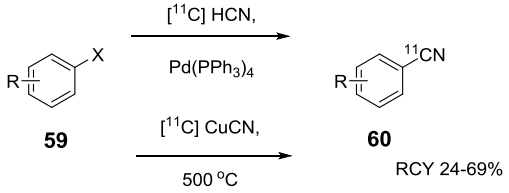

Scheme 19- Introducing [^{11}CN] group to aryl halides.[83, 84]

[^{11}C] HCN can be reacted directly with aryl halides **59** using palladium catalysis or it may be converted to [^{11}C] CuCN and then used to introduce the nitrile group *via* a Rosenmund-von Braun reaction.[83, 84] With the nitrile functionality in place amides, tetrazoles and carboxylic

acids can be conveniently synthesised allowing the generation of a wide range of radiolabelled molecules.[41]

It should be noted that there are a number of reactions such as rhodium catalysed carbonylations using and the use of [^{11}C] labelled phosgene that have been omitted. These will be covered in *section 2.0.2* discussing the synthesis of [^{11}C] labelled isocyanates.

These examples serve to highlight the diverse array of reactions available to the radiochemist utilising [^{11}C] and demonstrates the synthetic versatility of this radionuclide in comparison to [^{18}F]. Furthermore, as carbon is an element endogenous to the body it means that a tracer labelled with [^{11}C] it will follow the same biological pathways as the original molecule, providing a 'true tracer' of the process being analysed.[97] However, there are limitations associated with [^{11}C] chiefly its relatively short half-life. This places restrictions on the number of steps that can be used and unlike [^{18}F] requires the presence of an on-site cyclotron. Additionally gaseous [^{11}C] CO_2 and [^{11}C] CH_4 are difficult to handle requiring specialist equipment.[73] It should be noted that a short half-life can be beneficial clinically, allowing repeat studies to be carried out with a similar or lower dose than radionuclides with a longer half-life.[85]

1.2.3 Oxygen-15 and Nitrogen-13 Radiochemistry

As is this case with [^{11}C] both [^{15}O] and [^{13}N] are examples of nuclei whose stable isotopes are elements endogenous to the body. They are found in most biologically active compounds and therefore are seemingly ideal candidates for radiolabelling molecular probes. Unfortunately, as previously mentioned, their short half-lives restrict the amount of useful synthetic radiochemistry that can be performed using these radionuclides (*Table 1*).

Oxygen-15 can be produced in two forms: as [^{15}O] O_2, made in the $^{14}N(d,n)^{15}O$ nuclear reaction by bombarding a nitrogen-oxygen mixture with high energy deuterons, and as [^{15}O] H_2O made by irradiation of water with protons $^{16}O(p,pn)^{15}O$.[86] Both [^{15}O] O_2 and [^{15}O] H_2O can be used for blood flow studies in the brain and other organs.[87]

Nitrogen-13 is generated from H_2O using the $^{16}O(p,\alpha)^{13}N$ nuclear reaction in the form of [^{13}N] nitrate and nitrite salts. The commonly used form for labelling is as [^{13}N] ammonia. This can be prepared *via* the reduction of the aforementioned nitrogen salts using an Al/Cu/Zn alloy or can be

made directly by the addition of ethanol to the target to scavenge radical hydroxyl groups thus preventing oxidation. Much like [^{15}O] O_2 and H_2O [^{13}N] NH_3 can be used in blood flow studies. Other uses include the enzymatic synthesis of amino acids, the reaction of acid chlorides to form amides and the synthesis of [^{13}N]-*cis*platin **62** for measuring uptake of *cis*platin in the brain (*Scheme 20*).[88, 89]

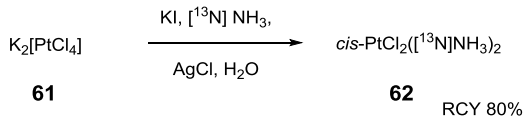

Scheme 20- Synthesis of [^{13}N]-*cis*platin.[89]

While [^{15}O] and [^{13}N] have demonstrated usefulness for the synthesis of a small number of probes, particularly those suited for perfusion studies. When compared to [^{18}F] and [^{11}C] their use in complex radiochemical syntheses is at best limited.

Now that the desirable properties of PET radiopharmaceuticals have been established and the synthetic methods for generating them described, some currently used molecular probes will be reviewed. This will be followed by an examination of more recent developments in imaging proliferation in cancer as well as outlining potential targets for the next generation of PET proliferation probes.

1.3 PET Imaging Probes

1.3.1 PET Probes for Imaging Glucose Metabolism

1.3.1.1 [^{18}F]-Fluorodeoxyglucose ([^{18}F]-FDG)

There are a vast number of radiotracers available for imaging cancers using PET. The current 'gold standard' molecular probe is undoubtedly the glucose analogue [^{18}F]-FDG, in which the C-2 hydroxyl group of glucose is replaced with an [^{18}F] radionuclide (*Figure 10*). The radiosynthesis of [^{18}F]-FDG has been previously covered (*Scheme 1 Section 1.2.1.1*).

1 **63**

Figure 10- [^{18}F]-FDG **1** and D-Glucose **63**.[90]

Cancerous cells show increased consumption of glucose and therefore an increased consumption of [^{18}F]-FDG in comparison to normal cells. As mentioned previously (see *Section 1.0.1*) cancerous cells are able to reprogram the manner in which they carry out glucose metabolism, limiting energy production to glycolysis.[7] This causes the net production of two (adenosine triphosphate) ATP molecules per molecule of glucose compared with thirty six ATP molecules in standard aerobic conditions. As such, additional glucose is required to generate the same amount of energy.[91] Enhanced glucose uptake is caused by an upregulation in expression of the glucose transporting membrane protein Glut 1, mediated by the transcription factors hypoxia inducing factor-1α (HIF-1α) and HIF-2α.[92]

When glucose is taken up by a cell for the purpose of glycolysis it follows a specific pathway to ATP production. However, when [^{18}F]-FDG is taken up, it only follows the initial steps of the glycolytic pathway (*Figure 11*).

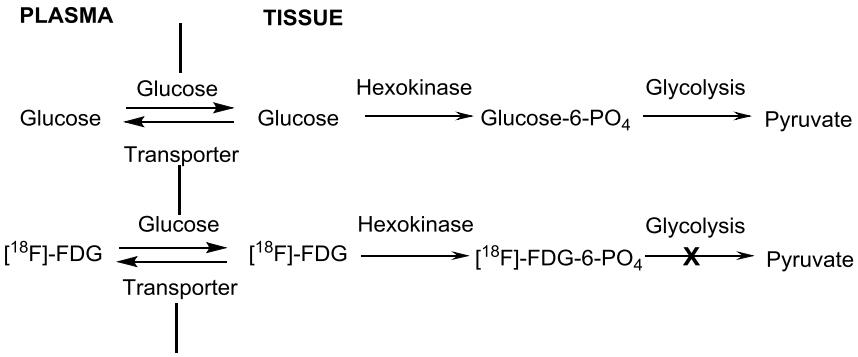

Figure 11- Uptake and usage of glucose and [^{18}F]-FDG in the glycolytic pathway.[36]

When [^{18}F]-FDG is transported into a tissue it is phosphorylated to 6-phospho-[^{18}F]-FDG under the control of hexokinase. Once in this state it cannot be further metabolised due to the presence of the C-2 fluorine, which is incompatible with phosphohexose isomerise and glycolysis cannot continue.[90] In addition, Glut transporters cannot deal with phosphorylated forms of glucose and remove 6-phospho-[^{18}F]-FDG from the cell.[21] [^{18}F]-FDG is therefore, trapped within the cancerous cell in its mono-phosphorylated state and will accumulate permitting imaging of a tumour. The amount of [^{18}F]-FDG retained in the lesion is proportional to the rate of glycolysis and so [^{18}F]-FDG is said to be a marker that images the rate of glycolysis.[51]

1.3.2 PET Probes for Imaging Proliferation: Nucleosides

Another class of compound commonly used for imaging tumours, and the primary focus of this thesis, are radiolabelled nucleosides. These probes differ from [^{18}F]-FDG in the physiological processes they image and their biodistribution patterns. Although these different classes have overlapping uses their different characteristics ensure they also have specific roles. For example, the natural biodistribution of [^{18}F]-FDG sees significant accumulation in the brain, heart, inflammatory tissues and bladder with lesser uptake in the liver and kidneys; whereas the nucleoside analogue [^{18}F]-FLT shows reduced accumulation in the brain and in inflamed tissues.[93]

1.3.2.1 3'-Deoxy-3'-[^{18}F]-fluorothymidine ([^{18}F]-FLT)

As was previously mentioned, cancerous cells show rapid proliferation and hence exhibit increased DNA synthesis in comparison to ordinary cells. It can be easily envisaged that

imaging proliferation would allow for the detection of cancers; 3'-deoxy-3'-[^{18}F]-fluorothymidine ([^{18}F]-FLT) **65** is a PET molecular probe highly suited to this purpose.[94] [^{18}F]-FLT is an analogue of the deoxyribonucleoside thymidine, **64** in which the hydroxyl group in the 3' position has been replaced by an [^{18}F] radionuclide (*Figure 12*).

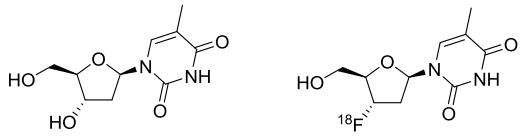

Figure 12- Deoxythymidine **64** and [^{18}F]-FLT **65**.

The synthesis of [^{18}F]-FLT proceeds *via* a simple nucleophilic substitution reaction on protected nucleoside precursor **66** using [^{18}F] KF.K_{222}, followed by hydrolysis to the product (*Scheme 21*).[95]

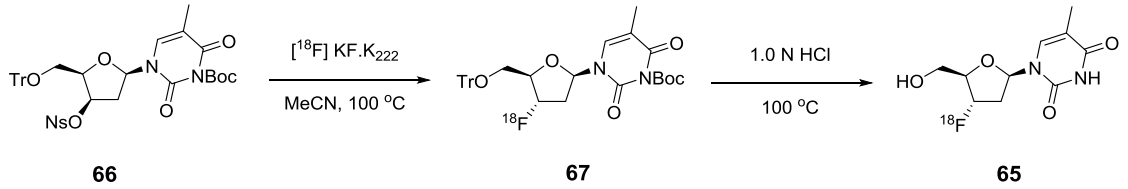

Scheme 21- Synthesis of [^{18}F]-FLT.[95]

There are two routes a cell can make use of to generate the nucleotides required for DNA synthesis, namely the DNA salvage and *de novo* pathways. In general, tissues utilise the *de novo* pathway. However, rapidly proliferating tissues show a strong reliance on the salvage pathway.[96]

The salvage pathway involves the synthesis of nucleotides using nucleosides and bases formed during DNA degradation. Thymidine and [^{18}F]-FLT are therefore actively transported into cells by carrier protein. Once in the cell they are phosphorylated by thymidine kinase 1 (TK1), an enzyme expressed during the DNA synthesis phase of the cell cycle (*Figure 13*).[96]

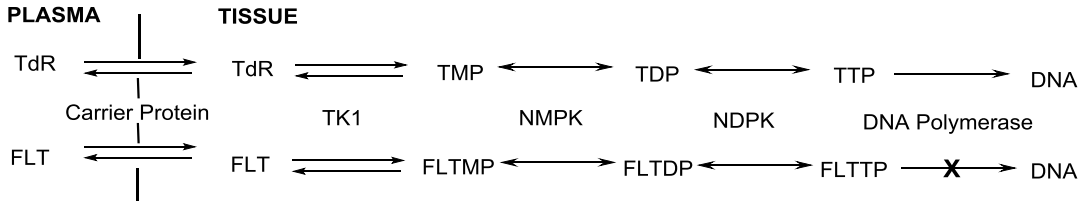

Figure 13- The DNA Salvage Pathway for Thymidine (TdR) and [^{18}F]-FLT.[96]

Thymidine is subsequently subjected to further phosphorylation by nucleoside monophosphate and nucleoside diphosphate kinases (NMPK and NDPK) before being incorporated into DNA by DNA polymerase[96]. [^{18}F]-FLT also undergoes further phosphorylation by NMPKs and NPDKs but cannot be incorporated into DNA due to the incompatibility of the 3' fluorine with DNA polymerase.[97] As such the detection of [^{18}F]-FLT accumulation within rapidly proliferating cells provides a measure of TK1 activity. Since TK1 activity has been shown to correlate with the extent of cellular replication, [^{18}F]-FLT serves to image proliferation. [^{18}F]-FLT has also been shown in various studies to be a sensitive probe for assessing tumour response to treatment.[98, 99]

However, there are also a number of issues with [^{18}F]-FLT. The main concern is that its uptake and retention by tumours is in general significantly lower than that of thymidine.[98] The likely cause of the problem of [^{18}F]-FLT uptake will be evaluated by comparison with carbon-11 radiolabelled thymidine.

1.3.2.2 [^{11}C]-Thymidine

The most widely studied molecular probes for cellular proliferation are [^{11}C] labelled thymidine compounds. [^{11}C]-thymidine nucleosides can be synthesised by labelling in two positions on the pyrimidine ring: either the 5-methyl position or the 2-carbonyl position. 5-[^{11}C]-methyl thymidine **70** is synthesised by the double deprotonation of bromide precursor **68**, followed by reaction of intermediate di-anion **69** with [^{11}C] CH_3I and then deprotection (*Scheme 22*).[100] Synthesis of 2-[^{11}C]-thymidine **74** is a slightly more involved. Firstly [^{11}C] phosgene is generated by reaction of [^{11}C] CH_4 with chlorine at high temperature to produce [^{11}C] CCl_4, which can then be oxidised over iron to form phosgene. This is further reacted with liquid ammonia to generate [^{11}C] urea **72**, which can be heated with diethyl β-methylmalate in the presence of sulfuric acid and sulfur trioxide to yield the radiolabeled thymine **73**. Finally the

base is enzymatically condensed with 2'-deoxyribose-1-phosphate using thymidine phosphorylase (*Scheme 22*).[101]

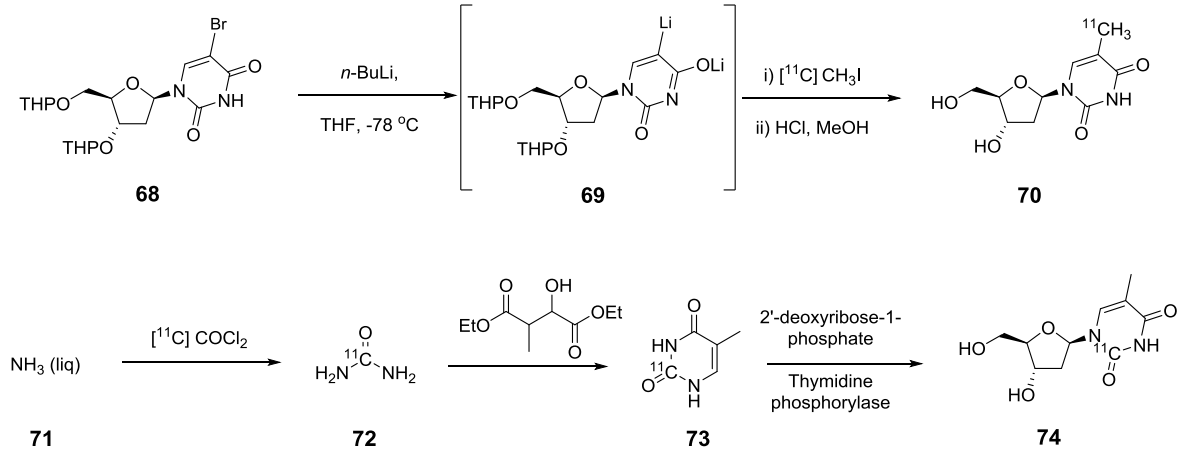

Scheme 22- Synthesis of 5-[methyl-^{11}C]-thymidine **70** and 2-[^{11}C]-thymidine **74**.[100, 101]

Unfortunately, these probes have several disadvantages which have led to [^{18}F]-FLT being considered a more suitable candidate for cancer imaging.[98] Principally is the fact that [^{11}C]-thymidine compounds are subject to rapid *in vivo* degradation by thymidine phosphorylase. This results in the production of numerous metabolites, creating images of a lower quality than [^{18}F]-FLT and making kinetic studies more complex.[98, 102]

Nevertheless, thymidine probes show a variety of properties that should be taken into account when considering the design of novel cancer imaging probes. For example, these compounds are better substrates for many nucleoside carrier proteins and for TK1, in comparison to [^{18}F]-FLT.[97] Additionally, and in contrast to [^{18}F]-FLT, [^{11}C]-thymidine compounds are suitable substrates for DNA polymerase. Upon entering the salvage pathway (*Figure 13*) they are completely phosphorylated and incorporated into DNA.[97] Studies in A549 tumour cells have shown that since [^{18}F]-FLT is not incorporated into DNA it is subject to a degree of dephosphorylation by a putative nucleotidase (dNT). As a result the phosphorylated [^{18}F]-FLT can be transported out of the cell following dephosphorylation by this nucleotidase, which could explain its poor uptake.[103] Since thymidine shows improved uptake and retention within proliferating cells when compared to [^{18}F]-FLT, it suggests that if one could design a [^{11}C]-thymidine molecule stable to thymidine phosphorylase, it could overcome the limitations of both FLT and thymidine compounds.[103] This would provide a metabolically robust compound that allows sensitive proliferation imaging.

Unfortunately, the stability of [^{18}F]-FLT to breakdown by thymidine phosphorylase has been attributed to the replacement of the 3' hydroxyl with [^{18}F].[102] As was previously mentioned, this [^{18}F] radiolabel contributes to the uptake issues of FLT making it a poorer substrate for TK1 and unreactive with DNA polymerase. It is clear that a different approach to enhancing the stability of nucleoside molecular probes is required.

1.3.3 Recent Developments in Imaging of Proliferation

1.3.3.1 Sulfur Based Pyrimidine Nucleosides

A recent study by Toyohara *et al*. reported the synthesis of a sulfur based thymidine nucleoside proliferation marker 5-[Methyl-^{11}C]thiothymidine using a Stille coupling with [^{11}C] CH_3I (*Scheme 23*).[104]

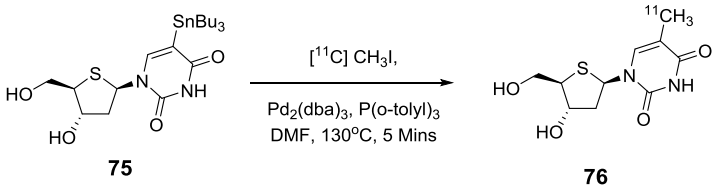

Scheme 23- Synthesis of 5-[Methyl-^{11}C]thiothymidine **76**.[104]

Although it should be noted that the results given are for *in vivo* studies in mice and not clinical data, this probe displays a number of exciting properties. For example, it exhibits relative metabolic stability in plasma, indicating that it will not suffer from the poor image quality seen in [^{11}C]-thymidine molecules. It is also efficiently incorporated into DNA *via* the salvage pathway due to the presence of the 3' hydroxyl group. As a result, 5-[methyl-^{11}C]-thiothymidine shows improved uptake in rapidly proliferating tissues in comparison to [methyl-^{3}H]-FLT; these results were mirrored in tumour models with **76** again showing higher accumulation.[104, 105]

Based on the initial data from *in vivo* mice studies for 5-[methyl-^{11}C]-thiothymidine, [^{11}C] thiothymidine nucleosides present an exciting prospect for the imaging of proliferation in cancers using PET. They appear to show superior properties to the current PET proliferation markers [^{18}F]-FLT and [^{11}C]-thymidine and hence warrant further investigation.

1.3.3.2 2'-Deoxy-2',2'-difluoro Nucleosides

Radu *et al* have reported the synthesis of a deoxycytidine based nucleoside analogue: 1-(2'-deoxy-2'-[^{18}F]-fluoroarabinofuranosyl) cytosine also known as [^{18}F]-FAC **78** (*Figure 14*).[106]

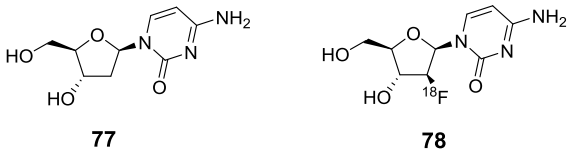

Figure 14- Deoxycytidine **77** and [^{18}F]-FAC **78**.[106]

Synthesis of [^{18}F]-FAC begins with introduction of the [^{18}F] fluoride radiolabel to furanose precursor **79**. This is subsequently transformed into bromide **81** using HBr in acetic acid, before being subjected to the Vorbrüggen glycosylation with *bis*-trimethylsilylated cytosine **82** and finally deprotected to the desired product **78** (*Scheme 24*).[107]

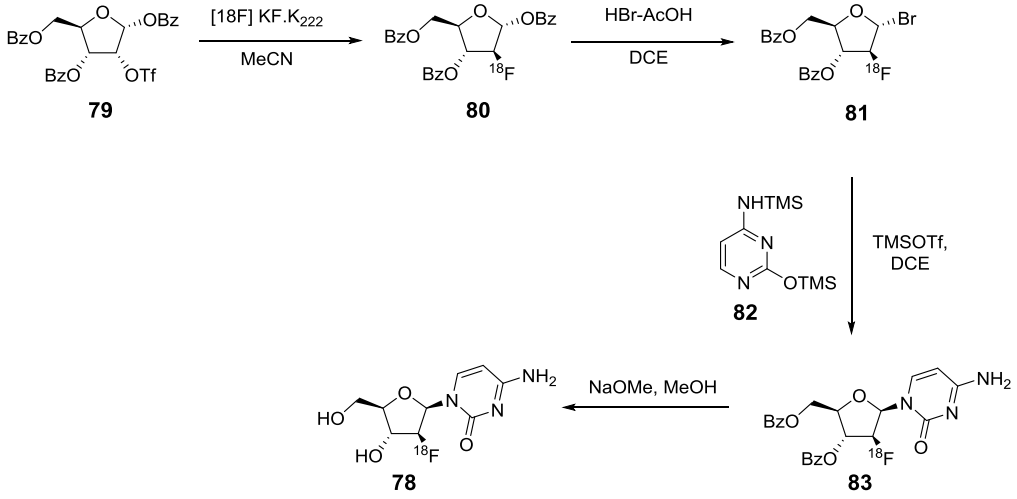

Scheme 24- Synthesis of [^{18}F]-FAC.[107]

In a similar fashion to deoxythymidine and [^{18}F]-FLT, [^{18}F]-FAC is taken up *via* a nucleoside salvage pathway in this case the deoxycytidine pathway. There are however, a number of differences in the pathways and the uptake of [^{18}F]-FAC itself. The initial phosphorylation for example, is performed by deoxycytidine Kinase (dCK) in place of TK1 (*Figure 15*). Another

key difference is evidence showing that [^{18}F]-FAC is a substrate for DNA polymerase and therefore is incorporated into DNA.[96, 106]

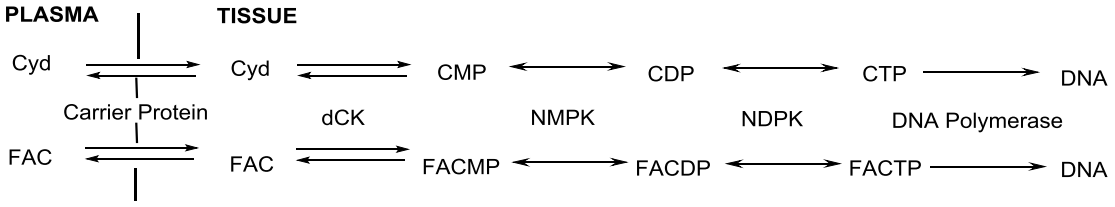

Figure 15- The DNA salvage pathway showing routes taken by deoxycytidine (Cyd) and [^{18}F]-FAC.[96]

Thus, [^{18}F]-FAC uptake occurs in cells showing increased expression of dCK including: myeloid and lymphatic cancers, a number of solid tumours, as well as lymphocytes and activated T-cells. [^{18}F]-FAC therefore serves to image dCK activity in these cells, allowing imaging of immune activation. Usefully [^{18}F]-FAC shows a different biodistribution pattern to [^{18}F]-FLT and [^{18}F]-FDG with significant quantities of the probe found in the thymus, spleen, intestines, bone marrow and liver.[106, 108] Another interesting potential use of [^{18}F]-FAC is in predicting the response to specific classes of nucleoside based chemotherapeutic agents. Cytarabine, fludarabine, gemcitabine and decitabine are all cytotoxic pro-drugs activated by dCK that suffer from poor response in tumour cells displaying reduced dCK activity.[109] Measuring [^{18}F]-FAC uptake would allow evaluation of the likelihood of a positive response to these drugs.[108]

Although [^{18}F]-FAC was the primary focus of Radu's report, mention was also made of another deoxycytidine nucleoside analogue, 2'-deoxy-2',2'-difluorocytidine (dFdc or gemcitabine) **84**, which showed superior selectivity and retention in proliferating T-cells in comparison to [^{18}F]-FAC. This could be attributed to the additional hydrogen bonding in the dCK active site between the *ribo*-fluorine and a tyrosine residue.[110] dFdc was not investigated for use as a PET imaging probe due to envisaged synthetic difficulties in generating a precursor to dFdc suitable for labelling with [^{18}F] fluoride (*Figure 16*).[106]

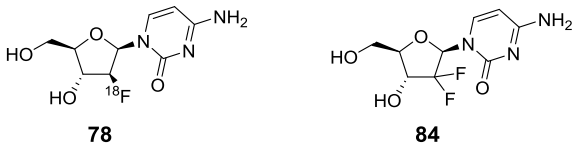

Figure 16- [^{18}F]-FAC **78** and dFdc **84**.[106]

While not strictly used for imaging proliferation, the useful properties exhibited by [^{18}F]-FAC and the improvements shown by dFdc warrant further investigation of this molecule through the use of different radiolabelling strategies.

Furthermore, the principle of replacing an *arabino*-fluorine with a germinal difluoro moiety could be applied to other nucleosides with the aim of altering their selectivity for thymidine kinase and deoxycytidine kinase enzymes (*Figure 17*).

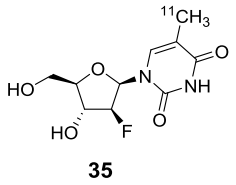

Figure 17- [^{11}C]-FMAU.[64]

For example, [^{11}C] and [^{18}F]-FMAU have both been shown to be stable *in vivo* and are incorporated into DNA giving them advantageous properties in comparison to [^{18}F]-FLT and [^{11}C]-Thymidine (*Figure 17*).[111, 112] Unfortunately, FMAU is known to be a better substrate for the cell cycle independent TK2 in comparison to TK1. This suggests that FMAU is perhaps not an ideal candidate for imaging the proliferation of tumours, as the uptake of TK2 selective nucleosides has been previously demonstrated not to correlate with the proliferation of tumours.[104] However, FMAU has also been shown to be a substrate for dCK.[106] Bearing in-mind the aforementioned favourable binding interactions for difluoro nucleoside analogues with dCK, it would be of interest to synthesise a di-fluoro analogue of this molecule and compare its selectivity for TK1, TK2 and dCK and utility as PET proliferation probe with that of [^{11}C]/[^{18}F]-FMAU.

1.4 Aims and Objectives

For the past ten years the Aboagye group has researched PET based imaging of proliferation in cancerous cells with a focus on [^{18}F]-FLT. As a result of the recent developments in sulfur based pyrimidine and 2'-deoxy-2',2'-difluoro nucleoside analogues, chemistry discovery efforts will now be focussed on the study of these molecules.

Sulfur Based Pyrimidine Nucleosides

The aim of this project was the development of novel methodology to facilitate synthesis of a number of [^{11}C] labelled thiothymidine nucleoside analogues. This was to be followed by an evaluation of their use as PET probes for imaging proliferation (*Figure 18*).

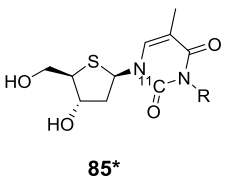

85*

Figure 18- 2-[^{11}C]-thiothymidine analogue with variable 'R' group.

The synthesis of these compounds was based on the generation of a novel precursor β-lactam nucleoside **86**. This would be heated to undergo an elimination reaction to yield an intermediate azetone **87**, which would then be reacted with a variety of [^{11}C]-isocyanates to allow the late stage introduction of the radiolabel (*Scheme 25*).

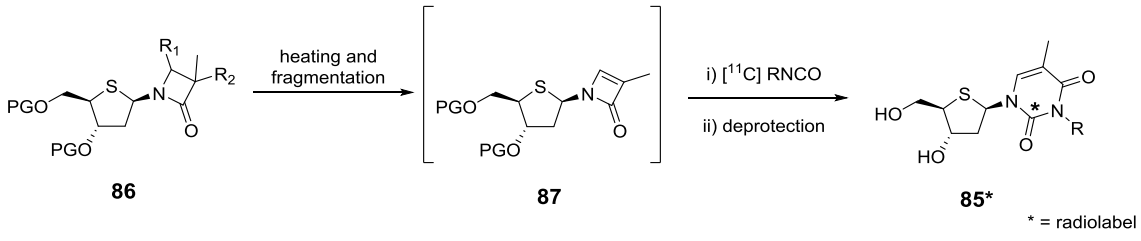

Scheme 25- A simplified illustration of the proposed synthesis of the 2-[^{11}C]-thiothymidine analogues.

The theoretical basis for azetones, their potential reactivity and the methods for producing [^{11}C]-isocyanates will be discussed in full in *Sections 2.0.1* and *2.0.2*.

2'-Deoxy-2',2'-difluoro Nucleosides

The aim of this project was to synthesise and radiolabel an analogue of dFdc with an [^{11}C] radiolabel in the 5-position of the cytosine ring **89*** using a Stille coupling strategy (*Scheme 26*).[64]

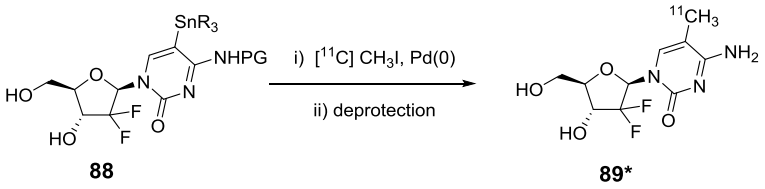

Scheme 26- Proposed synthesis of analogue **89***.

It was hoped that using stannane precursor **88** would permit easy access to **89***, circumventing the envisioned synthetic difficulties of producing an [^{18}F]-dFdc analogue while maintaining the desirable properties of selectivity and retention. Furthermore, a similar synthetic strategy could be applied to the synthesis of a 2',2'-difluoro analogue of [^{11}C]-FMAU **90*** (*Figure 19*).

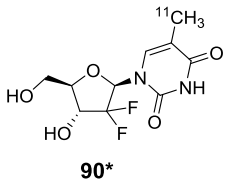

Figure 19- Di-fluoro [^{11}C]-FMAU analogue [^{11}C]-dFMAU **90***.

RESULTS AND DISCUSSION

2. Sulfur Based Pyrimidine Nucleosides

2.0 Overview

The aims of this project, as previously discussed (*Section 1.4*), were twofold: development of novel methodology to allow radiolabelling of precursor β-lactam nucleoside **86** and synthesis of precursor **86** itself (see *Section 2.2.1* for a proposed route).

2.0.1 Azetones

Outlined in *Scheme 27* the generation of an azetone intermediate and subsequent reaction with an [^{11}C] isocyanate would allow the late stage induction of a radiolabel as part of novel methodology for the synthesis of pyrimidine bases. Azetones, as a result of the anti-aromatic nature of their structure and its resonance forms (in violation of Hückel's $4n + 2$ rule), are highly reactive and unstable compounds (*Scheme 27)*.[113, 114]

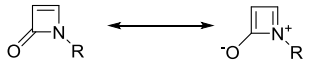

91 **92**

Scheme 27- Resonance forms of a generic unfunctionalised azetone.

During the late 1960s and early 1970s, Arbuzov and co-workers reported the synthesis of a number of stable azetones through the reaction of benzoyl isocyanates with a variety of alkynes (*Scheme 28*).[115, 116, 117] Unfortunately, these results could not be reproduced by other researchers.[118, 119] Pericás *et al.*, reported the synthesis of 2-phenyl-4,5-di-t-butoxy-l,3-oxazin-6-one **95** from similar starting materials to those used by Arbuzov and unambiguously assigned the structure using X-ray crystallography. They suggested that perhaps the products isolated by Arbuzov were not azetones but rather the corresponding 1,3-oxazin-6-ones derivatives (*Scheme 28*).[120]

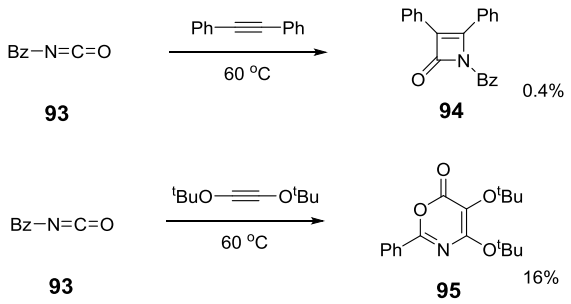

Scheme 28- Azetone synthesis reported by Arbuzov and 1,3-oxazin-6-one synthesis by Pericás.[117, 120]

In fact, the only other claim to isolation of an azetone was made by Wentrup *et al.* who reported the formation of an *N*-adamantylazetone **98** in equilibrium with its corresponding imidoylketene **97**. Using vacuum pyrolysis (FVP) of l-adamantyl-4-methyl-5-phenyl-2,3-dihydropyrrole-2,3-dione **96**, products were monitored by mass spectrometry and I.R. within an argon matrix at 18 °K (*Scheme 29*).[121]

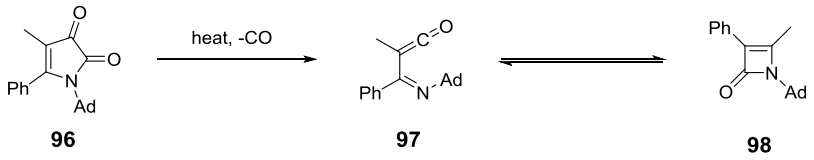

Scheme 29- Generation of an azetone by FVP.[121]

Benzo-fused forms of azetones (benzazetones) on the other hand, are known to be stable and have been synthesised and fully characterised.[114] Initially reported to be formed by the reaction of *N*-alkyl anthranil salts with triethylamine, benzazetones have been occasionally described in the literature including a more recent radiochemical synthesis by Långström *et al* (*Scheme 30*).[114, 122, 123]

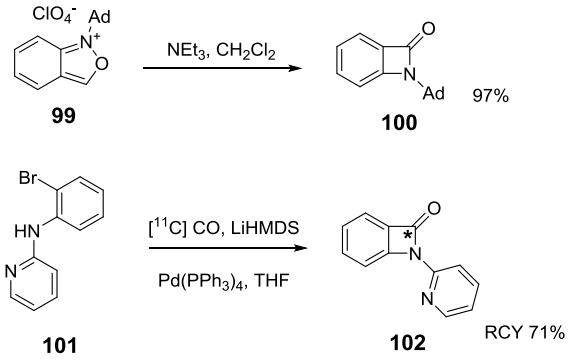

Scheme 30- Cold and radiochemical syntheses of benzazetones.[114, 123]

Unfortunately, these stable azetone derivatives are not suited for the desired methodology and the isolation of un-fused azetones in ambient conditions seems unlikely. However, despite discounting the possibility of forming stable azetones, Pericás *et al*. suggested the probability of an intermediate azetone **103** in their synthesis of **95**. These claims were substantiated through the use of computational methods (*Scheme 31*).[120]

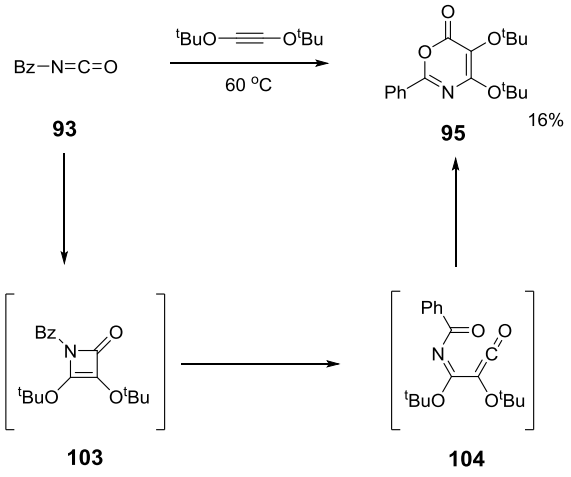

Scheme 31- Proposed mechanistic pathway to **95**, *via* an intermediate azetone **103** and imidoylketene **104**.[120]

Moreover, there here have been sporadic reports in the literature of reactions purporting to proceed *via* an intermediate azetone.[124, 125, 126] Of particular note are the examples of Alajarin *et al.* who described the synthesis of 1,3-oxazin-6-ones derivatives from *N*-Acyl-4-acyloxy-*β*-lactams, which followed on directly from the work of Pericás (*Scheme 32*).[127]

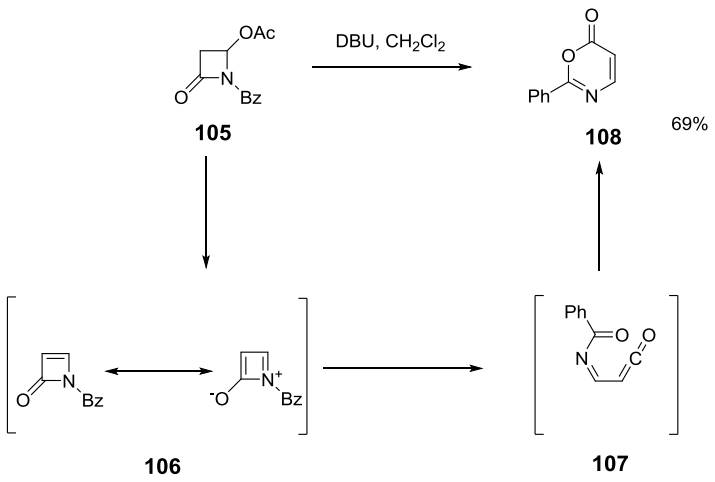

Scheme 32- Synthesis of 1,3-oxazin-6-one derivative **108**.

In this case, the proposed pathway involved an E1cB style β-elimination of acetate from **105** to generate the azetone **106**. This underwent a retro-[*4-exo-dig*] ring opening to generate the imidoylketene **107**, which reacted in a [*6-exo-dig*] ring closure to form **108**.[127] The authors subsequently published follow up computational studies on this process. Results complemented those of earlier work suggesting that proceeding *via* an azetone is the most energetically favourable pathway, despite being un-favoured by Baldwin's rules, to accessing the 1,3-oxazin-6-one analogues.[128]

From these observations one can conclude that there appears to be limited physical evidence for the existence of azetones such as **103** and **106**. However, indirect evidence from computational studies and from reactions purporting to proceed *via* these intermediates, suggests that developing methodology with the aim of utilising an azetone intermediate is an endeavour worthy of investigation.

In more detail, our proposed methodology involved the use of a β-lactam nucleoside precursor functionalised with a sulfoxide **109**, which could be heated to undergo *syn*-elimination forming the intermediate azetone **87** and benzene sulfenic acid (*Scheme 33*).[129]

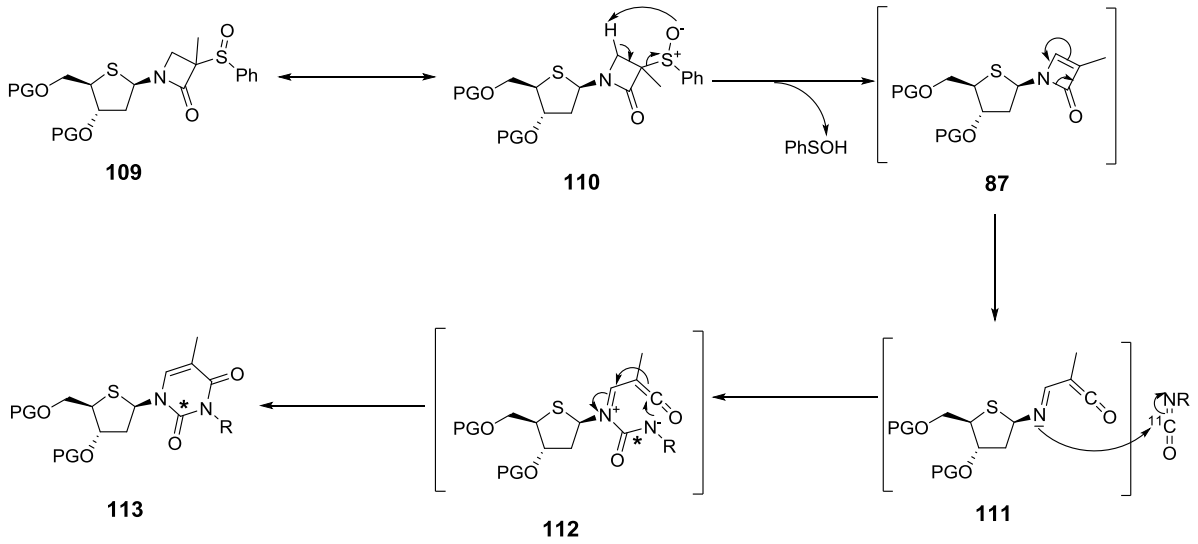

Scheme 33- Proposed mechanistic route to nucleosides **113**.

Electrocyclic ring opening of the unstable anti-aromatic lactam would result in the formation of intermediate imidoylketene **111**. This would subsequently undergo, by analogy with related transformations, stepwise addition with a variety of [^{11}C]-isocyanates leading to the isolation of nucleosides **113**.[130, 131]

2.0.2 Carbon-11 Labelled Isocyanates

Having outlined the proposed methodology for generating novel 2-[^{11}C]-thiothymidine nucleosides and discussed the theoretical basis behind this proposition, it would be prudent to briefly review the methods available for generating the required ^{11}C radiolabelled isocyanate precursors.

The most widely investigated method for generating [^{11}C]-isocyanates involve reactions with radiolabelled phosgene. As previously mentioned [^{11}C] phosgene is generated either by the reaction of [^{11}C] CH_4 with chlorine at elevated temperatures, followed by oxidation over iron granules in a stream of oxygen; or by reacting [^{11}C] CO with platinum tetrachloride.[73] Phosgene is then typically reacted directly with an amine, sometimes in the presence of base, to generate an isocyanate (*Scheme 34*).[132, 133]

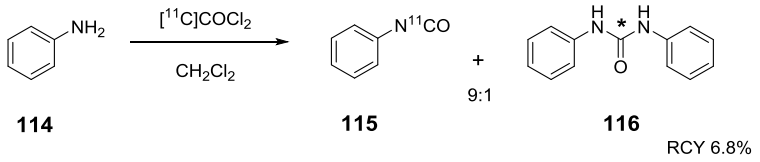

Scheme 34- Formation of phenyl-[^{11}C]-isocyanate **115** and urea by-product **116**.[132]

Note: RCY given for urea formed by administering excess aniline.

However, these methods tend to suffer from side reactions leading to the production of symmetrical [^{11}C]-ureas as a result of administration of excess amine. Particularly in the case of PET where microscale quantities are used and especially when using gaseous amines, this can prove to be problematic.[133]

Brown and co-workers have developed a number of methods for overcoming the problems associated with the formation of ureas as a side product. One such example involves the reaction of phosgene with sulfinylamines (*Scheme 35*).[134]

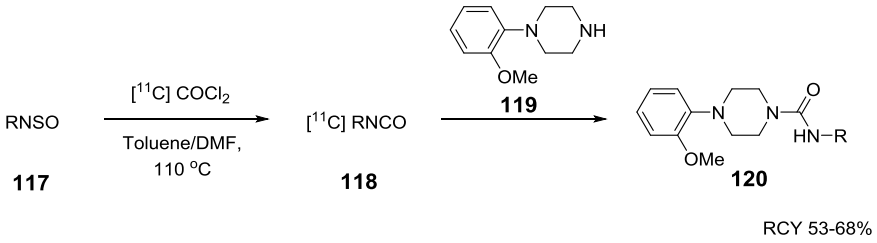

Scheme 35- Synthesis of [^{11}C]-isocyanates **118** using sulfinylamines.[134]

Sulfinylamines are well suited to this purpose being sufficiently reactive to form an isocyanate with phosgene but without sufficient nucleophilicity to further react with the isocyanate and form ureas. This permits further functionalization to unsymmetrical ureas as desired.[134] A further alternative developed by Brown *et al.* involves making use of the *N,N-bis*(trimethylsilyl)methylamine **121** (*Scheme 36*).[135]

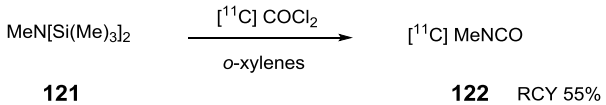

Scheme 36- Synthesis of methyl-[^{11}C]-isocyanate **122** using silyl-amines.[135]

Unfortunately, these methods generally suffer from low radiochemical yields and the production of phosgene itself is capricious.[73] More attractive methods make use of [^{11}C] CO or [^{11}C] CO_2 which are much more readily available.

An effective method for producing radiolabelled isocyanates and ureas without the use of [^{11}C] phosgene has been demonstrated by Långström *et al.* This method utilises the rhodium catalysed carbonylation of azides to form isocyanates (*Scheme 37*).[136]

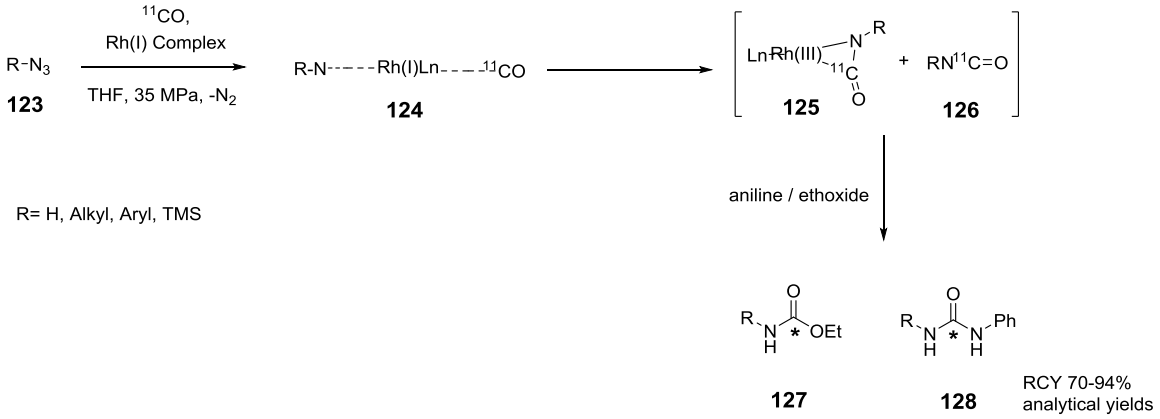

Scheme 37- Proposed pathway for [^{11}C]-isocyanate formation by carbonylation.[136, 137]

The initial decomposition of azide **123** results in the production of an intermediate nitrene, which undergoes reaction with [^{11}C] CO and the rhodium catalyst to yield a further intermediate in the form of isocyanate **126** or an isocyanate co-ordinated rhodium complex **125**. The isocyanates can then undergo undergo further conversion to ureas **128** and carbamates **127**.[136]

The ideal situation would involve the use of [^{11}C] CO_2 as it is available directly from the cyclotron without the need for any further manipulation. A promising example was reported by Van Tilburg *et al.* whereby phenyl-[^{11}C]-isocyanate was formed by the reaction of phenyl-triphenylphosphinimine with carbon dioxide (*Scheme 38*).[138]

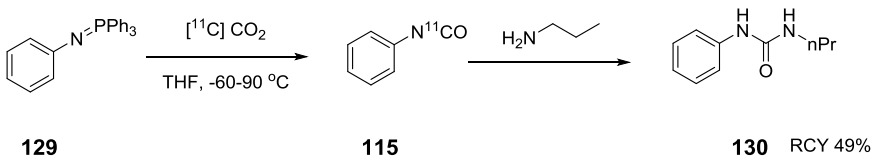

129 **115** **130** RCY 49%

Scheme 38- Reaction of [^{11}C] CO_2 with phenyl-triphenylphosphinimine to from isocyanate **115**.[138]

Trapping of [^{11}C] CO_2 in a solution of the triphenylphosphinimine **129** in THF with subsequent heating allowed the formation of the desired product **115**, which was then further reacted to form an unsymmetrical [^{11}C] labelled urea **130**. This was the only example used to illustrate the usefulness of this protocol. The potential for use of a variety of other phosphinimines was suggested, although the structural diversity of available phosphinimines may still prove be a limiting factor.[138]

Inspired by the work of Hooker *et al.* Wilson and co-workers have recently published a method for the synthesis of a wide variety [^{11}C]-isocyanates from [^{11}C] CO_2 (*Scheme 39*).[69, 139]

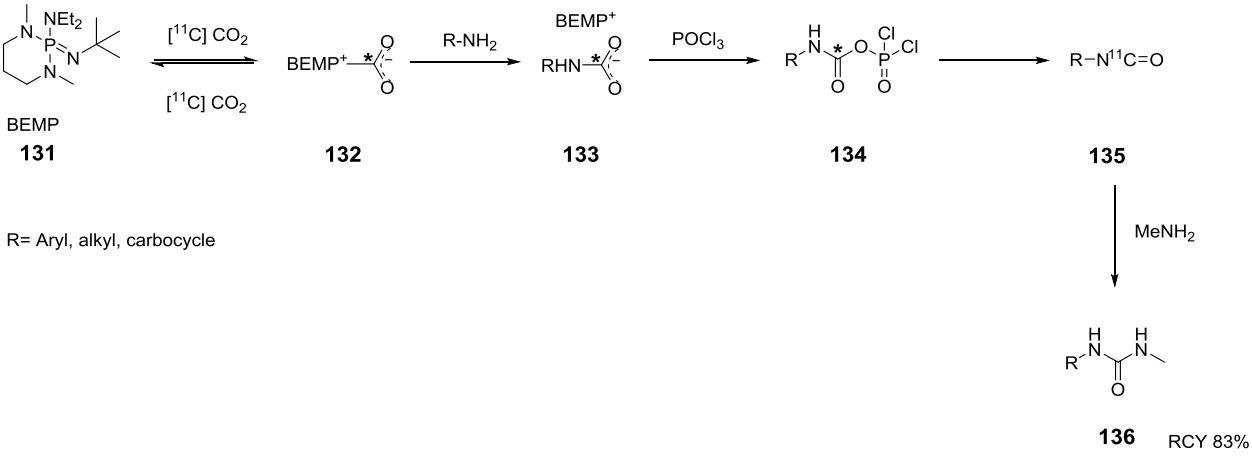

Scheme 39- Synthesis of [^{11}C]-isocyanates **135** by fixation of [^{11}C] CO_2.[139]

This protocol involves the fixation of [^{11}C] CO_2 using 2-*tert*-butylimino-2-diethylamino-1,3-dimethylperhydro-1,3,2-diazaphosphorine (BEMP) **131** in a solution of acetonitrile at ambient temperatures and pressures. Displacement of BEMP by an amine results in the formation of a carbamate salt **133**, which then upon addition of $POCl_3$ is dehydrated to form the isocyanate

135.[139] The authors demonstrated the scope of this reaction by successfully synthesising a variety of isocyanates and reacting these to form both [^{11}C] carbamates and ureas. As a result of the wide scope, mild conditions and the use of readily available [^{11}C] CO_2 this appears to be a most promising method. However, it should be noted this protocol does require careful stoichiometric control of reagent addition to avoiding the formation of symmetrical ureas, a problem inherent in many of these discussed methods.[139]

2.1 Methodology Studies

2.1.1 Synthesis of Sulfoxide Precursors

To assess the validity of the devised strategy for synthesising thymidine analogues from the corresponding β-lactam nucleosides and isocyanates, preliminary investigations were performed using more chemically simple systems. It was envisaged that a suitable sulfoxide precursor could be accessed by the thiation and oxidation of an unsubstituted nitrogen-protected β-lactam (*Scheme 40*).

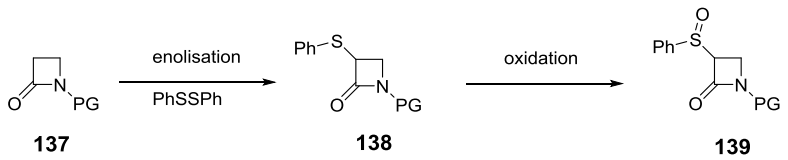

Scheme 40- Sulfoxide precursors for trial methodology studies.

Consultation of the literature prior to attempting this synthesis revealed conflicting views regarding the viability of enolates formed from unsubstituted β-lactams. Urbach and Kano, reported successful enolisation and reaction of *N*-silyl and *N-para*-methoxyphenyl (PMP) protected unsubstituted lactams.[140, 141] However, Wilson and Miller suggested that these systems were unsuitable for this purpose as a result of enolate instability, self-condensation and reaction *via* the alkoxide anion.[142, 143] To test these competing theories, synthesis and enolisation of both *N-tert*-butyldimethylsilyl (TBS) and *N*-PMP protected lactams **141** and **146** were performed (*Scheme 41*).

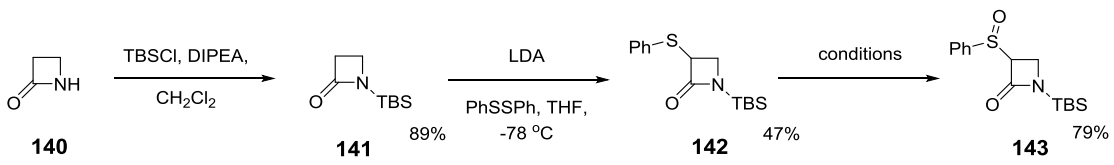

Scheme 41- Synthesis of *N*-silyl protected β-lactam **143**.

Protection of 2-azetidinone **140** with TBSCl proceeded smoothly giving **141** in good yields.[140] In corroboration with the report of Williams *et al.* initial attempts at thiation of **141** using standard

conditions (addition of the lactam to LDA, followed by stirring at −78 ^{o}C and then treatment with a solution of diphenyl disulfide) yielded only starting material. Fortunately, it was discovered that by modifying the addition of reactants so that both the lactam **141** and diphenyl disulfide were added simultaneously to a solution of LDA, sulfide **142** could be isolated in satisfying yields. Perhaps concurrent addition of the lactam and electrophile permitted immediate reaction of diphenyl disulfide with the enolate, which was highly unstable over more prolonged periods.

With multiple grams of sulfide **142** now in hand a variety of conditions were screened for oxidation to the sulfoxide (*Table 2*).

Entry	*Conditions*	*Time*	***Sulfoxide Yield (%)***	***Sulfone Yield (%)***	***Starting Material (%)***
1	NBS, Phosphate Buffer, H_2O_2, MeCN, 35^{o}C	48 h	0	0	20
2	$NaIO_4$: SiO_2 CH_2Cl_2, 140 ^{o}C Microwave	2.5 min	18	13	11
3	Ac_2O, H_2O_2, SiO_2, CH_2Cl_2,	36 h	79	0	0

Table 2- Conditions evaluated for oxidation of **142**.

Utilising hydrogen peroxide in acetonitrile with a phosphate buffer and catalytic *N*-bromosuccinimde resulted mainly in decomposition with some starting material recoverable (*Table 2,* entry 1).[144] Microwave mediated oxidation using sodium metaperiodate supported on silica gel was more successful (*Table 2,* entry 2).[145] However, full conversion was not observed, with over oxidation to the sulfone and decomposition also evident. Making use of milder conditions by reacting **142** with hydrogen peroxide and catalytic acetic anhydride at ambient temperature resulted in full conversion after 36 hours, with no over oxidation or decomposition observed (*Table 2,* entry 3).[146]

Having developed a suitable synthetic route for accessing diastereomeric sulfoxide precursors for the methodology studies, *N*-PMP protected lactam-sulfoxide **148** was also synthesised (*Scheme 42*).

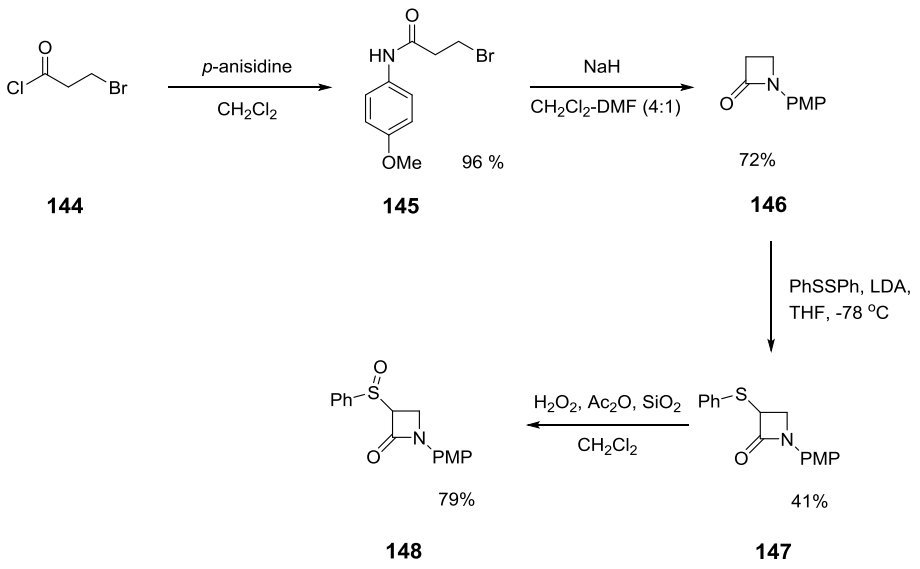

Scheme 42- Synthesis of *N*-paramethoxyphenyl protected β-lactam **148**.

Following the protocol of Easton *et al.*, reaction of 3-bromopropionyl chloride **144** with *para*-anisidine gave amide **145** in excellent yields. In an improvement over the literature procedure it was discovered that β-lactam **146** could be cyclised and isolated in a 72% yield by recrystallization from DMF, compared to 58% reported by flash silica column chromatography.[147] Problems were encountered during initial attempts at thiation of **146** due to insolubility of this lactam at −78 °C in THF. Thankfully, the enolate of **146** proved to be sufficiently soluble at low temperature. Therefore, by increasing the temperature of the lactam-diphenyl disulfide solution, followed by slow addition to a −78 °C solution of LDA in THF, solubility was maintained, allowing for successful reaction. Subsequent oxidation furnished exclusively sulfoxide **148**.[146]

Through completion of the synthesis of sulfoxides **143** and **148** it was demonstrated that enolisation and subsequent reaction of lactams **141** and **146** is possible given suitable modifications of addition methods. Moreover, attempts could now be made at *syn*-elimination of the sulfoxides and trapping of any resulting imidoylketenes.

2.1.2 Trial Reactions of Sulfoxide Precursors

For the purpose of these studies having two differently protected lactams was beneficial: the *N*-silyl protected lactam could be easily deprotected and subjected to further functionalization if the

methodology proved successful, whereas the *N*-PMP protected lactam would provide more robust protection should the TBS group prove labile to the heating needed for elimination of the sulfoxide to occur.[129, 148]

Sulfoxide **143** was subjected to various different conditions in an attempt to induce elimination of the sulfoxide (*Table 3*).

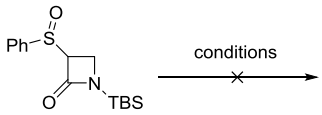

143

Table 3- Attempted elimination of sulfoxide **143**.

Entry	*Conditions**	***Yield (%)***
1	Toluene-d^8, 130 °C, 0.1 M, 4 h	0
2	5eq. Tosyl isocyanate, Toluene, 130 °C, 0.1 M, 4 h	0
3	5eq. Tosyl isocyanate, THF, 130 °C, 0.1 M, 24 h	0
4	5eq. Tosyl isocyanate, Furan, THF, 130 °C, 0.1 M, 24 h	0

*All reactions performed in a sealed tube.

Initial attempts were promising: a test reaction performed in deuterated toluene showed consumption of starting material leading to decomposition (*Table 3*, entry 1). It was hoped that this decomposition was proceeding *via* the azetone and therefore the imidoylketene, thus a number of attempts were made at trapping this intermediate. Trapping reactions carried out using tosyl isocyanate in either toluene or THF were unsuccessful leading only to decomposition (*Table 3*, entries 2 and 3). It was thought that benzenesulfenic acid produced as a by-product of the *syn*-elimination could be causing the observed decomposition. A further attempt was

therefore made using furan as a trap for the acid (*Table* 3, entry 4); however this again was unsuccessful. Another possible reason behind these observations could be the poor thermal stability of the sulfoxide itself, particularly due to the potential lability of the TBS group.

Indeed, these concerns proved to be justified as demonstrated in the attempted elimination of sulfoxide **148** (*Table 4*).

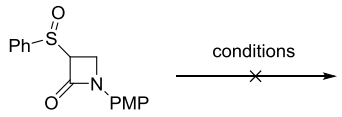

148

Table 4- Attempted elimination of sulfoxide **148**.

Entry	*Conditions*	***Result***
1	Toluene-d^8, 130 °C, 0.1 M, sealed tube, 24 h	Starting material
2	Toluene-d^8, 130 °C, 0.1 M, microwave, 24 h	Starting material
3	Toluene-d^8, 160 °C, 0.1 M, sealed tube, 24 h	Starting material
4	Toluene-d^8, 160 °C, 0.1 M, microwave, 24 h	Starting material

As in the case for sulfoxide **143** a test reaction was firstly carried out to observe consumption of **148**. Despite prolonged heating at high temperatures only starting material was recovered (*Table 4*, entry 1). Using microwave radiation and increasing the reaction temperature again gave no conversion (*Table 4*, entries 2, 3 and 4). Clearly *syn*-elimination of the sulfoxide was not occurring in these systems. Consequently, this also suggested that the observed decomposition of lactam **143** was due to instability of the TBS group to high temperatures rather than elimination and formation of the azetone.

2.1.3 Synthesis and Trial Reactions of Selenoxide Precursors

As a result of the unsuccessful sulfoxide fragmentations a more reactive system was proposed: the *syn*-elimination of selenoxides to their corresponding alkenes is known to occur spontaneously at room temperature.[149] It was therefore hoped that the increased reactivity of the selenoxides would allow the desired elimination reactions to occur where they had been unsuccessful in the more stable sulfoxide systems (*Scheme 43*).

Scheme 43- Proposed synthesis and elimination of *N*-PMP protected selenoxide.

It was envisaged that selenylation of **146** could be carried out using a procedure similar to that described for thiation of **146**. Oxidation of selenide **149** would be performed with DMDO at low temperatures to reduce the number of by-products in the mixture before warming the selenoxide **150** to room temperature to undergo elimination.

Problems were encountered when attempting selenylation of **146**: using a slight excess of LDA and phenylselenyl bromide resulted in the recovery of a large portion of starting material (60%), as well as a mixture of the desired *mono*-selenide **149** and the *bis*-selenide **151**. Presumably the pK_a of alpha carbonyl proton in **149** was lower than those in **146** resulting in a second deprotonation and reaction with another equivalent of the selenyl bromide to form **151**. It was therefore decided to attempt full conversion to **151** by using additional equivalents of phenylselenyl bromide and LDA. This resulted in starting material consumption and the formation of a mixture of the *mono* and *bis*-selenylated products in more acceptable yields (*Scheme 44*).

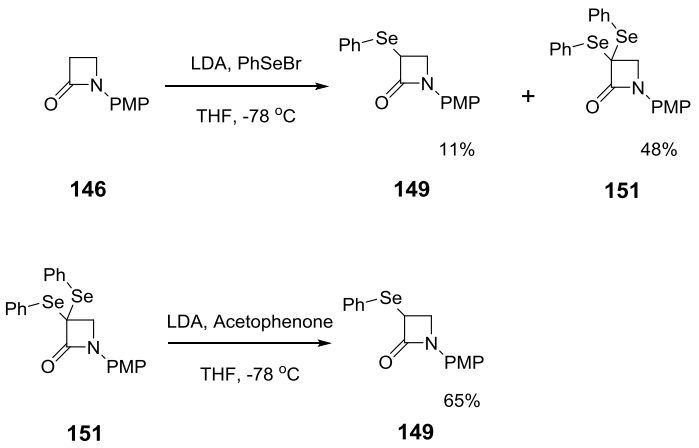

Scheme 44- Synthesis of selenide **149**.

The *bis*-selenide was then successfully *mono*-de-phenylselenylated using the enolate of acetophenone resulting in exclusive generation of **149** (*Scheme 44*).

With the desired selenide now available, oxidation to the selenoxide was performed using DMDO. As previously mentioned, DMDO was seen as an ideal reagent for this step due to the production of relatively unreactive acetone as a by-product which would make attempted reaction with the isocyanate more likely (*Scheme 45*).[150]

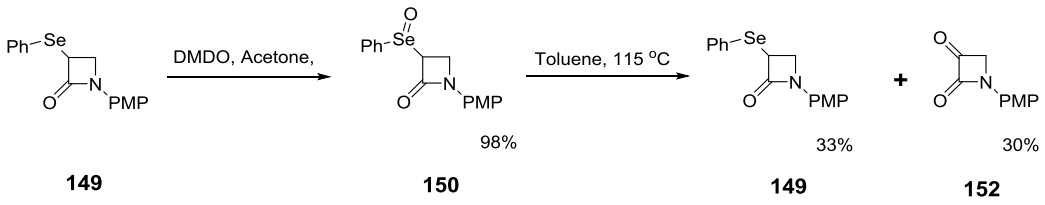

Scheme 45- Oxidation to and attempted elimination of selenoxide **150**.

As in previous examples, attempted eliminations were first carried out in the absence of an isocyanate to ascertain starting material consumption. Unexpectedly oxidation of **149** resulted in almost quantitative formation of the stable selenoxide **150**. This was considered somewhat peculiar as stable selenoxides are generally only isolatable in systems lacking β-protons.[151, 152] Nevertheless, isolation of **150** was deemed advantageous as the elimination reaction could be carried out as a separate step using solvents entirely unreactive to the intermediate ketene. When refluxed in toluene the selenoxide was fully converted, undergoing disproportionation to furnish

both keto β-lactam **152** and selenide **149** as products. This disproportionation implied that the reaction was occurring *via* a bimolecular process. In order to avoid this and favour elimination, the experiment was repeated at a low concentration (0.005 M) and at higher temperature by slow addition (10 hours) of **150** to refluxing xylenes. Unfortunately the same result was obtained.

By nature β-lactams are strained systems.[153] It is therefore possible that elimination was not observed as a result of this strained nature preventing the selenoxide from effecting deprotonation in the β-position (*Scheme 46*).

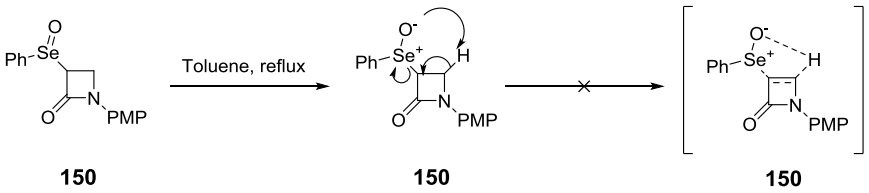

150 **150** **150**

Scheme 46- Transition state required for elimination.

2.1.4 Synthesis of Alternative Azetone Precursors

With both the sulfoxide and selenoxide systems failing to react *via* the anticipated pathways it was clear that an alternative approach to generating the azetone was needed. Pyrolysis of carboxylate salts is a common method for inducing decarboxylation. It was therefore proposed that heating potassium salt **153** in the presence of 18-crown-6 would result in decarboxylation, followed by elimination, giving rise to the desired azetone intermediate (*Scheme 47*).

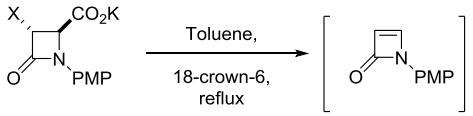

153 **154**

X = suitable leaving group

Scheme 47- Formation of the azetone **154** by decarboxylative elimination from **153**.

β-lactam **155** has been reported in the literature and was suggested as suitable starting point for the synthesis of a carboxylate salt analogous to **153** (*Scheme 48*).[154]

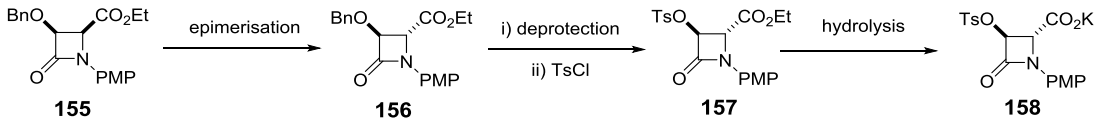

Scheme 48- Proposed synthesis of **158**.

Starting from **155**, base mediated epimerisation leading to the thermodynamically favoured trans-diastereomer could be followed by cleavage of the benzyl group of **156** to give the corresponding alcohol. Consequently, functionalization as a tosylate **157** and hydrolysis of the ester would furnish potassium salt **158**.

The synthesis began with the Staudinger cycloaddition of imine **160 (**formed by condensation of ethyl glyoxylate **159** with *para*-anisidine) with benzyloxyacetyl chloride to give the cis-β-lactam **155** (*Scheme 49*).[154, 155]

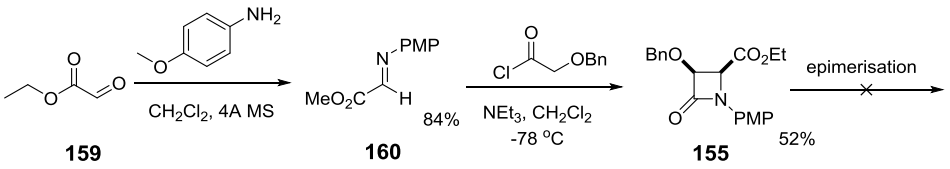

Scheme 49- Synthesis and attempted epimerisation of **155**.[154]

Epimerisation alpha to the ethyl ester proved to be difficult and a variety of conditions were evaluated (*Table 5*).

Entry	*Conditions*	*Result*
1	Na_2CO_3, MeCN:H_2O, 0.03 M	Starting material
2	$NHMe_2$, benzene, 0.1 M	Starting material
3	DBU, CH_2Cl_2, 0.1 M	Starting material

Table 5- Attempted epimerisation of lactam **155**.

The initially used conditions were based on the work of Alcaide *et al.* who reported the instability of similarly functionalised β-lactams to harsher conditions.[156] Unfortunately in these cases only starting material was recovered (*Table 5*, entries 1 and 2). Using a stronger base also resulted in no observable conversion (*Table 5*, entry 3).[157] It was thought that by synthesising the corresponding aldehyde of **155** the system could be made more susceptible to the epimerisation conditions by decreasing the pK_a of the proton alpha to the carbonyl functionality.

Aldehyde **164** was easily accessed in three steps using the procedure of Alcaide *et al.* (*Scheme 50*).[158]

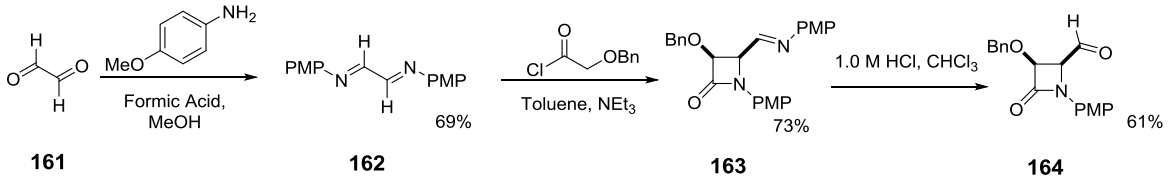

Scheme 50- Synthesis of aldehyde **164**.[158]

Condensation of *para*-anisidine with glyoxal **161** gave di-imine **162** in good yields.[159] Staudinger cycloaddition of **162** with benzyloxyacetyl chloride furnished β-lactam **163**, which could then be hydrolysed directly to the desired aldehyde. With aldehyde **164** in hand further attempts at epimerisation could be made. Unfortunately these efforts also resulted in the recovery of starting material (*Table 6*).[156]

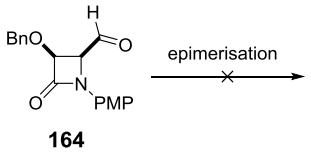

Table 6- Attempted epimerisation of aldehyde **164**.

Entry	*Conditions*	***Result***
1	Na_2CO_3, MeCN:H_2O, RT, 0.03 M	starting material
2	$NHMe_2$, benzene, RT, 0.10 M	starting material

With attempted epimerisation of the β-lactams **155** and **164** proving to be unsuccessful a new strategy was envisaged whereby the desired trans-geometry could be accessed by simple S_N2 reaction (*Scheme 51*).

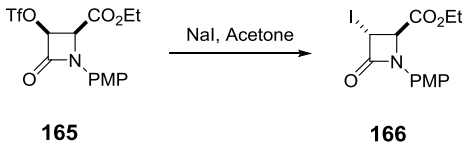

165 **166**

Scheme 51- Suggested synthesis of trans-β-lactam **166**.

Based on similar literature examples it was thought that displacing the triflate in **165** with sodium iodide would give exclusively the trans-lactam **166**.[160] Synthesis of **165** was relatively simple using lactam **155** as a starting point (*Scheme 52*).

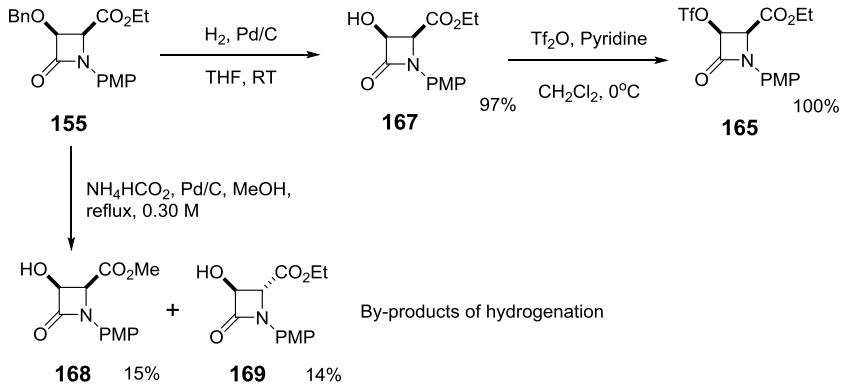

155 **167** **165**

168 15% **169** 14%

Scheme 52- Synthesis of triflate **165**.

A number of conditions were screened in order to find a suitable procedure for deprotection of benzyl ether **155** (*Table 7*).

Entry	*Conditions*	***Result***
1	H_2, $Pd(OH)_2/C$, MeOH, 0.12 M	Starting material
2	NH_4HCO_2, Pd/C, MeOH, reflux, 0.30 M	**167** 36%, **168** 15% **169** 14%
3	H_2, Pd/C, THF, 0.03 M	**167** 97%

Table 7- Deprotection of benzyl ether **155**.

Initial attempts at hydrogenation using Pearlman's Catalyst proved to be unsuccessful due to solubility issues of **155** in methanol (*Table 7*, entry 1).[154] Increasing the temperature to reflux and using ammonium formate overcame the solubility problems but also lead to the formation of two side products (*Table* 7, entry 2).[161] The presence of these could be attributed to heating of the mixture coupled with the action of ammonia released during the reaction: **168** is a product of trans-esterification with methanol and **169** is the epimerised form of the desired product. In order to prevent the formation of by-products, milder reaction conditions and a different solvent were used. Carrying out the hydrogenation in THF with palladium on carbon permitted deprotection at room temperature and resulted in excellent yields of **167** (*Table 7*, entry 3).[162]

Functionalization of **167** as its triflate ester occurred quantitatively and was followed by displacement of the triflate using sodium iodide.[160] Interestingly a 1:1 mixture of diastereomers **166** and **170** was recovered after reaction. Since a large excess of sodium iodide was used this outcome can be rationalised by the displacement of one iodide by another until an equilibrium mixture is reached (*Scheme 53*).

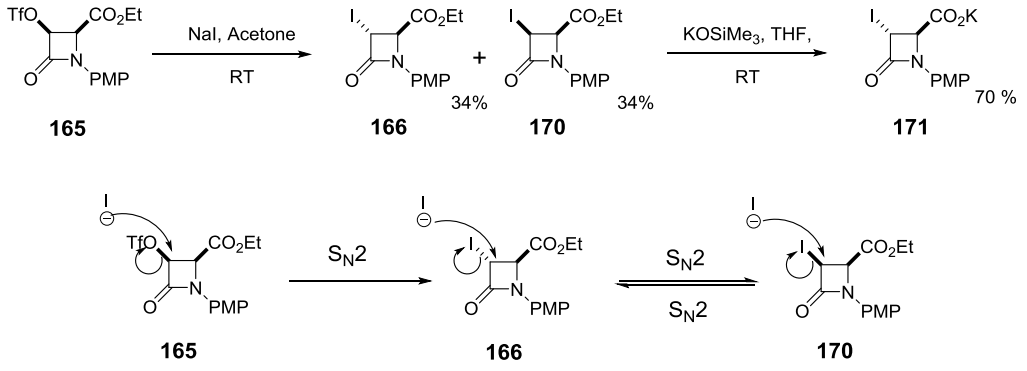

Scheme 53- Synthesis of potassium salt **171**.

Fortunately, these diastereomers could be easily separated. The final step in this synthesis was the hydrolysis of ethyl ester **166** to the corresponding potassium salt, which was accomplished in fair yields using potassium trimethylsilanolate (*Scheme 53*).[163]

With desired salt in hand the fragmentation reactions could now be attempted (*Table 8*).

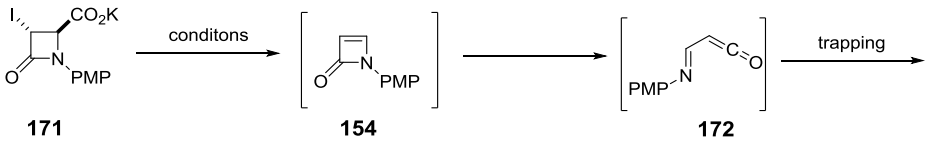

171 **154** **172**

Table 8- Attempted fragmentation of **171** and trapping of intermediate **172**.

Entry	*Conditions*	*Reaction Time*	***Result***
1	MeOH, 60-160 °C, 300 W, 0.1 M	30 min at each temperature	Decomposition
2	Antracene 5eq., 18-crown-6, *o*-xylenes, 125 °C, 0.5 M	16 h	Decomposition
3	**175** 10 eq., 125 °C	16 h	**176** and **177**, 55%
4	Adamantyl isocyanate 5eq., 18-crown-6, *o*-xylenes, 125 °C, 0.5 M	2 h	**180** 6%

As was the case with the sulfoxide and the selenoxide preliminary investigations were performed in the absence of other reactants in order to assess starting material consumption. Heating **171** in methanol using microwave irradiation at a variety of temperatures showed that temperatures in excess of 120 °C were required for starting material consumption (*Table 8*, entry 1). It was hoped that using methanol would result in trapping of the resultant intermediate ketene providing evidence of the azetone, however this proved not to be the case and decomposition was instead observed.

It was therefore decided to attempt trapping with a variety of different reagents. Efforts to capture the proposed imidoylketene intermediate in a Diels-Alder process with anthracene resulted only in decomposition of the starting material (*Table 8*, entry 2). A similar attempt

using diene **175** again resulted in decomposition of **171** with the isolation of the Diels-Alder product between two molecules of **175** (*Scheme 54*).

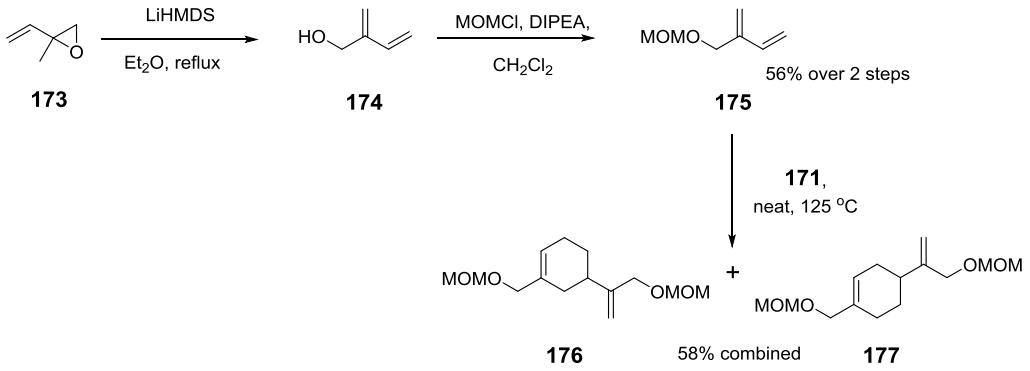

Scheme 54- Synthesis of diene **175** and reaction to form regioisomers **176** and **177**.

Diene **175** was synthesised in two steps by the opening and isomerisation of commercially available 2-methyl-2-vinyloxirane **173**, followed by protection of the resultant alcohol with chloromethyl methyl ether (MOMCl).[164] As a consequence of the highly volatile nature of both **174** and **175** yields for this synthesis were lower than may be expected, however sufficient material was synthesised in order to attempt the trapping reactions.

A final attempt at trapping was made using adamantyl isocyanate, which was chosen as the distinctive ^{1}H-NMR adamantyl peaks would allow easy identification of incorporation into products (*Table 8*, entry 4 and *Scheme 55*).

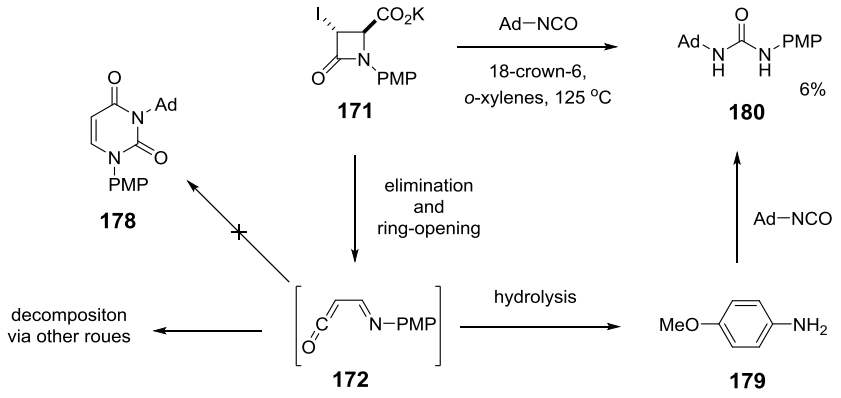

Scheme 55- Synthesis of urea **180** and proposed mechanistic route.

In this case, alongside unidentifiable decomposition, small quantities of urea **180** were isolated contaminated with another by-product. While by no means providing clear proof that this is the case, one possible explanation for the isolation of **180** is *via* an intermediate azetone (*Scheme 55*). Decarboxylation and elimination of **171** followed by ring opening of the azetone to form imidoylketene **172**, could be followed by hydrolysis to *para*-anisidine, which could then react with adamantly isocyanate to furnish urea **180**. While every effort was made to ensure the reaction was performed under anhydrous conditions it is possible that some moisture may have been retained by the hydroscopic salt allowing for hydrolysis of the imine. It can therefore be suggested that if the reaction is proceeding *via* an azetone intermediate the majority of the imidoylketene is decomposing *via* other pathways with small amounts being hydrolysed explaining the observations.

However, in the reports of Pericás and Alajarin, reactions of imidoylketenes formed from azetones were hypothesised to proceed *via* an intramolecular process (see *Section 2.0.*1 *Schemes 31* and *32)*.[120, 127] It has also been demonstrated that imidoylketenes generated from more stable sources are liable to undergo dimerisations (*Scheme 56*).[165]

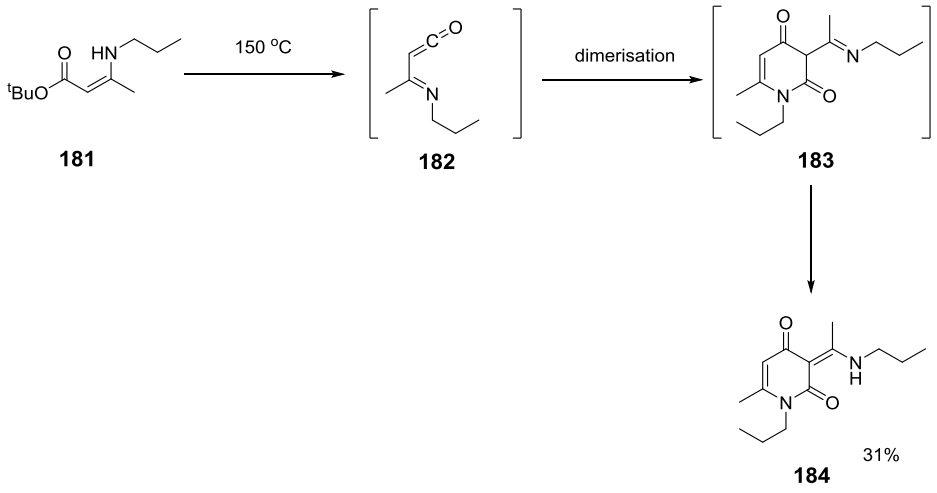

Scheme 56- Dimerisation of imidoylketene **182** reported by Zhou *et al.*[165]

This suggests that if the reaction was proceeding through an azetone, one could expect to see some additional evidence of intramolecular reaction or dimerisation. It is therefore also conceivable that decomposition to *para*-anisidine may be occurring by another unknown pathway.

2.2 Towards the Synthesis of Thiothymidine Nucleoside 85

2.2.1 Overview and Proposed Synthesis

In parallel to the methodology studies, efforts were also focussed on the development of a synthetic route for accessing the aforementioned novel β-lactam nucleoside precursor **193** and hence the thio-thymidine analogues themselves. A route was proposed which would complement and make use of the methodology studies (*Scheme 57*).

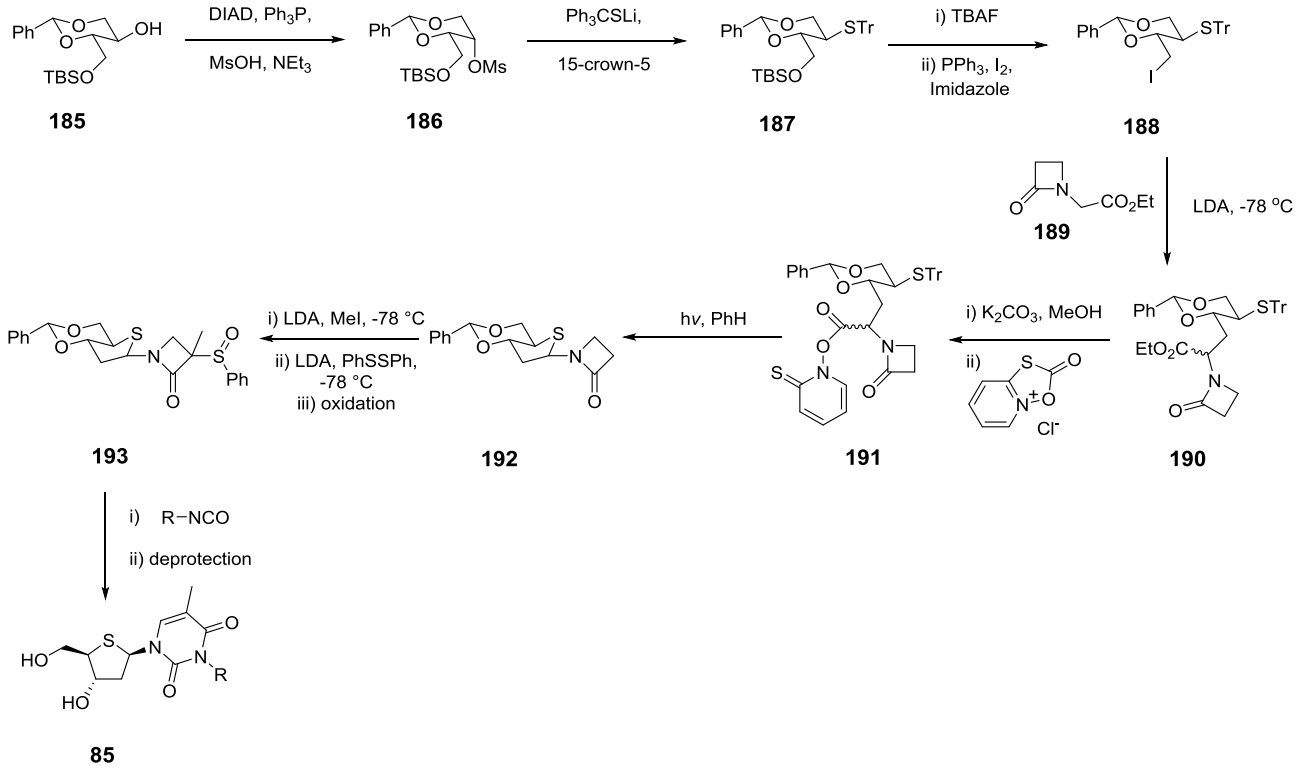

Scheme 57- Proposed synthesis of thiothymidine analogues **85**.

The synthesis would begin with Mitsunobu reaction of literature known alcohol **185** with methanesulfonic acid simultaneously introducing a leaving group and the desired stereochemistry. This would be followed by displacement of the mesylate in **186** with triphenylmethyl mercaptan, removal of the silyl protecting group and Appel reaction to furnish iodide **188**. Coupling of **188** and **189** and subsequent trans-esterification would yield Barton ester **191**. This could then be subjected to a radical decarboxylation, generating **192** which is in a suitable from to be subjected to the methodology that would be developed concurrently.

2.2.2 Synthesis of β-Lactam Coupling Partner **189**

β-lactam **189** was obtained using a two-step procedure described by Baggaley *et al* (*Scheme 58*).[166]

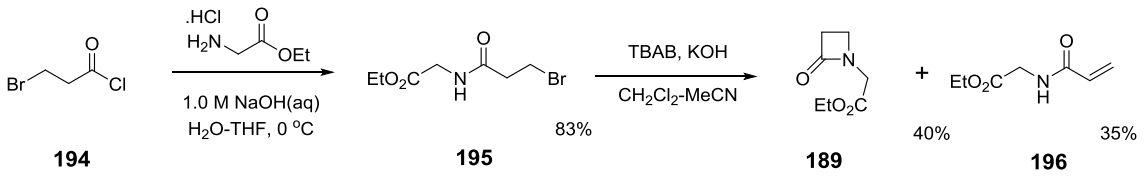

Scheme 58- Synthesis of lactam **189**.[166]

The acetylation of glycine ethyl ester hydrochloride with 3-bromopropionyl chloride gave amide **195** in high yields. Cyclisation to lactam **189** was carried out in the presence of potassium hydroxide. Yields, while being a good match for the literature, were relatively low as the result of the competing elimination process producing **196**.[166]

2.2.3 Synthesis and Inversion of Alcohol **185**

Alcohol **185** was easily accessible in four steps starting from D-glucose (*Scheme 59*).

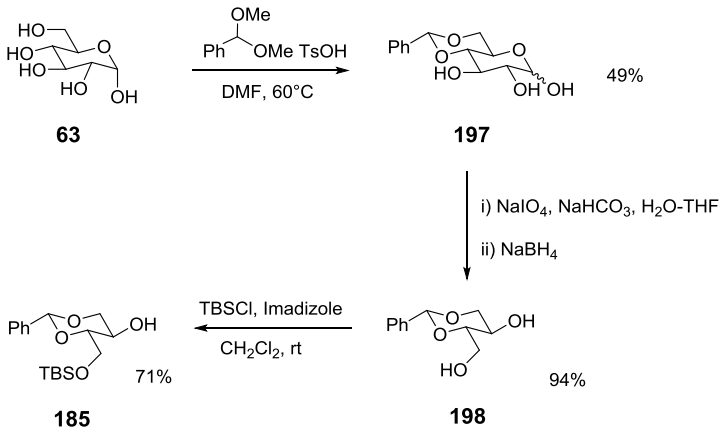

Scheme 59- Synthesis alcohol **185**.

The synthesis began with the protection of glucose **63** as its benzylidene acetal **197** using benzaldehyde dimethyl acetal.[167] Oxidative cleavage of **197** using sodium metaperiodate and an

excess of sodium bicarbonate was directly followed by reduction of the intermediate with sodium borohydride to give benzylidene-erythritol **198** in excellent yields.[168] Finally the primary alcohol of **198** was protected as its silyl ether using TBSCl and standard conditions to furnish **185**.[169]

It was originally envisaged that alcohol **185** could be displaced using methane sulfonic acid under Mitsonobu conditions to yield the inverted mesylate **186** as described by Anderson *et al* (*Scheme 57*).[170] Unfortunately these conditions were sufficiently acidic to result in silyl-deprotection of **185**. Milder conditions using benzoic acid, followed by hydrolysis and functionalization of the resultant alcohol to from **186** were therefore proposed (*Scheme 60*). [171]

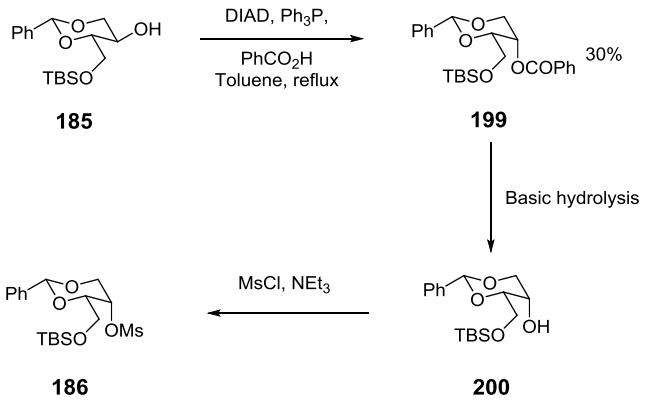

Scheme 60- Proposed route to mesylate **186**.

Despite prolonged heating at reflux, the Mitsonobu reaction would not proceed to completion giving poor yields of benzoate ester **199**. Possible reasons for the lack of full conversion can be attributed to hindrance associated with the cyclic system and the bulk of the silyl protecting group which could also hinder reaction at the alcohol.[172]

These results were unsatisfactory and it was clear a different approach was required for accessing the inverted alcohol **200**. A two-step oxidation and selective reduction protocol proved to be more successful (*Scheme 61*).

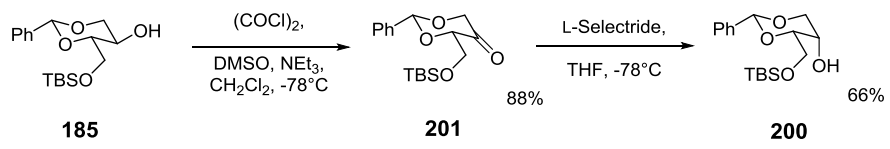

Scheme 61- Oxidation-reduction protocol for synthesis of **200**.

Swern oxidation of alcohol **185** to ketone **201** was followed by reduction using L-selectride. This process was high yielding and the reduction was highly diastereoselective furnishing almost exclusively axial alcohol **200**.[173, 174] The conformation was unambiguously assigned based on ^{1}H-NMR coupling constants.

2.2.4 Introducing the Sulfide Functionality: Synthesis of Thioether **203**

With the inverted alcohol now accessible, the next step was to introduce the sulfur moiety to form thioether **187**. As was previously outlined (*Scheme 57 Section 2.2.1*) the lithium salt of triphenylmethyl mercaptan was to be used to form **187**. However, due to the difficulty in handling this thiolate, the substitution reactions were first of all trialled using a simpler system with thiophenol as the nucleophile (*Table 9*)

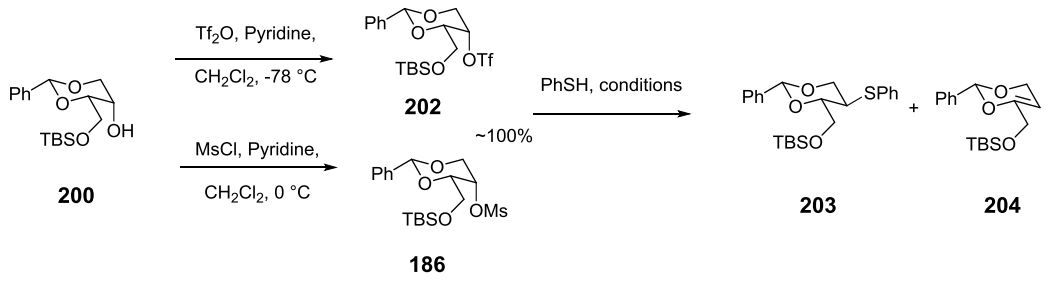

Table 9- Introducing the sulfide functionality to form **203**.

Entry	*Starting Material*	*Reaction Conditions*	*Temperature*	**203:204** *Ratio*	**Yield of 203 (%)**
1	Mesylate	Thiophenol, NaOH, DMF, Toluene (0.06 M)	Room temp	0 : 0	0
2	Triflate	Thiophenol, NEt_3, DMSO (0.15 M)	Room temp	50:50	20
3	Triflate	Thiophenol, NaH, DMSO-THF	Room temp	14:86	5
4	Triflate	Thiophenol, NEt_3, CH_2Cl_2 (0.10 M)	0 °C	64:36	28
5	Triflate	Thiophenol, NEt_3, CH_2Cl_2 (0.50 M)	−10 °C	70:30	32
6	Triflate	Thiophenol, NEt_3, CH_2Cl_2 (0.50 M)	−30 °C	80:20	40
7	Triflate	Thiophenol, NEt_3, CH_2Cl_2 (0.50 M)	−55 °C	80:20	38
8	Triflate	Thiophenol, Na_2CO_3, CH_2Cl_2 (0.10 M)	Room temp	60:40	22
9	Triflate	Thiophenol, Na_2CO_3, MeCN (0.50 M)	0 °C	64 : 36	30
10	Triflate	Thiophenol, Na_2CO_3, MeCN (0.50 M)	−10 °C	68:32	30
11	Triflate	Thiophenol, THF 18-crown-6, ^{t}BuOK (0.50 M)	−30 °C	65:35	25
12	Triflate	Thiophenol, THF 18-crown-6, ^{t}BuOK (0.50 M)	−55 °C	72:28	48

This transformation proved to be particularly challenging as a result of the competing elimination reaction. Both the triflate **202** and the mesylate **186** were easily accessible from alcohol **200** using standard conditions. Unfortunately the mesylate proved to be insufficiently reactive, with attempted displacement yielding only starting material (*Table 9,* entry 1).[175] Attempting the displacement using **202** was met with greater success: a preliminary reaction in DMSO and

triethylamine yielded both the desired **203** and the elimination product **204** in a 50:50 ratio, based on analysis of the crude 1H-NMR (*Table 9,* entry 2).[176] This provided a solid basis for further optimisation.

One idea was to pre-form the thiolate using sodium hydride to prevent the base from causing elimination (*Table 9,* entry 3). However, the sulfur anion was found to be sufficiently reactive to cause elimination itself. Following on from this, different conditions of concentration and temperature were evaluated using triethylamine and sodium carbonate as the bases (*Table 9,* entries 4–10).[177, 178] From these studies it was generally found that lowering the temperature increased the ratio of product to elimination product, with the best conditions utilising a higher concentration and triethylamine as the base (*Table 9*, entry 6). A final set of conditions using potassium *tert*-butoxide and THF at high concentrations were attempted. At −55 °C these conditions provided the highest yields (*Table 9,* entry 12).

Having completed the synthesis of thioether **203**, it was deemed prudent to validate the downstream reactions using this compound as a test system (*Scheme 62*).

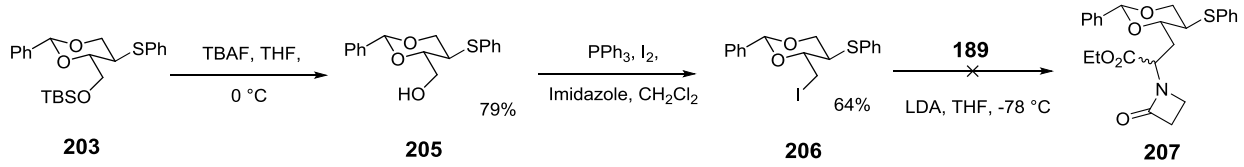

203 **205** **206** **207**

Scheme 62- Deprotection and functionalization of thioether **203**, followed by attempted alkylation of lactam **189** with **206**.

Silyl deprotection of thioether **203** proceeded smoothly using tetra-*n*-butylammonium fluoride (TBAF) and was followed by iodination of alcohol **205** in good yields using the Appel reaction.[179] Attempted alkylation of the enolate of β-lactam **189** with iodide **206**, gave no conversion. Since the focus of this project was the synthesis of **85**, with a different thioether in place, further attempts at this alkylation were not made.

2.2.5 Attempted Synthesis of Thioether **187**

Having established conditions to allow the generation of thioethers from triflate **202**, attention could now be focussed on the synthesis of **187** containing the triphenylmethane-sulfide moiety. Chadwick *et al.* reported the synthesis and isolation of lithium triphenylmethanethiolate co-ordinated with 15-crown-5, by deprotection of the corresponding mercaptan with *n*-BuLi under strictly anhydrous conditions.[180] It was hoped this product could be used directly in similar conditions to the formation of **203** (*Scheme 63*).

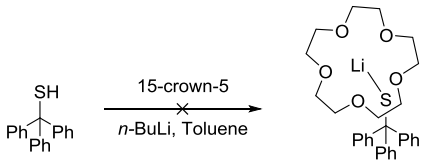

208 **209**

Scheme 63- Attempted synthesis of lithium triphenylmethanethiolate **209**.[180]

Unfortunately despite repeated attempts using glovebox techniques and Schlenk equipment to ensure the driest conditions isolation of the product was unsuccessful. As a result, efforts to directly react the mercaptan **208** with **202** were made (*Table 10*).

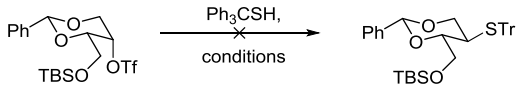

202 **187**

Table 10- Attempted reaction of **202** with triphenylmethanethiol.

Entry	*Conditions*	*Temperature*	***Result***
1	Triphenylmercaptan, THF 18-crown-6, ^{t}BuOK, (0.5 M)	−55 °C	**202** and **204**
2	Triphenylmercaptan, Toluene, 15-crown-5, *n*-BuLi, (0.5 M)	−55 °C	**204**

Unfortunately, using the conditions established for the reaction of **202** with thiophenol yielded only starting material and the elimination product (*Table 10*, entry 1). A further attempt made using Chadwick's conditions also produced similar results (*Table 10*, entry 2). It is likely that the bulky mercaptan is hindering reaction at the triflate preventing any substitution. Reviewing the literature showed similar types of reaction using conditions at reflux.[181, 182] However these are unsuited for this situation as such conditions are likely to favour elimination as well as decomposition of the unstable triflate **202**. An alternative method for generating sulfide **187** was therefore sought.

2.2.6 Alternative Routes to Thioether **187**

It was hoped that reacting **202** with thioacetic acid or a derivative salt, followed by hydrolysis of the resulting thioester **210** would provide the free thiol which could then be protected with trityl chloride to give the desired sulfide (*Scheme 64* and *Table 11*).

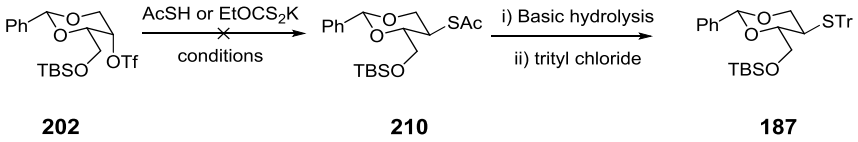

202 **210** **187**

Scheme 64- Alternative route to thioether **187.**

Entry	*Conditions*	***Result***
1	KSAc, DMF, 0.15 M	**204**
2	KSAc, DMF, −30 °C, 0.15 M	**204**
3	KSAc, DMF, −55 °C, 0.5 M	**204**
4	KSAc, THF, 18-crown-6 −55 °C, 0.5 M	**204**
5	AcSH, Cs_2CO_3 DMF, −55 °C, 0.5 M	**204**

Table 11- Attempted reaction of **202** with thioacetate salts.

Based on literature precedence, directly reacting **202** with potassium thioacetate was attempted at room temperature.[183] This lead only to elimination (*Table 11*, entry 1). Neither decreasing the

reaction temperature, nor making use of previously established conditions had any effect on the outcome of the reaction (*Table 11,* entries 2-4). A final attempt using thioacetic acid and a caesium base also resulted in elimination (*Table 11,* entry 5).[184] These results suggest that the thioacetate anion was insufficiently nucleophilic to favour the desired substitution reaction over the competing elimination.

Potassium ethyl xanthate was proposed as more nucleophilic sulfur source and could be reacted in a similar fashion to the thioacetate salts (*Scheme 64* and *Table 12)*.[185]

Entry	*Conditions*	***Result***
1	$EtOCS_2K$, DMF, 0.04 M	**204**
2	$EtOCS_2K$, DMF, 0 °C, 0.2 M	**204**
3	$EtOCS_2K$, DMF, −20 °C, 0.04 M	**204**
4	$EtOCS_2K$, THF, 18-crown-6 −10 °C, 0.2 M	**204**
5	$EtOCS_2K$, DMF, −40 °C, 0.2 M	**204**

Table 12- Attempted reaction of **202** with xanthate salts.

Initial attempts at room temperature based on literature procedures again resulted in elimination (*Table* 12, entry 1).[185] It was quickly apparent that decreasing the reaction temperature and altering concentration had little effect on the outcome of the reaction, with elimination occurring in all cases (*Table 12,* entries 2-5).

Since substitution reactions on **202** were clearly unviable, a different route to **187** was required. It was thought that thionation of ketone **201**, followed by reduction of the resulting thioketone **211** to form the thiol and then trityl protection as previously described would yield the desired thioether (*Scheme 65*).

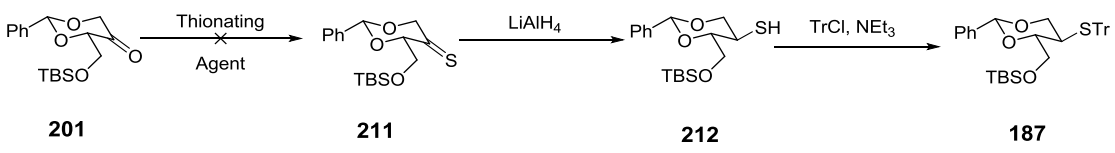

201 **211** **212** **187**

Scheme 65- Alternative route to **187** *via* thioketone **211**.

A number of attempts were made at the formation of the thioketone **211** making use of both Lawessons' reagent and phosphorous pentasulfide under a variety of reaction conditions *(Table 13)*.[186, 187]

Entry	*Conditions*	*Reaction Time*	***Result***
1	P_4S_{10}, HMDO, Toluene, Reflux, 1.0 M	1 h	Decomposition
2	Lawessons' reagent, Toluene, Reflux, 1.0 M	1 h	Decomposition
3	P_4S_{10}, Pyridine, Reflux, 0.1 M	1 h	Decomposition
4	P_4S_{10}, Pyridine, CH_2Cl_2, Reflux, 0.1 M	1 h	Decomposition

Table 13- Attempted thionation of ketone **201**.

Despite a variety of attempts, decomposition was observed in all cases (*Table 13*, entries 1-4). This can be attributable to the presence of enolizable protons alpha to the ketone which allows for the formation of dimeric sulphides leading to degradation of the compounds.[188]

Having made numerous unsuccessful attempts at synthesising thioether **187**, it was apparent that the route being used was not viable. Thioether **187** either needed to be developed from an alternative starting point or perhaps another route for generating the nucleoside altogether was required. Due to time constraints further investigations of this project were not possible.

2.3 Conclusion and Further Work

The goal of developing methodology to allow the synthesis of thymidine nucleobase analogues by reaction of isocyanates with imidoylketene intermediates, generated from β-lactams, was unsuccessful. Nevertheless efficient syntheses were developed for accessing novel β-lactam structures functionalised as sulfoxides, selenoxides and potassium salts **143**, **148**, **150** and **171** (*Figure 20*).

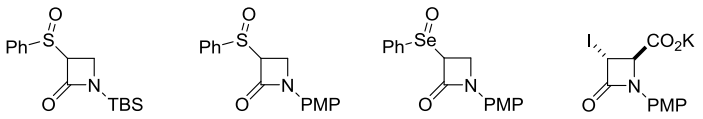

143 **148** **150** **171**

Figure 20- Novel β-lactam structures synthesised.

Of particular note was isolation of the stable selenoxide **150** due to the rarity of such molecules in the literature. Additionally, while no desired trapping of isocyanates was observed, potassium salt **171** may have fragmented to an azetone as evidenced by the isolation of urea **180**.

The synthesis of β-lactam nucleoside precursor **193** and hence nucleoside analogues **85** was not completed. Problems were encountered in attempted installation of the sulfide moiety in thioether **187** as a result of a competing elimination process. The route concluded following a ten step synthesis of sulfide **206** (*Figure 21*).

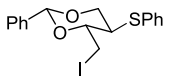

206

Figure 21- Sulfide **206**.

Looking forward, an alternative method of generating the desired azetone could be through the use of a nucleoside precursor such as **213** (*Scheme 66*).

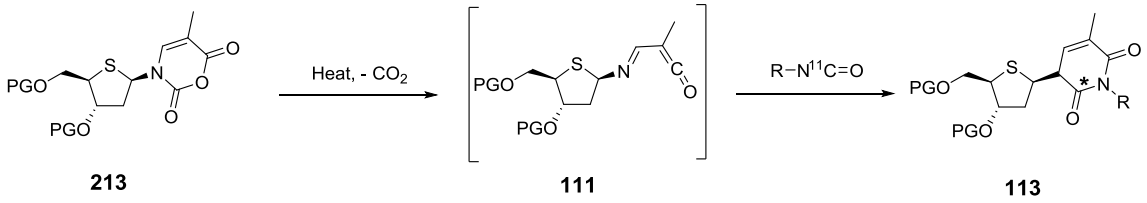

Scheme 66- Alternative method for accessing nucleoside analogues **85**.

This method is particularly attractive as 1,3-oxazine-2,4-(6*H*)-dione **215** is a literature known compound and thus the usefulness of the proposed methodology could be easily assessed. **215** is readily synthesised from the reaction of maleic anhydride with trimethylsilyl azide (*Scheme 67*).[189, 190]

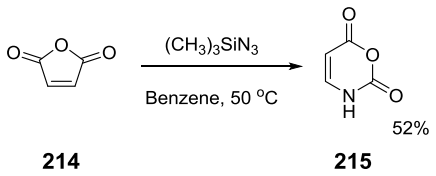

Scheme 67- Synthesis of **215**.[189]

Furthermore the corresponding nucleoside of **215** has been synthesised *via* Vorbrüggen reaction with modified ribose sugar **216** by Chwang and Bobek (*Scheme 68*).[191, 192]

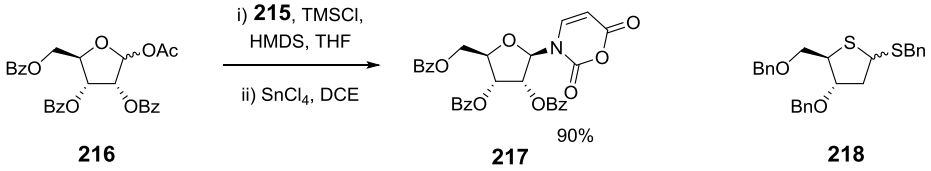

Scheme 68- Synthesis of nucleoside **217** and alternative glycosyl donor thiofuranose **218**.[191]

One could therefore envisage that replacement of ribose **216** with benzyl 3,5-di-*O*-benzyl-2-deoxy-1,4-dithio-D-*erythro*pentofuranoside **218** would allow access to a thio-nucleoside analogous to **213** (*Scheme 68*). **218** is available in seven steps from 2-deoxy-D-ribose and its use as a glycosyl donor in Vorbrüggen reactions is well known.[193]

Finally, there are reported examples using similar compounds to those proposed for the formation and reaction of imidoylketenes (S*cheme 69*).[165]

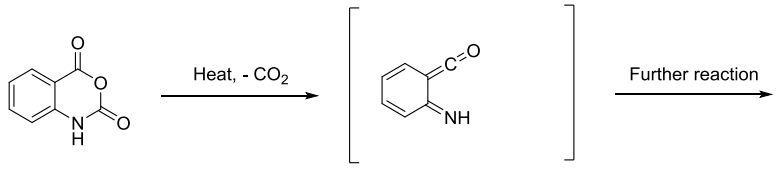

219 **220**

Scheme 69- Reported methodology for generating imidoylketenes from **219**.[165]

3. Synthesis and Radiolabelling of 2'-Deoxy-2',2'-difluoro Nucleoside Analogues

3.0 Overview

Outlined in the project aims and objectives (*Section 1.4*) the synthesis and radiolabelling of two 2',2'-difluoro nucleoside analogues **90*** and **89*** was planned. It was believed these could be obtained from their corresponding protected nucleosides **221β** and **222β** by iodination, stannylation and finally Stille coupling with [^{11}C] CH_3I as described by Samuelsson *et al* (*Scheme 70*).[64]

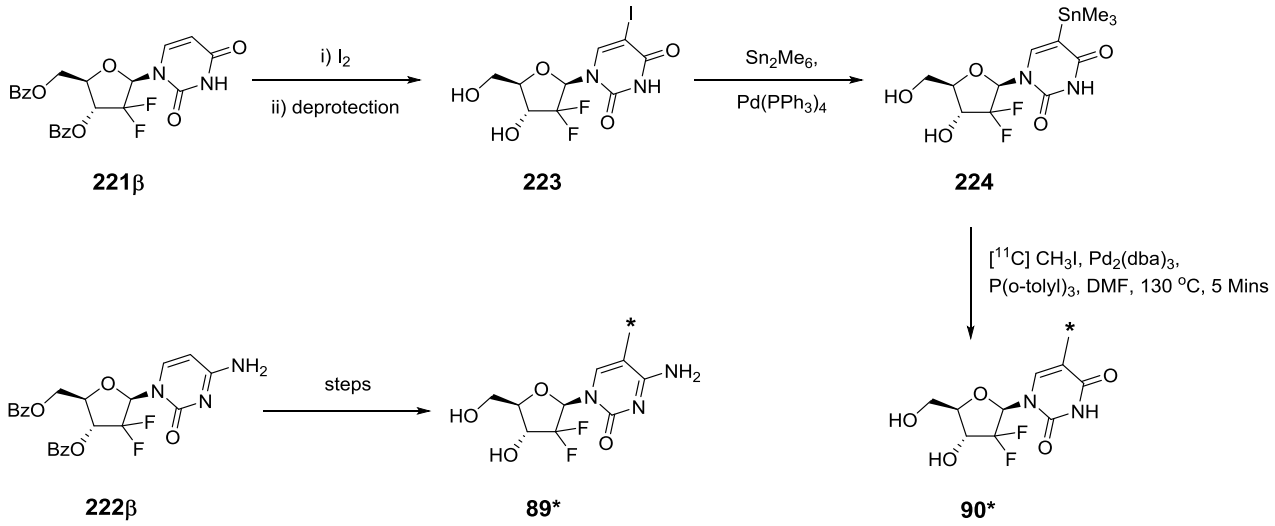

Scheme 70- Planned synthesis of **90*** and **89***, both compounds were expected to be accessible *via* similar methods.

Chou *et al.* have reported the synthesis of both **221β** and **222β** from simple starting materials and their work was used as a basis for this project.[194]

3.1 Cold Synthesis of dFMAU 90

3.1.1 Synthesis of Protected Glyceraldehyde **225**

Chou's methods made use of 2,3-*O*-isopropylidene-D-glyceraldehyde **225** as a starting material, which can be readily synthesised from D-mannitol (*Scheme 71*).[195]

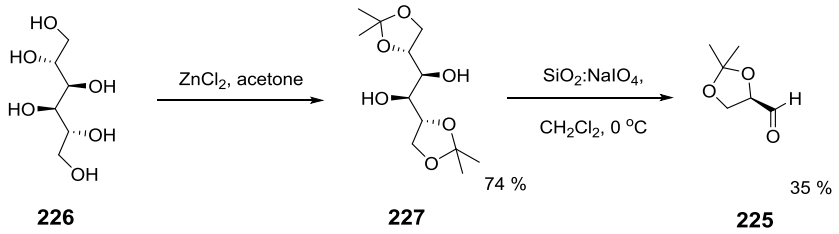

Scheme 71- Synthesis of protected glyceraldehyde **225**.

D-Mannitol **226** was easily protected as its diacetonide **227** using acetone and zinc chloride.[195] Cleavage of the diacetonide to unstable aldehyde **225** was carried out using silica supported sodium metaperiodate as described by Shing *et al*. It was reported that simple filtration of the reaction mixture yielded products of suitable purity for further reaction; however, this was not found to be the case.[196] Pure aldehyde was hence obtained by distillation of the crude residue as reported by Schmid and Bryant.[197]

3.1.2 Synthesis of Ribonolactone **228**

Ribonolactone **228** was synthesised in four steps from aldehyde **225** starting with a Reformatskii reaction to introduce the key difluoro-moiety (*Scheme 72*).

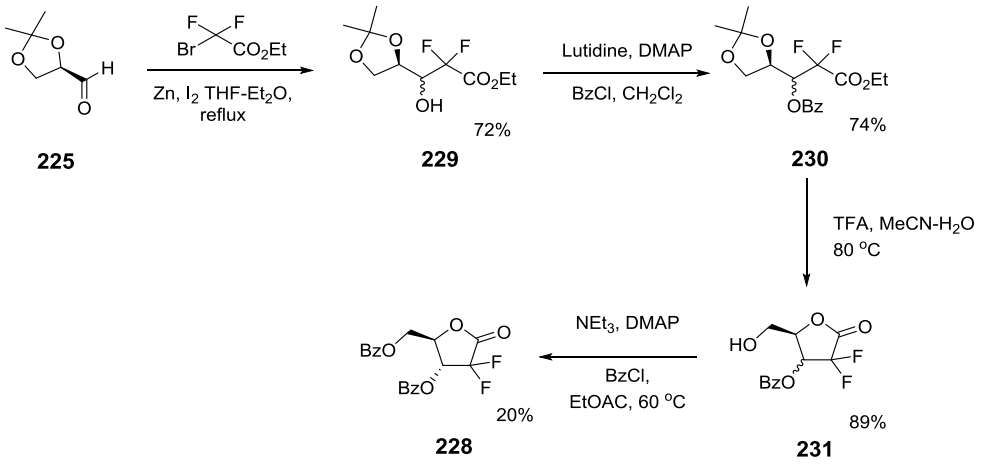

Scheme 72- Synthesis of ribonolactone **228**.[194]

The Reformatskii reaction of ethyl bromodifluoroacetate with **225** presented some difficulties.[198] An initial attempt made using zinc dust activated by acetic acid lead to poor conversion.[199] This was rectified by altering the method of activation: stirring with 0.2 equivalents of iodine served to fully activate the zinc and lead to satisfying yields of diastereomeric **229**.[200] A 2.3:1.0 ratio of *trans* and *cis* diastereomers were recovered, which is in agreement with the polar Felkin-Anh model.

Benzoylation of alcohol **229** was followed by deprotection of the acetonide **230** under acidic conditions. Spontaneous *5-exo-trig* cyclisation of the resultant intermediate to **231**, under aezeotropic distillation is favoured by Baldwin's rules. Lactone **231** was further benzoylated to give an epimeric mixture of **228**, which was recrystallized to furnish exclusively the *ribo* anomer in similar yields to the literature.[194]

3.1.3 Synthesis of Protected Nucleoside **221β**

With sufficient quantities of **228** available, the synthesis was continued with introduction of the uracil nucleobase (*Scheme 73*).

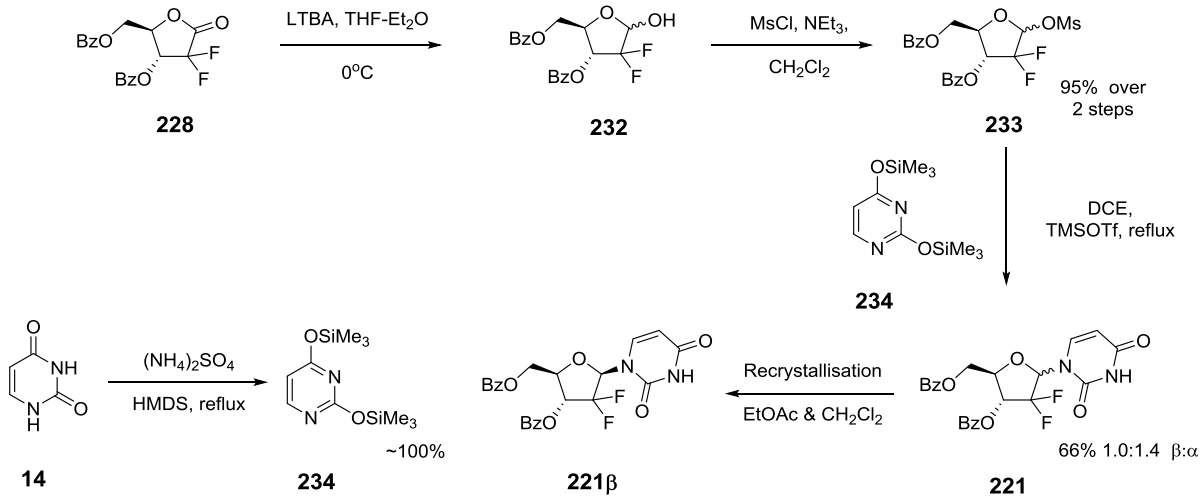

Scheme 73- Synthesis of protected nucleoside **221β**.[194]

Ribonolactone **228** was selectively reduced using lithium tri-*tert*-butoxyaluminum hydride to yield lactol **232.** This was subsequently mesylated to furnish **233** in excellent yields over the two steps. Silylated uracil **234** was synthesised by refluxing uracil **14** with hexamethyldisilizane (HMDS) in the presence of ammonium sulphate. **234** was directly reacted with mesylates **233** under the Vorbrüggen protocol to give the blocked anomeric nucleoside. In an improvement from the literature procedure, recrystallization from ethyl acetate then dichloromethane was found to give exclusively the desired β-anomer.[194]

3.1.4 Completion of the Synthesis

The synthesis of **90** was completed by functionalization of the protected nucleoside **221β** as a stannane followed by Stille coupling with methyl iodide (*Scheme 74*).

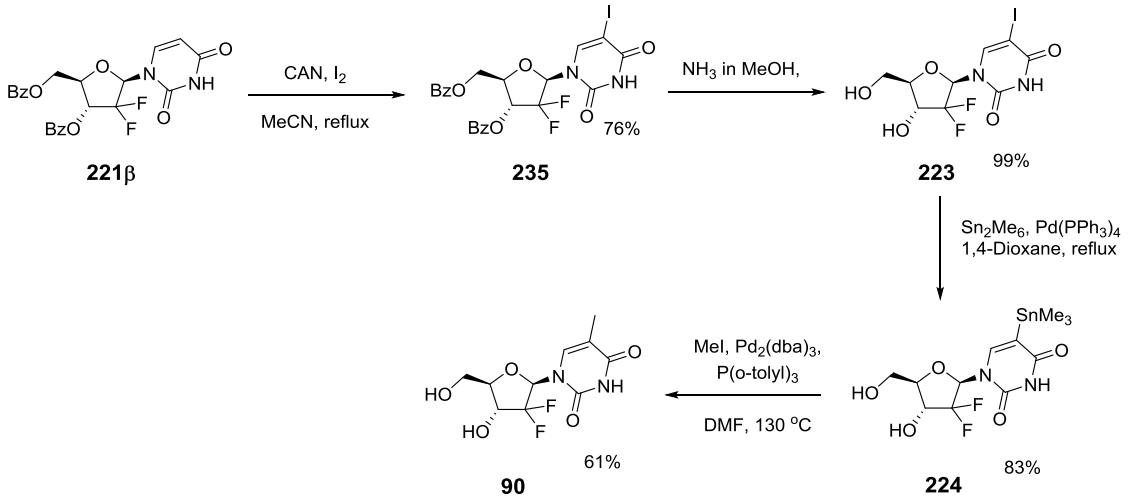

Scheme 74- End stage synthesis of **90**.

Refluxing **221β** with iodine monochloride in CH_2Cl_2 resulted in starting material recovery.[201] Altering iodinating conditions to ceric ammonium nitrate and iodine gave **235** in good yields.[202] Removal of the benzoyl protecting groups in **235** using methanolic ammonia was followed by coupling of the iodide **223** with hexamethylditin to furnish stannane **224**.[104] Preliminary attempts at the Stille coupling of **224** with methyl iodide were unsuccessful resulting in starting material recovery. It was observed that the reported colour change (from purple to deep yellow) corresponding to the *in situ* formation of the bis(tris(2-tolyl)phosphine)palladium ($Pd[P(o\text{-tolyl})_3]_2$) catalyst was not occurring during the course of the reaction.[64] This suggested that there were issues with the quality of the commercially available tris(dibenzylideneacetone)dipalladium ($Pd_2(dba)_3$) catalyst. The catalyst was therefore synthesised from palladium dichloride ($PdCl_2$) and dibenzylideneacetone according to the procedures of Ukai *et al* and recrystallized as its chloroform adduct to ensure high purity (*Scheme 75*).[203]

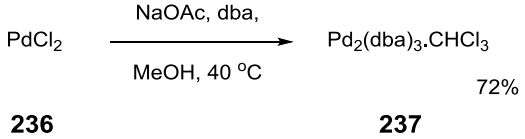

Scheme 75- Preparation of the catalyst **237**.[203]

Fortunately, this catalyst proved to be sufficiently pure for successful reaction, generating the desired product **90**.

3.2 Radiochemical Synthesis of [^{11}C]-dFMAU 90*

3.2.1 Production of Carbon-11 Methyl Iodide

Following the successful synthesis of cold dFMAU preparations were made for the synthesis of the radiolabelled nucleoside. Due to the discontinuation of carbon-11 production at the Hammersmith Campus, all radiochemistry was performed with our collaborators at the Wolfson Brain Imaging Centre (WBIC), University of Cambridge headed by Dr Franklin Aigbirhio and under the supervision of Dr Patrick Riss.

[^{11}C] CH_3I used in the radiochemical synthesis was produced using the so-called 'dry method' by radical iodination of [^{11}C] CH_4 at high temperatures using the GE Medical Systems PET trace MeI Microlab instrumentation. In more detail: [^{11}C] CO_2 from the cyclotron target is firstly adsorbed on molecular sieves in oven A (*Figure 22*).[204, 205]

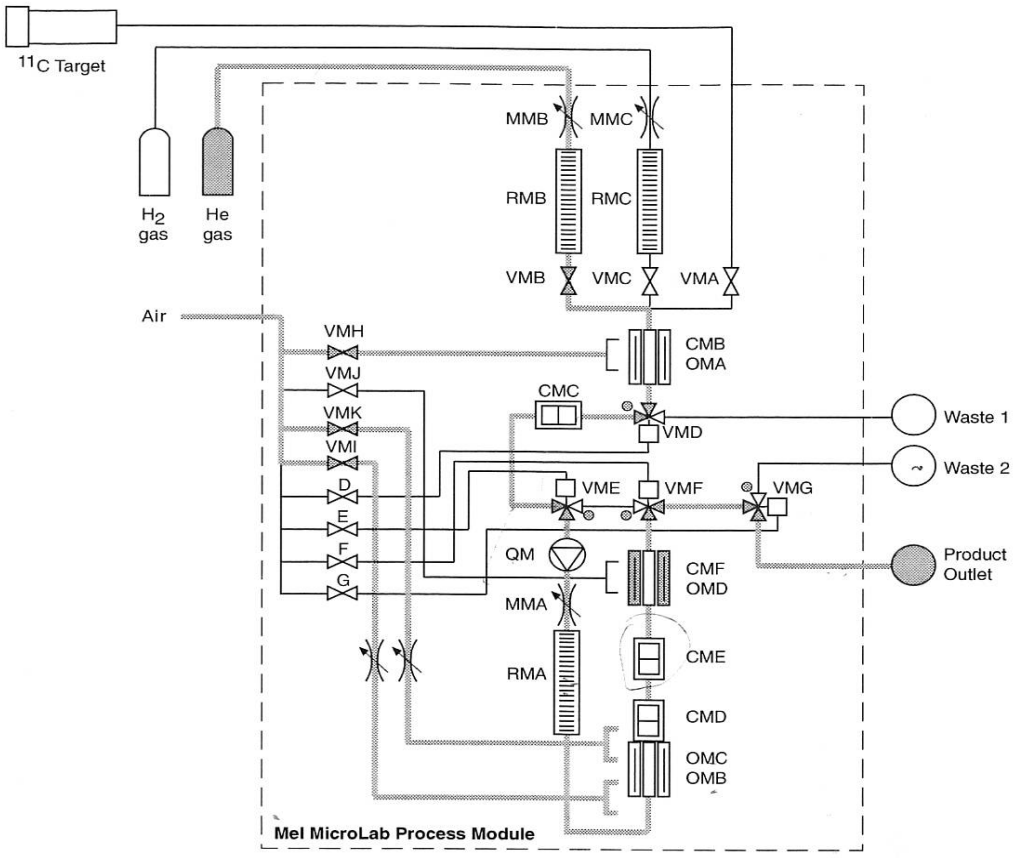

Figure 22- Schematic of [^{11}C] CH_3I synthesis module. VM = valve, OM = oven.[204]

Hydrogen is then released into the system and oven A is sealed and heated, releasing the [^{11}C] CO_2 which is reduced by hydrogen and the nickel catalyst to form [^{11}C] CH_4. The [^{11}C] CH_4 is released under a flow of helium into the methyl iodide conversion components of the system containing ovens B, C and D. Iodine is heated to 700 ^{o}C and vaporised on oven B and is reacted with [^{11}C] CH_4 to form [^{11}C] CH_3I on oven C. [^{11}C] CH_3I is subsequently trapped on the adsorbent Porapak polymers in oven D. Recirculation of [^{11}C] CH_4 through the system is continued until conversion to [^{11}C] CH_3I is complete. Finally, any unreacted [^{11}C] CH_4 is released as waste before the trapped [^{11}C] CH_3I is released and trapped in a solution of DMF heating oven D in a stream of helium.[204, 205]

3.2.2 Synthesis of [^{11}C]-dFMAU **90***

Radiolabelling of **224** using [^{11}C] CH_3I was successfully carried out according to the procedures of Samuelsson *et al*. to give the novel radiolabelled nucleoside **90*** (*Scheme 76*).[64]

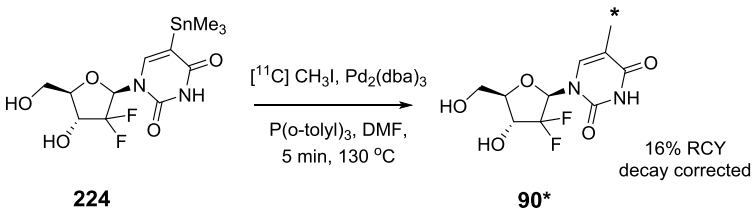

Scheme 76- Radiolabelling of **224** with [^{11}C] CH_3I.[64]

When the synthesis was performed manually, decay-corrected radiochemical yields of 16% (n=2) and radiochemical purity of >97% (after HPLC) were achieved after reacting for five minutes. In order to minimise contact with radioactivity and perform a more streamlined and efficient production, the synthesis was adapted for automation using the GE Tracerlab FX_C® synthesis module. This resulted in similar radiochemical purity but unfortunately gave lower radiochemical yields of 5% (n=3). This was thought to be a result of blocked filters and tubes during transfer of the reaction mixture from the reaction vessel to the HPLC caused by palladium deposits. Confirmation of the product identity was performed by spiking a crude analytical sample of the radiolabelled material with authentic cold sample of **90** (*Figure 23*).

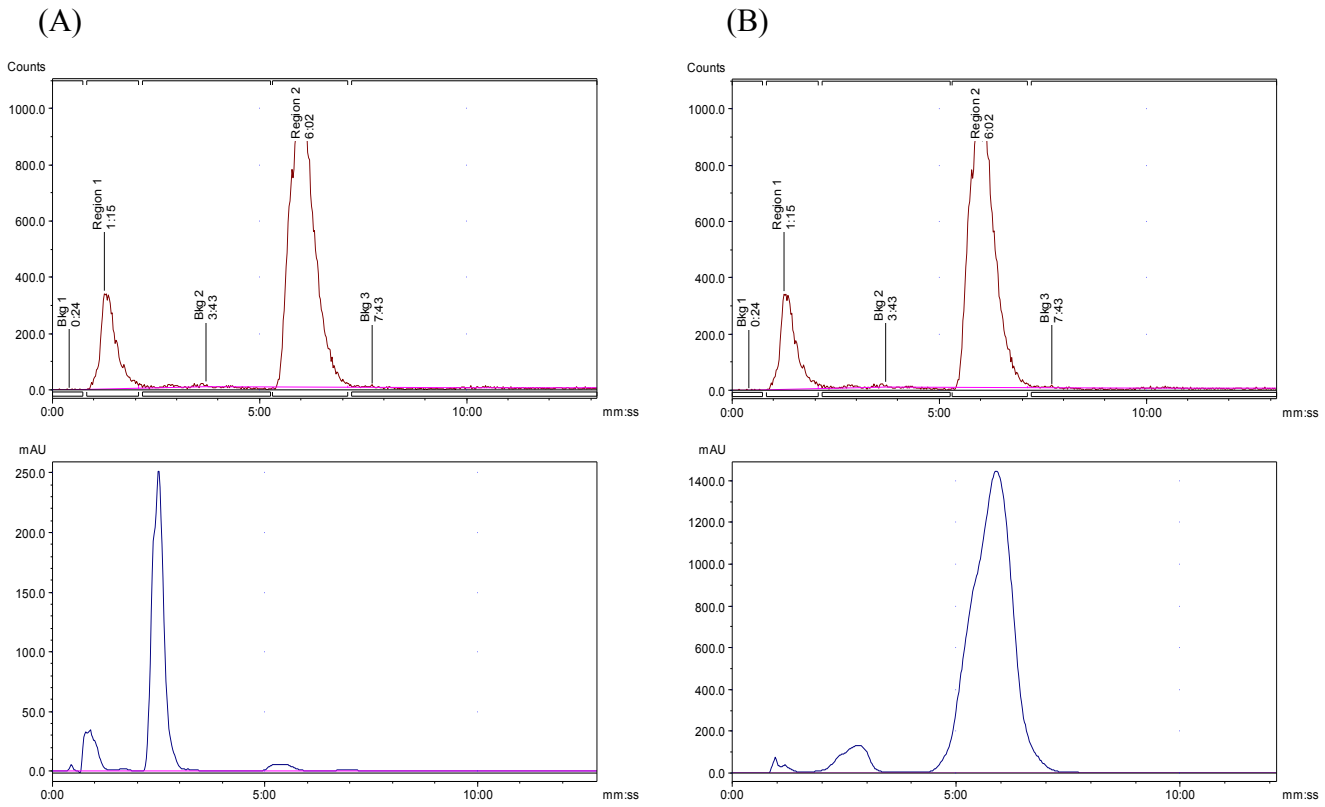

Figure 23- (A) UV and activity traces for radiolabelled **90*** and (B) traces for a sample spiked with cold **90**.

Further efforts to optimise the synthesis of **90*** involved investigations into developing a method suited for use with a microfluidic reactor. Microfluidic syntheses involve the controlled injection of reaction components through a network of small channels, typically with 10-500 µm dimensions, which form a microfluidic reactor.[206] Microfluidic systems offer numerous advantages which are particularly useful to the PET radiochemist, including: rate acceleration by increased mixing of components and enhanced heat transport as a result of the increased surface area (particularly important when considering the short half-lives of PET radionuclides), the ability to easily perform reactions using small amounts of reagent (in µM-pM range) as is typical in PET syntheses, ease of automation which allows direct integration with HPLC purification for example and the small space requirements which allow easier shielding of the user from radioactivity.[206, 207]

For these reasons, it was hoped that using the Advion NanoTek® microfluidic system would allow for an automated synthesis of the radiolabelled product while also decreasing the reaction time. A variety of conditions were investigated (*Table 14*).

Entry	*Temperature (^{o}C)*	*Flow Rate (1:1)*	***Result***
1	130	60 μL min^{-1}	No Conversion
2	140	60 μL min^{-1}	No Conversion
3	150	60 μL min^{-1}	No Conversion
4	160	60 μL min^{-1}	No Conversion
5	170	60 μL min^{-1}	No Conversion
6	180	60 μL min^{-1}	No Conversion
7	190	60 μL min^{-1}	No Conversion
8	200	60 μL min^{-1}	No Conversion
9	140	30 μL min^{-1}	No Conversion
10	140	25 μL min^{-1}	No Conversion
11	140	20 μL min^{-1}	No Conversion
12	140	15 μL min^{-1}	No Conversion

Table 14- Conditions evaluated for the microfluidic radiochemical synthesis of **90***.

Note: Total reactor volume = 30 μL.
Flow rate corresponds to injection of $^{11}CH_3I$ in DMF from one pump and the remaining reaction components in DMF from another in a 1:1 mixture.

Initial conditions were based upon those used in the standard radiolabelling reaction to form **90***, the difference being the residence time in the reactor (i.e. reaction time) was 15 seconds in comparison to five minutes when performed in a vial (*Table 14*, entry 1). In this case, no conversion of the starting material was observed. It was thought the problem could be due to temperature differences between the reactor and the reaction mixture itself. The temperature was therefore increased incrementally to a maximum of 200 ^{o}C to no avail (*Table 14*, entries 2-8). A second line of thought centred on the residency time within the reactor itself, decreasing the flow rate leading to an eventual residency time of one minute also did not result in conversion of **224** (*Table 14*, entries 9-12). Aside from the reaction time, the failure to isolate any product could be attributed to the lower concentration of reactants caused by the larger surface area of the microfluidic system. Indeed, in Samuelssons' report, it was noted that lowering the reaction concentration gave reduced yields.[64] Perhaps it is a combination of both the lower reaction concentration and reduced reaction time which lead to these results.

Despite being unable to isolate any product from the microfluidic synthesis and the relatively low radiochemical yields attained from the Tracerlab system, biological testing of radiolabelled **90*** for TK1 selectivity was nevertheless carried out. It should be noted that compounds prepared in radiochemical yields of less than 5% (decay-corrected) are still suitable for biological studies, as such the yield of **90*** was less problematic than may be expected.[208]

3.3 Biological Assay of [^{11}C]-dFMAU 90*

The assay used to test the activity of **90*** for TK1 was developed by Roberta Sala our collaborator at the Hammersmith Campus and is adapted from the work of Toyohara *et al*.[209] Briefly, TK1 expressing cells (TK1+) were grown until they achieved 60-70% confluency, whereupon they were lysed and suspended in a homogenised buffer suited for reaction. These cells were then incubated with radiolabelled **90*** and additional reaction buffer, allowing the extent of phosphorylation to be assessed (*Table 15*).

Entry	*Conditions**	*Incubation Time*	***Phosphorylation (%)***
1	Buffer, **90***, 37 ^{o}C	40 min	0
2	Buffer, TK1+ cell lysate, **90***, 0 ^{o}C	40 min	0
3	Buffer, TK1- cell lysate, **90***, 37 ^{o}C	40 min	0
4	Buffer, TK1+ cell lysate, **90***, 37 ^{o}C	20 min	0
5	Buffer, TK1+ cell lysate, **90***, 37 ^{o}C	40 min	< 1
6	Buffer, TK1+ cell lysate, **90***, CIP, 37 ^{o}C	40 min	0

Table 15- Results for TK1 assay of **90***.

*Each experiment was repeated three times and carried out using 20 µL of cell lysate, 180 µL of buffer (50 mM Tris-HCl pH 7.5, 2.5 mM ATP, 2.5 mM $MgCl_2$) and 100 µL of activity (50 MBq in 5 mL). Experiments performed under the guidance of Dr Patrick Riss at the WBIC University of Cambridge.

A number of control experiments were carried out in order to validate the results of the assay. Negative controls performed with cell lysates not expressing TK1 (TK1-) and with TK1+ cell lysates but at 0 ^{o}C, as expected, resulted in zero phosphorylation of **90*** (*Table 15*, entries 2 and 3). A blank experiment containing no cell lysate gave an identical result (*Table 15*, entry 1). Unfortunately, incubation of TK1+ cell lysate with **90*** for 20 minutes and 40 minutes resulted in minimal phosphorylation of the nucleoside (*Table 15*, entries 4 and 5). These results suggest that **90*** is not a substrate for TK1. A final experiment was performed using standard conditions with the addition of the alkaline phosphatase (CIP). Had a new peak been observed in any previous experiments, this would have allowed confirmation that it was a product of phosphorylation.

Since **90*** shows no TK1 activity, assays to assess its dCK activity need to be performed. Following discussions with our collaborators several other factors were suggested that could account for these results: **90*** was formulated in 6% EtOH:H_2O and low phosphorylation rates with non-radioactive samples in EtOH have been observed in the past. Additionally there might be traces of palladium or tin left in the formulation, which could have poisoned the kinase, leading to low conversion.

3.4 Towards the Synthesis of 5-Methyl-Gemcitabine 89

3.4.1 Modification of the Synthetic Route

With the cold and radiosynthesis of **90** completed, focus was turned to the synthesis and radiosynthesis of methylated gemcitabine. As previously mentioned, it was thought that the strategy for generation of this compound would be similar to that used in accessing **90**. However, in this case a slight modification of the route was required to account for the *N*4-amine in **89** (*Scheme 77*).

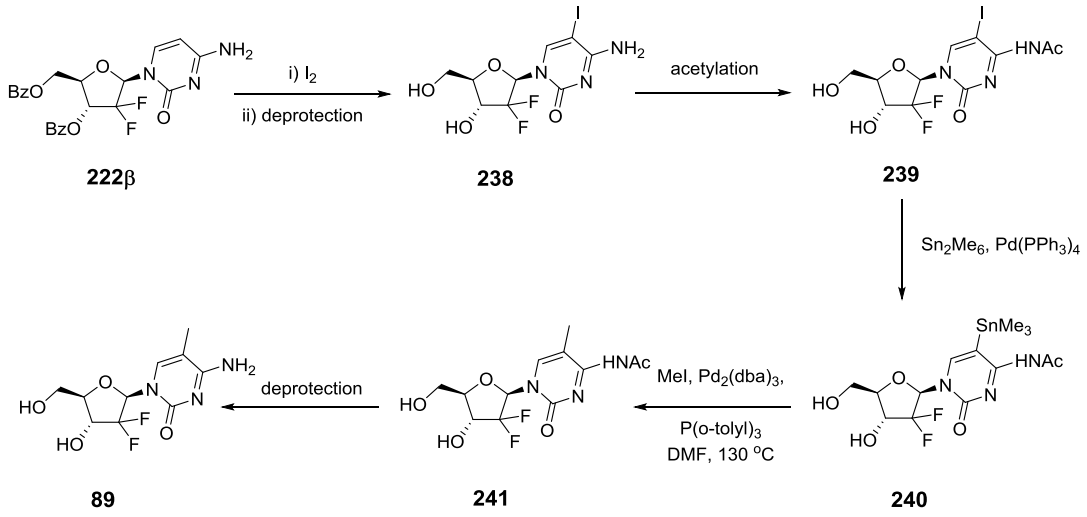

Scheme 77- Proposed synthesis of **89**.

Amines are known to be poisons for a number of catalysts including platinum and palladium.[210] Consequently, it was envisaged that protection of the *N*4-amine of **238** would be required to prevent catalyst poisoning as well as decrease the chance of other side-reactions with methyl iodide and during the palladium catalysed steps. Indeed, Reddington *et al.* have reported the necessity of such protection in 5-iodo-2'-deoxycytidine for successful Heck reaction with *N*-allyl-trifluoroacetamide.[211]

3.4.2 Synthesis of Gemcitabine **84**

Making use of mesylate intermediate **233** as a starting point, the synthesis of benzoyl-protected gemcitabine were completed according to methods of Chou (*Scheme 78*).[194]

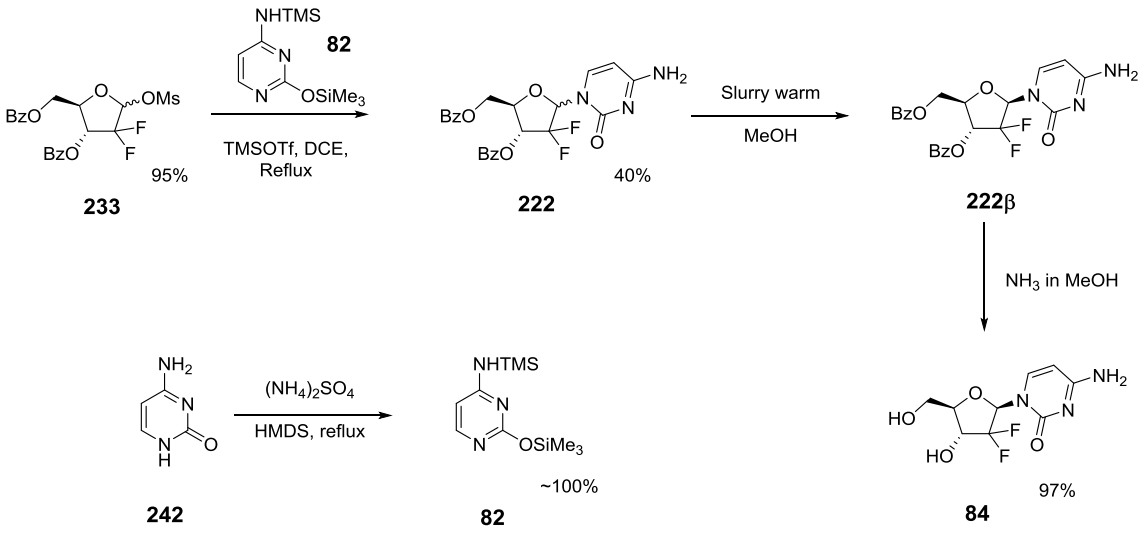

Scheme 78- Synthesis of gemcitabine **84**.[194]

Cytosine was silylated to form **82** by refluxing in HMDS in the presence of ammonium sulfate. This was then reacted with mesylate **233** (synthesis described in *Scheme 71 Section 3.1.3*) using the Vorbrüggen reaction to give the blocked anomeric nucleoside **222**. The yield of **222** was slightly lower in comparison to the given literature values.[194] This was thought to be partly due to changing solvents from 1,1,2-trichloroethane to 1,2-dichloroethane which meant the reaction was performed at a lower temperature and took longer to complete. Should the reaction be repeated 1,1,2-trichloroethane will be used. Isolation of the desired β-anomer **222β** could be easily performed by slurrying the anomeric mixture in warm methanol followed by filtration to recover the insoluble beta-product. Basic deprotection of the blocked nucleoside led to almost quantitative yields of cold gemcitabine.[194]

3.4.3 Attempted Synthesis of **89**

Iodination of the 5-position of cytosine ring proved to be somewhat challenging, requiring a variety of conditions to be screened before a suitable method was discovered (*Table 16*).

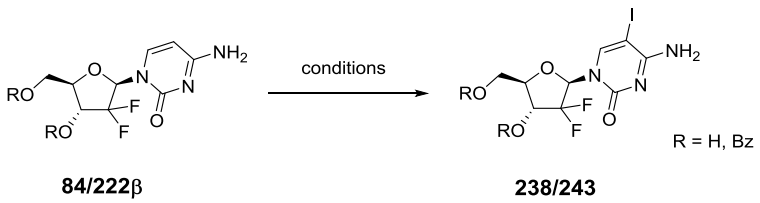

84/222β **238/243**

Table 16- Iodination of nucleosides **222β** and **84**.

Entry	*Starting Material*	*Conditons*	***Yield***
1	**84**	I_2, HIO_3, AcOH:H_2O:CCl_4 (1:0.12:1), 0.13 M, 45 ^oC, 4 h	27%
2	**84**	NIS, DMF, 200W, 70 ^oC, 1.0 M, 10 min	29%
3	**222β**	I_2, HIO_3, AcOH:H_2O:CCl_4 (1:0.12:1), 0.13 M, 45 ^oC, 4 h	10%
4	**84**	I_2, HIO_3, AcOH:H_2O:CCl_4 (1:0.12:1), 0.03 M, 45 ^oC, 4 h	61%

Protocols making use of iodine and iodic acid were found to be amongst the most commonly used methods for iodinating cytidine and deoxycytidine in the literature.[212] Unfortunately using these conditions with **84** in a mixture of tetrachloromethane, acetic acid and water resulted in poor yields of **238** as well as the formation of an unidentified by-product (*Table 16*, entry 1). This side-product proved difficult to separate from **238** using flash silica column chromatography and contributed to the low yields. Using microwave irradiation and *N*-iodosuccinimde resulted in incomplete reaction and poor yields of **238** (*Table 16*, entry 2).[213] Cheng *et al* reported high yields for the iodination of cytidine, using iodine and iodic acid, with acetyl protection of the alcohol functionalities in place.[214] Disappointingly attempts at replicating this procedure with **222β** gave low yields of **243** with a number of side products also observed. A final set of conditions whereby a lower concentration was used and purification was performed by recrystallization, led to good yields of **238** (*Table 16*, entry 4).[215] It is probable that recrystallization of the crude mixture from water was the main factor behind the observed increase in yield as this negated the need for difficult chromatographic separation of **238** and the by-products.

With iodide **238** now easily accessible, acetylation of the *N*4-amine was carried out to ensure the nucleoside was suitably functionalised for use with palladium chemistry (*Scheme 79*).

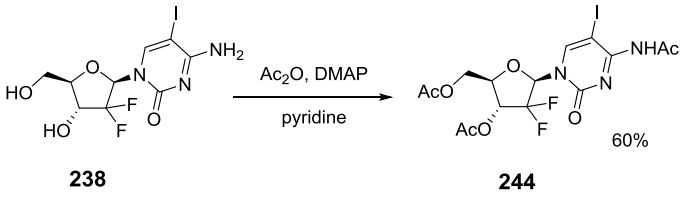

238 **244**

Scheme 79- Acetylation of **238**.[216]

Efforts to selectively protect the amine with a single equivalent of acetic anhydride, in DMF, resulted in incomplete reaction and low yields.[211] Increasing the equivalents of acetic anhydride to a slight excess resulted in a mixture of protected products. As a result it was decided to attempt global protection of **238**. Fortunately this strategy proved to be more successful furnishing **244** in adequate yields.[216]

The penultimate step of the synthesis was stannylation of **244** to generate a precursor suitable for radiolabelling (*Scheme 80*).

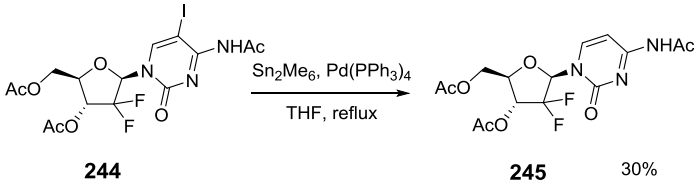

244 **245**

Scheme 80- Protodestannylation of **244** to **245**.

Attempted stannylation of **244** with hexamethylditin lead mainly to decomposition with **245** the product of protodestannylation identifiable by ^{1}H NMR.[104] Unfortunately **245** could not be isolated cleanly, although high resolution mass spectrometry allowed confirmation of its identity. The replacement of hexamethylditin with the more sterically encumbered and less reactive *bis*(tributyltin) was suggested as a means of avoiding this problem. However, with only small quantities of precursor **222β** available and other projects showing promising developments, as well as providing possible alternative solutions to the problems of radiolabelling deoxycytidine

analogues, it was decided to switch focus to these assignments with the possibility of revisiting the stannylation reaction in the future.

3.5 Conclusion and Further Work

The synthesis and radiolabelling of the novel nucleoside analogue **90*** was successfully completed in 14 steps, making use of a Stille coupling to introduce the radiolabel (*Figure 24*).

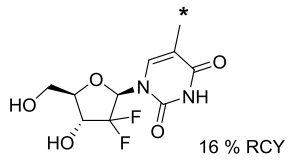

90*

Figure 24- Novel radiolabelled nucleoside **90***.

Despite proving not to be a substrate for TK1, **90*** could still prove to be useful for PET applications should it show activity for dCK. It is hoped assays for dCK will be performed in the future in order to assess this probes utility. It must also be noted that carrying out the radiosynthesis of **90*** in a clinical PET lab meant only intermittent visits to Cambridge were possible. As a result of the sporadic nature of this work, as well as the departure of the authors' primary laboratory supervisor, the specific activity of **90*** remains uncalculated. Should the probe prove useful in other assays and carbon-11 production facilities remain unavailable at Hammersmith Hospital, further collaborations will need to be established in order to calculate this value.

Attempted synthesis of 5-methyl-gemcitabine concluded with an unexpected protodestannylation reaction yielding **245** during efforts to form stannane **244** (*Figure 25*).

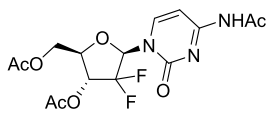

245

Figure 25- **245** product of protodestannylation.

Potential solutions to a number of the challenges experienced in the syntheses of these nucleosides were identified in work which is discussed in the following chapter.

4. 2'-Deoxy-2',2'-difluoro Nucleoside Analogues for Radiolabelling with Fluorine-18 and other Biomedical Applications

4.0 Overview

4.0.1 Alternative Radiolabelling Strategies for 2',2'-difluoro Nucleosides

One of the main problems encountered during radiosynthesis of **90*** was not specifically a synthetic challenge but rather the lack of carbon-11 production facilities locally. The ability to synthesise 2'-deoxy-2',2'-difluoro nucleosides analogues suitable for radiolabelling with fluorine-18 was desirable for two reasons: firstly, it would allow use of the fluorine-18 services available at Hammersmith Hospital and secondly, it would also provide a radiolabelled nucleoside with a substantially longer half-life.

With this in mind, a deoxyuridine-nucleoside analogue hydroxymethylated in the 5-position was proposed as a suitable precursor for fluorination (*Scheme 81*).

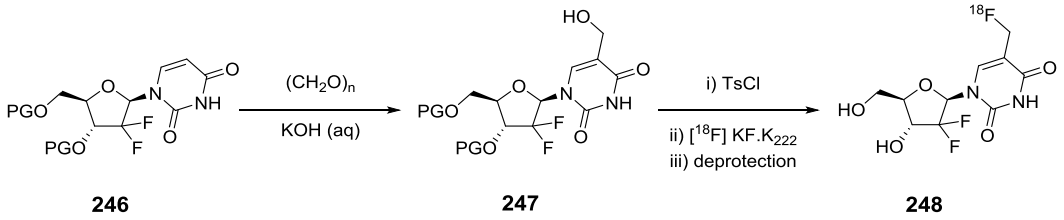

Scheme 81- Proposed route to a [^{18}F]-dFMAU analogue **248**.

Hydroxymethylation of uracil bases using a KOH (aq) solution and *para*-formaldehyde was first reported with full characterisation by Cline *et al.* in the 1950s.[217] Since then there have been a number of reports describing the use of this reaction and its modifications with varying degrees of success. Recent examples include the hydroxymethylation of uracil, uridine and deoxyuridine analogues by Gavriliu, Chung, Hudson and Dai.[218, 219, 220, 221] If a nucleoside such as **247** could be accessed then functionalization of the alcohol as a tosylate followed by displacement with [^{18}F]-KF would provide a viable strategy to accessing a [^{18}F] labelled analogue of dFMAU **90**.

4.0.2 2',2'-difluoro Nucleoside Analogues for Other Biomedical Applications

The synthesis of **247** would also present the opportunity for the synthesis of a variety of other nucleoside analogues with chemically interesting structures and potentially useful biological properties (*Figure 26*).

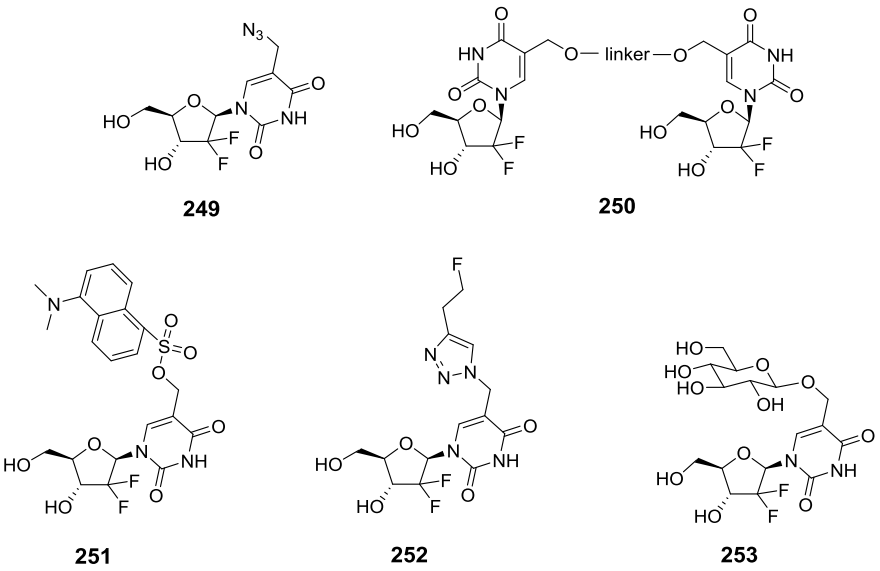

Figure 26- 2'-Deoxy-2',2'-difluoro nucleoside analogue targets.

Nucleoside reverse transcriptase inhibitors have revolutionised the treatment of HIV/AIDS (human immunodeficiency virus/acquired immunodeficiency syndrome) since their introduction in the late 1980s.[222] Azidothymidine (AZT) **254** in this respect is a pioneer for this class of drug molecule and remains clinically relevant today (*Figure 27*).

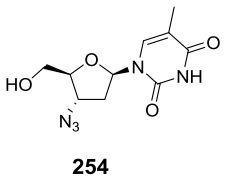

Figure 27- AZT.[222]

The success of AZT can be attributed to its high selectivity for HIV reverse transcriptase in comparison to DNA polymerase as well as the presence of the azido group which permits facile

crossing of phospholipid bilayers as well as the blood brain barrier.[223, 224] An AZT analogue such as **249** could perhaps mimic some of the interesting properties of this drug. Starting from **247**, azide **249** should be relatively simple to synthesise using the methods of Seio *et al.* (*Scheme 82*).[225]

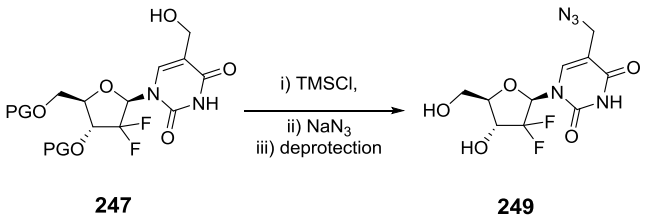

Scheme 82- Proposed synthesis of AZT analogue **249**.

[^{18}F]-FOT **255** is a nucleoside analogue previously described in our group with potential use in the imaging of proliferation in cancer.[226] During the synthesis a Huisgen cycloaddition was used to introduce the triazole functionality (*Figure 28*).

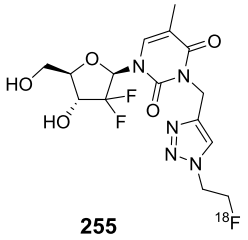

Figure 28- [^{18}F]-FOT.[226]

Assuming the synthesis of the protected azide **256** (*Scheme 82*) was successful, the opportunity to carry out a Huisgen cycloaddition to generate the corresponding nucleoside triazole analogue **252** would become available (*Scheme 83*).

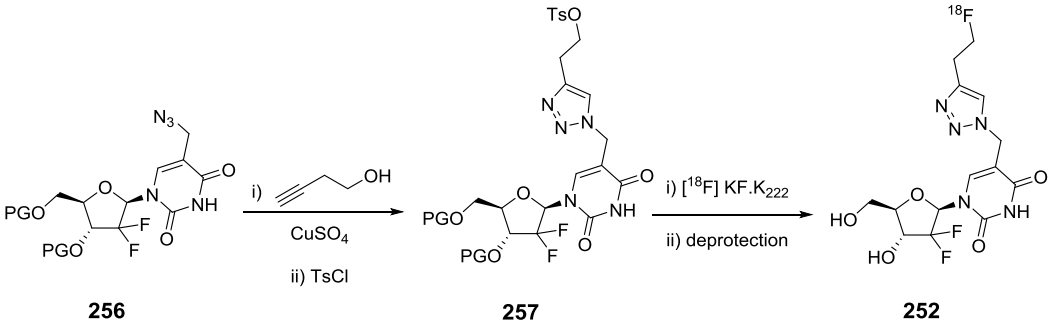

Scheme 83- Proposed synthesis of [^{18}F]-FOT analogue **252**.

The cold synthesis and radiosynthesis of **252** would be a logical step in assessing the utility of nucleosides bearing the triazole functionality as PET proliferation markers for cancer.

Covalently linked bivalent nucleosides have also shown potential for use in several areas, including: combined allosteric and direct inhibition of HIV reverse transcriptase, the study of DNA repair mechanisms and as inhibitors of ribonucleotide reductase (an important target for chemotherapeutic agents).[227, 228, 229] Using **247** and a simple linker would provide a means of accessing these types of structure, with the addition of the difluoro-moiety, in the form of dinucleoside **250** (*Scheme 84*).

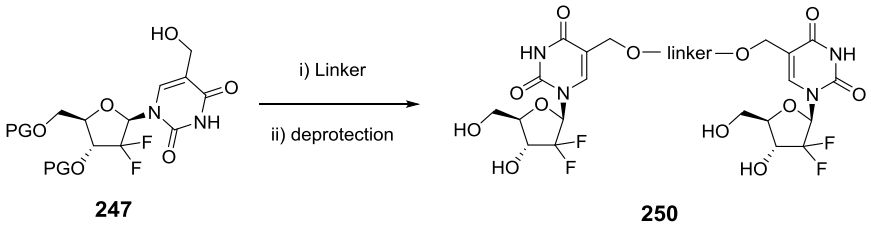

Scheme 84- Proposed synthesis of dinucleoside analogue **250**.

Optical imaging techniques such as fluorescent imaging (see *Section 1.0.2* for a greater discussion of optical imaging techniques) have applications for *in vitro* cellular imaging and in fluorescence based assays.[230] Labelling **247** with dansyl chloride, for example, could provide another means of evaluating the usefulness of 2'-deoxy-2',2'-difluoro nucleoside analogues for imaging tumours (*Scheme 85*).

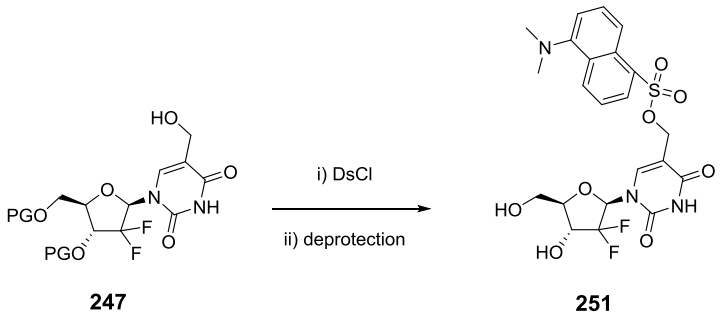

Scheme 85- Proposed syntheses of dansylated nucleoside **251**.

Finally, the modified nucleoside analogue 5-(β-D-glucopyranosyloxymethyl)-2'-deoxyuridine **258** is expressed by a number of Kinetoplastida protozoa including the parasites Trypanosoma Brucei and Leishmania which cause the diseases sleeping sickness and Leishmaniasis.[231] It has been demonstrated that **258** is essential for the survival of the Leishmania parasite, although its function has yet to be unambiguously determined.[231] Synthesis of **258** was carried out by de Kort *et al.* with the aims of evaluating the biological and physical effects of incorporating this nucleoside into DNA in order to further understand its function.[232] Generation of a similar analogue could be used to complement these studies (*Scheme 86*).

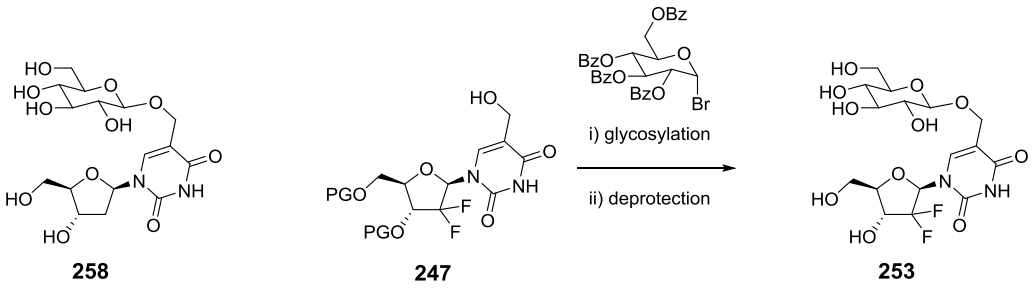

Scheme 86- Proposed synthesis of glycosylated nucleoside **253**.[232]

4.1 Synthesis of Hydroxymethylated Nucleoside 270β

4.1.1 Trial Reactions with Uracil

In order to verify the suitability of the hydroxymethylation procedure, trial reactions were carried out with uracil (*Table 17*).

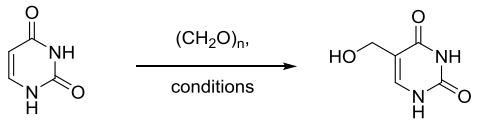

14 **259**

Table 17- Trial reactions with uracil.

Entry	*Conditions*	***Yield***
1	(CH_2O)n, 0.5 N KOH (aq) 60 °C, 72 h	66%
2	(CH_2O)n, 0.5 N KOH (aq) 200 W, 90 °C, 2 h	58%
3	(CH_2O)n, NEt_3, H_2O 60 °C, 16 h	73%

Stirring uracil with *para*-formaldehyde in 0.5 N KOH (aq) according to the protocol described by Cline gave the product in 66 % yield (*Table 17*, entry 1).[217] Abdel-Raham *et al.* reported an improvement of this procedure using microwave heating and higher temperatures to dramatically accelerate the reaction; these conditions allowed the generation of **259** in two hours, albeit in reduced yields (*Table 17*, entry 2).[233] The final conditions investigated used triethylamine in water in place of 0.5 N KOH (aq) and gave the best yields of **259** after stirring for 16 hours (*Table 17*, entry 3).[220] It was decided to adopt these conditions for future endeavours as they not only gave best yield, but also had the simplest purification avoiding the use of acidic resins as in the previous examples (*Table 17*, entries 1 and 2).[217, 233]

4.1.2 Attempted Hydroxymethylation of Nucleosides

Having established the most suitable method for hydroxymethylation of uracil, the reaction could now be used for the synthesis of a nucleoside analogous to **247** (*Scheme 87*).

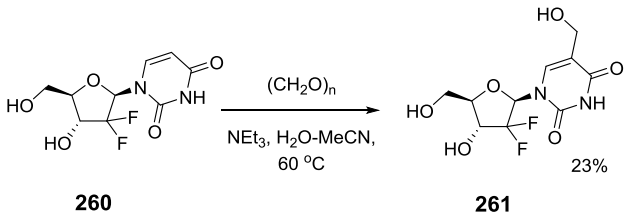

260 **261**

Scheme 87- Hydroxymethylation of **260**.[220]

The reaction was firstly attempted on the free nucleoside **260**. It was found that acetonitrile was required in addition to water in order to maintain full solubility of the reactants.[221] Yields for this step were poor and completion required heating for 72 hours. Nevertheless, **261** could be isolated and it was hoped that further attempts would prove to be more successful (*Scheme 88*).

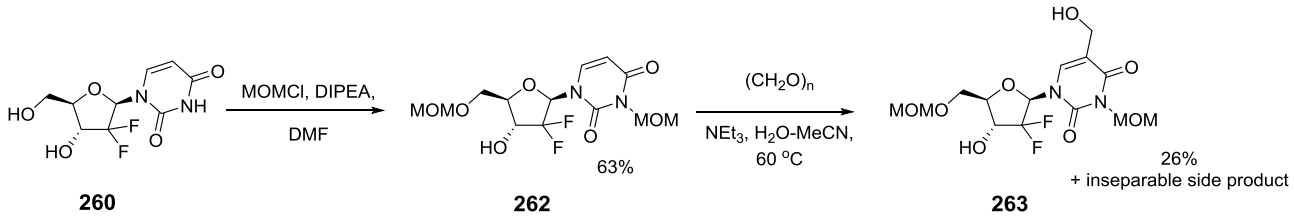

260 **262** **263**

Scheme 88- Hydroxymethylation of **262**.

260 was firstly protected as its methoxymethyl ether **262**.[234] Protection was necessary to allow differentiation between the primary hydroxyl groups following hydroxymethylation, to permit further functionalization. A MOM protection was chosen as it would be stable to the reaction conditions while also ensuring the molecule was sufficiently polar to maintain solubility. The protected nucleoside **262** was further reacted to furnish **263** along with small amounts of an inseparable side product, a result corroborated by the reports of Chung *et al*.[235] Unfortunately yields for this reaction were also poor. Attempts made using the other conditions outlined in *Table 17* gave similarly low yields.

With small quantities of the hydroxymethylated nucleoside **263** available it was deemed prudent to utilise this material to trial the synthesis of one of the desired analogues. In this case introduction of the dansyl group, considered to be the simplest transformation, was performed (*Scheme 89*).

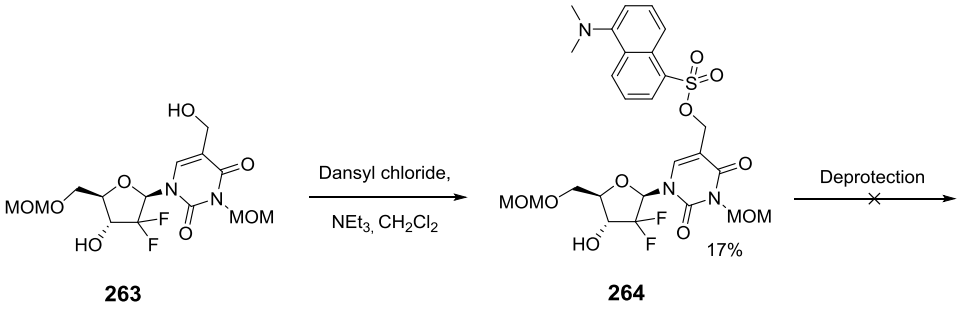

Scheme 89- Attempted synthesis of dansylated analogue **251**.

Dansylation of **263** furnished **264** in low yields.[236] This was attributed to the presence of impurities from the previous step. Nonetheless, sufficient material was recovered to allow attempts to be made at deprotection on a small scale (*Table 18*).

Entry	*Conditons*	***Result***
1	$MgCl_2$, *n*-PrSH, CH_2Cl_2, 0.5 M	Starting Material
2	$ZnCl_2$, *n*-PrSH, CH_2Cl_2, 0.5 M	Starting Material
3	$ZnBr_2$, *n*-PrSH, CH_2Cl_2, 0.5 M	Starting Material
4	6.0 N HCl, THF, 0.5 M	Epimerisation

Table 18- Attempted deprotection of nucleoside **264**.

Unfortunately despite trying numerous conditions removal of the methoxymethyl ether groups of **264** proved to be unsuccessful. Initial efforts using milder conditions with a variety of Lewis acids and 1-propanethiol yielded only starting material (*Table 18*, entries 1, 2 and 3).[237] Making use of harsher conditions resulted in epimerisation of the nucleoside (*Table 18*, entry 4).[238]

As a result of the poor yields for the hydroxymethylation step and difficulties in removing the methoxymethyl ether protecting groups, it was clear a different approach to generating large quantities of an intermediate analogous to **247** needed for synthesis of the desired analogues was required.

4.1.3 Alternative Routes to Hydroxymethylated Nucleosides

Dai *et al.* also reported difficulties when attempting hydroxymethylation on a similar protected nucleoside system. As a solution they performed a palladium catalysed carbonylation on a 5-iodo-nucleoside precursor, followed by Luche reduction to the corresponding primary alcohol.[221] Inspired by these results attempts were made to apply this protocol to the generation of a nucleoside similar to **247** (*Scheme 90*).

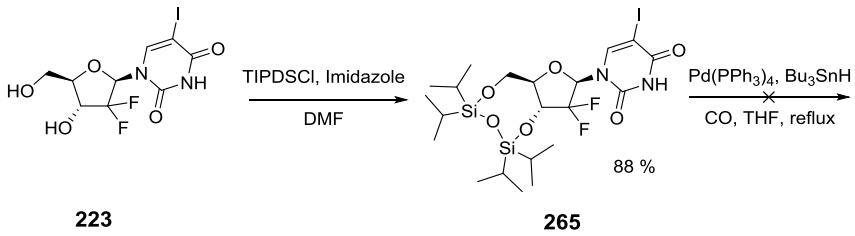

Scheme 90- Attempted carbonylation of **265**.[221]

The synthesis started with protection of iodide **223** (reported in *section 3.1.4*) using 1,3-dichloro-1,1,3,3-tetraisopropyl disiloxane (TIPDSCl) proceeding in a good yield.[239] Unfortunately attempts at carbonylation led to incomplete reaction as well as the production of a number of side-products which prevented clean isolation of the desired material. Dai *et al***.** reported the carbonylation using 50 psi of carbon monoxide.[221] These pressures could not be attained using the available equipment and was cited as a probable cause for the incomplete reaction.

Reviewing the literature revealed other alternative strategies for accessing hydroxymethylated nucleosides akin to **247** including photochemical mono-bromination of thymidine nucleosides followed by hydrolysis.[240] However, since the original reactions with uracil (*Table 17*) were high yielding and did not require the use of specialist equipment it was decided to revisit these and use a different approach to incorporating this moiety.

Brulíková and Uchida described the synthesis of nucleotide analogues modified in the 5-position by pre-functionalization of the nucleobases used in the Vorbrüggen reaction.[241, 242] Encouraged by these reports attempts were made at directly using 5-hydroxymethyluracil **259** with the mesylate precursor **233** (*Scheme 91*).

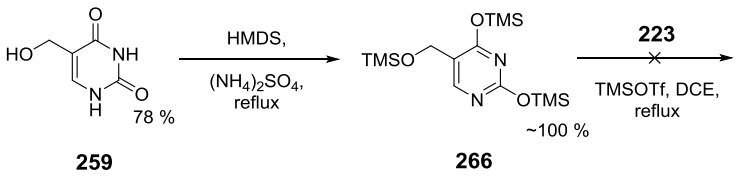

Scheme 91- Attempted Vorbrüggen reaction of **266** and **233**.

Silylation of this **259** and subsequent coupling with mesylates **233** (see *Section 3.1.3* for synthesis) was unsuccessful. *Zhang et al*. also reported problems with this transformation on similar nucleosides, citing solubility issues of **266** during the glycosylation. Silyl protection of **259** prior to coupling was purported to alleviate these difficulties (*Scheme 92*).[243]

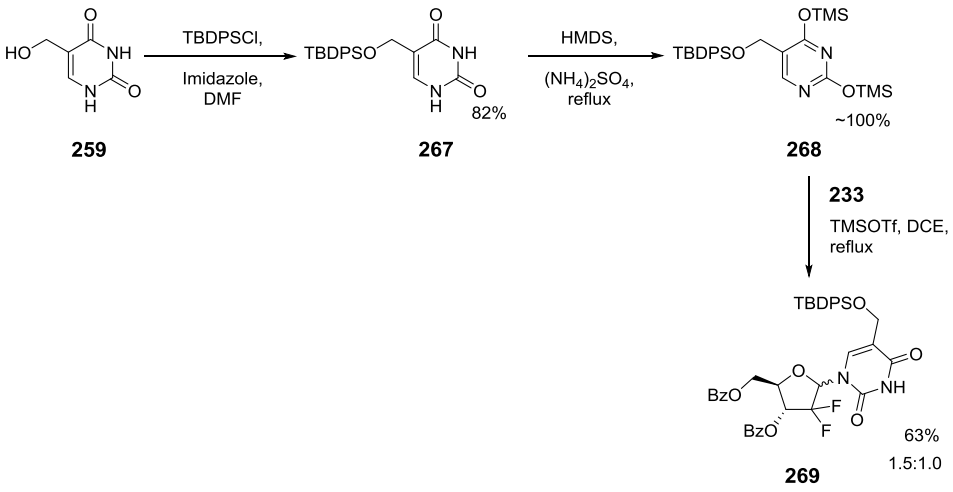

Scheme 92- Vorbrüggen glycosylation of **268** and **233**.[243]

Protection of **259** with *tert*-butyldiphenylsilyl chloride (TBDPSCl) and subsequent silylation with HMDS proceeded smoothly to furnish **268**. Coupling of **268** with mesylates **233** gave the desired nucleoside **269** as a mixture of anomers. Separation of the anomers proved to be difficult. Only partial separation was possible by column chromatography and re-crystallisation was not possible. Based on the crystallisation of similar nucleosides in the literature, it was

hoped that removing the bulky non-polar TBDPS group would render the nucleoside more susceptible to re-crystallisation (*Scheme 93*).[244]

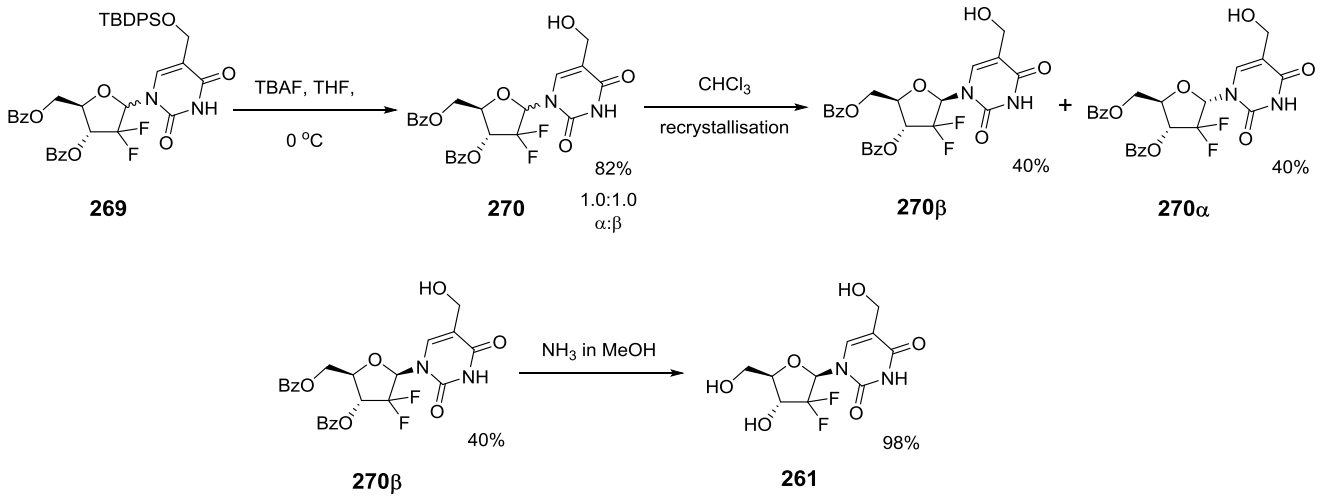

Scheme 93- Deprotection of **269** and separation of the anomers.

Unexpectedly deprotection of **269** using excess of TBAF lead to epimerisation of the nucleoside giving rise to a one-to-one anomeric mixture.[245] This could be rationalised by the presence of water in the TBAF solution, which would lead to the formation of HF and this could in turn cause the observed epimerisation. Indeed, Hogrefe *et al.* have reported the presence of significant quantities of water even in newly purchased bottles of TBAF.[246] Pleasingly, recrystallization of the anomeric mixture from chloroform allowed complete separation of the anomers. The identity of the β-anomer was ascertained by 2D-NOESY experiments (see *Supporting Data*). Further confirmation of this assignment was obtained by deprotection of **270β** to **261** and comparison of the NMR data with that of an authentic sample of **261** formed from literature known compounds. (*Scheme 87*, *Section 4.1.2*).

Using this route, multi-grams quantities of **270β** could be made rapidly and efficiently, thus permitting continued efforts into synthesis of the desired analogues (*Figure 24*).

4.2 Synthesis of 2'-Deoxy-2',2'-difluoro Nucleoside Analogues

4.2.1 Synthesis of Fluorinated Nucleoside **271**

The fluorinated nucleoside analogue **271** was the primary target in the hope that a rapid turnaround of the 'cold' compound would give sufficient time for radiochemistry to be performed. As outlined previously (*Scheme 79 Section 4.0.1*) functionalization of **270β** with a suitable leaving group was to be followed by displacement with fluoride (*Table 19*).

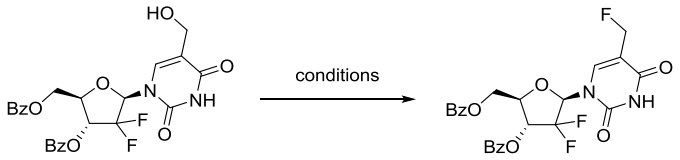

270β **271**

Table 19- Synthesis of protected fluorinated nucleoside **271**.

Entry	*Conditions*	***Result***
1	Tf_2O, Pyridine, THF, −78 °C to 0 °C	Decomposition
2	TsCl, Pyridine, THF	Decomposition
3	DAST, THF, −15 °C	**271**, 35%

Unfortunately efforts at forming the tosylate and triflate of **270β** resulted in decomposition (*Table 19*, entries 1 and 2).[247] It was thought this could be due to reaction through the unprotected uracil amide of **270β**, a process which was also evident in the protection of **260** with MOMCl (*Scheme 86 Section 4.1.2*). Furthermore, reaction at this position is known in the literature an example being in the synthesis of [^{18}F]-FOT.[226] The use of fluorinating reagents such as diethylaminosulfur trifluoride (DAST) was suggested as alternative method for producing the desired nucleoside. DAST was the reagent of choice as the synthesis of [^{18}F]-DAST has been reported in the literature meaning this protocol would be translatable to a radiochemical synthesis.[248] Fluorination of **270β** using DAST under standard conditions was successful (*Table 19*, entry 3).[249]

The final step of the synthesis was deprotection of the benzoyl groups in **271** using ammonia in methanol, unfortunately this lead to the isolation of amine **272** (*Scheme 94*).

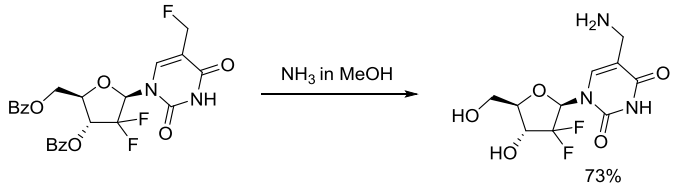

271 **272**

Scheme 94- Attempted deprotection of fluorinated nucleoside **271**.

It was proposed that the uracil system was causing activation of the primary fluoride of **271** increasing its lability and permitting displacement by ammonia to give **272**. Additional attempts at deprotection gave similar results, lending further credence to this hypothesis (*Table 20*).

Entry	*Conditions*	***Result***
1	K_2CO_3, MeOH	**273** 76%
2	K_2CO_3, EtOH	**274** 72%
3	K_2CO_3, ^{i}PrOH	Starting material

Table 20- Attempted deprotection of **271**.

Using potassium carbonate with methanol and ethanol furnished the deprotected methyl (**273**) and ethyl (**274**) of ethers of **270β** respectfully (*Table 20*, entries 1 and 2).[250] A final attempt using isopropanol as the solvent yielded starting material. In this case steric hindrance appears to have prevented any reaction. (*Table 20*, entry 3).

From these results it was clear that a different protecting strategy was needed as basic deprotection resulted in substitution of the fluoride group. Future endeavours could make use of acid sensitive trityl or acetyl protecting groups to prevent the unwanted substitution reactions.

4.2.2 Synthesis of AZT and FOT Analogues **249** and **252**

The AZT analogue **249** was easily synthesised in three steps from **270β** (*Scheme 95*).

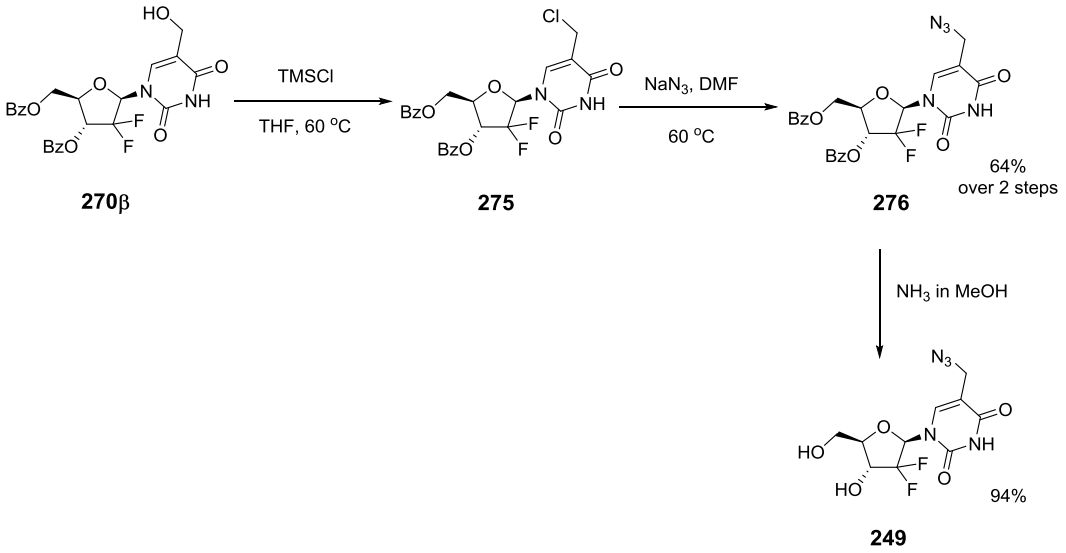

Scheme 95- Synthesis of AZT analogue **249**.[225]

Hydroxymethylated nucleoside **270β** was converted to the chloride and then displaced with sodium azide as described by Seio *et al* to give **276** in a good yield over two steps.[225] Cleavage of the benzoyl groups in **276** yielded the desired AZT analogue **249** in an excellent yield. With azide **276** readily available the synthesis of FOT analogue **252** was carried out (*Scheme 96*).

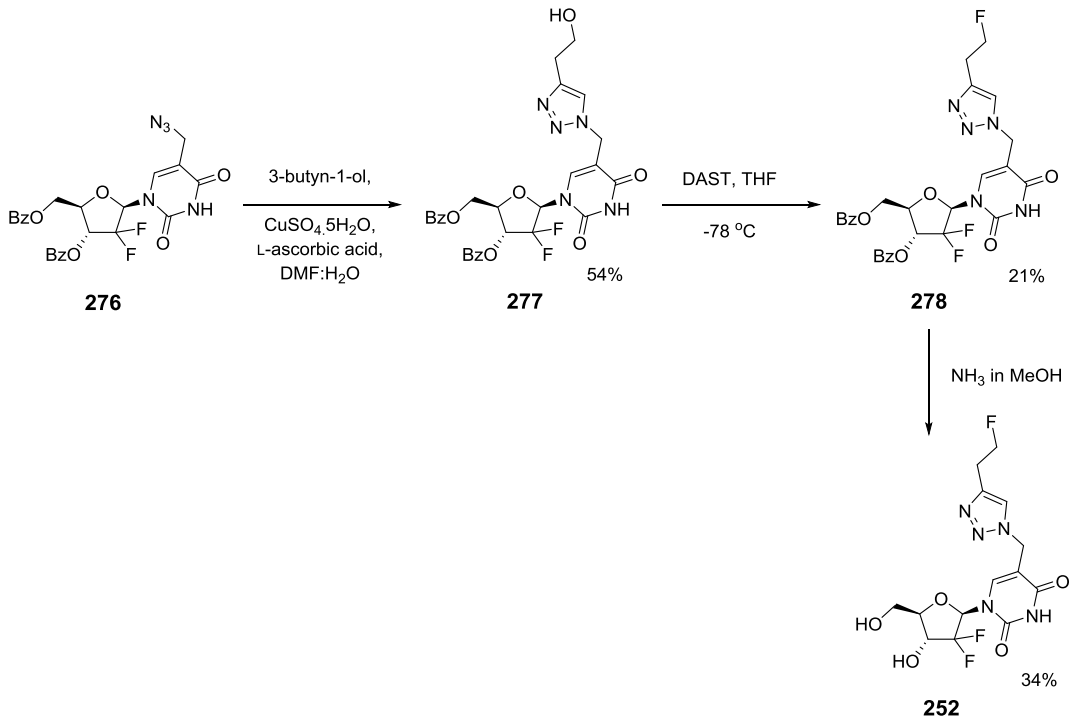

Scheme 96- Synthesis of FOT analogue **252**.[226]

Using standard copper catalysed azide-alkyne cycloaddition conditions with **276** and 3-butyn-1-ol, triazole **277** was generated in a 54% yield.[226] Having proven useful in previous efforts, DAST was used for fluorination to form **278**; this was followed by basic de-protection to give the final compound **252**. Yields for the final two steps were relatively low: 21% and 34% respectively. However, this was not of great concern as these steps were performed using small quantities of material (less than 10 mg of **278** was used in the de-protection) and it is believed that yields would see improvement on scale-up.

Having completed the synthesis of **252**, efforts were made to develop a route more suitable for radiochemistry. [^{18}F]-DAST may be synthesised; however the specific activity of this reagent is comparatively low therefore the use of [^{18}F] fluoride is preferable.[248] An alternative strategy was proposed involving synthesis of a tosylate analogue of **277**. (*Scheme 97*)

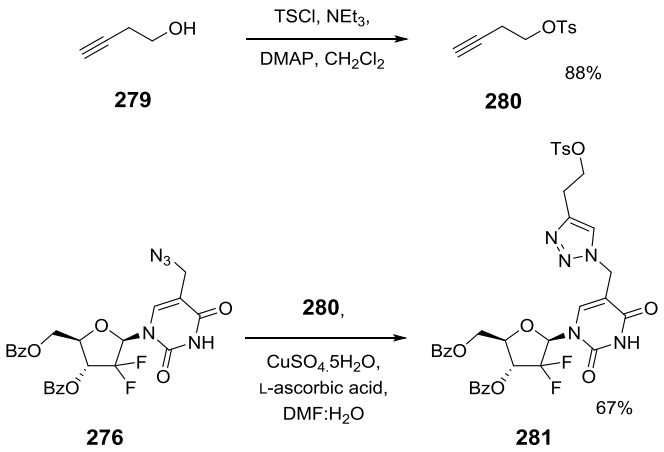

Scheme 97- Synthesis of radiochemical precursor **281**.[251]

Having experienced problems in forming the tosylate of **270β** (*Table 19 Section 4.2.1*) the decision was made to introduce the tosyl functionality at earlier stage of the synthesis; as such, 3-butyn-1-ol **279** was reacted with tosyl chloride to form **280**, which was used directly in the Huisgen cycloaddition with **276**.[251] Tosylate **281** was recovered in good yields, providing a suitable precursor for radiochemical synthesis of **252**.

4.2.3 Synthesis of Dansylated and Dinucleoside Analogues **250** and **251**

It was originally envisaged that dansylation of **270β** would allow easy access to analogue **250** (*Scheme 85*). However, bearing in mind the previously encountered problems when attempting to functionalise the primary alcohol of **270β** as well as the issues in deprotection of fluoride **271** (*Scheme 94 Section 4.2.1*), it was decided instead to convert **270β** to the corresponding amine. It was hoped that replacement of the alcohol with an amine, followed by reaction with dansyl chloride would provide the more stable sulfonamide functionality. The required amine was accessible by reduction of azide **276** (*Table 21*).

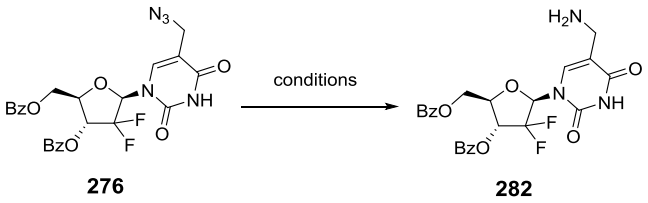

Table 21- Reduction of **276** to amine **282**.

Entry	*Conditions*	***Result***
1	H_2, Pd/C, MeOH, 60 ^oC	Debenzoylation
2	H_2, Pd/C, 1,4-dioxane, 60 ^oC	14%
3	PPh_3, THF-H_2O	74%

Problems were encountered when attempting reduction of **276** by hydrogenation. Heating **276** with methanol (to ensure solubility) and palladium on carbon under hydrogen gave a number of side products with displacement of the benzoyl protecting groups evident (*Table 20*, entry 1).[252] Altering the solvent to 1,4-dioxane, in which **276** was fully soluble, in an effort to alleviate these problems gave a sluggish reaction that did not fully complete (*Table 20*, entry 2). Fortunately, reduction using Staudinger methodology provided a mild procedure for accessing the desired amine in good yields (*Table 20*, entry 3).[253] With **282** now in hand synthesis of the dansylated analogue was completed. (*Scheme 98*)

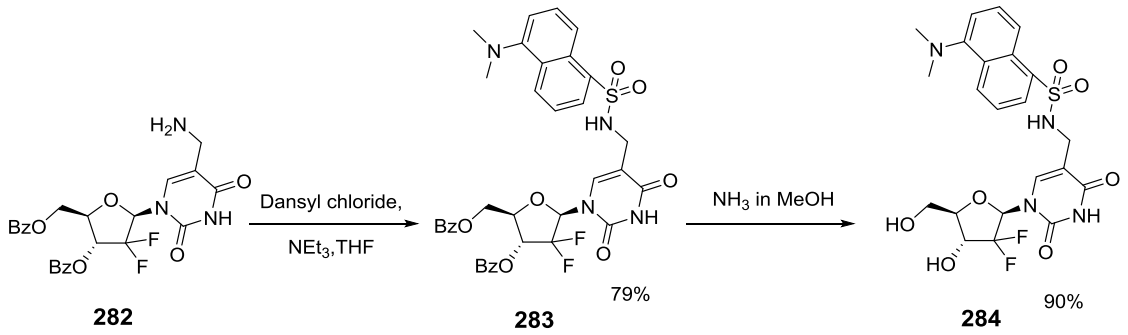

Scheme 98- Synthesis of dansylated analogue **284**.[236]

Pleasingly reaction of **282** with dansyl chloride proceeded smoothly to furnish **283**.[236] The sulfonamide linkage also ensured that displacement by ammonia during deprotection did not occur yielding exclusively **284**.

With some quantity of amine **282** remaining from endeavours towards **284**, the opportunity for synthesis of a bivalent nucleoside analogous to **251** was apparent (*Scheme 99*).

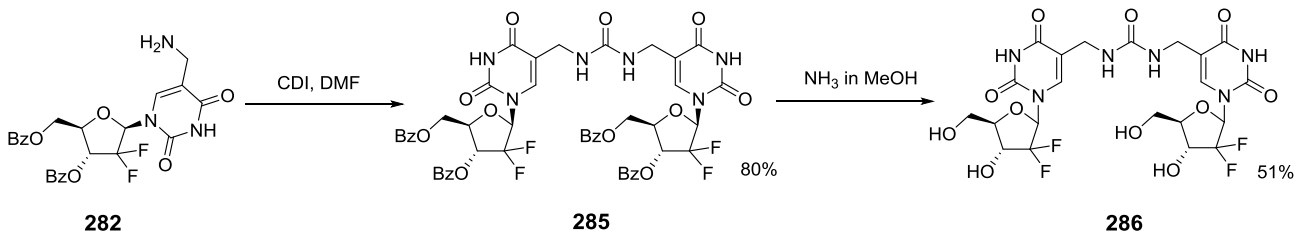

Scheme 99- Synthesis of bivalent nucleoside analogue **285**.

Two equivalents of **282** were reacted with a single equivalent of CDI to generate the di-nucleoside **285**.[254] The urea linkage in **285** also proved stable to deprotection using the standard conditions to give the final product **286**.

4.2.4 Synthesis of Glycosylated Nucleoside Analogue **253**

The final target was the glycosylated nucleoside **253**. De Kort *et al*. reported the synthesis of a similar analogue **258** (*Scheme 86 Section 4.0.2*) by glycosylation of a hydroxymethylated nucleoside using modified D-glucose.[232] This methodology would be the basis for our synthesis. The glycosyl donor was firstly synthesised according to the procedure of Sjölin *et al.* (*Scheme 100*).[255]

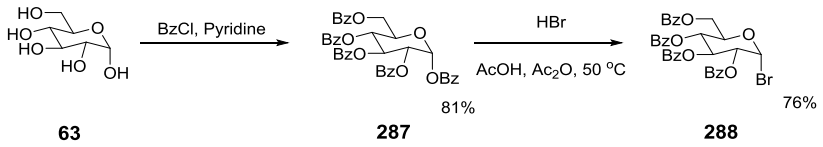

Scheme 100- Synthesis of glycosyl donor **288**.[255]

D-glucose was fully protected using benzoyl chloride to furnish **287**. This was then transformed using hydrobromic acid to form the glycosyl donor **288**.[255] The next step was to use **288** for Koenigs-Knorr glycosylation of nucleoside **270β** (*Table 22*).

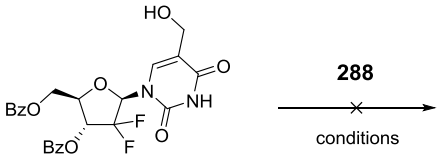

270β

Table 22- Attempted glycosylation of nucleoside **270β** with **288**.

Entry	*Conditions*	*Result*
1	AgOTf, 3Å MS, MeCN	Starting material
2	$Hg(CN)_2$, $HgBr_2$, MeCN	Starting material

In de Korts' report glycosylation was performed using mercury bromide and mercury cyanide.[232] In order to avoid using these highly toxic reagents and alternative protocol was identified using silver triflate as the promoter; unfortunately only starting material was recovered under these conditions (*Table 21*, entry 1).[255] Returning to the Helferich reaction also only yielded starting material (*Table 21*, entry 2).

It was decided to investigate the use of different glycosylation methods with different donors and so acetimidate **290** was synthesised (*Scheme 101*).

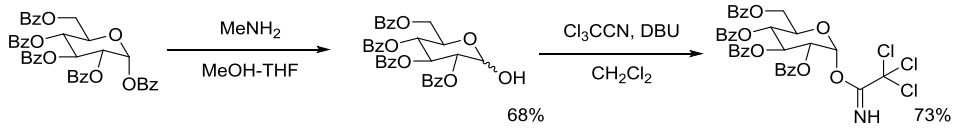

287 **289** **290**

Scheme 101- Synthesis of alternative glycosyl donor **290**.[256]

Selective deprotection of benzoyl protected glucose **287** using methylamine gave an anomeric mixture of glucopyranose **289**. Further reaction of **289** with trichloroacetonitrile furnished acetimidate **290** in good yields.[256] With **290** in hand Schmidt glycosylation of **270β** could be attempted (*Scheme 102*).

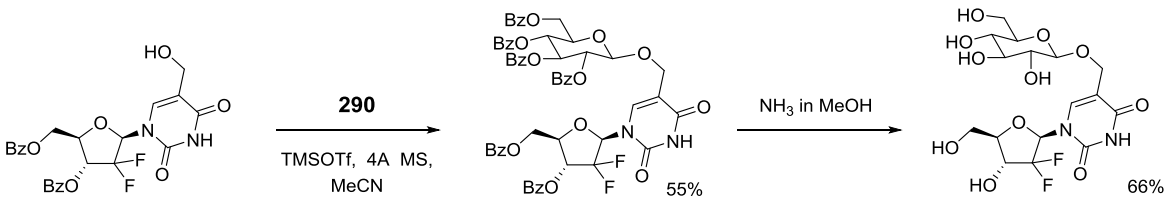

270β **291** **253**

Scheme 102- Synthesis of glycosylated nucleoside **253**.

Pleasingly, making use of TMSOTf as the promoter gave **291** in good yields.[232] Deprotection using ammonia in methanol yielded the final product **253**.

4.3 Conclusion and Further Work

Adapting the methods of Uchida and Zhang led to the development of a route permitting the facile generation of multiple gram quantities of hydroxymethylated nucleoside **270β**.[242, 243] By performing hydroxymethylation of uracil at an early stage of the synthesis, the somewhat cumbersome hydroxymethylation of nucleosides, which tend to lead to low yields, was avoided (*Scheme 103*).

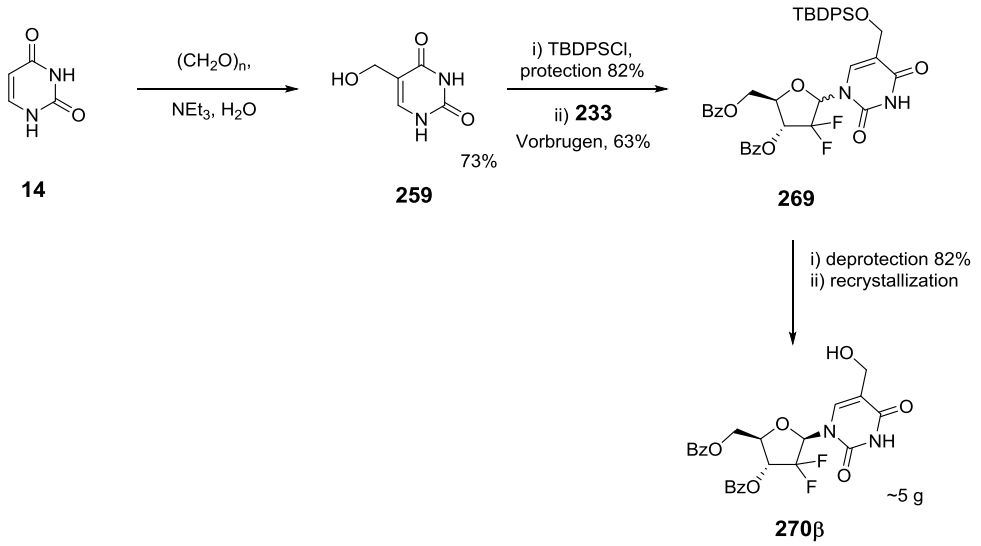

Scheme 103- Route to nucleoside **270β**.

It was also demonstrated that hydroxymethylated nucleoside **270β** can be used for the synthesis of a diverse array of structures (*Figure 29*).

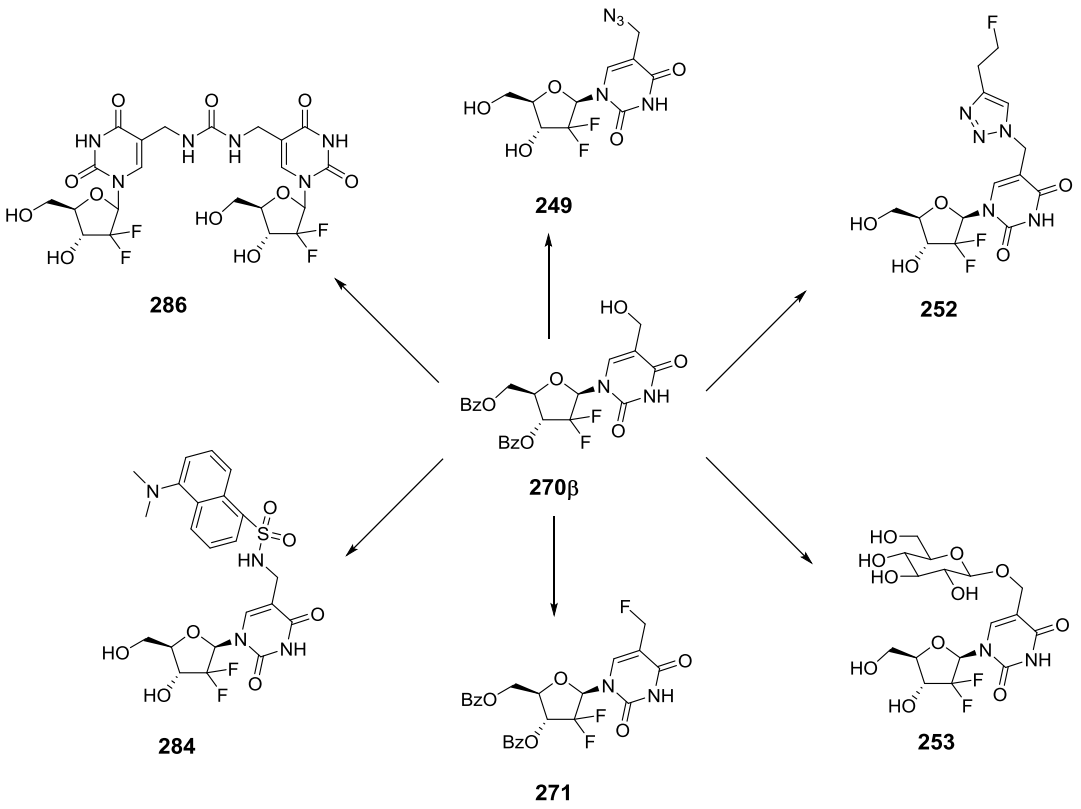

Figure 29- Nucleoside analogues synthesised.

While problems were encountered in deprotection of the fluorinated analogue **271**, it is believed that altering the protecting groups to avoid the use of basic deprotection would allow access to the final product. Inspiration can be taken from the radiosynthesis of [^{18}F]-FLT which makes use of the acid labile trityl protecting group (*Scheme 21 Section 1.3.2.1*).[95] If these issues can be overcome radiolabelling with [^{18}F]-DAST would be the logical next step. Furthermore, this synthesis could be adapted for use in generating a similarly labelled dFdc analogue, which would provide a suitable solution to issues highlighted in the conclusion of chapter three (*Section 3.5*) (*Figure 30)*.

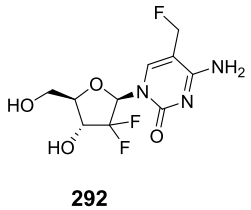

Figure 30- dFdc analogue **292**.

The AZT analogue **249** could now be tested to determine its usefulness as an inhibitor of HIV reverse transcriptase. In the case of the dimer **286**, the synthesis acted as a proof of concept showing how these nucleosides can be linked together. Further studies could focus on linking different nucleosides together and examining their properties as combined direct and allosteric inhibitors of HIV reverse transcriptase.

Generation of the protected azide **276** permitted the synthesis, *via* a Huisgen cycloaddition, of **252** an analogue of the PET tracer FOT (*Scheme 104*).[226]

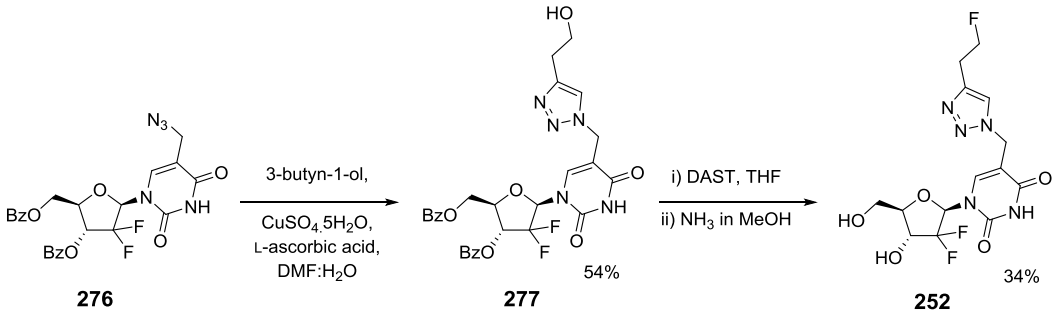

Scheme 104- Synthesis of triazole nucleoside analogue.

Having completed the synthesis of the cold compound and its tosylated precursor **281**, future endeavours should focus on adapting this molecule for radiochemical synthesis by using [^{18}F]-KF to displace the tosylate.

Dansylation to form **284** provided further demonstration of the diverse range of structures that can be formed from **270β**. Incorporation of other fluorophores such as rhodamine and fluorescein derivatives could be followed by an investigation of the use of these molecules for *in vitro* imaging (*Figure 31*).[230]

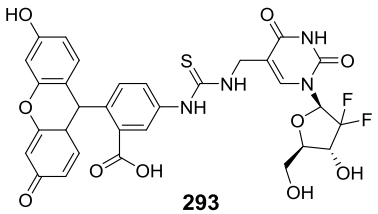

Figure 31- Fluorescein labelled nucleoside.

Finally glycosylated analogue **253** was synthesised by Schmidt glycosylation of **270β** using modified glucose. As previously mentioned this molecule could be used to complement studies assessing the function of **258** and its role in Kinetoplastid protozoa.[232]

Experimental

All chemicals were used as received or purified using standard procedures. Solvents were dried by standard techniques and distilled under nitrogen before use. Tetrahydrofuran was distilled from sodium with benzophenone indicator. Toluene was distilled from sodium. Dichloromethane and methanol were distilled from calcium hydride. *N,N*-Dimethylformamide, dimethylsulfoxide, aceonte, 1,4-dioxane, acetonitrile, 1,2-dichloroethane, ethanol, *tert*-butanol, benzene and *o*-xylene were purchased anhydrous and used as received. All experiments were carried out in oven-dried glassware under an inert atmosphere of nitrogen or argon.

Analytical thin layer chromatography (TLC) was performed using pre-coated Merck aluminium or glass backed plates (Silicagel 60 F254). Visualization was by ultraviolet light (366 nm and 254 nm) and/or treatment with potassium permanganate or vanillin stains followed by heating as appropriate. Flash column chromatography was carried out on Merck 9385 Kieselgel 60 (230-400 mesh).

NMR spectra were recorded on a Bruker DRX-400 spectrometer using an internal deuterium lock at ambient probe temperatures. Alternatively, spectra were recorded at 500 MHz (^{1}H NMR) and 125 MHz (^{13}C NMR) by the NMR Service, Imperial College London, Department of Chemistry. Chemical shifts (δ) are quoted in parts per million (ppm) and are referenced to a residual solvent peak. Coupling constants (*J*) are quoted in Hertz (Hz) to the nearest 0.1 Hz. Assignments were determined on the basis of unambiguous chemical shift and coupling pattern. Additional experiments (COSY, DEPT-135, HSQC, HMBC and NOESY) were used to aid assignments but are not included.

Low and high resolution mass spectrometry (EI, CI, ESI) were recorded by the Mass Spectrometry Service, Imperial College London, Department of Chemistry using a Micromass Platform II and Micromass AutoSpec-Q spectrometer.

Microanalyses were determined at London Metropolitan University Microanalysis Service.

Infra-red (IR) spectra were obtained using a Perkin-Elmer Spectrum BX II FT-IR System monitoring from 4000-700 cm^{-1}, with automatic background subtraction. All samples were run neat. Absorption maxima are reported in wave numbers (cm^{-1}).

Melting points were obtained on a Reichert-Thermovar melting point apparatus and are uncorrected.

Optical rotations were measured at 25 °C on a Perkin-Elmer 241 polarimeter with a path length of 1 dm, using a sodium lamp (λ = 589 nm, D-line); $[\alpha]_D^{25}$ values are reported in 10^{-1} deg cm^2 g^{-1} and concentrations (c) are quoted in g/100 mL.

Results and Discussion Section 2.

1-[*tert*-Butyl(dimethyl)silyl]azetidin-2-one 141

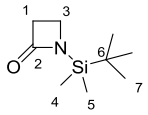

A solution of DIPEA (3.7 mL, 21.2 mmol) in CH_2Cl_2 (8 mL) was added dropwise to a solution of 2-azetidinone (1.00 g, 14.1 mmol) and *tert*-butyldimethylsilylchloride (2.44 g, 16.2 mmol) in CH_2Cl_2 (12 mL) and the reaction mixture stirred for 24 hours at room temperature. The solvent was then removed *in vacuo* and the resulting residue partitioned between Et_2O (30 mL) and H_2O (15 mL), aqueous layer extracted with Et_2O (3 × 30 mL). The combined organic layers were dried over $MgSO_4$ and concentrated *in vacuo* to yield the crude product. The crude product was purified using flash silica column chromatography (20% EtOAc in 40-60 petroleum ether) to give the product (2.32 g, 89%) as a colourless oil.
The data were in agreement with the published data.[140]

^{1}H-NMR (400 MHz, $CDCl_3$): δ_H = 0.23 (s, 6H^{4+5}), 0.95 (s, 9H^7), 3.06 (t, 2H^3, *J*=4.6Hz), 3.18 (t, 2H^1, *J*=4.6Hz).

^{13}C-NMR (400 MHz, $CDCl_3$): δ_C = -6.2 (C-4,5), 18.5 (C-6), 26.0 (C-7), 36.7 (C-1), 39.0 (C-3), 172.9 (C-2).

MS (ES+) m/z = 186 $[M+H]^+$.

1-(*tert*-Butyldimethylsilyl)-3-(phenylthio)azetidin-2-one 142

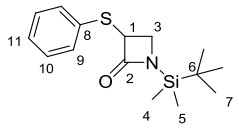

To a solution of diisopropylamine (2.5 mL, 17.8 mmol) in THF (30 mL) at 0 ^oC was added 1.0 M *n*-BuLi in hexanes (17.8 mL, 17.8 mmol) and the resulting solution stirred for 30 minutes at 0 ^oC. The solution was then cooled to −78 ^oC and added dropwise to a −78 ^oC solution of β-lactam **141**

(2.2 g, 11.9 mmol) and diphenyl disulfide (2.86 g, 13.1 mmol) in THF (70 mL). The reaction mixture was allowed to slowly warm to room temperature overnight and then poured into saturated NH_4Cl (aq) (180 mL) and extracted with CH_2Cl_2 (180 mL). The organic layer was separated and washed with H_2O (3 × 60 mL), dried over $MgSO_4$ and concentrated *in vacuo*. The crude product was purified using flash silica column chromatography (5% EtOAc in 40-60 petroleum ether) to yield the product (1.64 g, 47%) as a white solid.

^{1}H-NMR (400 MHz, $CDCl_3$): δ_H = 0.10 (s, 3H$^{4/5}$), 0.11 (s, 3H$^{4/5}$), 0.80 (s, 9H^7), 3.02 (dd, 1H^3, *J*=6.4Hz, *J*=3.0Hz), 3.53 (m, 1H^3), 4.41 (dd, 1H^1, *J*=5.7Hz, *J*=3.0Hz), 7.31 (m, 3H-Ar), 7.55 (m, 2H-Ar).

^{13}C-NMR (400 MHz, $CDCl_3$): δ_C = -6.3 (C-4,5), 18.3 (C-6), 25.7 (C-7), 44.4 (C-3), 53.3 (C-1), 128.2 (CH-Ar), 129.1 (CH-Ar), 131.4 (C-8), 133.7 (CH-Ar), 171.1 (C-2).

IR ν_{max} (neat) = 2943, 2924, 2856, 1729 cm^{-1}

MS (ES+) m/z = 294 $[M+H]^+$.
HRMS (ES+) calculated 294.1348 for $C_{15}H_{24}NOSSi$, observed 294.1354 $[M + H]^+$.

mp (CH_2Cl_2)= 68-70 ^oC.

1-(*tert*-Butyldimethylsilyl)-3-(phenylsulfinyl)azetidin-2-one 143

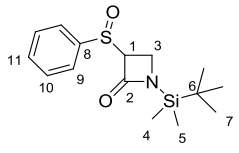

To a mixture of **142** (100 mg, 0.12 mmol), Ac_2O (36 µL, 0.38 mmol) and SiO_2 (68 mg) in dichloromethane (1.7 mL) was added 30% H_2O_2 (aq) (41 µL, 0.41 mmol). The reaction mixture was stirred for 36 hours at room temperature then filtered through a sintered funnel and the collected solid washed with CH_2Cl_2 (10 mL). The filtrate was washed sequentially with saturated $NaHSO_3$ (aq) (10 mL), saturated $NaHCO_3$ (aq) (10 mL) and Brine (10 mL), then dried

over $MgSO_4$ and concentrated *in vacuo*. The crude product was purified using flash silica column chromatography (20% EtOAc in 40-60 petroleum ether) to yield the product (83 mg, 79%) as a white solid in a 1.0:1.3 mixture of diastereomers.

^{1}H-NMR (400 MHz, $CDCl_3$): δ_H = 0.03 (s, $3H^{4/5A}$), 0.06 (s, $3H^{4/5A}$), 0.23 (s, $3H^{4/5B}$), 0.27 (s, $3H^{4/5B}$), 0.80 (s, $9H^{7A}$), 0.97 (s, $9H^{7B}$), 3.19 (dd, $1H^{3B}$, *J*=6.7Hz, *J*=5.5Hz), 3.38-3.49 (m, $2H^{3A}$), 3.67 (dd, $1H^{3B}$, *J*=6.8Hz, *J*=2.9Hz), 4.33 (dd, $1H^{1B}$, *J*=5.4Hz, *J*=2.9Hz), 4.72 (dd, $1H^{1A}$, *J*=5.3Hz, *J*=3.0Hz), 7.53 (m, 6H-Ar), 7.65 (m, 2H-Ar), 7.72 (m, 2H-Ar).

^{13}C-NMR (400 MHz, $CDCl_3$): δ_C = -6.5 (C-4/5B), -6.5 (C-4/5B), -6.3(C-4/5A), -6.2 (C-4/5A), 18.2 (C-6B), 18.5 (C-6A), 25.7 (C-7B), 25.9 (C-7A), 35.9 (C-3B), 37.8 (C-3A), 69.5 (C-1A), 71.8 (C-1B), 124.0 (CH-Ar), 125.3 (CH-Ar), 129.1 (CH-Ar), 129.4 (CH-Ar), 131.3 (CH-Ar), 131.7 (CH-Ar), 138.7 (C-8A/B), 141.9 (C-8A/B), 165.0 (C=O), 165.7 (C=O).

IR ν_{max} (neat) = 2954, 2924, 2856, 1733, 1048 cm^{-1}

MS (ES+) m/z = 310 $[M+H]^+$, 332 $[M+Na]^+$.
HRMS (ES+) calculated 310.1297 for $C_{15}H_{24}NO_2SSi$, observed 310.1304 $[M+H]^+$.

3-Bromo-*N*-(4-methoxyphenyl)propionamide 145

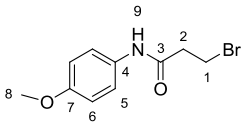

To a solution of *para*-anisidine (5.00 g, mmol) in CH_2Cl_2 (16 mL) was added 3-bromopropionyl chloride (2.15 mL, 21.4 mmol) dropwise and the resulting solution stirred for 3 hours at room temperature. The reaction mixture was then diluted with CH_2Cl_2 (100 mL), washed with H_2O (2 × 100 mL), dried over $MgSO_4$ and concentrated *in vacuo* to yield the product as a purple powder (5.15 g, 94%). The product was used directly in the next step with no further purification.
The data were in agreement with the published data.[147]

^{1}H-NMR (400 MHz, $CDCl_3$): δ_H = 2.88 (t, 2H[1], *J*=6.6Hz) 3.66 (t, 2H[2], *J*=6.6Hz) 3.76 (s, 3H[8]) 6.82 (m, 2H[6]) 7.38 (m, 2H[5]) 7.87 (s, 1H[9]).

^{13}C-NMR (400 MHz, $CDCl_3$): δ_C = 27.4 (C-1), 40.3 (C-2), 55.5 (C-8), 114.1 (C-6), 122.4 (C-5), 130.5 (C-4), 156.7 (C-7), 168.3 (C-3).

IR ν_{max} (neat) = 3250, 2831, 1651, 1603 cm^{-1}

MS (ES+) m/z = 258 $[M+H]^+$.
HRMS (ES+) calculated 258.0130 for $C_{10}H_{13}NO_2Br$, observed 258.0135 $[M+H]^+$.

1-(4-Methoxyphenyl)azetidin-2-one 146

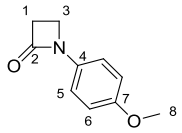

NaH (60% in mineral oil, 1.33 g, 33.2 mmol) was washed with hexanes (2 × 20 mL) and then suspended in a CH_2Cl_2-DMF mixture (4:1, 850 mL). To this was added, slowly over a period of 6 hours, a solution of the propionamide **145** (5.20 g, 20.2 mmol) in a CH_2Cl_2-DMF mixture (4:1, 340 mL). The reaction mixture was then stirred overnight at room temperature before being quenched with saturated NH_4Cl (aq) (800 mL). The organic layer was separated and washed with brine (3 × 1000 mL), H_2O (1000 mL), dried over $MgSO_4$ and concentrated *in vacuo* leaving approximately 10 mL of DMF. The product precipitated upon standing and cooling yielding the β-lactam (2.42 g, 70%) as white crystals.
The data were in agreement with the published data.[147]

^{1}H-NMR (400 MHz, $CDCl_3$): δ_H = 3.09 (t, 2H[3], *J*=4.4Hz) 3.59 (t, 2H[1], *J*=4.4Hz) 3.78 (s, 3H[10]) 6.87 (m, 2H[6]) 7.30 (m, 2H[5]).

^{13}C-NMR (400 MHz, $CDCl_3$): δ_C = 36.1 (C-3), 38.1 (C-1), 55.5 (C-8), 114.4 (C-6), 117.4 (C-5), 132.3 (C-4), 156.0 (C-7), 163.9 (C-2).

IR ν_{max} (neat) = 2950, 1727 cm^{-1}

MS (ES+) m/z = 178 $[M+H]^+$.
HRMS (ES+) calculated 178.0868 for $C_{10}H_{12}NO_2$, observed 178.0865 $[M+H]^+$.

1-(4-Methoxyphenyl)-3-(phenylsulfanyl)azetdin-2-one 147

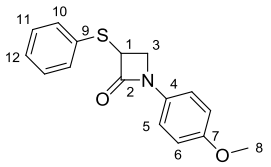

To a solution of diisopropylamine (3.08 mL, 22.0 mmol) in THF (50 mL) at –78 °C was added 1.1 M *n*-BuLi in hexanes (20 mL, 22.0 mmol) and the resulting solution stirred for 30 minutes at 0 °C. The solution was then cooled to –78 °C and a –15 °C solution of azetidinone **146** (1.95 g, 11.0 mmol) and diphenyl disulfide (2.64 g, 12.1 mmol) in THF (42 mL) added dropwise. The reaction mixture was allowed to slowly warm to room temperature overnight, then poured into saturated NH_4Cl (aq) (200 mL) and extracted with CH_2Cl_2 (300 mL). The organic layer was separated and washed with H_2O (2 × 400 mL), dried over $MgSO_4$ and concentrated *in vacuo*. The crude product was purified using flash silica column chromatography (25% EtOAc in 40-60 petroleum ether) to yield the product (1.27 g, 40%) as a yellow solid.

^{1}H-NMR (400 MHz, $CDCl_3$): δ_H = 3.49 (dd, 1H^3, *J*=6.0Hz, *J*=2.6Hz) 3.81 (s, 3H^8) 4.01 (m, 1H^3) 4.55 (dd, 1H^1, *J*=5.4Hz, *J*=2.6Hz) 6.88 (m, 2H-Ar) 7.32 (m, 5H-Ar) 7.58 (m, 2H-Ar).

^{13}C-NMR (400 MHz, $CDCl_3$): δ_C = 46.3 (C-3), 50.9 (C-1), 55.5 (C-8), 114.3 (C-6), 117.7 (C-5), 128.0 (CH-Ar), 129.2 (CH-Ar), 131.4 (C-Ar), 132.1(C-Ar), 132.2 (CH-Ar), 156.3 (C-Ar), 162.5 (C-2).

IR ν_{max} (neat) = 3048, 3003, 2943, 1733 cm^{-1}

MS (ES+) m/z = 286 $[M+H]^+$.
HRMS (ES+) calculated 286.0902 for $C_{16}H_{16}NO_2S$, observed 286.0902 $[M+H]^+$.

mp (CH_2Cl_2)= 82-85 ^oC.

3-(Benzenesulfinyl)-1-(4-Methoxyphenyl)azetidine-2-one 148

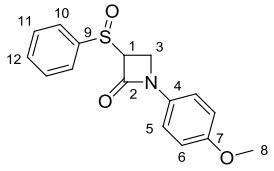

To a mixture of the sulphide **147** (800 mg, 2.8 mmol), Ac_2O (0.29 mL, 3.1 mmol) and SiO_2 (560 mg) in CH_2Cl_2 (14 mL) was added 30% H_2O_2 (aq) (0.34 mL, 3.4 mmol). The reaction mixture was stirred for 36 hours at room temperature then filtered through a celite padded frit. The filtrate was then washed sequentially with saturated $NaHSO_3$ (aq) (100 mL), saturated $NaHCO_3$ (aq) (100 mL) and brine (10 mL), then dried over $MgSO_4$ and concentrated *in vacuo*. The crude product was purified using flash silica column chromatography (50% EtOAc in 40-60 petroleum ether) to give the product (670 mg, 79%) as a pale yellow solid in a 1.0:1.3 mixture of diastereomers.

^{1}H-NMR (400 MHz, $CDCl_3$): δ_H = 3.60 (dd, 1H^{3A}, *J*=6.2Hz, *J*=5.4Hz) 3.77 (s, 3H^{8B}) 3.79 (s, 3H^{8A}) 3.84 (m, 2H^{3B}) 4.11 (dd, 1H^{3A}, *J*=6.3Hz, *J*=2.5Hz) 4.35 (dd, 1H^{1A}, *J*=5.2Hz, *J*=2.5Hz) 4.58 (dd, 1H^{1B}, *J*=4.6Hz, *J*=3.3Hz) 6.81 (m, 2H) 6.88 (m, 2H) 7.16 (m, 2H) 7.30 (m, 2H) 7.55 (m, 6H-Ar) 7.70 (m, 2H-Ar) 7.75 (m, 2H-Ar).

^{13}C-NMR (400 MHz, $CDCl_3$): δ_C = 37.5 (C-3A), 44.8 (C-3B), 55.4, 55.5 (C-8A), 67.2, 69.4 (C-1B), 114.4 (CH-Ar), 114.8 (CH-Ar), 117.4 (CH-Ar), 117.9 (CH-Ar), 123.9 (CH-Ar), 124.5 (CH-Ar), 129.1 (CH-Ar), 129.5 (CH-Ar), 130.8 (C-Ar), 131.1 (C-Ar), 131.6 (CH-Ar), 131.8 (CH-Ar), 138.9 (C-Ar), 141.6 (C-Ar),156.1 (C-Ar), 156.5 (C-Ar),156.7 (C=O), 157.2 (C=O).

IR ν_{max} (neat) = 3057, 2944, 2834, 1766, 1746 cm^{-1}

MS (ES+) m/z = 302 $[M+H]^+$, 365 $[M+Na+MeCN]^+$.
HRMS (ES+) calculated 302.0851 for $C_{16}H_{15}NO_3S$, observed 302.0838 $[M+H]^+$.

1-(4-Methoxyphenyl)-3,3-bis(phenylselanyl)azetidin-2-one 151

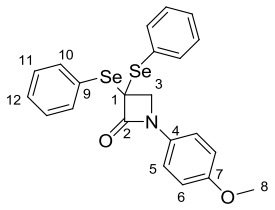

To a solution of diisopropylamine (1.52 mL, 10.9 mmol) in THF (20 mL) at −78 °C was added 1.57 M *n*-BuLi in hexanes (6.90 mL, 10.9 mmol) and the resulting solution stirred for 30 minutes at 0 °C. The solution was then cooled to −78 °C and a −15 °C solution of azetidinone **146** (840 mg, 4.74 mmol) and phenyl selenium bromide (2.45 g, 10.4 mmol) in THF (20 mL) added dropwise. The reaction mixture was allowed to slowly warm to room temperature overnight and then quenched with H_2O (60 mL), extracted into Et_2O (2 × 60 mL), dried over $MgSO_4$ and concentrated *in vacuo*. The crude product was purified using flash silica column chromatography (15% EtOAc in 40-60 petroleum ether) to yield the product (1.11 g, 48%) as a yellow oil and the monoselenide **149** (168 mg, 11%) as a yellow solid.

^{1}H-NMR (400 MHz, $CDCl_3$): δ_H = 3.68 (s, 2H^3) 3.74 (s, 3H^8) 6.74 (m, 2H, Ar-H) 6.98 (m, 2H, Ar-H) 7.32 (m, 6H, Ar-H) 7.73 (m, 4H, Ar-H).

^{13}C-NMR (400 MHz, $CDCl_3$): δ_C = 48.2 (C-1), 53.3 (C-3), 55.4 (C-8), 114.2 (CH-Ar), 117.8 (CH-Ar), 127.2 (C-Ar), 129.2 (CH-Ar), 129.4 (CH-Ar), 130.7 (C-Ar), 136.5 (CH-Ar), 156.3 (C-Ar), 163.5 (C-2).

IR ν_{max} (neat) = 3072, 3023, 2960, 2838, 1733 cm^{-1}

MS (ES+) m/z = 490 $[M+H]^+$, 553 $[M+Na+MeCN]^+$.
HRMS (ES+) calculated 489.9824 for $C_{22}H_{20}NO_2Se_2$, observed 489.9821 $[M+H]^+$.

mp (CH_2Cl_2)= 82-84 °C.

1-(4-Methoxyphenyl)-3-(phenylselanyl)azetidin-2-one 149

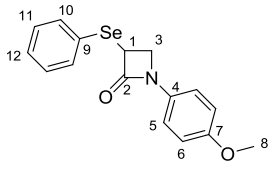

To a solution of diisopropylamine (0.04 mL, 0.20 mmol) in THF (0.8 mL) at −78 °C was added 2.06 M *n*-BuLi in hexanes (0.12 mL, 0.25 mmol) and the resulting solution stirred for 30 minutes at 0 °C. The solution was then cooled to −78 °C and a −78 °C solution of acetophenone (0.23 mL, 0.20 mmol) and the bis-selenide **151** (100 mg, 0.20 mmL) in THF (1.0 mL) added dropwise. The reaction mixture was allowed to slowly warm to room temperature overnight and then quenched with H_2O (10 mL), extracted into Et_2O (2 × 20 mL), dried over $MgSO_4$ and concentrated *in vacuo*. The crude product was purified using flash silica column chromatography (15% EtOAc in 40-60 petroleum ether) to yield the product (40 mg, 61%) as a yellow solid.

^{1}H-NMR (400 MHz, $CDCl_3$): δ_H = 3.47 (dd, 1H^3, *J*=6.2Hz, *J*=2.5Hz) 3.80 (s, 3H^8) 4.02 (m, 1H^1) 4.56 (dd, 1H^3, *J*=5.4 Hz, *J*=2.5Hz) 6.85 (m, 2H, Ar-H) 7.21 (m, 2H, Ar-H) 7.30 (m, 3H, Ar-H) 7.69 (m, 2H, Ar-H)

^{13}C-NMR (400 MHz, $CDCl_3$): δ_C = 42.6 (C-1), 46.4 (C-3), 55.4 (C-8), 114.3 (CH-Ar), 117.6, (CH-Ar) 126.2 (C-Ar), 128.5 (CH-Ar), 129.2 (CH-Ar), 131.5 (C-Ar), 135.0 (CH-Ar), 156.2 (C-Ar), 163.2 (C-2).

IR ν_{max} (neat) = 3053, 2960, 1733 cm^{-1}

MS (ES+) m/z = 334 $[M+H]^+$.
HRMS (ES+) calculated 334.0346 for $C_{16}H_{16}NO_2Se$, observed 334.0338 $[M+H]^+$.

mp (Et_2O) = 82-84 °C.

Dimethyldioxirane

To a 1 litre 3-necked flask containing a mixture of $NaHCO_3$ (45 g, 0.53 mol) in H_2O (120 mL) and acetone (100 mL) at 0 ^oC, was added oxone (90 g, 0.59 mol) in 3 portions during 10 minutes. The reaction mixture was stirred for 15 minutes before being allowed to warm to room temperature and the product collected by distillation (30 mbar), as a pale yellow solution (0.10 M in acetone, by titration with thioanisole) into a chilled receiving flask at −78 ^oC. The product was stored over anhydrous Na_2SO_4 at −25 ^oC.[150]

3-(Benzeneseleninyl)-1-(4-methoxyphenyl)azetidin-2-one 150

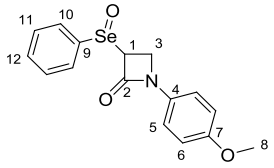

To a solution of the selenide **149** (340 mg, 1.05 mmol) in acetone (5.3 mL) was added a 0.09 M solution of dimethyldioxirane in acetone (12.9 mL, 1.16 mmol) and the mixture stirred for 20 minutes at room temperature. The reaction mixture was then concentrated *in vacuo* and purified using flash silica column chromatography (2% MeOH in $CHCl_3$) to yield the product (347 mg, 98%) as a white solid in a 1.0:1.3 mixture of diastereomers.

^{1}H-NMR (400 MHz, $CDCl_3$): δ_H = 3.53 (dd, 1H^{3B}, *J*=7.1Hz, *J*=2.0Hz) 3.59 (dd, 1H^{3A}, *J*=6.4Hz, *J*=5.3Hz) 3.73 (s, 3H^{8B}) 3.75-3.77 (m, 1H^{3B}) 3.78 (s, 3H^{8A}) 4.07 (dd, 1H^{3A}, *J*=6.4Hz, *J*=2.2Hz) 4.42 (dd, 1H^{1A}, *J*=5.2Hz, *J*=2.3Hz) 4.77 (dd, 1H^{1B}, *J*=5.0Hz, *J*=2.0Hz) 6.72-6.75 (m, 2H-Ar) 6.85-6.89 (m, 2H-Ar) 6.94-6.96 (m, 2H-Ar) 7.27-7.29 (m, 2H-Ar) 7.42-7.48 (m, 3H-Ar) 7.55-7.60 (m, 3H-Ar) 7.75-7.79 (m, 4H-Ar).

^{13}C-NMR (400 MHz, $CDCl_3$): δ_C = 37.5 (C-3A), 39.2 (C-3B), 55.4 (C-8B), 55.5 (C-8A), 62.0 (C-1A), 64.0 (C1-B), 114.2(CH-Ar), 114.4 (CH-Ar), 117.6 (CH-Ar), 117.9 (CH-Ar), 125.7(CH-Ar), 126.5 (CH-Ar), 129.4 (CH-Ar), 130.0 (CH-Ar), 130.4 (C-Ar), 131.1 (C-Ar), 131.8 (CH-Ar),

132.2 (CH-Ar), 135.1 (C-Ar), 139.1 (C-Ar), 156.6 (C-Ar), 156.7 (C-Ar), 157.8 (C=O), 158.2 (C=O).

IR ν_{max} (neat) = 2966, 1737 cm^{-1}

MS (ES+) m/z = 350 $[M+H]^+$, 372 $[M+Na]^+$.
HRMS (ESI) calculated 350.0295 for $C_{16}H_{16}NO_3Se$, observed 350.0293 $[M+H]^+$.

1-(4-Methoxyphenyl)-3-(phenylselanyl)azetidin-2-one 149 and
l-(*p*-Methoxyphenyl)azetidine-2,3-dione 152

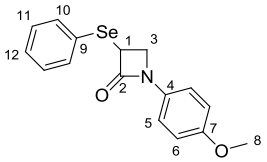

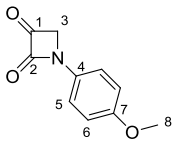

Selenoxide **150** (100 mg, 0.30 mmol) in toluene (3 mL) was heated in a sealed tube at 120 ^oC for 36 hours. The reaction mixture was then concentrated *in vacuo* and purified using flash silica column chromatography (100% $CHCl_3$) to yield selenide **149** (32 mg, 33%) and diketone **152** (17 mg, 30%).
The data were in agreement with the published data.[257]

^{1}H-NMR (400 MHz, $CDCl_3$): δ_H = 3.84 (s, $3H^8$) 4.29 (s, $2H^3$) 6.96-7.00 (m, $2H^6$) 7.48-7.51 (m, $2H^5$).

^{13}C-NMR (400 MHz, $CDCl_3$): δ_C = 55.6 (C-8), 59.6 (C-3), 114.8 (C-6), 119.0 (C-5), 130.7 (C-4), 158.1 (C-7), 159.3 (C-2), 190.6 (C-1).

IR ν_{max} (neat) = 1814, 1741 cm^{-1}

MS (ES+) m/z = 192 $[M+H]^+$.
HRMS (ES+) calculated 192.0622 for $C_{10}H_{10}NO_3$, observed 192.0613 $[M+H]^+$.

***N-p*-Methoxybenzyl-α-iminoglyoxalate 160**

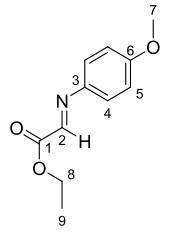

To a solution of ethyl-glyoxylate (50% in toluene, 0.48 mL, 2.4 mmol) in CH_2Cl_2 (8 mL) was added dropwise a solution of *para*-anisidine (296 mg, 2.4 mmol) in CH_2Cl_2 (4 mL) and the resulting solution stirred for 30 minutes at room temperature before being treated with 4Å molecular sieves and stirred for a further 1 hour. The reaction mixture was then filtered and concentrated *in vacuo* to yield the product (419 mg, 84%) as yellow oil, which was used directly in the next step with no further purification.
The data were in agreement with the published data.[155]

^{1}H-NMR (400 MHz, $CDCl_3$): δ_H = 1.40 (t, 3H^9, *J*=7.1Hz) 3.84 (s, 3H^7) 4.41 (q, 2H^8, *J*=7.1Hz) 6.91-6.94 (m, 2H^5) 7.35-7.37 (m, 1H^4) 7.94 (s, 1H^2)

^{13}C-NMR (100 MHz, $CDCl_3$): δ_C = 14.3 (C-9) 55.5 (C-7) 61.9 (C-8) 114.5 (C-5) 123.6 (C-4) 141.4 (C-3) 148.0 (C-2) 160.5 (C-6) 163.6 (C-1).

Ethyl 3-(benzyloxy)-1-(4-methoxyphenyl)-4-oxoazetidine-2-carboxylate 155

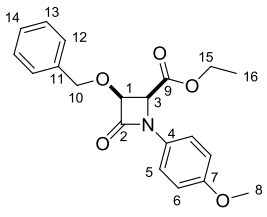

To a −78 ^{o}C solution of imine **160** (230 mg, 1.11 mmol) and NEt_3 (0.31 mL, 2.22 mmol) in CH_2Cl_2 (3 mL) was added benzyloxyacetyl chloride (0.26 mL, 1.67 mmol) dropwise. The solution was then warmed to room temperature and stirred overnight. The reaction mixture was then concentrated *in vacuo* and the crude residue purified using flash silica column

chromatography (20% EtOAc in 40-60 petroleum ether) to yield the product (201 mg, 51%) as a white solid.
The data were in agreement with the published data.[154]

^{1}H-NMR (400 MHz, $CDCl_3$): δ_H = 1.25 (t, 3H^{16}, *J*=7.2Hz) 3.82 (s, 3H^8) 4.28 (q, 2H^{15}, *J*=7.2Hz) 4.74 (d^3, 1H, *J*=5.2Hz) 4.83 (s, 2H^{10}) 5.04 (d, 1H^1, *J*=5.1Hz) 6.88-6.91 (m, 2H^6) 7.30-7.32 (m, 2H^5) 7.36-7.40 (m, 5H^{12,13,14})

^{13}C-NMR (100 MHz, $CDCl_3$): δ_C = 14.2 (C-16) 55.5 (C-8) 59.2 (C-3) 62.0 (C-15) 73.3 (C-10) 81.7 (C-1) 114.4 (CH-Ar) 118.4 (CH-Ar) 127.9 (CH-Ar), 128.2 (CH-Ar), 128.5 (CH-Ar) 130.4 (C-Ar) 136.4 (C-Ar) 156.8 (C-Ar) 162.7 (C-2) 167.6 (C-9).

IR ν_{max} (neat) =2962, 1742 cm^{-1}

MS (ES+) m/z = 356 $[M+H]^+$.
HRMS (ES+) calculated 356.1498 for $C_{20}H_{22}NO_5$, observed 356.1506 $[M+H]^+$.

1,4-Bis(4'-methoxyphenyl)-1,4-diazabuta-1,3-diene 162

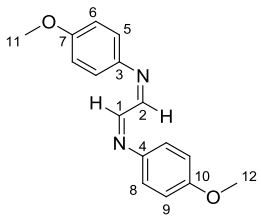

A mixture of 40% glyoxal (aq) (0.50 mL, 4.30 mmol), *para*-anisidine (1.06 g, 8.60 mmol) and catalytic formic acid in MeOH (14 mL) were stirred at room temperature for 1 hour. The precipitated solids were collected by filtration, washed with cold MeOH and dried under vacuum to give the product (805 mg, 70%) as a yellow powder.
The data were in agreement with the published data.[159]

^{1}H-NMR (400 MHz, $CDCl_3$): δ_H = 3.85 (s, 6H^{11+12}) 6.93-6.98 (m, 4H) 7.32-7.36 (m, 4H) 8.42 (s, 2H^{1+2}).

^{13}C-NMR (100 MHz, $CDCl_3$): δ_C = 55.5 (C-11+12), 114.6 (C6+9), 123.1 (C5+8), 143.0 (C3+4), 157.6 (C7+10), 159.8 (C1+2).

MS (ES+) m/z = 269 $[M+H]^+$.
HRMS (ES+) calculated 268.1290 for $C_{16}H_{17}N_2O_2$, observed 269.1310 $[M+H]^+$.

3-(Benzyloxy)-4-formyl-1-(4-methoxyphenyl)azetidin-2-one 164

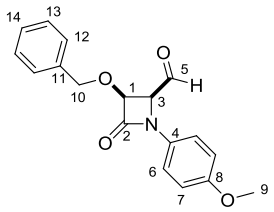

To a suspension of the di-imine **162** (690 mg, 2.57 mmol) and NEt_3 (0.43 mL, 3.09 mmol) in toluene (24 mL) was added a solution of benzoxyacetyl chloride (0.45 mL, 2.83 mmol) in toluene (12 mL) dropwise and the resulting solution stirred overnight at room temperature. The reaction mixture was diluted with $CHCl_3$ (100 mL), washed sequentially with saturated $NaHCO_3$ (aq) (50 mL) and H_2O (2 × 50 mL), then dried over $MgSO_4$ and concentrated *in vacuo*.
A solution of the crude lactam (350 mg, 0.84 mmol) in $CHCl_3$ (16 mL) was stirred with 5% HCl (aq) (8.4 mL) overnight at room temperature. The reaction was then diluted with $CHCl_3$ (50 mL), washed sequentially with 1.0 M HCl (aq) (2 × 20 mL), H_2O (20 mL) and brine (20 mL), then dried over $MgSO_4$ and concentrated *in vacuo*. The crude material was re-crystallised from EtOAc and hexanes (1:1) to yield the product (160 mg, 61%) as a brown solid.
The data were in agreement with the published data.[158]

^{1}H-NMR (400 MHz, $CDCl_3$): δ_H = 3.82 (s, 3H^9) 4.51 (dd, 1H^3, *J*=3.9Hz, *J*=5.2Hz) 4.75 (d, 1H^{10}, *J*=11.6Hz) 4.86 (d, 1H^{10}, *J*=11.7Hz) 5.07 (d, 1H^1, *J*=5.2Hz) 6.89-6.91 (m, 2H^7) 7.28-7.30 (m, 2H^6) 7.36-7.41 (m, 5H$^{12\text{-}14}$) 9.74 (d, 1H^5, *J*=3.8Hz).

^{13}C-NMR (100 MHz, $CDCl_3$): δ_C = 55.5 (C-9), 63.2 (C-3), 73.6 (C-10), 82.7 (C-1), 114.6 (CH-Ar), 118.1 (CH-Ar), 128.3 (CH-Ar), 128.5 (CH-Ar), 128.6(CH-Ar), 130.5 (C-Ar), 135.8 (C-Ar), 157.0 (C-Ar), 162.9 (C-2), 198.9 (C-5).

IR ν_{max} (neat) =2838, 1737, 1511 cm^{-1}

MS (CI+) m/z = 329 $[M+NH_4]^+$.
HRMS (CI+) calculated 329.1501 for $C_{18}H_{21}N_2O_4$, observed 329.1487 $[M+NH_4]^+$.

Ethyl 3-hydroxy-1-(4-methoxyphenyl)-4-oxoazetidine-2-carboxylate 167

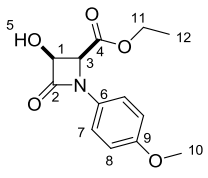

A round bottomed flask containing 10% Pd on carbon (50 mg, 0.05 mmol) was evacuated and backfilled with nitrogen three times and then evacuated and refilled with hydrogen. To this was added a solution of β-lactam **155** (106 mg, 0.30 mmol) in THF (10 mL) and the mixture stirred under hydrogen (1 atm) overnight. The reaction mixture was filtered through a celite padded frit and then concentrated *in vacuo* to yield the product as a white solid (77 mg, 97%).
The data were in agreement with the published data.[154]

^{1}H-NMR (400 MHz, $CDCl_3$): δ_H = 1.31 (t, 3H^{12}, *J*=7.1Hz) 3.71 (d, 1H^5, *J*=9.5Hz) 3.78 (s, 3H^{10}) 4.32 (q, 2H^{11}, *J*=7.1Hz) 4.69 (d, 1H^3, *J*=5.2Hz) 5.21 (dd, 1H^1, *J*=9.5Hz, *J*=5.1Hz) 6.85-6.88 (m, 2H^8) 7.27-7.30 (m, 2H^7).

^{13}C-NMR (100 MHz, $CDCl_3$): δ_C = 14.2 (C-12), 55.5 (C-10), 59.7 (C-3), 62.4 (C-11), 77.3 (C-1), 114.5 (C-8), 118.4 (C-7), 130.3 (C-6), 156.9 (C-9), 164.3 (C-2), 168.7 (C-4).

IR ν_{max} (neat) = 3239, 2942, 1719 cm^{-1}

MS (ES+) m/z = 266 $[M+H]^+$.

HRMS (ES+) calculated 265.1028 for $C_{13}H_{16}NO_5$, observed 266.1036 $[M+H]^+$.

Ethyl 1-(4-methoxyphenyl)-4-oxo-3-[(trifluoromethane)sulfonyloxy]azetidine-2-carboxylate 165

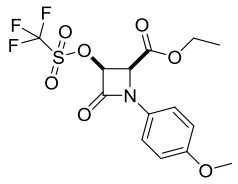

To a −78 °C solution of the alcohol **167** (70 mg, 0.26 mmol) and pyridine (90 μL, 1.14 mmol) in CH_2Cl_2 (1.75 mL) was added Tf_2O (90 μL, 0.52 mmol) slowly and the mixture warmed to 0 °C and stirred for 1 hour. The reaction mixture was diluted with CH_2Cl_2 (10 mL), washed with H_2O (2 × 10 mL), combined aqueous layers re-extracted with CH_2Cl_2 (10 mL) and the combined organic layers dried over $MgSO_4$ and concentrated *in vacuo* to yield the crude product as a yellow solid. This was used directly in the following step with no further purification.

Ethyl 3-iodo-1-(4-methoxyphenyl)-4-oxoazetidine-2-carboxylate 166 and 170

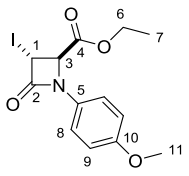

166

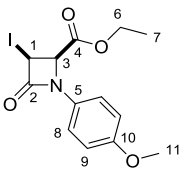

170

To a solution of triflate **165** (100 mg, 0.25 mmol) in acetone (2.5 mL) was added NaI (292 mg, 1.95 mmol) and the resulting suspension stirred for 48 hours at room temperature. The reaction mixture was then concentrated *in vacuo* and partitioned between Et_2O (10 mL) and H_2O (10 mL). The aqueous layer was re-extracted with Et_2O (10 mL), the combined organic layers dried over $MgSO_4$ and then concentrated *in vacuo*. The crude material was purified using flash silica column chromatography (30% EtOAc in 40-60 petroleum ether) to yield the trans-β-lactam (33 mg, 35%) and the cis-β-lactam (31 mg, 33%) as pale yellow amorphous solids.

Trans-diastereomer 166

^{1}H-NMR (400 MHz, $CDCl_3$): δ_H = 1.31 (t, 3H^{7}, *J*=7.2Hz) 3.82 (s, 3H^{11}) 4.31 (m, 2H^{6}) 4.63 (d, 1H^{3}, *J*=2.0Hz) 5.07 (d, 1H^{1}, *J*=1.9Hz) 6.88-6.92 (m, 2H^{9}) 7.29-7.32 (m, 2H^{8}).

^{13}C-NMR (100 MHz, $CDCl_3$): δ_C = 14.1 (C-1), 15.1 (C-7), 55.5 (C-11), 62.1 (C-3), 62.6 (C-6), 114. (C-9), 118.2 (C-8), 130.6 (C-5), 157.0 (C-10), 160.4 (C-2), 168.3 (C-4).

IR: v_{max} (neat) = 2984, 1760, 1512 cm^{-1}

Cis-diastereomer 170

^{1}H-NMR (400 MHz, $CDCl_3$): δ_H = 1.36 (t, 3H, *J*=7.2Hz) 3.82 (s, 3H) 4.31-4.44 (m, 2H^{6}) 4.81 (d, 1H^{3}, *J*=5.7Hz) 5.43 (d, 1H^{1}, *J*=5.7Hz) 6.89-6.92 (m, 2H^{9}) 7.26-7.30 (m, 2H^{8}).

^{13}C-NMR (100 MHz, $CDCl_3$): δ_C = 14.3 (C-1), 17.5 (C-7), 55.5 (C-11), 56.6 (C-3), 62.4 (C-6), 114.5 (C-9), 118.2 (C-8), 130.4 (C-5), 157.0 (C-10), 161.5 (C-2), 169.3 (C-4).

IR: v_{max} (neat) = 2995, 1749, 1513 cm^{-1}

MS (ES+) m/z = 376 $[M+H]^+$.

HRMS (ES+) calculated 376.0046 for $C_{13}H_{15}NO_4I$, observed 376.0056 $[M+H]^+$.

3-Iodo-1-(4-methoxyphenyl)-4-oxoazetidine-2-carboxylic acid 171

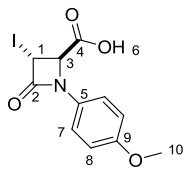

A solution of β-lactam **166** (76 mg, 0.20 mmol) in THF (1 mL) was treated with potassium trimethylsilanolate (43 mg, 0.30 mmol) and the resulting suspension stirred at room temperature for 10 minutes. The reaction mixture was then concentrated *in vacuo,* dissolved in H_2O (10 mL) and washed with EtOAc (2 ×10 mL). Acidification of the aqueous layer using 1.0 M HCl (aq)

(15 mL) was followed by extraction into CH_2Cl_2 (2 x 10 mL). Combined organic layers were dried over $MgSO_4$ and concentrated under reduced pressure to yield the product (42 mg, 60%) as a yellow gum.

^{1}H-NMR (400 MHz, $CDCl_3$): δ_H = 3.82 (s, 3H^{10}) 4.66 (d, 1H^3, *J*=2.0Hz) 5.13 (d, 1H^1, *J*=2.0Hz) 5.41 (br s, 1H^6) 6.89-6.93 (m, 2H^8) 7.30-7.34 (m, 2H^7).

^{13}C-NMR (100 MHz, $CDCl_3$): δ_C = 14.7 (C-1), 55.6 (C-10), 61.7 (C-3), 114.7 (C-8), 118.3 (C-7), 130.4 (C-5), 157.2 (C-9), 160.5 (C-2), 171.8 (C-4).

IR ν_{max} (neat) = 3460, 2932, 1734, 1612 cm^{-1}

MS (ES-) m/z = 346 [M-H]$^-$.
HRMS (ES-) calculated 345.9576 for $C_{11}H_9NO_4I$, observed 345.9588 [M-H]$^-$.

2-Methylidenebut-3-en-1-ol 174

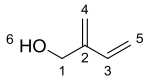

To a −78 ^{o}C solution of HMDS (0.64 mL, 3.04 mmol) in Et_2O (2.40 mL) was added 2.5 M *n*-BuLi (1.14 mL, 2.85 mmol) dropwise. The resulting mixture was warmed to room temperature during 30 minutes then 2-methyl-2-vinyloxirane (0.23 mL, 2.38 mmol) added and the solution refluxed for 24 hours. The reaction mixture was then cooled to room temperature poured into cold 1.0 M HCl (aq) (20 mL), stirred for 1 hour and extracted into Et_2O (3 × 10 mL). Combined organic layers were washed sequentially with saturated $NaHCO_3$ (aq) (10 mL) and brine (10 mL), then dried over $MgSO_4$ and concentrated *in vacuo* to yield the crude product as a volatile, colourless oil. This was used directly in the next step with no further purification.

^{1}H-NMR (400 MHz, $CDCl_3$): δ_H = 1.54 (s, 1H^6) 4.38 (s, 2H^1) 5.14-5.19 (m, 2H^5) 5.29-5.34 (m, 2H^4) 6.43 (dd, 1H^3, *J*=17.9Hz, *J*=11.1Hz).

^{13}C-NMR (100 MHz, $CDCl_3$): δ_C = 62.6 (C-1), 114.1 (C-5), 115.7 (C-4), 136.3 (C-3), 145.2 (C-2).

Methoxy[(2-methylidenebut-3-en-1-yl)oxy]methane 175

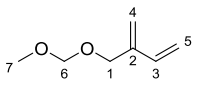

To a solution of the crude isoprenol **174** (700 mg, 8.3 mmol) and DIPEA (3.04 mL, 17.5 mmol) in CH_2Cl_2 (70 mL) was added chloromethyl methyl ether (1.26 mL, 16.6 mmol) dropwise and the resulting solution stirred for 16 hours at room temperature. The reaction mixture was quenched with H_2O (200 mL) and extracted with CH_2Cl_2 (2 × 150 mL). The combined organic layers were then washed with 1.0 M HCl (aq) (15-0 mL), dried over $MgSO_4$ and concentrated *in vacuo*. The crude material was purified by flash silica column chromatography (8% Et_2O in pentane) to yield the product (596 mg, 56%, over 2 steps) as a volatile, colourless oil.

^{1}H-NMR (400 MHz, $CDCl_3$): δ_H = 3.43 (s, 3H^7) 4.28 (s, 2H^1) 4.71 (s, 2H^6) 5.14-5.23 (m, 2H^5) 5.31-5.36 (m, 2H^4) 6.43 (dd, 1H^3, *J*=17.8Hz, *J*=11.0Hz).

^{13}C-NMR (100 MHz, $CDCl_3$): δ_C = 55.4 (C-7), 66.7 (C-1), 95.7 (C-6), 114.4 (C-5), 117.5 (C-4), 136.6 (C-3), 142.2 (C-2).

IR ν_{max} (neat) = 2934, 2887, 1598 cm^{-1}

HRMS: Did not provide spectra suitable for interpretation.

1-((methoxymethoxy)methyl)-5-(3-(methoxymethoxy)prop-1-en-2-yl)cyclohex-1-ene 176 and 1-((methoxymethoxy)methyl)-4-(3-(methoxymethoxy)prop-1-en-2-yl)cyclohex-1-ene 177

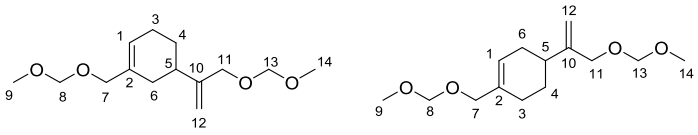

A mixture of β-lactam salt **171** (75 mg, 0.20 mmol) and diene **175** (250 mg, 1.95 mmol) was heated at 125 ^{o}C for 16 hours in a sealed tube. The reaction mixture was cooled to room temperature, diluted with EtOAc (15 mL) and washed with H_2O (15 mL). The organic layer was dried over $MgSO_4$ and concentrated *in vacuo* to yield the crude product. The crude product was purified using flash silica column chromatography (10% Et_2O in pentane) to yield the product (72 mg, 58%) as a 1.0:1.0 mixture of regioisomers.

^{1}H-NMR (400 MHz, $CDCl_3$): δ_H = 1.45-2.31 (m, 14H^{3,4,5,6}), 3.39-3.40 (m, 12H^{9,14}), 3.94 (br, s 4H^{7}), 4.08 (m, 4H^{11}), 4.64-4.67 (m, 8H^{8,13}), 4.96-4.98 (m, 2H^{12}), 5.09-5.12 (m, 2H^{12}), 5.67-5.77 (m, 2H^{1}).

^{13}C-NMR (100 MHz, $CDCl_3$): δ_C = 25.5 (C-3), 26.5 (C-3), 27.5 (C-4), 27.6 (C-4), 30.9 (C-6), 31.9 (C-6), 36.9 (C-5), 37.0 (C-5), 55.2 (C-9), 55.3 (C-14), 69.4 (C-11), 69.4 (C-11), 71.5 (C-7), 71.8 (C-7), 95.5 (C-8/13), 95.7 (C-8/13), 110.5 (C-12), 110.5 (C-12), 124.6 (C-1), 125.0 (C-1), 134.0 (C-2), 134.2 (C-2), 149.8 (C-10), 149.8 (C-10).

IR ν_{max} (neat) = 2926, 2883, 2839 cm^{-1}

MS (ES+) m/z = 279 $[M+Na]^+$.
HRMS (ES+) calculated 279.1572 for $C_{14}H_{24}O_4Na$, observed 279.1592 $[M+Na]^+$.

1-(Adamantan-1-yl)-3-(4-methoxyphenyl)urea 180

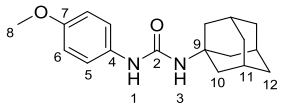

A suspension of β-lactam salt **171** (80 mg, 0.21 mmol), 1-adamantyl isocyanate (186 mg, 1.05 mmol) and 18-crown-6 (55 mg, 0.21 mmol) in *o*-xylene (0.5 mL) was heated at 130 ^{o}C for 2 hours. The reaction mixture was cooled to room temperature, diluted with EtOAc (10 mL) and washed with H_2O (15 mL). The organic layer was dried over $MgSO_4$ and concentrated *in vacuo* to yield the crude product. The crude product was purified using flash silica column chromatography (30% EtOAc in 40-60 petroleum ether) to yield the product (4 mg, 6%) as an orange solid.

The data were in agreement with the published data.[258]

^{1}H-NMR (400 MHz, $CDCl_3$): δ_H = 1.63-1.69 (m, 6H^{12}), 1.95 (dd, 6H^{10}, *J*=9.6Hz, *J*=2.9Hz), 2.02-2.10 (m, 3H^{11}), 3.79 (s, 3H^{8}), 4.36 (s, 1H^{1}), 5.87 (s, 1H^{3}), 6.83-6.87 (m, 2H-Ar), 7.14-7.18 (m, 2H-Ar).

^{13}C-NMR (100 MHz, $CDCl_3$): δ_C = 29.5 (C-11), 36.4 (C-12), 42.3 (C-10), 51.2 (C-9), 55.5 (C-8), 114.5 (C-6), 124.5 (C-5), 131.4 (C-4), 155.3 (C-7), 157.0 (C-2).

IR ν_{max} (neat) = 3323, 2905, 1628, 1553 cm^{-1}

MS (ES+) m/z = 301 $[M+H]^+$.

HRMS (ES+) calculated 301.1916 for $C_{18}H_{25}N_2O_2$, observed 301.1922 $[M+H]^+$.

4,6-*O*-Benzylidene-D-glucopyranose 197

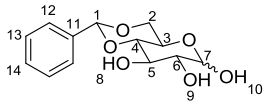

To oven dried anhydrous D-glucose (10 g, 55.5 mmol) was added catalytic *para*-toluenesulfonic acid (50 mg), benzaldehyde dimethyl acetal (9.2 mL, 61.1 mmol) and DMF (40 mL). The resulting suspension was heated under reduced pressure (330 mbar) at 60 ^{o}C for 30 minutes until the glucose had dissolved. The reaction was quenched by cooling and the addition of excess NEt_3 (1.5 mL), then concentrated *in vacuo* to yield the crude product. The crude product was purified using flash silica column chromatography (0.1% NEt_3 in EtOAc) to yield the product (7.3 g, 49%) as a white solid in a 1.0:1.5 mixture of α and β-anomers.
The data were in agreement with the published data.[167]

^{1}H-NMR (400 MHz, DMSO-d_6): δ_H = 3.02 (td, 1H$^{6\alpha}$, *J*=7.9Hz, *J*=5.2Hz), 3.23-3.43 (m, 5H$^{3\alpha,4\alpha,4\beta,5\alpha,6\beta,}$), 3.59-3.69 (m, 3H$^{2\alpha,2\beta,5\beta}$), 3.80 (td, 1H$^{3\beta}$, *J*=10.0Hz, *J*=4.8Hz), 4.09 (dd, 1H$^{2\beta}$, *J*=9.9Hz, *J*=4.8Hz), 4.16 (dd, 1H$^{2\alpha}$, *J*=10.2Hz, *J*=4.0Hz), 4.43-4.47 (m, 1H$^{7\alpha}$), 4.81 (d, 1H$^{9\beta}$, *J*=6.9Hz), 4.97-5.00 (m, 1H$^{7\beta}$), 5.10 (d, 1H$^{8\beta}$, *J*=5.0Hz), 5.18 (d, 1H$^{9\alpha}$, *J*=5.1Hz), 5.23 (d, 1H$^{8\alpha}$, *J*=4.7Hz), 5.56 (s, 1H$^{1\beta}$), 5.57 (s, 1H$^{1\alpha}$), 6.55 (d, 1H$^{10\beta}$, *J*=4.8Hz), 6.84 (d, 1H$^{10\alpha}$, *J*=6.6Hz), 7.36-7.40 (m, 6H-Ar), 7.43-7.46 (m, 4H-Ar).

^{13}C-NMR (400 MHz, DMSO-d_6): δ_C = 62.4 (C-3β), 66.2 (C-3α), 68.5 (C-2α), 68.9 (C-2β), 70.1 (C-5α), 73.3 (C-5β), 73.4 (C-6α), 76.2 (C-6β), 81.4 (C-4α), 82.2 (C-4β), 93.6 (C-7β), 98.1 (C-7α), 101.1 (C-1α), 101.3 (C-1β),126.8 (CH-Ar), 126.8 (CH-Ar), 128.5 (CH-Ar), 129.3 (CH-Ar), 138.3 (C-Ar), 138.4 (C-Ar).

Note: missing 2 × CH-Ar due to overlapping peaks.

IR ν_{max} (neat) = 3314, 1386 cm^{-1}

MS (ES+) m/z = 269 $[M+H]^+$.
HRMS (ES+) calculated 269.1025 for $C_{13}H_{17}O_6$, observed 269.1035 $[M+H]^+$.

1,3-Benzylidene-L-erythritol 198

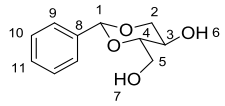

A mixture of glucopyranose **197** (7.0 g, 25.9 mmol), sodium metaperiodate (11.4 g, 53.1 mmol) and sodium bicarbonate (5.8 g, 84.0 mmol) in THF-H_2O (1.0:2.3, 265 mL) was stirred at room temperature for 1 hour. The reaction was then cooled to 0 ^oC, sodium borohydride (2.00 g, 53.1 mmol) was added and the reaction mixture stirred for a further hour at 0 ^oC. The precipitate was then filtered off, the filtrate extracted with ethyl acetate (2 x 200 mL), washed with saturated Na_2SO_4 (aq)-$NaHCO_3$ (aq) (1:1, 2 × 200 mL) and dried over $MgSO_4$. The organic layer was concentrated *in vacuo* to yield the product (5.09 g, 94%) as a white solid.
The data were in agreement with the published data.[168]

^{1}H-NMR (400 MHz, DMSO-d_6): δ_H = 3.46-3.58 (m, 4H^{2,3,4,5}), 3.71-3.78 (m, 1H^5), 4.07-4.13 (m, 1H^2), 4.64 (t, 1H^7, *J*=5.7Hz), 5.17 (d, 1H^6, *J*=5.0Hz), 5.50 (s, 1H^1), 7.35-7.37 (m, 3H-Ar), 7.44-7.46 (m, 2H-Ar).

^{13}C-NMR (400 MHz, DMSO-d_6): δ_C = 61.3 (C-3, 5), 71.2 (C-2), 83.6 (C-4), 100.6 (C-1), 126.8 (CH-Ar), 128.4 (CH-Ar), 129.0 (CH-Ar), 138.8 (C-8).

IR ν_{max} (neat) = 3282, 2947, 1454 cm^{-1}

MS (CI) m/z = 211 $[M+H]^+$, 228 $[M+NH_4]^+$.
HRMS (CI+) calculated 228.1236 for $C_{11}H_{18}O_4N$, observed 228.1241 $[M+NH_4]^+$.

(4*S*,5*R*)-4-((*tert*-Butyldimethylsilyloxy)methyl)-2-phenyl-1,3-dioxan-5-ol 185

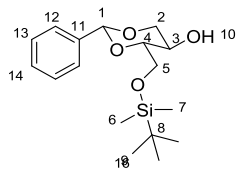

A solution of diol **198** (4.88 g, 23.2 mmol) and imidazole (1.74 g, 25.5 mmol) in anhydrous CH_2Cl_2 (430 mL) was stirred at 0 ^oC while TBSCl (4.37 g, 29.0 mmol) was added during 5 minutes. The resulting milky solution was stirred overnight at room temperature, then excess ethanol amine (2.5 mL) added and the mixture stirred for a further 30 minutes. The reaction mixture was diluted with H_2O (300 mL), extracted with CH_2Cl_2 (2 × 250 mL), the combined organic layers washed with brine (300 mL), dried over $MgSO_4$ and concentrated *in vacuo*. The crude product was purified using flash silica column chromatography (20% acetone in 40-60 petroleum ether) to yield the product (6.10 g, 81%) as a colourless, viscous oil.
The data were in agreement with the published data.[169]

^{1}H-NMR (400 MHz, $CDCl_3$): δ_H = 0.12 (s, 3H$^{6/7}$), 0.13 (s, 3H$^{6/7}$), 0.92 (s, 9H^9), 3.46 (d, 1H^{10}, *J*=1.2Hz), 3.62-3.67 (m, 1H^5), 3.74-3.77 (m, 1H^3), 3.85 (dd, 1H^2, *J*=9.6Hz, *J*=8.8Hz), 3.88-4.01 (m, 1H^4), 4.04 (dd, 1H^2, *J*=9.7Hz, *J*=4.6Hz), 4.33 (dd, 1H^5, *J*=10.9Hz, *J*=5.3Hz), 5.50 (s, 1H^1), 7.34-7.39 (m, 3H), 7.45-7.48 (m, 2H).

^{13}C-NMR (400 MHz, $CDCl_3$): δ_C = -5.6 (C-6/7), -3.6 (C-6/7), 18.6 (C-8), 25.8 (C-9), 66.3 (C-5), 66.6 (C-4), 70.5 (C-2), 78. 9 (C-3), 101.1 (C-1), 126.1 (CH-Ar), 128.3 (CH-Ar), 129.0 (CH-Ar), 137.4 (C-11).

IR ν_{max} (neat) = 3473, 2958, 2860, 1251 cm^{-1}

MS (ES+) m/z = 325 $[M + H]^+$, 347 $[M+Na]^+$, 388 $[M+Na+MeCN]^+$.
HRMS (ES+) calculated 325.1835 for $C_{17}H_{29}O_4Si$, observed 325.1837 $[M+H]^+$.

(4*S*,5*S*)-4-((*tert*-Butyldimethylsilyloxy)methyl)-2-phenyl-1,3-dioxan-5-yl benzoate 199

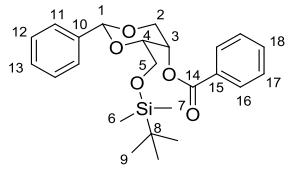

To a 0 °C solution of alcohol **185** (100 mg, 0.31 mmol) in toluene (3.0 mL) was added triphenylphosphine (420 mg, 1.54 mmol) and benzoic acid (188 mg, 1.54 mmol). To the resulting solution was then added DIAD (0.30 mL, 1.54 mmol), the reaction heated to reflux and stirred for 72 hours. The reaction mixture was diluted with saturated $NaHCO_3$ (aq) (7 mL), extracted with CH_2Cl_2 (3 × 6 mL), dried over magnesium sulphate and concentrated *in vacuo*. The crude product was purified using flash silica column chromatography (20% EtOAc in 40-60 petroleum ether) to yield the product (40 mg, 29%) as a colourless oil.

^{1}H-NMR (400 MHz, $CDCl_3$): δ_H = -0.09 (s, 3H$^{6/7}$), -0.03 (s, 3H$^{6/7}$), 0.81 (s, 9H^9), 3.81-3.89 (m, 2H^2), 4.20 (dd, 1H^5, *J*=13.0Hz, *J*=1.4Hz), 4.25 (ddd, 1H^3, *J*=7.8Hz, *J*=6.0Hz, *J*=1.6Hz), 4.49 (dd, 1H^5, *J*=13.0Hz, *J*=1.3Hz), 5.12-5.14 (m, 1H^4), 5.66 (s, 1H^1), 7.36-7.42 (m, 3H-Ar), 7.44-7.48 (m, 2H-Ar), 7.53-7.60 (m, 3H-Ar), 8.13-8.15 (m, 2H-Ar).

^{13}C-NMR (400 MHz, $CDCl_3$): δ_C = -5.5 (C-6/7), -5.4 (C-6/7), 18.1 (C-8), 25.7 (C-9), 61.3 (C-5), 65.4 (C-4), 69.6 (C-2), 78.2 (C-3), 101.3 (C-1), 126.2 (CH-Ar), 128.3 (CH-Ar), 128.4 (CH-Ar), 129.1 (CH-Ar), 129.8 (CH-Ar), 130.1 (C-15), 133.1 (CH-Ar), 137.9 (C-10), 166.1 (C-14).

IR ν_{max} (neat) = 2930, 2857, 1722, 1271 cm^{-1}

MS (ESI) m/z: Did not provide spectra suitable for interpretation.

(2*R*,4*S*)-4-[[*tert*-Butyl(dimethyl)silyl]methyl]-2-phenyl-1,3-dioxan-5-one 201

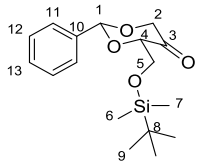

To a solution of oxalyl chloride (2.26 mL, 26.7 mmol) in CH_2Cl_2 (80 mL) at −78 °C was added DMSO (3.80 mL, 53.4 mmol). After 5 minutes a solution of alcohol **185** (5.78 g, 17.8 mmol) in CH_2Cl_2 (25 mL) was added and the reaction mixture stirred at −78 °C for 1 hour. The reaction mixture was then treated with NEt_3 (11.2 mL, 80.1 mmol), before being slowly warmed to 0 °C and stirred for 15 minutes. The solution was then poured into cold saturated NH_4Cl (aq) (250 mL), extracted with EtOAc (2 × 300 mL), dried over $MgSO_4$ and concentrated *in vacuo*. The crude product was purfied using flash silica column chromatography (15% EtOAc in 40-60 petroleum ether) to yield the product (5.06 g, 88%) as a yellow oil.

^{1}H-NMR (400 MHz, $CDCl_3$): δ_H = 0.06 (s, 3H$^{6/7}$), 0.08 (s, 3H$^{6/7}$), 0.89 (s, 9H^9), 4.06-4.09 (m, 2H^5), 4.39-4.50 (m, 2H^2), 4.52-4.54 (m, 1H^4), 5.94 (s, 1H^1), 7.39-7.44 (m, 3H-Ar), 7.54-7.58 (m, 2H-Ar).

^{13}C-NMR (400 MHz, $CDCl_3$): δ_C = -5.4 (C-6/7), -5.3 (C-6/7), 18.3 (C-8), 25.8 (C-9), 62.8 (C-5), 72.6 (C-2), 84.1 (C-4), 99.2 (C-1), 126.2 (CH-Ar), 128.4 (CH-Ar), 129.2 (CH-Ar), 137.1 (C-10), 205.2 (C-3).

IR ν_{max} (neat) = 2928, 2857, 1738, 1253 cm^{-1}

MS (ES+) m/z = 323 $[M+H]^+$.
HRMS (ES+) calculated 323.1679 for $C_{17}H_{27}O_4Si$, observed 323.1669 $[M+H]^+$.

(4*S*,5*S*)-4-[[*tert*-Butyl(dimethyl)silyl]oxymethyl]-2-phenyl-1,3-dioxan-5-ol 200

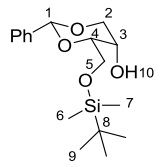

To a −78 °C solution of ketone **201** (4.50 g, 14.0 mmol) in THF (26 mL) was added 1.0 M L-selectride in THF (26.5 mL, 26.5 mmol) dropwise and the resulting solution stirred at −78 °C for 3 hours. The reaction mixture was then warmed to room temperature and treated with 10% NaOH (aq) (250 mL), the layers were separated and the aqueous layer was extracted with EtOAc (3 × 300 mL). The combined organic layers were dried over $MgSO_4$ and concentrated *in vacuo* to yield the crude product. The crude product was purified using flash silica column chromatography (15% EtOAc in 40-60 petroleum ether) to yield the product (3.82 g, 84%) as a colourless oil.

^{1}H-NMR (400 MHz, $CDCl_3$): δ_H = 0.08 (s, 3H$^{6/7}$), 0.09 (s, 3H$^{6/7}$), 0.91 (s, 9H^9), 2.83 (d, 1H^{10}, *J*=10.2Hz), 3.70-3.74 (m, 1H^3), 3.80 (dd, 1H^5, *J*=10.1Hz, *J*=5.3Hz), 3.91 (dd, 1H^5, *J*=10.1Hz, *J*=6.7Hz), 3.98 (ddd, 1H^4, *J*=6.7Hz, *J*=5.3Hz, *J*=1.1Hz), 4.08 (dd, 1H^2, *J*=11.9Hz, *J*=1.3Hz), 4.25 (dd, 1H^2, *J*=11.9Hz, *J*=1.9Hz), 5.59 (s, 1H^1), 7.35-7.40 (m, 3H-Ar), 7.48-7.51 (m, 2H-Ar).

^{13}C-NMR (400 MHz, $CDCl_3$): δ_C = -5.4 (C-6/7), -5.4 (C-6/7), 18.3 (C-8), 25.8 (C-9), 62.4 (C-5), 63.7 (C-4), 72.7 (C-2), 79.8 (C-3), 101.4 (C-1), 126.0 (CH-Ar), 128.2 (CH-Ar), 129.0 (CH-Ar), 137.4 (C-Ar).

IR ν_{max} (neat) = 3465, 2958, 2927, 1250 cm^{-1}

MS (ES+) m/z = 325 $[M+H]^+$, 347 $[M+Na]^+$.
HRMS (ESI) calculated 325.1835 for $C_{17}H_{29}O_4Si$, observed 325.1837 $[M+H]^+$.

(4*S*,5*S*)-4-((*tert*-Butyldimethylsilyloxy)methyl)-2-phenyl-1,3-dioxan-5-yl trifluoromethanesulfonate 202

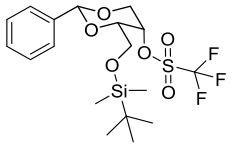

To a stirred solution of alcohol **200** (300 mg, 0.92 mmol) and pyridine (0.33 mL, 4.07 mmol) in CH_2Cl_2 (6.0 mL) at −78 °C, was added trifluoromethanesulfonate anhydride (0.31 mL, 1.85 mmol) dropwise. The resulting solution was warmed to 0 °C and stirred for 2 hours. The reaction was then diluted with CH_2Cl_2 (30 mL), washed with H_2O (3 × 20 mL), dried over $MgSO_4$ and concentrated *in vacuo* to yield the crude product as an orange residue which was used directly in the proceeding step with no further purification.

***tert*-Butyl-dimethyl-[[(2*R*,4*S*,5*R*)-2-phenyl-5-phenylsulfanyl-1,3-dioxan-4-yl]methoxy]silane 203**

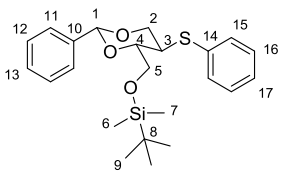

To a stirred suspension of 1.0 M ^{t}BuOK in THF (1.5 mL, 1.50 mmol) and 18-crown-6 (138 mg, 0.52 mmol) in THF (1.0 mL) at −55 °C was added thiophenol (0. 16 mL, 1.50 mmol). To this was added a solution of triflate **202** (470 mg, 1.03 mmol) in THF (1.2 mL). The reaction mixture was stirred for 48 hours at −55 °C and then treated with saturated $NaHCO_3$ (aq) (10 mL) and extracted into Et_2O (25 mL). The organic layer was washed with H_2O (15 mL), brine (15 mL), dried over $MgSO_4$ and concentrated *in vacuo* to yield the crude product. The crude product was purified using flash silica column chromatography (40% CH_2Cl_2 in 40-60 petroleum ether) to yield the product (206 mg, 48%) as a colourless oil.

^{1}H-NMR (400 MHz, $CDCl_3$): δ_H = 0.04 (s, 3H$^{6/7}$), 0.06 (s, 3H$^{6/7}$), 0.09 (s, 9H^9), 3.51-3.57 (m, 1H^3), 3.76 (ddd, 1H^4, *J*=10.6Hz, *J*=4.0Hz, *J*=1.9Hz), 3.79 (m, 1H^2) 4.03 (dd, 1H^5, *J*=11.5Hz, *J*=

1.9Hz), 4.10 (dd, 1H[5], *J*= 11.5 Hz, *J*=4.0Hz), 4.34 (dd, 1H[2], *J*=11.4Hz, *J*=5.1Hz), 5.20 (s, 1H[1]), 7.24-7.36 (m, 6H-Ar), 7.46-7.52 (m, 4H-Ar).

^{13}C-NMR (400 MHz, $CDCl_3$): δ_C = -5.3 (C-6/7), -5.1 (C-6/7), 18.4 (C-8), 25.9 (C-9), 41.7 (C-3), 63.3 (C-5), 71.0 (C-2), 81.4 (C-4), 101.4 (C-1), 126.2 (CH-Ar), 127.5 (CH-Ar), 128.2 (CH-Ar), 128.9 (CH-Ar), 129.1 (CH-Ar), 132.3 (C-Ar), 138.0 (C-Ar).

Note: missing 1 × CH-Ar due to overlapping signals.

IR ν_{max} (neat) = 3031, 2956, 2927, 2855, 1252 cm^{-1}

MS (EI+) m/z = 417 $[M+H]^+$.
HRMS (EI+) calculated 417.2051 for $C_{23}H_{33}O_3SSi$, observed 417.2057 $[M+H]^+$.

[(4*S*,5*R*)-2-Phenyl-5-phenylsulfanyl-1,3-dioxan-4-yl]methanol 205

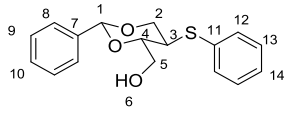

1.0 M TBAF in THF (0.79 mL, 0.79 mmol) was added dropwise to a 0 ^oC solution of the protected alcohol **203** (300 mg, 0.72 mmol) in THF (1.2 mL). The reaction mixture was then warmed to room temperature and stirred for a further 15 minutes at this temperature, before being poured into H_2O (10 mL) and extracted into Et_2O (2 × 30 mL). The combined organic layers were dried over $MgSO_4$ and concentrated *in vacuo* to yield the crude product. The crude product was purified using flash silica column chromatography (15% EtOAc in 40-60 petroleum ether) to yield the product (173 mg, 79%) as an amorphous, white solid.

^{1}H-NMR (400 MHz, $CDCl_3$): δ_H = 2.07 (t, 1H[6], *J*=6.8Hz), 3.43-3.51 (m, 1H[3]), 3.81-3.87 (m, 1H[2]), 3.85 (ddd, 1H[4], *J*=10.5Hz, *J*= 5.0Hz, *J*= 2.6Hz), 3.98 (ddd, 1H[5], *J*=12.0Hz, *J*=6.8Hz, *J*=5.1Hz) 4.11 (ddd, 1H[5], *J*=12.0Hz, *J*=6.8Hz, *J*=2.6Hz), 4.38 (dd, 1H[2], *J*=11.4Hz, *J*=5.1Hz) 5.54 (s, 1H[1]), 7.33-7.42 (m, 6H-Ar), 7.48-7.53 (m, 4H-Ar).

^{13}C-NMR (400 MHz, $CDCl_3$): δ_C = 41.9 (C-3), 63.0 (C-5), 70.8 (C-2), 80.7 (C-4), 101.3 (C-1), 126.1 (CH-Ar), 128.0 (CH-Ar), 128.4 (CH-Ar), 129.3 (CH-Ar), 132.2 (C-Ar), 132.7 (CH-Ar), 137.5 (C-Ar).

Note: missing 1 × CH-Ar due to overlapping signals.

IR ν_{max} (neat) = 3348, 3071, 2975, 2858, 1138 cm^{-1}

MS (EI+) m/z: 302 $[M]^+$.
HRMS (EI+) calculated 302.0977 for $C_{17}H_{18}O_3S$, observed 302.0977 $[M]^+$.

(4*R*,5*R*)-4-(Iodomethyl)-2-phenyl-5-phenylsulfanyl-1,3-dioxane 206

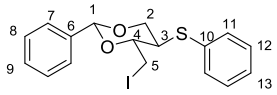

Triphenylphosphine (290 mg, 1.12 mmol), imidazole (284 mg, 1.12 mmol) and I_2 (142 mg, 1.12 mmol) were added to a solution of alcohol **205** (170 mg, 0.56 mmol) in CH_2Cl_2 (10 mL). The reaction mixture was stirred for 3 hours at room temperature then concentrated *in vacuo* to yield the crude product, which was purified using flash silica column chromatography (2.5% EtOAc in 40-60 petroleum ether) to yield the product (147 mg, 64%) as a white solid.

^{1}H-NMR (400 MHz, $CDCl_3$): δ_H = 3.31 (ddd, 1H^3, *J*=11.2Hz, *J*=9.9Hz, *J*=5.0Hz), 3.56-3.66 (m, 2H^{4,5}), 3.81-3.90 (m, 2H^{2,5}) 4.33 (dd, 1H^2, *J*=11.5Hz, *J*=5.0Hz) 5.57 (s, 1H^1) 7.37-7.46 (m, 6H-Ar), 7.51-7.55 (m, 4H-Ar).

^{13}C-NMR (400 MHz, $CDCl_3$): δ_C = 7.9 (C-5), 47.0 (C-3), 70.5 (C-2), 78.7 (C-4), 101.2 (C-1), 126.1 (CH-Ar), 128.3 (CH-Ar), 129.1 (CH-Ar), 129.4 (CH-Ar), 131.5 (C-Ar), 133.3 (CH-Ar), 137.4 (C-Ar).

Note: missing 1 × CH-Ar due to overlapping signals.

IR ν_{max} (neat) = 2982, 2855, 1215 cm^{-1}

MS (EI+) m/z = 412 $[M]^+$.
HRMS (EI+) calculated 411.9994 for $C_{17}H_{17}IO_2S$, observed 411.9989 $[M]^+$.

mp (CH_2Cl_2) = 62-66 ^oC.

Ethyl 3-Bromopropionamidoacetate 195

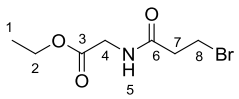

To a stirred solution of glycine-ethyl-ester hydrochloride (100 mg, 0.72 mmol) in H_2O-THF (1:1, 4.0 mL) at 0 ^oC, was added a solution of 3-bromopropionyl (80 μL, 0.72 mmol) chloride in THF (1.0 mL) during 10 minutes, maintaining a pH between 5.5-6.5 using 1.0 M NaOH (aq). The reaction mixture was then stirred for 30 minutes, before being warmed to room temperature and stirred for a further hour. The reaction mixture was then extracted into EtOAc (25 mL), washed with brine (2 × 30 mL), dried over $MgSO_4$ and concentrated *in vacuo*. The crude product was triturated twice with 40-60 petroleum ether (5.0 mL) to yield the product (141 mg, 83%) as a white solid.
The data were in agreement with the published data.[166]

^{1}H-NMR (400 MHz, $CDCl_3$): δ_H = 1.29 (t, $3H^1$, *J*=7.2Hz), 2.84 (t, $2H^7$, *J*=6.7Hz), 3.63 (t, $2H^8$, *J*=6.7Hz), 4.06 (d, $2H^4$, *J*=5.0Hz), 4.23 (q, $2H^2$, *J*=7.2Hz), 6.18 (d, $1H^5$, *J*=5.1Hz).

^{13}C-NMR (400 MHz, $CDCl_3$): δ_C = 14.1 (C-1), 26.8 (C-8), 39.3 (C-7), 41.5 (C-4), 61.7 (C-2), 169.8 (C-3), 207.1 (C-6).

IR ν_{max} (neat) = 3286, 2986, 1741, 1647 cm^{-1}

MS (ES+) m/z = 238 $[M+H]^+$.
HRMS (ES+) calculated 238.0079 for $C_7H_{13}BrNO_3$, observed 238.0085 $[M+H]^+$.

Ethyl-(2-oxoazetidin-1-yl)acetate 189

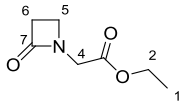

Pulverised KOH (360 mg, 6.41 mmol) and tetrabutylammonium bromide (348 mg, 1.08 mmol) were suspended in a CH_2Cl_2-MeCN solution (19:1, 110 mL) and stirred vigorously at room temperature. To this was added a solution of bromide **195** (1.22 g, 5.13 mmol) in CH_2Cl_2-MeCN (19:1, 110 mL) during 6 hours. Additional KOH (360 mg, 6.41 mmol) and tetrabutylammonium bromide (348 mg, 1.08 mmol) were added and the reaction stirred overnight. The reaction mixture was then filtered and the filtrate concentrated *in vacuo* to yield the crude product. The crude product was purified using flash silica column chromatography (50% ethyl acetate in 40-60 petroleum ether) to yield the product (314 mg, 39% yield) as a colourless oil.
The data were in agreement with the published data.[166]

^{1}H-NMR (400 MHz, $CDCl_3$): δ_H = 1.28 (t, 3H^1, *J*=7.2Hz), 3.03 (t, 2H^6, *J*=4.2Hz), 3.42 (t, 2H^5, *J*=4.2Hz), 3.98 (s, 2H^4), 4.20 (q, 2H^2, *J*=7.1Hz).

^{13}C-NMR (400 MHz, $CDCl_3$): δ_C = 14.1 (C-1), 37.7 (C-6), 40.0 (C-5), 41.5 (C-4), 61.7 (C-2), 165.5 (C-7), 170.0 (C-3).

IR ν_{max} (neat) = 2986, 1729 cm^{-1}

MS (ES+) m/z = 180 $[M+Na]^+$.
HRMS (ES+) calculated 180.0637 for $C_7H_{11}NO_3Na$, observed 180.0652 $[M+Na]^+$.

Results and Discussion Section 3.

1,2:5,6-Di-*O*-isopropylidene-D-mannitol 227

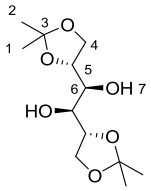

$ZnCl_2$ (40.3 g, 0.30 mol) was heated to a melt *in vacuo* (3 mbar) then cooled to room temperature under argon. To this was added anhydrous acetone (390 mL) and D-mannitol (20.0 g, 0.11 mol) and the resulting suspension stirred for 16 hours at room temperature. The reaction mixture was poured into 7.0 M K_2CO_3 (aq) (140 mL), stirred vigorously and the precipitated solid filtered and washed with acetone. The filtrate was concentrated *in vacuo* to remove acetone and then extracted with Et_2O (2 × 400 mL), the combined organic layers were dried over $MgSO_4$ and concentrated *in vacuo*. Hexane (400 mL) was then added, the resulting suspension stirred for 20 minutes, stored at 0 ^oC for 1 hour and then filtered and washed with cold hexane to yield the product (21.1 g, 73%) as a white solid.
The data were in agreement with the published data.[195]

^{1}H-NMR (400 MHz, $CDCl_3$): δ_H = 1.36 (s, 6 $H^{1/2}$), 1.42 (s, 6$H^{1/2}$), 2.60 (d, 2H^7, *J*=6.7Hz), 3.73-3.77 (m, 2H^6), 3.97 (dd, 2H^4, *J*=8.5Hz, *J*=5.6Hz), 4.12 (dd, 2H^4, *J*=8.5Hz, *J*=6.4Hz), 4.16-4.22 (m, 2H^5).

^{13}C-NMR (100 MHz, $CDCl_3$): δ_C = 25.2 (C-1/2), 26.7 (C-1/2), 66.7 (C-4), 71.2 (C-6), 76.3 (C-5), 109.4 (C-3).

IR ν_{max} (neat) = 3309, 2982, 1371 cm^{-1}

MS (ES+) m/z = 263 $[M+H]^+$, 285 $[M+Na]^+$.
HRMS (ES+) calculated 263.1495 for $C_{12}H_{23}O_6$, observed 263.1504 $[M+H]^+$.

2,3-*O*-Isopropylidene-D-glyceraldehyde 225

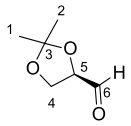

Silica supported sodium metaperiodate ($NaIO_4$:SiO_2):
$NaIO_4$ (25.7 g, 0.12 mol) was suspended in H_2O (50 mL) and heated to 80 ^oC. Silica gel (100 g) was then added followed by vigorous shaking and stirring.

To a stirred suspension of $NaIO_4$:SiO_2 (115 g) in CH_2Cl_2 (190 mL) at 0 ^oC was added a solution of protected acetonide **227** (10.0 g, 38.2 mmol) in CH_2Cl_2 (190 mL). The reaction mixture was then stirred for 30 minutes at 0 ^oC and then filtered. The collected solids were washed with CH_2Cl_2 and the filtrate was concentrated *in vacuo*. The crude product was purified by vacuum distillation (head temperature 50–54^oC at 18 mbar) to give the product (6.27 g, 64%) as an unstable colourless liquid.
The data were in agreement with the published data.[197]

^{1}H-NMR (400 MHz, $CDCl_3$): δ_H = 1.41 (s, 3H$^{1/2}$), 1.48 (s, 3H$^{1/2}$), 4.10 (dd, 1H^4, *J*=8.6Hz, *J*=4.8Hz), 4.20 (dd^4, 1H, *J*=8.6Hz, *J*=7.8Hz), 4.41 (m, 1H^5), 9.72 (d, 1H^6, *J*=1.8Hz).

^{13}C-NMR (100 MHz, $CDCl_3$): δ_C = 25.1 (C-1), 26.3 (C-2), 65.6 (C-4), 79.9 (C-5), 110.1 (C-3), 201.9 (C-6).

Ethyl 3-[(4*R*)-2,2-dimethyl-1,3-dioxolan-4-yl]-2,2-difluoro-3-hydroxy-propanoate 229

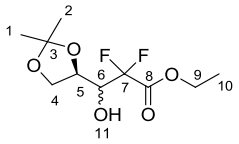

To a suspension of Zn dust (8.8 g, 140 mmol) and I_2 (1.4 g, 0.31 mmol) in Et_2O (45 mL) was added a mixture of aldehyde **225** (3.5 g, 27 mmol) and ethyl bromodifluoroacetate (4.5 mL, 35 mmol) in THF (90 mL) and Et_2O (45 mL). The resulting solution was refluxed for 1 hour. The reaction mixture was cooled and poured into cold 1.0 M HCl (aq) (150 mL), extracted into Et_2O (2 × 300 mL), the combined organics were washed with brine (150 mL), saturated $NaHCO_3$ (aq) (150 mL), dried over $MgSO_4$ and concentrated *in vacuo*. The crude product was purified using flash silica column chromatography (20% EtOAc in 40-60 petroleum ether) to yield the product as a colourless oil containing a 1.0:2.3 mixture of cis (B) and trans (A) diastereomers (5.2 g, 76%).
The data were in agreement with the published data.[194]

^{1}H-NMR (400 MHz, $CDCl_3$): δ_H = 1.36 (m, 18H$^{1,2,10A+B}$), 2.69 (d, 1H^{11A}, *J*=4.3Hz), 2.93 (d, 1H^{11B}, *J*=8.7Hz), 3.88-4.40 (m, 12H$^{4,5,6,9A+B}$).

^{13}C-NMR (100 MHz, $CDCl_3$): δ_C = 13.9 (C-10A+B), 25.0 (C-1A/B), 25.3 (C-1A/B), 26.2 (C-2A+B), 63.2 (C-9A), 63.3 (C-9B), 65.5 (d, C-4A, $^4J_{C\text{-}F}$=2.6 Hz), 66.4 (C-4B), 70.7-71.0 (m, C-6B), 71.8 (dd, C-6A, $^2J_{C\text{-}F}$=24.9Hz, $^2J_{C\text{-}F}$=23.0Hz), 72.2 (C-5B), 73.4 (C-5A), 109.7 (C-3A), 110.3 (C-3B), 113.9 (dd, C-7, $J_{C\text{-}F}$=254.0, $J_{C\text{-}F}$=254.8Hz), 163.0 (C-8A/B), 163.3 (C-8A/B).

Note: assigning peaks for individual diastereomers was difficult due to overlapping peaks.

IR ν_{max} = 3456, 2995, 1763 cm^{-1}

MS (ES+) m/z = 255 $[M+H]^+$.
HRMS (ES+) calculated 255.1044 for $C_{10}H_{17}F_2O_5$, observed 255.1038 $[M+H]^+$.

Ethyl 3-(benzoyloxy)-3-[(4*R*)-2,2-dimethyl-1,3-dioxolan-4-yl]-2,2-difluoropropanoate 230

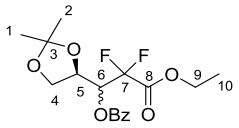

A solution of benzoyl chloride (0.27 mL, 2.36 mmol) in CH_2Cl_2 (2.5 mL) was added dropwise to a solution of alcohol **229** (500 mg, 1.97 mmol), 2,6-lutidine (0.45 mL, 3.93 mmol) and DMAP (151 mg, 1.24 mmol) in CH_2Cl_2 (2.5 mL) at 35 ^oC. The reaction mixture was then stirred for 3 hours, cooled to room temperature, diluted with CH_2Cl_2 (10 mL) and washed sequentially with 1.0 M HCl (aq) (10 mL), saturated $NaHCO_3$ (aq) (10 mL), H_2O (10 mL), dried over $MgSO_4$ and concentrated *in vacuo*. The crude product was purified using flash silica column chromatography (10% EtOAc in 40-60 petroleum ether) to yield the product as a colourless oil containing a 1.0:2.3 mixture of cis (B) and trans (A) diastereomers (520 mg, 74%).
The data were in agreement with the published data.[194]

^{1}H-NMR (400 MHz, $CDCl_3$): δ_H = 1.32 (m, 18H$^{1,2,10A+B}$), 4.00 (dd, 1H^{4B}, *J*=8.9Hz, *J*=5.9Hz), 4.06 (dd, 1H^{4A}, *J*=8.9Hz, *J*=5.8Hz), 4.12-4.19 (m, 2H^{4A+B}), 4.23-4.26 (m, 4H^{9A+B}), 4.50-4.54 (m, 1H^{5A}), 4.55-4.60 (m, 1H^{5B}), 5.70 (ddd, 1H^{6B}, *J*=13.8Hz, $^3J_{H\text{-}F}$=7.6Hz, $^3J_{H\text{-}F}$=5.8Hz), 5.83-5.91 (m, 1H^{6A}), 7.44-7.49 (m, 4H-Ar), 7.58-7.63 (m, 2H-Ar), 8.06-8.10 (m, 4H-Ar).

^{13}C-NMR (100 MHz, $CDCl_3$): δ_C = 13.8 (C-10A+B), 25.1 (C-1A), 25.4 (C-1B), 26.0 (C-2B), 26.1 (C-2A), 63.3 (C-9B), 63.4 (C-9A), 65.6 (C-4A), 65.8 (d, C-4B, $^4J_{C\text{-}F}$=3.5Hz), 70.8 (dd, C-6A, $^2J_{C\text{-}F}$=25.4Hz, $^2J_{C\text{-}F}$=22.8Hz), 71.1-71.7 (m, C-6B), 72.3 (C-5B), 72.5 (C-5A), 110.1 (C-3A), 110.2 (C-3B), 112.80 (t, C-7A, $J_{C\text{-}F}$=258.5Hz), 128.6 (CH-Ar), 128.7 (CH-Ar), 130.1 (CH-Ar), 130.1 (CH-Ar), 133.7 (CH-Ar), 133.9 (CH-Ar), 161.8 (C=O), 162.3 (C=O), 164.6 (C=O), 164.8 (C=O).

Note: assigning peaks for individual diastereomers was difficult, missing 2 × C-Ar and C-7B due to overlapping peaks assigning peaks.

IR ν_{max} = 2988, 1767, 1736 cm^{-1}

MS (CI+) m/z = 359 $[M+H]^+$.

HRMS (CI+) calculated 359.1306 for $C_{17}H_{21}F_2O_3$, observed 359.1299 $[M+H]^+$.

2-Deoxy-2,2-difluoro-D-pentofuranos-1-ulose-3-benzoate 231

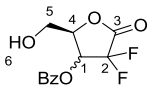

A mixture of the propionate **230 (**0.58 g, 1.63 mmol), H_2O (0.17 mL, 9.13 mmol) and trifluoroacetic acid (0.03 mL, 0.39 mmol) in MeCN (3.3 mL) was refluxed at 80 ^oC for 3 hours. Using azeotoropic distillation the MeCN was removed and replaced by dry toluene and the reaction heated at 100 ^oC for a further hour. The mixture was then cooled to room temperature and concentrated *in vacuo* to yield the crude oil (0.39 g, 89%) as a 1.0:2.3 mixture of *xylo* (B) and *ribo* (A) epimers which were used directly in the next step without further purification.
The data were in agreement with the published data.[194]

Data for *ribo* epimer.

^{1}H-NMR (400 MHz, $CDCl_3$): δ_H = 3.96 (dd, 1H^5, *J*=13.0Hz, *J*=3.3Hz) 4.11 (dd, 1H^5, *J*=13.0Hz, *J*=2.7Hz) 4.90 (m, 1H^4) 5.79 (ddd, 1H^1, *J*=11.5Hz, $^3J_{H\text{-}F}$=9.3Hz, $^3J_{H\text{-}F}$=5.7Hz) 7.48 (m, 2H-Ar) 7.63 (m, 1H-Ar), 8.06 (m, 2H-Ar).

IR ν_{max} = 3457, 2948, 1815, 1724 cm^{-1}

MS (ES+) m/z = 273 $[M+H]^+$.
HRMS (ES+) calculated 273.0575 for $C_{12}H_{11}F_2O_5$, observed 273.0577 $[M+H]^+$.

2-Deoxy-2,2-difluoro-D-*ribo*-pentofuranose-1-ulose-3,5-dibenzoate 228

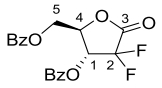

To a solution of lactone **231** (250 mg, 0.92 mmol) in EtOAc (1.6 mL) was added pyridine (0.16 mL. 1.84 mmol) and DMAP (14 mg, 0.10 mmol) and the resulting mixture heated to 65 ^{o}C. A solution of benzoyl chloride (0.12 mL, 1.10 mmol) in EtOAc (1.6 mL) was then added and the solution stirred for 2 hours. The reaction mixture was cooled to 5 ^{o}C, filtered through a celite padded frit and concentrated *in vacuo* to give the crude product as a mixture of epimers (225 mg, 65%). Recrystallisation from CH_2Cl_2-Heptane yielded the desired product (70 mg, 20%) as a white solid.
The data were in agreement with the published data.[194]

$[\alpha]_D^{25}$ (c = 1.0, $CHCl_3$) +49.6

^{1}H-NMR (400 MHz, $CDCl_3$): δ_H = 4.71 (dd, 1H^5, *J*=12.7Hz, *J*=4.4Hz), 4.78 (dd, 1H^5, *J*=12.7Hz, *J*=3.9Hz), 5.00 (m, 1H^4), 5.75 (ddd, 1H^1, $^3J_{H\text{-}F}$=12.2Hz, $^3J_{H\text{-}F}$=5.9Hz, *J*=4.6Hz), 7.45-7.53 (m, 4H-Ar), 7.59-7.70 (m, 2H-Ar), 8.03-8.10 (m, 4H-Ar).

^{13}C-NMR (100 MHz, $CDCl_3$): δ_C = 62.2 (C-5), 69.5 (dd, C-1, $^2J_{C\text{-}F}$=31.0Hz, $^2J_{C\text{-}F}$=15.7Hz), 78.4 (d, C-4, $^3J_{C\text{-}F}$=5.9Hz), 111.48 (dd, C-2, $J_{C\text{-}F}$ =262.6Hz, $J_{C\text{-}F}$=257.9Hz), 127.4 (C-Ar), 128.6 (CH-Ar), 128.7 (C-Ar), 128.8 (CH-Ar), 129.8 (CH-Ar), 130.2 (CH-Ar), 133.7 (CH-Ar), 134.5 (CH-Ar), 162.5 (C=O), 164.6 (C=O), 165.7 (C=O).

IR ν_{max} = 3070, 1817, 1805, 1725, 1711 cm^{-1}

Anal. calculated for $C_{19}H_{14}F_2O_6$: C, 60.64; H, 3.75. Found: C, 60.51; H, 3.65.

mp (CH_2Cl_2-Heptane) = 107-108 ^{o}C

2-Deoxy-2, 2-difluoro-D-ribofuranos-1-ulose-3,5-dibenzoate 232

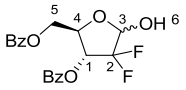

To a 0 °C solution of furanose **228** (10.0 g, 26.6 mmol) in Et_2O-THF (1:1, 110 mL) was added $LiAlH(O^tBu)_3$ (10.2 g, 40.0 mmol) portion-wise during 40 minutes and the resulting suspension warmed to room temperature and stirred for 1.5 hours. The reaction mixture was quenched by dropwise addition of MeOH (20 mL), then diluted with Et_2O (200 mL) and washed sequentially with 1.0 M HCl (aq) (200 mL), saturated $NaHCO_3$ (aq) (150 mL), saturated Rochelle's salt (aq) (2 × 200 mL) and H_2O (200 mL). The organic layer was then dried over $MgSO_4$ and concentrated *in vacuo* to yield the product (10.0 g, 99.8%) as colourless oil in a 1.0:1.5 mixture of β and α anomers. This was used directly in the next step with no further purification.
The data were in agreement with the published data.[194]

^{1}H-NMR (400 MHz, $CDCl_3$): δ_H = 4.45-4.49 (m, 1H$^{4\beta}$), 4.60 (dd, 1H$^{5\alpha}$, *J*=12.0Hz, *J*=4.3Hz), 4.67-5.69 (m, 2H$^{5\beta}$), 4.71-4.80 (m, 2H$^{4\alpha,5\alpha}$), 5.33-5.36 (m, 1H$^{3\beta}$), 5.47-5.52 (m, 2H$^{1+3\alpha}$), 5.73 (td, 1H$^{1\beta}$, $^3J_{H\text{-}F}$=10.1Hz, *J*=6.2Hz), 7.38-7.50 (m, 8H-Ar), 7.54-7.66 (m, 4H-Ar), 8.04-8.10 (m, 8H-Ar).

^{13}C-NMR (100 MHz, $CDCl_3$): δ_C = 63.2 (C-5α), 64.3 (C-5β), 71.3 (dd, C-1α, $^2J_{C\text{-}F}$=29.0Hz, $^2J_{C\text{-}F}$ =16.0Hz), 72.0 (dd, C-1β, $^2J_{C\text{-}F}$=36.4Hz, $^2J_{C\text{-}F}$=17.6Hz), 77.2 (C-4α), 79.5 (C-4β), 95.5-96.4 (m, C-3α+β), 121.5 (t, C-2α/β, $J_{C\text{-}F}$=261.0Hz), 122.3 (t, C-2α/β, $J_{C\text{-}F}$=256.1Hz), 128.0 (C-Ar), 128.5 (CH-Ar), 128.6 (CH-Ar), 129.6 (CH-Ar), 129.8 (CH-Ar), 129.9 (CH-Ar), 130.1 (CH-Ar), 133.0 (CH-Ar), 133.4 (CH-Ar), 133.5 (CH-Ar), 133.9 (CH-Ar), 134.0 (CH-Ar). 165.2 (C=O), 165.3 (C=O), 166.3 (C=O), 166.5 (C=O).

Note: missing 3 × C-Ar and 1 × CH-Ar due to overlapping peaks.

IR ν_{max} (neat) = 3453, 2955, 1719 cm^{-1}

MS (ES+) m/z = 379 $[M+H]^+$.
HRMS (ES+) calculated 379.0993 for $C_{19}H_{17}F_2O_6$, observed 379.0974 $[M+H]^+$.

2-Deoxy-2, 2-difluoro-D-ribofuranos-1-ulose-3,5-dibenzoate-1-methanesulfonate 233

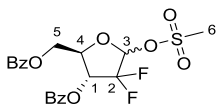

To a solution of hemiacetal **232 (**20.0 g, 52.9 mmol) in CH_2Cl_2 (210 mL) at 0 ^oC was added NEt_3 (13.9 mL, 100 mmol) and methanesulfonyl chloride (7.0 mL, 90.0 mmol). The resulting solution was warmed to room temperature and stirred for 2 hours. The reaction mixture was then diluted with CH_2Cl_2 (500 mL) and washed sequentially with 1.0 M HCl (aq) (500 mL), saturated $NaHCO_3$ (aq) (300 mL), H_2O (500 mL), dried over $MgSO_4$ and concentrated *in vacuo* to yield the product as orange oil (21.3 g, 88%) in a 1.0:1.5 mixture of β and α anomers.
The data were in agreement with the published data.[194]

^{1}H-NMR (500 MHz, $CDCl_3$): δ_H = 3.02 (s, 3H$^{6\beta}$), 3.18 (s, 3H$^{6\alpha}$), 4.60 (dd, 1H$^{5\beta}$, *J*=12.3Hz, *J*=4.4Hz), 4.64-4.69 (m, 2H$^{4\beta,5\beta}$), 4.72-4.78 (m, 2H$^{5\alpha}$), 4.84 (dd, 1H$^{4\alpha}$, *J*=7.9Hz, *J*=4.0Hz), 5.57 (dd, 1H$^{1\alpha}$, $^3J_{H\text{-}F}$=16.4Hz *J*=4.2Hz), 5.94 (dt, 1H$^{1\beta}$, *J*=15.3Hz, $^3J_{H\text{-}F}$=7.1Hz), 6.03-6.05 (m, 1H$^{3\beta}$), 6.14 (dd, 1H$^{3\alpha}$, $^3J_{H\text{-}F}$=6.0Hz, $^3J_{H\text{-}F}$=1.1Hz), 7.42-7.51 (m, 8H-Ar), 7.58-7.67 (m, 4H-Ar), 8.03-8.09 (m, 8H-Ar).

^{13}C-NMR (125 MHz, $CDCl_3$): δ_C = 40.2 (C-6α), 40.3 (C-6β), 62.5 (C-5α), 63.0 (C-5β), 69.4 (dd, C-1β, $^2J_{C\text{-}F}$=26.0Hz, $^2J_{C\text{-}F}$=15.6Hz), 71.0 (dd, C-1α, $^2J_{C\text{-}F}$=36.8Hz, $^2J_{C\text{-}F}$=17.4Hz), 79.72 (d, C-4β, $^3J_{C\text{-}F}$=7.7Hz), 82.7 (C-4α), 98.8 (dd, C-3β, $^2J_{C\text{-}F}$=42.0Hz, $^2J_{C\text{-}F}$=25.0Hz), 99.6 (dd, C-3α, $^2J_{C\text{-}F}$=46.2Hz, $^2J_{C\text{-}F}$=25.0Hz), 118.3-122.9 (m, C-2α+β), 127.9 (C-Ar), 128.0 (C-Ar), 128.9 (C-Ar), 129.1 (CH-Ar), 128.5 (CH-Ar), 128.7 (CH-Ar), 128.7 (CH-Ar), 128.8 (CH-Ar), 129.8 (CH-Ar), 130.1 (CH-Ar), 130.2 (CH-Ar), 133.5 (CH-Ar), 133.7 (CH-Ar), 134.2 (CH-Ar), 134.2 (CH-Ar), 164.9 (C=O), 165.0 (C=O), 165.8 (C=O), 165.9 (C=O).

Note: missing 1 × C-Ar due overlapping peaks.

IR: v_{max} = 3030, 1724 cm^{-1}
HRMS: Did not provide spectra suitable for interpretation.

2'-Deoxy-2',2'-difluoruridine-3',5'-dibenzoate 221β

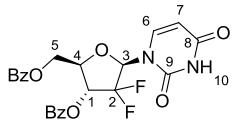

Uracil (8.9 g, 79.3 mmol) and $(NH_4)_2SO_4$ (628 mg, 4.76 mmol) were refluxed in HMDS (220 mL) for 12 hours, then cooled to room temperature and concentrated *in vacuo*. The resulting residue was dissolved in DCE (150 mL), treated with TMSOTf (14.4 mL, 79.3 mmol) and a solution of mesylates **233** (21.3 g, 46.7 mmol) in DCE (80 mL) added. The mixture was heated to reflux and stirred for 24 hours, then cooled to room temperature and the solvent removed *in vacuo*. The resulting gum was dissolved in EtOAc (800 mL) then washed sequentially with H_2O (2 × 600 mL), saturated $NaHCO_3$ (aq) (600 mL) and brine (600 mL) dried over $MgSO_4$ and concentrated *in vacuo* to yield the crude product (3.92 g, 66%) as a 1.0:1.4 mixture of β and α-anomers. Recrystallisation of the crude material, once from EtOAc and once from CH_2Cl_2 yielded exclusively the β-anomer (4.65 g, 21%) as a white solid.
The data were in agreement with the published data.[194]

^{1}H-NMR (400 MHz, $CDCl_3$): δ_H = 4.57-4.60 (m, 1H^4), 4.69 (dd, 1H^5, *J*=12.5Hz, *J*=4.3Hz), 4.83 (dd, 1H^5, *J*=12.5Hz, *J*=3.1Hz), 5.62-5.68 (m, 1H^1), 5.67 (dd, 1H^7, *J*=8.2Hz, *J*=2.1Hz), 6.39 (dd, 1H^3, $^3J_{H\text{-}F}$=11.8Hz, $^3J_{H\text{-}F}$=6.3Hz),7.39 (dd, 1H^6, *J*=8.2Hz, *J*=2.1Hz), 7.49 (m, 4H-Ar), 7.65 (m, 2H-Ar), 8.07 (m, 4H-Ar), 8.23 (s, 1H^{10}).

^{13}C-NMR (100 MHz, $CDCl_3$): δ_C = 62.4 (C-5) 71.3 (dd, C-1, $^2J_{C\text{-}F}$=16.8Hz, $^2J_{C\text{-}F}$= 4.7Hz) 78.5 (C-4) 83.1 (dd, C-3, $^2J_{C\text{-}F}$=37.5Hz, $^2J_{C\text{-}F}$=21.0Hz) 103.2 (C-7) 120.77 (dd, C-2, $J_{C\text{-}F}$ =259.1Hz, $J_{C\text{-}F}$ =266.6Hz) 127.7 (C-Ar) 128.7 (CH-Ar) 128.8 (CH-Ar) 129.0 (C-Ar) 129.6 (CH-Ar) 130.1 (CH-Ar) 133.7 (CH-Ar) 134.3 (CH-Ar) 139.6 (d, C-6, $^4J_{C\text{-}F}$=3.2Hz) 149.7 (C=O) 161.8 (C=O) 164.8 (C=O) 165.9 (C=O).

IR: ν_{max} = 3189, 3060, 2970, 1723, 1689 cm^{-1}

MS (ES+) m/z = 473 $[M+H]^+$.
HRMS (ES+) calculated 473.1160 for $C_{23}H_{19}N_2F_2O_7$, observed 473.1150 $[M+H]^+$.

2'-Deoxy-2',2'-difluorouridine 260

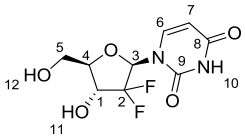

To a solution of the protected nucleoside **221β** (390 mg, 0.42 mmol) in MeOH (83 mL) at 0 ^{o}C was added 7.0 M NH_3 in MeOH (17 mL, 116 mmol). The resulting solution was warmed to room temperature and stirred for 16 hours. The solvents were removed *in vacuo* and the resultant residue partitioned between H_2O (80 mL) and EtOAc (80 mL). The organic layer was re-extracted with H_2O (80 mL) and the combined aqueous layers concentrated *in vacuo* to yield the product (197 mg, 90%) as a colourless amorphous solid.
The data were in agreement with the published data.[194]

^{1}H-NMR (400 MHz, D_2O): δ_H = 3.75 (dd, 1H^{5}, *J*=13.1Hz, *J*=4.4Hz), 3.90 (dd, 1H^{5}, *J*=13.1Hz, *J*=2.0Hz), 3.96 (m, 1H^{4}), 4.26 (td, 1H^{1}, $^{3}J_{H\text{-}F}$=11.8Hz, *J*=8.5Hz), 5.80 (d, 1H^{7}, *J*=8.1Hz), 6.09 (m, 1H^{3}), 7.67 (d, 1H^{6}, *J*=8.1Hz).

^{13}C-NMR (100 MHz, D_2O): δ_C = 59.3 (C-5), 69.2 (dd, C-1, $^{2}J_{C\text{-}F}$=25.6Hz, 20.7Hz) 80.46 (d, C-4, $^{3}J_{C\text{-}F}$=7.8Hz) 84.13 (dd, C-3, $^{2}J_{C\text{-}F}$=39.3Hz, 25.3Hz), 102.5 (C-7), 122.1 (dd, C-2, $J_{C\text{-}F}$= 260.6Hz, 259.5Hz), 141.4 (C-6), 151.4 (C-9), 165.9 (C-8).

IR ν_{max} (neat) = 3266, 1686 cm^{-1}

MS (ES+) m/z = 265 $[M+H]^{+}$.
HRMS (ES+) calculated 265.0636 for $C_9H_{11}N_2F_2O_5$, observed 265.0635 $[M+H]^{+}$.

(2*R*,3*R*,5*R*)-2-[(Benzoyloxy)methyl]-4,4-difluoro-5-(5-iodo-2,4-dioxo-1,2,3,4-tetrahydropyrimidin-1-yl)oxolan-3-yl benzoate 235

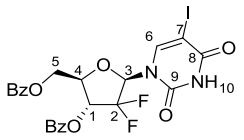

A mixture of the protected nucleoside **221β** (300 mg, 0.64 mmol), I_2 (102 mg, 0.40 mmol) and ceric ammonium nitrate (175 mg, 0.32 mmol) in MeCN (6.4 mL) were refluxed at 80 ^oC for 4 hours, then cooled to room temperature and stirred for 16 hours. The solvent was removed *in vacuo* and the resulting residue dissolved in cold EtOAc (20 mL) and washed with brine (10 mL) and 5% $NaHSO_3$ (aq) (5 mL). The aqueous layers were extracted with EtOAc (20 mL) and the combined organic layers were washed sequentially with 5% $NaHSO_3$ (aq) (5 mL), brine (15 mL) and H_2O (10 mL) dried over $MgSO_4$ and concentrated *in vacuo*. The crude product was purified using flash silica column chromatography (4% acetone in $CHCl_3$) to yield the product (290 mg, 76%) as a white powder.

^{1}H-NMR (500 MHz, $CDCl_3$): δ_H = 4.59-4.62 (m, 1H^4), 4.76 (dd, 1H^5, *J*=12.6Hz, *J*=3.8Hz), 4.84 (dd, 1H^5, *J*=12.6Hz, *J*=2.9Hz), 5.65 (ddd, 1H^1, $^3J_{H\text{-}F}$=14.9Hz, $^3J_{H\text{-}F}$=4.9Hz, *J*=1.7Hz), 6.37 (dd, 1H^3, $^3J_{H\text{-}F}$=12.4Hz, $^3J_{H\text{-}F}$=5.7Hz), 7.48-7.52 (m, 4H-Ar), 7.60-7.67 (m, 2H-Ar), 7.81 (d, 1H^6, $^4J_{H\text{-}F}$=2.3Hz), 8.08-8.10 (m, 4H-Ar), 8.28 (s, 1H^{10}).

^{13}C-NMR (125 MHz, $CDCl_3$): δ_C = 62.3 (C-5), 69.2 (C-7), 71.4 (dd, C-1, $^2J_{C\text{-}F}$=35.4Hz, $^2J_{C\text{-}F}$=16.5Hz), 79.0 (C-4), 83.2 (dd, C-3, $^2J_{C\text{-}F}$=36.0Hz, $^2J_{C\text{-}F}$=21.1Hz), 120.44 (dd, C-2, $J_{C\text{-}F}$= 259.1Hz, 258.5Hz), 127.7 (C-Ar), 128.7 (CH-Ar), 128.8 (CH-Ar), 128.9 (C-Ar), 129.8 (CH-Ar), 130.1 (CH-Ar), 133.7 (CH-Ar), 134.4 (CH-Ar), 144.1 (C-6), 149.3 (C=O), 158.8 (C=O), 164.8 (C=O), 166.0 (C=O).

IR ν_{max} (neat) = 3252, 3049, 1729, 1723, 1694 cm^{-1}

MS (ES+) m/z = 599 $[M+H]^+$.
HRMS (ES+) calculated 599.0127 for $C_{23}H_{18}N_2F_2O_7I$, observed 599.0102 $[M+H]^+$.

1-[(2*R*,4*R*,5*R*)-3,3-Difluoro-4-hydroxy-5-(hydroxymethyl)oxolan-2-yl]-5-iodo-1,2,3,4-tetrahydropyrimidine-2,4-dione 223

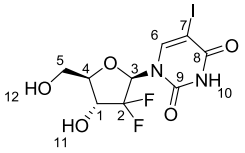

To a solution of iodide **235** (280 mg, 0.47 mmol) in MeOH (95 mL) at 0 °C was added 7.0 M NH_3 in MeOH (9.4 mL, 59.3 mmol) and the resulting solution warmed to room temperature and stirred for 16 hours. The solvents were removed *in vacuo* and the resultant residue partitioned between CH_2Cl_2 (50 mL) and H_2O (50 mL). The organic layer was extracted with water (2 × 50 mL) and the combined aqueous layers then concentrated under reduced pressure to yield the product (182 mg, 99%) as an off white amorphous solid.

^{1}H-NMR (400 MHz, MeOD-d_4): δ_H = 3.78 (dd, 1H^5, *J*=12.6Hz, *J*=2.5Hz), 3.90 (dt, 1H^4, *J*=8.4Hz, *J*=2.4), 3.93-3.97 (m, 1H^5), 4.32 (td, 1H^1, $^3J_{H\text{-}F}$=12.4Hz, *J*=8.5Hz), 6.09-6.13 (m, 1H^3), 8.44 (s, 1H^6).

^{13}C-NMR (100 MHz, MeOD-d_4): δ_C = 59.9 (C-5) 69.1 (C-7) 69.6-70.0 (m, C-1) 82.8 (d, C-4, $^3J_{C\text{-}F}$=8.1Hz) 85.0-86.0 (m, C-3) 122.60 (dd, C-2, $J_{C\text{-}F}$=261.1Hz, $J_{C\text{-}F}$=258.6) 146.1 (C-6) 151.8 (C-9) 162.4 (C-8).

IR ν_{max} (neat) = 3400, 3059, 1700, 1671 cm^{-1}

MS (ES+) m/z = 391 $[M+H]^+$.
HRMS (ES+) calculated 390.9603for $C_9H_{10}N_2F_2O_5I$, observed 390.9605 $[M+H]^+$.

1-[(2*R*,4*R*,5*R*)-3,3-Difluoro-4-hydroxy-5-(hydroxymethyl)oxolan-2-yl]-5-(trimethylstannyl)-1,2,3,4-tetrahydropyrimidine-2,4-dione 224

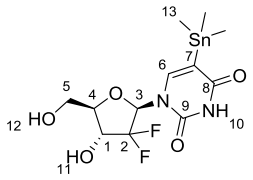

Iodide **223** (75 mg, 0.19 mmol) was dissolved in 1,4-dioxane (3 mL) at 50 ^{o}C, then cooled to room temperature and hexamethylditin (90 µL, 0.42 mmol) and $Pd(PPh_3)_4$ (5 mg, 5 µmol) added. The reaction mixture was then stirred at reflux for 20 hours, cooled to room temperature and concentrated *in vacuo*. The crude product was purified using flash silica column chromatography (25% acetone in CH_2Cl_2) to yield the product (67 mg, 83%) as a white solid.

^{1}H-NMR (400 MHz, CD_3OD): δ_H = 0.25 (s, 9H^{13}), [d, $^{2}J_{H}$-^{119}$_{Sn}$=58.8Hz, d, $^{2}J_{H}$-^{117}$_{Sn}$=56.3Hz] 3.75 (dd, 1H^{5}, *J*=12.6Hz, *J*=2.5Hz), 3.87 (dt, 1H^{4}, *J*=8.6Hz, *J*=2.5Hz), 3.92-3.95 (m, 1H^{5}), 4.31 (td, 1H^{1}, $^{3}J_{H-F}$=12.5Hz , *J*=8.6Hz,), 6.16 (t, 1H^{3}, $^{3}J_{H-F}$=7.8Hz), 7.62 (s, 1H^{6}), [d, $^{3}J^{119}$Sn-H=37.5Hz].

^{13}C-NMR (100 MHz, CD_3OD): δ_C = -9.5 (C13), [d, J_{C}-^{117}$_{Sn}$=365.5Hz, d, J_{C}-^{119}$_{Sn}$=382.4Hz] 59.8 (C-5), 70.03 (t, C-1, $^{2}J_{C-F}$=22.6Hz), 82.22 (t, C-4, $^{3}J_{C-F}$=4.0Hz), 85.1-85.6 (m, C-3), 113.8 (C-7), 124.21 (t, C-2, $^{1}J_{C-F}$=258.0Hz), 145.3 (C-6), 152.7 (C-9), 168.6 (C-8).

IR ν_{max} (neat) = 3269, 1697, 1648, 1601 cm^{-1}

HRMS Did not provide spectra suitable for interpretation.

mp (acetone) = 73-76 ^{o}C.

2'-Deoxy-2',2'-difluorothymidine 90

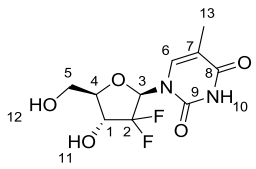

A mixture of $Pd_2(dba)_3$ (124 mg, 0.12 mmol), tri(*o*-tolyl)phosphine (143 mg, 0.47 mmol) and stannane **224** (100mg, 0.23 mmol) in DMF (30 mL) was purged with argon for 10 minutes, then treated with a solution of methyl iodide (40 mg, 0.28 mmol) in DMF (3mL). The resulting mixture was heated at 130 ^{o}C for 10 minutes then cooled to room temperature, the catalyst removed by filtration and the filtrate concentrated *in vacuo*. The crude product was purified using flash silica column chromatography (7% MeOH in $CHCl_3$) to yield the product (39 mg, 61%) as a colourless oil.

^{1}H-NMR (500 MHz, MeOD-d$_4$): δ_H = 1.87 (s, 3H^{13}), 3.78 (dd, 1H^{5}, *J*=12.7Hz, *J*=3.1Hz), 3.87 (dt, 1H^{4}, *J*=8.4Hz, *J*=2.7Hz), 3.94 (m, 1H^{5}), 4.30 (td, 1H^{1}, $^{3}J_{H\text{-}F}$=12.2Hz, *J*=8.4Hz), 6.12 (dd, 1H^{3}, $^{3}J_{H\text{-}F}$=9.1Hz, $^{3}J_{H\text{-}F}$=6.8Hz), 7.71 (s, 1H^{6}).

^{13}C-NMR (125 MHz, MeOD-d$_4$): δ_C = 12.4 (C-13) 60.4 (C-5) 70.30 (dd, C-1, $^{2}J_{C\text{-}F}$=25.6Hz, $^{2}J_{C\text{-}F}$ =20.4Hz), 82.5 (d, C-4, $^{3}J_{C\text{-}F}$=8.4Hz), 85.18 (dd, C-3, $^{2}J_{C\text{-}F}$ =40.1Hz, $^{2}J_{C\text{-}F}$ =25.2Hz), 111.7 (C-7), 124.01 (dd, C-2, $J_{C\text{-}F}$ =253.1Hz, $J_{C\text{-}F}$ =263.1Hz), 137.4 (C-6), 152.2 (C-9), 166.0 (C-8).

IR ν_{max} (neat) = 3374, 1692 cm^{-1}

MS (ES+) m/z = 279 $[M+H]^+$.
HRMS (ES+) calculated 279.0793 for $C_{10}H_{13}N_2F_2O_5$, observed 279.0790 $[M+H]^+$.

2',2'-Difluoro-2'-deoxycytidine-3',5'-dibenzoate 222β

Cytosine (4.82g, 43.4 mmol) and $(NH_4)_2SO_4$ (0.34 g, 2.60 mmol) in HMDS (100 mL) were refluxed for 16 hours, then cooled to room temperature and concentrated *in vacuo*. The resulting residue was dissolved DCE (80 mL), treated with TMSOTf (7.9 mL, 43.4 mmol) and then a solution of mesylates **233** (11.8 g, 25.9 mmol) in DCE (50 mL) added. The resulting solution was heated at reflux for 48 hours then cooled to room temperature and concentrated *in vacuo*. The resultant residue taken up in EtOAc (150 mL), washed with H_2O (2 × 150 mL), saturated $NaHCO_3$ (aq) (150 mL) and then concentrated to approximately one third volume resulting in the precipitation of a white solid. This was collected by filtration, washed with cold EtOAc and then vacuum dried to give the product (4.91 g, 40%) in a 1.0:1.0 mixture of β and α-anomers. Trituration with hot MeOH allowed isolation of the insoluble β-product (1.99 g, 16%) as a white solid.

The data were in agreement with the published data.[194]

^{1}H-NMR (500 MHz, DMSO-d$_6$): δ_H = 4.67-4.77 (m, 3H^{4,5}), 5.79 (d, 1H^8, *J*=7.5Hz), 5.80-5.84 (m, 1H^1), 6.38 (br, s, 1H^3), 7.46-7.49 (m, 2H-Ar/2H^{10}), 7.56-7.59 (m 2H-Ar), 7.62-7.67 (m, 2H-Ar), 7.72-7.75 (m 1H-Ar), 7.94-7.96 (m, 2H-Ar), 8.04-8.06 (m, 2H-Ar).

^{13}C-NMR (125 MHz, DMSO-d$_6$): δ_C = 63.4 (C-5), 71.7 (dd, C-1, $^2J_{C\text{-}F}$=26.3Hz, $^2J_{C\text{-}F}$=22.3Hz), 75.6 (C-4) 78.8 (t, C-3, $^2J_{C\text{-}F}$=33.4Hz) 94.99 (C-8), 121.72 (dd, C-2, $J_{C\text{-}F}$=268.8Hz, $J_{C\text{-}F}$=254.4Hz), 128.0 (C-Ar), 128.7 (CH-Ar), 128.9 (CH-Ar), 129.1 (CH-Ar), 129.2 (CH-Ar), 129.6 (CH-Ar), 133.6 (CH-Ar), 134.2 (CH-Ar), 141.8 (C-Ar), 154.3 (C=O), 164.3 (C=O), 165.3 (C=O), 165.7 (C-7).

IR ν_{max} (neat) = 3366, 3176, 1719, 1631 cm^{-1}

MS (ES+) m/z = 472 $[M+H]^+$.

HRMS (ES+) calculated 472.1320 for $C_{23}H_{20}N_3F_2O_6$, observed 472.1331 $[M+H]^+$.

2'-Deoxy-2',2'-difluorocytidine 84

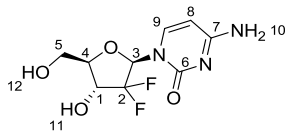

To a solution of protected nucleoside **222β** (600 mg, 1.27 mmol) in MeOH (120 mL) at 0 ^{o}C was added 7.0 M NH_3 in MeOH (25 mL, 178 mmol) and the resulting solution warmed to room temperature and stirred for 16 hours. The solvents were removed *in vacuo* and the resultant residue partitioned between EtOAc (125 mL) and H_2O (125 mL). The organic layer was extracted with H_2O (2 × 125 mL) and the combined aqueous layers concentrated under reduced pressure to yield the product (335 mg, 100%) as an amorphous white solid.
The data were in agreement with the published data.[194]

^{1}H-NMR (400 MHz, D_2O): δ_H = 3.75 (dd, 1H^{5}, *J*=13.1Hz, *J*=4.3Hz), 3.90 (dd, 1H^{5}, *J*=13.1Hz, *J*=2.2Hz), 3.92-3.96 (m, 1H^{4}), 4.23 (td, 1H^{1}, $^{3}J_{H\text{-}F}$=12.0Hz, *J*=8.7Hz), 5.96 (d, 1H^{8}, *J*=7.6Hz), 6.10 (t, 1H^{3}, $^{3}J_{H\text{-}F}$=7.9Hz), 7.64 (d, 1H^{9}, *J*=7.6Hz).

^{13}C-NMR (100 MHz, D_2O): δ_C = 59.3 (C-5), 69.20 (t, C-1, $^{2}J_{C\text{-}F}$=23.3Hz), 80.02 (t, C-4, $^{3}J_{C\text{-}F}$ =4.2Hz), 84.90 (t, C-3, $^{2}J_{C\text{-}F}$=31.2Hz), 96.4 (C-8), 123.5 (d, C-2, $J_{C\text{-}F}$=257.9Hz), 141.2 (C-9), 157.2 (C-6), 166.3 (C-7).

IR: v_{max} (neat) = 3232, 3206, 1666, 1639 cm^{-1}

MS (ES+) m/z = 264 $[M+H]^+$, 286 $[M+Na]^+$.
HRMS (ES+) calculated 263.0796 for $C_9H_{12}N_3F_2O_4$, observed 264.0800 $[M+H]^+$.

4-Amino-1-[(2*R*,4*R*,5*R*)-3,3-difluoro-4-hydroxy-5-(hydroxymethyl)oxolan-2-yl]-5-iodo-1,2-dihydropyrimidin-2-one 238

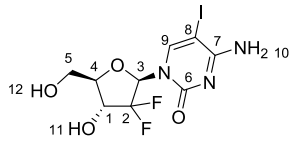

A mixture of gemcitabine **84** (123 mg, 0.47 mmol), I_2 (119 mg, 0.47 mmol) and iodic acid (83 mg, 0.47 mmol) in AcOH-H_2O-CCl_4 (8:3:2, 23 mL) was heated at 45 ^oC for 4 hours. The reaction mixture was then concentrated *in vacuo* and recrystallized from H_2O to yield the product (111 mg, 61%) as a white solid.

^{1}H-NMR (500 MHz, MeOD-d$_4$): δ_H = 3.78 (dd, 1H^5, *J*=12.7Hz, *J*=2.7Hz), 3.90 (td, 1H^4, *J*=8.5Hz, *J*=2.5Hz), 3.95 (dd, 1H^5, *J*=13.0Hz, *J*=2.5Hz), 4.28 (dt, 1H^1, $^3J_{H\text{-}F}$=12.3Hz, *J*=8.6Hz), 6.14-6.17 (m, 1H^3), 8.38 (s, 1H^9).

^{13}C-NMR (125 MHz, MeOD-d$_4$): δ_C = 57.6 (C-8), 60.0 (C-5), 69.7-70.1 (m, C-1), 82.5-82.6 (m, C-4), 85.7-86.2 (m, C-3), 123.89 (t, C-2, $J_{C\text{-}F}$=258.6Hz), 148.6 (C-9), 156.9 (C-6), 166.0 (C-7).

IR v_{max} (neat) = 3321, 3211, 1623 cm^{-1}

MS (ES+) m/z = 389 $[M+H]^+$, 452 $[M+MeCN+Na]^+$.
HRMS (ES+) calculated 389.9762 for $C_9H_{11}N_3F_2O_4I$, observed 389.9768 $[M+H]^+$.

(2*R*,3*R*,5*R*)-5-(4-Acetamido-5-iodo-2-oxopyrimidin-1(2H)-yl)-2-(acetoxymethyl)-4,4-difluorotetrahydrofuran-3-yl acetate 244

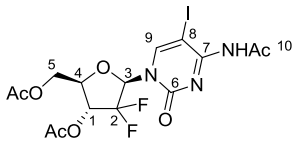

To a solution of iodide **238** (190 mg, 0.49 mmol) and DMAP (6.1 mg, 0.05 mmol) in pyridine (3.0 mL) was added acetic anhydride (0.41 mL, 4.40 mmol) and the resulting solution stirred for 16 hours. The reaction mixture was quenched with saturated $NaHCO_3$ (aq) (20 mL), extracted into EtOAc (2 × 30 mL), the combined organic layers washed with H_2O (30 mL), dried over $MgSO_4$ and concentrated *in vacuo*. The crude material was purified using flash silica column chromatography (3% acetone in $CHCl_3$) to yield the product (138 mg, 59%) as an amorphous solid.

^{1}H-NMR (500 MHz, $CDCl_3$): δ_H = 2.17 (s, 3H-Ac), 2.19 (s, 3H-Ac), 2.21 (s, 3H-Ac), 4.35 (dd, 1H^4, *J*=8.9Hz, *J*=3.8Hz), 4.42-4.45 (m, 2H^5), 5.26-5.31 (m, 1H^1), 6.36-6.40 (m, 1H^3), 7.93 (s, 1H^9).

^{13}C-NMR (125 MHz, $CDCl_3$): δ_C = 20.4 (C-Ac), 20.8 (C-Ac), 40.4 (C-8), 61.8 (C-5), 70.53 (dd, C-3, $^2J_{C\text{-}F}$=33.6Hz, $^2J_{C\text{-}F}$=18.4Hz), 78.4 (C-4), 83.3-84.5 (br, s, C-1), 149.0 (C-9), 159.1 (C=O), 168.9 (C=O), 170.2 (C=O).

Note: missing C-7, 1× C-Ac and C-2 due to a weak signal and overlapping peaks.

IR ν_{max} (neat) = 3347, 1746, 1711, 1668 cm^{-1}

MS (ES+) m/z = 516 $[M+H]^+$, 538 $[M+Na]^+$.
HRMS (ES+) calculated 516.0079 for $C_{15}H_{17}N_3F_2O_7I$, observed 516.0062 $[M+H]^+$.

Results and Discussion Section 4.

2'-Deoxy-2',2'-difluorouridine 260

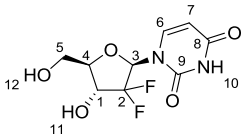

To a solution of the protected nucleoside **221β** (390 mg, 0.42 mmol) in MeOH at 0 ^{o}C (83 mL) was added 7.0 M NH_3 in MeOH (17 mL, 116 mmol). The resulting solution was warmed to room temperature and stirred for 16 hours. The solvents were removed *in vacuo* and the resultant residue partitioned between H_2O (80 mL) and EtOAc (80 mL). The organic layer was re-extracted with H_2O (80 mL) and the combined aqueous layers concentrated *in vacuo* to yield the product (197 mg, 90%) as a colourless amorphous solid.
The data were in agreement with the published data.[194]

^{1}H-NMR (400 MHz, D_2O): δ_H = 3.75 (dd, 1H^{5}, *J*=13.1Hz, *J*=4.4Hz), 3.90 (dd, 1H^{5}, *J*=13.1Hz, *J*=2.0Hz), 3.96 (m, 1H^{4}), 4.26 (td, 1H^{1}, $^{3}J_{H\text{-}F}$=11.8Hz, *J*=8.5Hz), 5.80 (d, 1H^{7}, *J*=8.1Hz), 6.09 (m, 1H^{3}), 7.67 (d, 1H^{6}, *J*=8.1Hz).

^{13}C-NMR (100 MHz, D_2O): δ_C = 59.3 (C-5), 69.2 (dd, C-1, $^{2}J_{C\text{-}F}$=25.6Hz, 20.7Hz) 80.46 (d, C-4, $^{3}J_{C\text{-}F}$=7.8Hz) 84.13 (dd, C-3, $^{2}J_{C\text{-}F}$=39.3Hz, 25.3Hz), 102.5 (C-7), 122.1 (dd, C-2, $J_{C\text{-}F}$= 260.6Hz, 259.5Hz), 141.4 (C-6), 151.4 (C-9), 165.9 (C-8).

IR ν_{max} (neat) = 3266, 1686 cm^{-1}

MS (ES+) m/z = 265 $[M+H]^{+}$.
HRMS (ES+) calculated 265.0636 for $C_9H_{11}N_2F_2O_5$, observed 265.0635 $[M+H]^{+}$.

1-[(2*R*,4*R*,5*R*)-3,3-Difluoro-4-hydroxy-5-(hydroxymethyl)oxolan-2-yl]-5-(hydroxymethyl)-1,2,3,4-tetrahydropyrimidine-2,4-dione 261

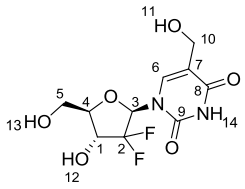

To a solution of nucleoside **260** (280 mg, 1.06 mmol), in H_2O:MeCN (7:3, 3.75 mL) was added *para*-formaldehyde (302 mg, 10.6 mmol) and NEt_3 (1.05 mL, 7.42 mmol) and the resulting solution stirred for 3 days at 60 ^oC. The reaction mixture was concentrated *in vacuo* and the crude residue purified using (15% MeOH in CH_2Cl_2) to yield the product (71 mg, 23%) as a colourless gum.

^{1}H-NMR (400 MHz, MeOD-d$_4$): δ_H = 3.79 (dd, 1H^5, *J*=12.5Hz, *J*=3.1Hz), 3.88-3.97 (m, 2H^{4+5}), 4.30-4.36 (m, 3H^{1+10}), 6.15-6.19 (m, 1H^3), 7.87 (s, 1H^6).

^{13}C-NMR (100 MHz, MeOD-d$_4$): δ_C = 57.9 (C-10), 60.5 (C-5), 70.4 (dd, C-1, $^2J_{C\text{-}F}$ 24.9Hz, $^2J_{C\text{-}F}$ =20.6Hz), 82.6 (d, C-4, $^3J_{C\text{-}F}$ =8.0Hz), 85.3 (dd, C-3, $^2J_{C\text{-}F}$ =40.2Hz, $^2J_{C\text{-}F}$ =24.8Hz), 115.6 (C-7), 125.4 (t, C-2, $J_{C\text{-}F}$=258.6.3Hz), 138.8 (C-6), 152.0 (C-9), 164.8 (C-8).

IR ν_{max} (neat) =3344, 2927, 1677 cm^{-1}

MS (ES-) m/z = 293 [M-H]$^-$.
HRMS (ES-) calculated 293.0585 for $C_{10}H_{11}N_2F_2O_6$, observed 293.0579 [M-H]$^-$.

1-[(2*R*,4*R*,5*R*)-3,3-Difluoro-4-hydroxy-5-[(methoxymethoxy)methyl]oxolan-2-yl]-4-(methoxymethoxy)-1,2-dihydropyrimidin-2-one 262

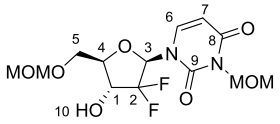

To a solution of the nucleoside **260** (90 mg, 0.34 mmol) in DMF (2.8 mL) at 0 ^{o}C was added DIPEA (0.24 mL, 1.42 mmol) followed by dropwise addition of chloromethyl methyl ether (0.1 mL, 1.36 mmol). The resulting solution was warmed to room temperature and stirred for 16 hours. The reaction was quenched by the addition of H_2O (10 mL), then extracted into EtOAc (2 × 10 mL), washed with 1.0 M HCl (aq) (10 mL) and then a mixture of H_2O:brine (1:1, 2 × 20 mL). The organic layers were dried over $MgSO_4$, concentrated *in vacuo* and purified using flash silica column chromatography (4% MeOH in $CHCl_3$) to yield the product as a colourless oil (76 mg, 63%).

^{1}H-NMR (400 MHz, $CDCl_3$): δ_H = 2.68 (dd, 1H^{10}, *J*=6.2Hz, *J*=1.5Hz), 3.40 (s, 3H (CH_3)), 3.44 (s, 3H (CH_3)), 3.83 (dd, 1H^{5}, *J*=11.5Hz, *J*=3.5Hz), 3.93 (dd, 1H^{5}, *J*=11.6Hz, *J*=1.8Hz), 4.09 (m, 1H^{4}), 4.36 (m, 1H^{1}), 4.71 (s, 2H (CH_2)), 5.37 (d, 1H, *J*=9.6Hz (CH_2)), 5.40 (d, 1H, *J*=9.6Hz (CH_2)), 5.81 (d, 1H^{7}, *J*=8.2Hz), 6.26 (dd, 1H^{3}, $^{3}J_{H\text{-}F}$=8.7Hz, $^{3}J_{H\text{-}F}$ =7.1Hz), 7.53 (d, 1H^{6}, *J*=8.2Hz).

^{13}C-NMR (100 MHz, $CDCl_3$): δ_C = 55.6 (CH_3, MOM), 57.9 (CH_3, MOM), 64.9 (C-5), 70.5 (dd, C-1, $^{2}J_{C\text{-}F}$=28.5Hz, $^{2}J_{C\text{-}F}$ =19.2Hz), 72.1 (CH_2, MOM), 80.1 (d, C-4, $^{3}J_{C\text{-}F}$=7.6Hz), 84.2 (dd, C-3, $^{2}J_{C\text{-}F}$=41.0Hz, $^{2}J_{C\text{-}F}$=22.4Hz), 96.8 (CH_2, MOM), 102.5 (C-7), 121.9 (dd, C-2, $^{1}J_{C\text{-}F}$=261.8Hz, $^{1}J_{C\text{-}F}$=258.0Hz), 138.1 (C-6), 151.0 (C-8), 162.2 (C-9).

IR ν_{max} (neat) = 3385, 2931, 1719, 1665 cm^{-1}

MS (CI+) m/z = 353 $[M+H]^+$, 370 $[M+NH_4]^+$.
HRMS (CI+) calculated 353.1160 $C_{13}H_{19}F_2N_2O_7$, observed 353.1165 $[M+H]^+$.

1-[(2*R*,4*R*,5*R*)-3,3-Difluoro-4-hydroxy-5-[(methoxymethoxy)methyl]oxolan-2-yl]-5-(hydroxymethyl)-4-(methoxymethoxy)-1,2-dihydropyrimidin-2-one 263

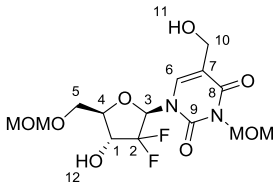

A suspension of protected nucleoside **262** (92 mg, 0.26 mmol) and *para*-formaldehyde (20 mg, 0.63 mmol) in 0.5 N KOH (aq) (0.5 mL) was stirred at 60 ^{o}C for 3 days. The reaction mixture was then concentrated *in vacuo* and purified using flash silica column chromatography (4% MeOH in $CHCl_3$) to yield the starting material (25 mg, 27%) and a mixture of the product and an inseparable, unidentifiable side-product (29 mg, 29%) as a gum, which was used directly in the next step with no further purification.

^{1}H-NMR (500 MHz, $CDCl_3$): δ_H = 3.41 (s, 3H (CH_3)), 3.45 (s, 3H (CH_3)), 3.84 (dd, 1H^{5}, *J*=11.6Hz, *J*=3.1Hz), 3.95 (br, d, 1H^{5}, *J*=11.6Hz), 4.09 (dt, 1H^{4}, *J*=7.7Hz, *J*=3.0Hz), 4.37-4.46 (m, 3H^{1+10}), 4.73 (s, 2H (CH_2)), 5.38 (d, 1H, *J*=9.6Hz (CH_2)), 5.41 (d, 1H, *J*=9.6Hz (CH_2)), 6.27 (dd, 1H^{3}, $^{3}J_{H\text{-}F}$=9.6Hz, $^{3}J_{H\text{-}F}$=5.4Hz), 7.70 (s, 1H^{6}).

^{13}C-NMR (125 MHz, $CDCl_3$): δ_C = 55.7 (CH_3, MOM) 58.1 (CH_3, MOM) 59.4 (C-10) 64.7 (C-5) 70.0 (dd, C-1, $^{2}J_{C\text{-}F}$ =27.4Hz, $^{2}J_{C\text{-}F}$ =19.6Hz) 72.2 (CH_2, MOM) 80.0 (d, C-4, $^{3}J_{C\text{-}F}$ =7.9Hz) 83.9-84.6 (m, C-3) 96.7 (CH_2, MOM) 113.6 (C-7) 124.6 (t, C-2, $^{1}J_{C\text{-}F}$=261.2Hz) 135.2 (C-6) 150.7 (C-8) 162.7 (C-9).

IR ν_{max} (neat) = 3274, 2950, 1708, 1656 cm^{-1}

MS (ES+) m/z = 383 $[M+H]^{+}$.
HRMS (ES+) calculated 383.1226 for $C_{14}H_{21}N_2F_2O_8$, observed 383.1257 $[M+H]^{+}$.

{1-[(2*R*,4*R*,5*R*)-3,3-Difluoro-4-hydroxy-5-[(methoxymethoxy)methyl]oxolan-2-yl]-4-(methoxymethoxy)-2-oxo-1,2-dihydropyrimidin-5-yl}methyl 5-(dimethylamino)-naphthalene-1-sulfonate 264

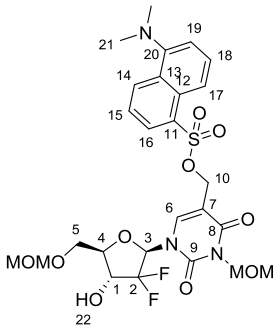

To a solution of the hydroxymethylated nucleoside **263** (60 mg, 0.17 mmol) and triethylamine (70 µL, 0.52 mmol) in CH_2Cl_2 (3 mL) was added dansyl chloride (86 mg, 0.35 mmol). After stirring for 24 hours additional equivalents of triethylamine (70 µL, 0.52 mmol) and dansyl chloride (86 mg, 0.35 mmol) were added and reaction continued for a further 12 hours. The mixture was then concentrated *in vacuo* and purified using flash silica column chromatography (100% $CHCl_3$) to yield the product as yellow gum (18 mg, 17%).

^{1}H-NMR (400 MHz, $CDCl_3$): δ_H = 2.55-2.58 (m, 1H^{22}), 2.92 (s, 6H^{21}), 3.36 (s, 3H(CH_3)), 3.43 (s, 3H (CH_3)), 3.51 (dd, 1H^5, *J*=11.8Hz, *J*=2.4Hz), 3.82 (br, d, 1H^5, *J*=11.6Hz), 4.25 (dt, 1H^4, *J*=7.8Hz, *J*=2.1Hz), 4.41 (br s, 2H (CH_2)), 4.47 (d, 1H^{10}, *J*=6.6Hz), 4.58 (d, 1H^{10}, *J*=6.5Hz), 5.10-5.17 (m, 1H^1), 5.34 (d, 1H, *J*=9.6Hz (CH_2)), 5.38 (d, 1H, *J*=9.6Hz (CH_2)), 6.19 (t, 1H^3, $^3J_{H\text{-}F}$=7.7Hz), 7.25 (d, 1H^{19}, *J*=7.5Hz), 7.62 (m, 3H$^{6,\ 15,\ 18}$), 8.25 (d, 1H^{16}, *J*=8.6Hz), 8.33 (dd, 1H^{17}, *J*=7.3Hz, *J*=0.8Hz), 8.68 (d, 1H^{14}, *J*=8.6Hz).

^{13}C-NMR (100 MHz, $CDCl_3$): δ_C = 45.42 (C-21), 55.74 (CH_3, MOM), 58.03 (CH_3, MOM), 59.31 (CH_2, MOM), 63.63 (C-5), 72.17 (CH_2, MOM), 73.71 (t, C-1, $^2J_{C\text{-}F}$ =24.0Hz), 77.80 (C-4), 84.0-84.9 (br, s, C-3), 96.67 (C-10), 113.28 (C-7), 115.89 (C-19), 119.00 (C-16), 122.92 (C-18), 129.22 (C-15), 129.81 (C-12/13), 129.86 (C-11), 130.44 (C-12/13), 130.94 (C-17), 132.72 (C-14), 134.92 (C-6), 150.55 (C-20), 152.00 (C-8), 162.51 (C-9).

Note: missing C-2 due to overlapping signals.

IR ν_{max} (neat) = 3478, 2928, 1718, 1675 cm^{-1}

MS (ES+) m/z = 616 $[M+H]^+$, 638 $[M+Na]^+$.
HRMS (ES+) calculated 616.1776 for $C_{26}H_{32}F_2N_3O_{10}S$, observed 616.1767 $[M+H]^+$.

1-((6a*R*,8*R*,9a*R*)-9,9-Difluoro-2,2,4,4-tetraisopropyltetrahydro-6H-furo[3,2-f][1,3,5,2,4]trioxadisilocin-8-yl)-5-iodopyrimidine-2,4(1H,3H)-dione 265

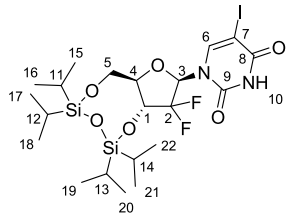

To a solution of iodide **223** (210 mg, 0.54 mmol) and imidazole (165 mg, 2.42 mmol) in DMF (1.1 mL) at 0 ^oC was added 1,3-dichloro-1,1,3,3-tetraisopropyl disiloxane (0.19 mL, 0.59 mmol) dropwise and the resulting solution warmed to room temperature and stirred for 16 hours. The reaction mixture was then diluted with EtOAc (20 mL), washed sequentially with brine (15 mL) and H_2O (15 mL), dried over $MgSO_4$ and concentrated *in vacuo*. The crude product was purified using flash silica column chromatography (100% CH_2Cl_2) to yield the product (302 mg, 88%) as colourless oil.

^{1}H-NMR (400 MHz, DMSO-d_6): δ_H = 1.12 (m, 28H$^{11\text{-}22}$), 3.96 (ddd, 1H^4, J=9.8Hz, J=2.5Hz, J=1.4Hz), 4.06 (dd, 1H^5, J=13.6Hz, J=2.5Hz), 4.23 (d, 1H^5, J=13.4Hz), 4.34 (td, 1H^1, J=13.6Hz, J=9.6Hz), 6.10 (m, 1H^3), 7.86 (s, 1H^6), 8.28 (s, 1H^{10}).

^{13}C-NMR (100 MHz, DMSO-d_6): δ_C = 12.4 (C-11-14), 12.6 (C-11-14), 12.9 (C-11-14), 13.5 (C-11-14), 16.7 (C-15-22), 16.8 (C-15-22), 16.9 (C-15-22), 17.1 (C-15-22), 17.2 (C-15-22), 17.4 (C-15-22), 17.6 (C-15-22), 17.7 (C-15-22), 59.1 (C-5), 69.0 (C-1), 79.4 (C-4), 84.4 (C-3), 142.6 (C-6), 149.2 (C-9), 164.6 (C-8).

Note: missing C-2 and C-7 due to weak signals.

IR ν_{max} (neat) = 2947, 2868, 1702, 1612 cm^{-1}

MS (ES+) m/z =633 $[M+H]^+$.
HRMS (ES+) calculated 633.1125 for $C_{21}H_{36}N_2O_6F_2Si_2I$, observed 633.1130 $[M+H]^+$.

5-Hydroxymethyluracil 259

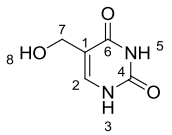

A suspension of uracil (2.5 g, 22.3 mmol) and *para*-formaldehyde (2.0 g, 66.9 mmol) in H_2O (75 mL) was treated with NEt_3 (4.6 mL, 33.4 mmol), then heated to 60 ^oC and stirred for 16 hours. The reaction mixture was then concentrated *in vacuo*, triturated with H_2O and EtOH (1:1, 20 mL), stirred for 1 hour at 0 ^oC, filtered and washed with cold EtOH to yield the product (2.3 g, 73 %) as a white solid.
The data were in agreement with the published data.[220]

^{1}H-NMR (400 MHz, DMSO-d_6): δ_H = 4.10 (d, $2H^7$, *J*=5.3Hz) 4.85 (t, $1H^8$, *J*=5.3Hz) 7.24 (s, $1H^2$) 10.73 (s, br, $1H^3$) 11.05 (s, br, $1H^5$).

^{13}C-NMR (100 MHz, DMSO-d_6): δ_C = 56.2 (C-7), 113.2 (C-1), 138.6 (C-2), 151.8 (C-6), 164.2 (C-4).

IR ν_{max} (neat) = 3010, 1737, 1662 cm^{-1}

MS (CI+) m/z =160 $[M+NH_4]^+$.
HRMS (CI+) calculated 160.0722 for $C_5H_{10}N_3O_3$, observed 160.0715 $[M+NH_4]^+$.

5-{[(*tert*-Butyldiphenylsilyl)oxy]methyl}-uracil 267

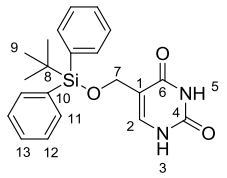

To a solution of 5-hydroxymethyl uracil **259** (2.3 g, 16.2 mmol) and imidazole (1.4 g, 21.1 mmol) in DMF (23 mL) was added TBDPSCl (5.0 mL, 19.4 mmol) and the resulting solution stirred for 24 hours at room temperature. The reaction mixture was then concentrated *in vacuo* and re-crystallised twice from MeOH:$CHCl_3$ (7:3) to yield the product as a white solid (5.0 g, 81%).

The data were in agreement with the published data.[243]

^{1}H-NMR (400 MHz, $CDCl_3$): δ_H = 1.00 (s, 9H^9), 4.36 (s, 2H^7), 7.27 (d, 1H^2, *J*=5.4Hz), 7.41-7.48 (m, 6H^{11+13}), 7.63-7.66 (m, 4H^{12}), 10.76 (d, 1H^3, *J*=5.4Hz,) 11.13 (s, br, 1H^5).

^{13}C-NMR (400 MHz, $CDCl_3$): δ_C = 19.2 (C-8), 27.1 (C-9), 59.3 (C-7), 114.6 (C-1) 128.4 (C-12), 130.4 (C-13), 133.2 (C-10) 135.5 (C-11), 138.6 (C-2), 151.6 (C-6), 163.9 (C-4).

IR ν_{max} (neat) = 2939, 1720, 1680 cm^{-1}

MS (ES+) m/z = 381 $[M+H]^+$.

HRMS (ES+) calculated 381.1634 for $C_{21}H_{25}N_2O_3Si$, observed 381.1639 $[M+H]^+$.

(2*R*,3*R*)-2-[(Benzoyloxy)methyl]-5-(5-{[(*tert*-butyldiphenylsilyl)oxy]methyl}-2,4-dioxo-1,2,3,4-tetrahydropyrimidin-1-yl)-4,4-difluorooxolan-3-yl benzoate 269

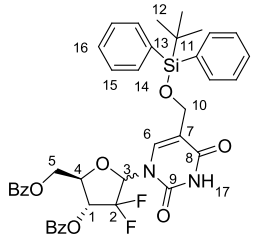

Protected uracil **267** (1.98 g, 5.21 mmol) and $(NH_4)_2SO_4$ (41 mg, 0.30 mmol) were refluxed in HMDS (26 mL) for 16 hours, then cooled to room temperature and concentrated *in vacuo*. The resulting residue was dissolved in DCE (8 mL), TMSOTf (0.94 mL, 5.21 mmol) was added and the mixture treated with a solution of mesylates **233** (1.40 g, 3.07 mmol) in DCE (22 mL). After refluxing for 16 hours, the reaction mixture was cooled to room temperature and the solvent removed *in vacuo*. The resulting gum was dissolved in CH_2Cl_2 (100 mL) then washed sequentially with H_2O (2 ×100 mL), saturated $NaHCO_3$ (aq) (100 mL) and brine (100 mL) then dried over $MgSO_4$ and concentrated *in vacuo* to yield the crude product. The crude product was purified using flash silica column chromatography (100% CH_2Cl_2) to yield the product (2.27 g, 63%) as a colourless solid in a 1.5:1.0 mixture of anomers.

^{1}H-NMR (400 MHz, $CDCl_3$): δ_H = 1.03 (s, 9H$^{12\alpha}$), 1.05 (s, 9H$^{12\beta}$), 4.53-4.72 (m, 10H$^{4,5,\ 10\alpha+\beta}$), 5.56-5.60 (m, 1H$^{1\beta}$), 5.82 (dt, 1H$^{1\alpha}$, $^3J_{H\text{-}F}$=10.4Hz, J=5.2Hz), 6.37 (dd, 1H$^{3\beta}$, $^3J_{H\text{-}F}$=11.6Hz, $^3J_{H\text{-}F}$ =6.5Hz), 6.53 (t, 1H$^{3\alpha}$, $^3J_{H\text{-}F}$=7.0Hz), 7.34-7.64 (m, 34H-Ar), 7.98-8.09 (m, 8H-Ar), 8.37 (s, 2H$^{17\alpha+\beta}$).

^{13}C-NMR (100 MHz, $CDCl_3$): δ_C = 19.2 (C-11), 19.2 (C-11), 26.7 (C-12), 26.7 (C-12), 58.7 (C-10), 58.8 (C-10), 63.1 (C-5), 63.3 (C-5) 71.6-71.9 (m, C-1α+β), 77.8 (C-4β), 81.2 (C-4α), 83.4 (C-3β), 85.1 (C-3α), 114.5 (C-7), 115.1 (C-7), 127.7-128.9 (m, C-2α+β), 127.9 (CH-Ar), 128.5 (CH-Ar), 128.6 (CH-Ar), 128.7 (CH-Ar), 129.7 (CH-Ar), 129.8 (CH-Ar), 130.0 (C-Ar), 130.1 (CH-Ar), 132.5 (C-Ar), 132.6 (C-Ar), 133.5 (CH-Ar), 133.6 (CH-Ar), 134.2 (CH-Ar), 134.3 (CH-Ar), 134.7 (C-Ar), 135.3 (C-Ar) 135.4 (CH-Ar), 135.4 (CH-Ar), 149.7 (C=O), 149.7 (C=O), 161.1 (C=O), 161.2 (C=O), 164.6 (C=O), 164.6 (C=O), 165.8 (C=O), 165.9 (C=O).

Note: missing multiple CH-Ar and C-Ar due to overlapping peaks. At this point the identity of the anomers could not be ascertained α and β were arbitrarily assigned to allow easier analysis of the NMR data.

IR ν_{max} (neat) = 1721, 1689 cm^{-1}

MS (ES+) m/z = 741 $[M+H]^+$.
HRMS (ES+) calculated 741.2444 for $C_{40}H_{39}F_2N_2O_8Si$, observed 741.2426 $[M+H]^+$.

(2*R*,3*R*,5*R*)-2-[(Benzoyloxy)methyl]-4,4-difluoro-5-[5-(hydroxymethyl)-2,4-dioxo-1,2,3,4-tetrahydropyrimidin-1-yl]oxolan-3-yl benzoate 270β

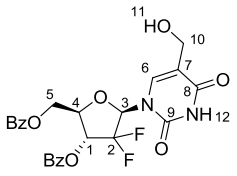

To a solution of protected nucleoside **269** (380 mg, 0.51 mmol) in THF (51 mL) at 0 °C was added 1.0 M TBAF in THF (0.64 mL, 0.64 mmol) dropwise and the resulting solution warmed to room temperature and stirred for 16 hours. The reaction mixture was then concentrated *in vacuo* and purified using flash silica column chromatography (3% MeOH in $CHCl_3$) to yield the product (207 mg, 81%) as a 1:1 mixture of anomers. Recrystallisation from $CHCl_3$ yielded pure β-anomer (207 mg, 40%) as colourless needles.

^{1}H-NMR (500 MHz, DMSO-d_6): δ_H = 4.15 (d, 2H^{10}, *J*=5.2Hz), 4.72 (qd, 2H^5, *J*=12.4Hz, *J*=4.1Hz), 4.82 (m, 1H^4), 5.11 (t, 1H^{11}, *J*=5.3Hz), 5.74-5.80 (m, 1H^1), 6.43 (t, 1H^3, $^3J_{H\text{-}F}$=9.4Hz), 7.47-7.51 (m, 2H-Ar), 7.56-7.60 (m, 2H-Ar), 7.61 (s, 1H^6), 7.63-7.74 (m, 2H-Ar), 7.97-7.98 (m, 2H-Ar) ,8.05-8.07 (m, 2H-Ar), 11.74 (s, 1H^{12}).

^{13}C-NMR (125 MHz, DMSO-d_6): δ_C = 55.7 (C-10), 62.9 (C-5), 71.1-71.4 (m, C-1), 75.7 (C-4), 83.4-84.4 (br, s, C-3), 115.0 (C-7), 121.54 (t, C-2, $J_{C\text{-}F}$=261.7Hz), 127.9 (C-Ar), 128.8 (CH-Ar), 128.9 (CH-Ar), 129.0 (C-Ar), 129.2 (CH-Ar), 129.7 (CH-Ar), 133.6 (CH-Ar), 134.2 (CH-Ar), 136.5 (C-6), 150.0 (C=O), 162.2 (C=O), 164.3 (C=O). 165.4 (C=O).

IR ν_{max} (neat) = 3431, 1713, 1697 cm^{-1}

MS (ES+) m/z = 503 $[M+H]^+$.
HRMS (ES+) calculated 503.1266 for $C_{24}H_{21}N_2F_2O_8$, observed 503.1283 $[M+H]^+$.

mp ($CHCl_3$)= 160-162 ^oC.

1-[(2*R*,4*R*,5*R*)-3,3-Difluoro-4-hydroxy-5-(hydroxymethyl)oxolan-2-yl]-5-(hydroxymethyl)-1,2,3,4-tetrahydropyrimidine-2,4-dione 261

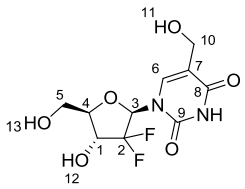

To a solution of nucleoside **270β** (50 mg, 0.1 mmol) in MeOH (2.0 mL) at 0 ^oC was added 7.0 M NH_3 in MeOH (1.1 mL, 8.0 mmol) and the resulting solution warmed to room temperature and stirred for 16 hours. The solvents were removed *in vacuo* and the resultant residue partitioned between H_2O (10 mL) and EtOAc (10 mL). The organic layer was re-extracted with H_2O (2 × 10 mL) and the combined aqueous layers concentrated under reduced pressure to yield the product (28 mg, 95%) as a colourless amorphous solid.

^{1}H-NMR (400 MHz, MeOD-d_4): δ_H = 3.79 (dd, 1H^5, *J*=12.5Hz, *J*=3.1Hz), 3.88-3.97 (m, 2H$^{4+5,}$) 4.30-4.36 (m, 3H$^{1+10,}$) 6.15-6.19 (m, 1H^3), 7.87 (s, 1H^6).

^{13}C-NMR (100 MHz, MeOD-d_4): δ_C = 57.9 (C-10), 60.5 (C-5), 70.42 (dd, C-1, $^2J_{C\text{-}F}$ 24.9Hz, $^2J_{C\text{-}F}$ =20.6Hz), 82.62 (d, C-4, $^3J_{C\text{-}F}$ =8.0Hz), 85.29 (dd, C-3, $^2J_{C\text{-}F}$ =40.2Hz, $^2J_{C\text{-}F}$ =24.8Hz), 115.6 (C-7), 125.39 (t, C-2, $J_{C\text{-}F}$=258.6.3Hz), 138.8 (C-6), 152.0 (C-9), 164.8 (C-8).

IR ν_{max} (neat) =3344, 2927, 1677 cm^{-1}

MS (ES-) m/z = 293 $[M-H]^-$.

HRMS (ES-) calculated 293.0585 for $C_{10}H_{11}N_2F_2O_6$, observed 293.0579 $[M-H]^-$.

(2*R*,3*R*,5*R*)-2-[(Benzoyloxy)methyl]-4,4-difluoro-5-[5-(fluoromethyl)-2,4-dioxo-1,2,3,4-tetrahydropyrimidin-1-yl]oxolan-3-yl benzoate 271

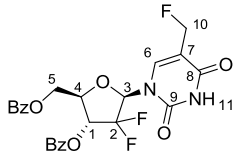

A solution of the nucleoside **270β** (100 mg, 0.20 mmol) in THF (0.70 mL) was added dropwise to a −15 °C solution of DAST (28 µl, 0.21 mmol) in THF (0.55 mL), stirred at this temperature for 30 minutes and then warmed to room temperature and stirred for a further hour. The reaction mixture was then poured into cold H_2O (10 mL), extracted into CH_2Cl_2 (10 mL), washed with H_2O (10 mL), dried with $MgSO_4$ and concentrated *in vacuo*. The crude product was purified using flash silica column chromatography (2% MeOH in CH_2Cl_2) to yield the product (25 mg, 25%) as a white solid.

^{1}H-NMR (500 MHz, DMSO-d$_6$): δ_H = 4.70-4.84 (m, 3H^{5+4}), 5.02 (d, 2H^{10}, $^2J_{H-F}$=48.6Hz), 5.76-5.91 (m, 1H^1), 6.42 (t, 1H^3, $^3J_{H-F}$=7.8Hz), 7.47 (t, 2H-Ar, *J*=7.4Hz), 7.58 (t, 2H-Ar, *J*=7.3Hz), 7.63-7.75 (m, 2H-Ar), 7.93-7.96 (m, 2H-Ar), 8.02-88.06 (m, 2H-Ar), 8.07-8.09 (m, 1H^6), 11.96 (s, 1H^{11}).

^{13}C-NMR (125 MHz, DMSO-d$_6$): δ_C = 63.3 (C-5), 71.46 (dd, C-1, $^2J_{C-F}$=25.3Hz, $^2J_{C-F}$=22.1Hz), 75.7 (C-4), 77.15 (d, C-10, J_{C-F}=162.6Hz) 83.4-84.5 (br, s, C-3), 109.68 (d, C-7, $^2J_{C-F}$ =18.3Hz), 121.53 (t, C-2, J_{C-F}=261.4Hz), 127.9 (C-Ar), 128.7 (CH-Ar), 128.9 (CH-Ar), 129.0 (C-Ar), 129.2 (CH-Ar), 129.7 (CH-Ar), 133.6 (CH-Ar), 134.3 (CH-Ar), 142.3 (d, C-6, $^3J_{C-F}$ =6.9Hz), 149.8 (C=O), 161.9 (C=O), 164.3 (C=O), 165.3 (C=O).

IR ν_{max} (neat) = 1724, 1700 cm^{-1}

MS (ES-) m/z = 503 $[M-H]^-$.
HRMS (ES-) calculated 503.1066 for $C_{24}H_{18}N_2F_3O_7$, observed 503.1084 $[M-H]^-$.

mp (THF) = 152-156 ^{o}C.

1-[(2*R*,4*R*,5*R*)-3,3-Difluoro-4-hydroxy-5-(hydroxymethyl)oxolan-2-yl]-5-(methoxymethyl)-1,2,3,4-tetrahydropyrimidine-2,4-dione 273

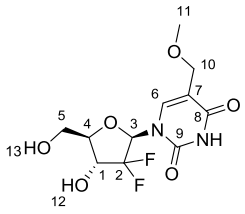

To a suspension of fluoride **271** (18 mg, 0.04 mmol) in MeOH (1.0 mL) at room temperature was added K_2CO_3 (7 mg, 0.05 mmol). The reaction mixture was stirred for 30 minutes, then concentrated *in vacuo* and purified using flash silica column chromatography (7 % MeOH in CH_2Cl_2) to yield the product (9 mg, 76%) as a colourless gum.

^{1}H-NMR (400 MHz, MeOD-d$_4$): δ_H = 3.37 (s, 3H^{11}), 3.80 (dd, 1H^{5}, *J*=12.6Hz, *J*=2.9Hz), 3.92 (dt, 1H^{4}, *J*=8.4Hz, *J*=2.6Hz), 3.97 (br d, 1H^{5}, *J*=12.8Hz), 4.14 (d, 1H^{10}, *J*=12.4Hz), 4.20 (d, 1H^{10}, *J*=11.6Hz), 4.32 (td, 1H^{1}, $^{3}J_{H\text{-}F}$=12.2Hz, *J*=8.4Hz), 6.15-6.19 (m, 1H^{3}), 7.98 (s, 1H^{6}).

^{13}C-NMR (100 MHz, MeOD-d$_4$): δ_C = 58.4 (C-11), 60.3 (C-5), 67.8 (C-10), 70.2 (dd, C-1, $^{2}J_{C\text{-}F}$=25.9Hz, $^{2}J_{C\text{-}F}$=19.9Hz), 82.6 (d, C-4, $^{3}J_{C\text{-}F}$=8.4Hz), 85.2 (dd, C-3, $^{2}J_{C\text{-}F}$=40.3Hz, $^{2}J_{C\text{-}F}$=24.5Hz), 112.4 (C-7), 124.0 (dd, C-2, $J_{C\text{-}F}$ =259.0Hz, $J_{C\text{-}F}$ =258.1Hz), 140.3 (C-6), 151.9 (C-9), 164.7 (C-8).

IR ν_{max} (neat) = 3363, 3072, 1682 cm^{-1}

MS (ES+) m/z = 309 [M+H]$^{+}$.
HRMS (ES+) calculated 309.0898 for $C_{11}H_{15}N_2F_2O_6$, observed 309.0916 [M+H]$^{+}$.

(2*R*,3*R*,5*R*)-5-[5-(Azidomethyl)-2,4-dioxo-1,2,3,4-tetrahydropyrimidin-1-yl]-2-[(benzoyloxy)methyl]-4,4-difluorooxolan-3-yl benzoate 276

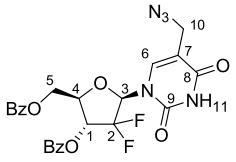

To a solution of nucleoside **270β** (400 mg, 0.80 mmol) in 1,4-dioxane (8 mL) was added TMSCl (0.50 mL, 4.00 mmol). After 5 hours at 65 ^{o}C additional TMSCl was added (0.5 mL, 4.00 mmol) and the reaction stirred for 16 hours at this temperature. The mixture was then concentrated *in vacuo,* the residue re-dissolved in DMF (8 mL), sodium azide (312 mg, 4.80 mmol) added and the solution stirred for 5 hours at 65 ^{o}C. The solvents were then removed under reduced pressure and the resulting solid partitioned between EtOAc (60 mL) and brine (60 mL). The organic layer was dried using $MgSO_4$, concentrated *in vacuo* and the crude material purified using flash silica column chromatography (2% MeOH in CH_2Cl_2, dry loaded using 1,4-dioxane) to yield the product as a white solid (288 mg, 68% over 2 steps).

^{1}H-NMR (500 MHz, DMSO-d$_6$): δ_H = 4.01 (d, 1H^{10}, *J*=13.6Hz), 4.05 (d, 1H^{10}, *J*=13.6Hz), 4.68-4.71 (m, 1H^{4}), 4.76-4.82 (m, 2H^{5}), 5.81 (m, 1H^{1}), 6.40 (t, 1H^{3}, $^{3}J_{H\text{-}F}$=8.9Hz), 7.47 (t, 2H-Ar, *J*=7.8Hz), 7.57 (t, 2H-Ar, *J*=7.8Hz), 7.63-7.74 (m, 2H-Ar), 7.88 (s, 1H^{6}), 7.95 (dd, 2H-Ar, *J*=8.2Hz, *J*=1.1Hz), 8.04 (dd, 2H-Ar, *J*=8.2Hz, *J*=1.1Hz), 11.92 (s, 1H^{11}).

^{13}C-NMR (125 MHz, DMSO-d$_6$): δ_C = 46.5 (C-10), 63.3 (C-5), 71.3-71.7 (m, C-1), 75.7 (C-4), 83.2-84.4 (br, s, C-3), 109.31 (C-7), 121.59 (t, C-2, $J_{C\text{-}F}$ =261.6Hz), 127.9 (C-Ar), 128.7(CH-Ar), 128.9 (CH-Ar), 129.0 (C-Ar), 129.2 (CH-Ar), 129.7 (CH-Ar), 133.6 (CH-Ar), 134.3 (CH-Ar), 139.9 (C-6), 149.8 (C=O), 162.4 (C=O), 164.3 (C=O), 165.4 (C=O).

IR v_{max} (neat) = 3279, 2096, 1722, 1689 cm^{-1}

HRMS: Did not provide spectra suitable for interpretation.

mp (acetone) = 170-176 ^{o}C.

5-(Azidomethyl)-1-[(2*R*,4*R*,5*R*)-3,3-difluoro-4-hydroxy-5-(hydroxymethyl)oxolan-2-yl]-1,2,3,4-tetrahydropyrimidine-2,4-dione 249

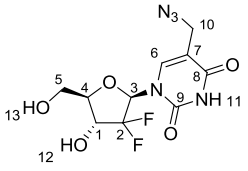

To a solution of the benzoyl protected azide **276** (30 mg, 60 μmol) in MeOH (3.0 mL) at 0 ^{o}C was added 7.0 M NH_3 in MeOH (0.7 mL, 4.80 mmol) and the resulting solution warmed to room temperature and stirred for 16 hours. The solvents were removed *in vacuo* and the resultant residue purified using flash silica column chromatography (5% MeOH in CH_2Cl_2) to yield the product (18 mg, 94%) as an amorphous colourless solid.

^{1}H-NMR (500 MHz, MeOD-d$_4$): δ_H = 3.80 (dd, 1H^5, *J*=12.6Hz, *J*=2.9Hz), 3.90-3.93 (m, 1H^4), 3.96 (br, d, 1H^5, *J*=12.9Hz), 4.08 (s, 2H^{10}), 4.32 (td, 1H^1, $^{3}J_{H\text{-}F}$=12.2Hz, *J*=8.4Hz), 6.13-6.17 (m, 1H^3), 8.05 (s, 1H^6).

^{13}C-NMR (125 MHz, MeOD-d$_4$): δ_C = 48.2 (C-10), 60.3 (C-5), 70.18 (dd, C-1, $^{2}J_{C\text{-}F}$ =26.5Hz, $^{2}J_{C\text{-}F}$ *J*=19.4Hz) 82.77 (d, C-4, $^{3}J_{C\text{-}F}$ =8.4Hz) 85.30 (dd, C-3, $^{2}J_{C\text{-}F}$ =40.8Hz, $^{2}J_{C\text{-}F}$ =23.9Hz) 110.79 (C-7) 123.96 (t, C-2, $J_{C\text{-}F}$=255.1Hz) 140.6 (C-6), 151.8 (C-9), 164.7 (C-8).

IR v_{max} (neat) = 3311, 2109, 1707, 1680 cm^{-1}

Anal. calculated for $C_{10}H_{11}F_2N_5O_5$: C, 37.63; H, 3.47; N, 21.94. Found: C, 37.51; H, 3.39; N, 21.87.

(2*R*,3*R*,5*R*)-5-[5-(Aminomethyl)-2,4-dioxo-1,2,3,4-tetrahydropyrimidin-1-yl]-2-[(benzoyloxy)methyl]-4,4-difluorooxolan-3-yl benzoate 282

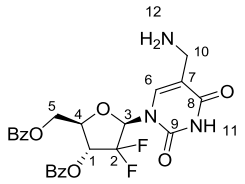

To a solution of the azide **276** (100 mg, 0.19 mmol) in THF:H_2O (10:1, 3.8 mL) was added triphenylphosphine (296 mg, 1.14 mmol) and the reaction mixture stirred for 16 hours at room temperature. The solvents were removed *in vacuo* and the crude material purified using flash silica column chromatography (5-10% MeOH in CH_2Cl_2) to yield the product (70 mg, 74%) as an amorphous white solid.

^{1}H-NMR (500 MHz, THF-d_8): δ_H = 3.38 (s, 2H^{10}), 4.12 (br s, 2H^{12}), 4.72 (m, 3H^{4+5}), 5.78-5.83 (m, 1H^1), 6.38 (t, 1H^3, $^3J_{H\text{-}F}$=9.1Hz), 7.42-7.66 (m, 7H-Ar), 8.00-8.14 (m, 4H-Ar).

^{13}C-NMR (125 MHz, THF-d_8): δ_C = 36.8 (C-10), 61.1 (C-5) 69.90 (dd, C-1, $^2J_{C\text{-}F}$ =28.5Hz, $^2J_{C\text{-}F}$ =20.5Hz), 75.3 (C-4), 82.2-82.9 (br, s, C-3), 114.7 (C-7), 122.10 (t, C-2, $J_{C\text{-}F}$=259.3Hz) 126.5 (CH-Ar), 126.6 (CH-Ar), 126.8 (C-Ar), 127.6 (CH-Ar), 127.9 (C-Ar), 127.9 (CH-Ar), 131.2 (CH-Ar), 131.8 (CH-Ar), 131.6 (CH-Ar), 148.3 (C=O), 160.6 (C=O), 162.4 (C=O), 163.5 (C=O).

IR ν_{max} (neat) = 2960, 1728, 1720 1673 cm^{-1}

MS (ES+) m/z = 502 $[M+H]^+$.
HRMS (ES+) calculated 502.1420 for $C_{24}H_{22}N_3F_2O_7$, observed 502.1426 $[M+H]^+$.

(2*R*,3*R*,5*R*)-2-[(Benzoyloxy)methyl]-5-{5-[5-(dimethylamino)naphthalene-1-sulfonamidomethyl]-2,4-dioxo-1,2,3,4-tetrahydropyrimidin-1-yl}-4,4-difluorooxolan-3-yl benzoate 283

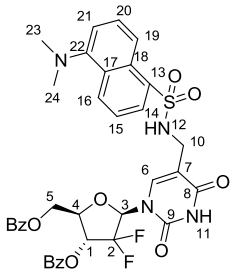

A room temperature solution of amine **282** (30 mg, 60 μmol) and NEt_3 (11 μl, 80 μmol) in THF (1.2 mL) was treated with dansyl chloride (19 mg, 70 μmol) and stirred for 16 hours. The reaction mixture was then concentrated *in vacuo* dissolved in CH_2Cl_2 (15 mL), washed with H_2O (10 mL), dried over $MgSO_4$ and the solvents removed *in vacuo*. The crude material was purified using flash silica column chromatography (2% MeOH in CH_2Cl_2) to yield the product (35 mg, 79%) as a pale green fluorescent solid.

^{1}H-NMR (400 MHz, $CDCl_3$): δ_H = 2.82 (s, 6H^{23+24}), 3.60 (dd, 1H^{10}, *J*=15.4Hz, *J*=6.5Hz), 3.78 (dd, 1H^{10}, *J*=15.4Hz, *J*=6.5Hz), 4.57-4.61 (m, 1H^4), 4.77 (dd, 1H^5, *J*=12.5Hz, *J*=4.6Hz), 4.87 (dd, 1H^5, *J*=12.5Hz, *J*=3.1Hz), 5.58-5.63 (m, 1H^1), 5.88 (t, 1H^{12}, *J*=6.5Hz), 6.20 (dd, 1H^3, $^3J_{H\text{-}F}$=12.0Hz, $^3J_{H\text{-}F}$=6.1Hz), 7.11 (d, 2H-Ar, *J*=8.1Hz), 7.40 (dd, 1H-Ar, *J*=8.3Hz, *J*=7.5Hz),7.47-7.52 (m, 5H-Ar), 7.59-7.67 (m, 2H-Ar), 8.06-8.14 (m, 6H-Ar), 8.44 (d, 1H-Ar, *J*=8.5Hz), 8.64 (s, 1H^{11}).

^{13}C-NMR (100 MHz, $CDCl_3$): δ_C = 40.7 (C-10), 45.3 (C-23+24), 62.5 (C-5), 71.5 (dd, C-1, $^2J_{C\text{-}F}$ =34.8Hz, $^2J_{C\text{-}F}$ =16.9Hz), 78.9 (C-4), 82.6-83.4 (br, s, C-3), 110.3 (C-7), 115.2 (CH-Ar), 118.7 (CH-Ar), 123.3 (CH-Ar), 127.8 (C-Ar), 128.5 (CH-Ar), 128.8 (CH-Ar), 128.9 (CH-Ar), 128.9 (C-Ar), 129.2 (C-Ar), 129.5 (CH-Ar), 129.6 (C-Ar), 129.8 (CH-Ar), 130.2 (CH-Ar), 130.3 (CH-Ar), 133.9 (CH-Ar), 134.3 (CH-Ar), 135.5 (C-Ar), 137.3 (CH-Ar), 149.0 (C=O), 151.9 (C-Ar), 162.0 (C=O), 164.8 (C=O), 166.0 (C=O).

Note: missing C-2 due to multiple overlapping peaks.

IR ν_{max} (neat) = 3058, 1720, 1680 cm^{-1}

MS (ES+) m/z = 735 $[M+H]^+$.
HRMS (ES+) calculated 735.1936 for $C_{36}H_{33}N_4F_2O_9S$, observed 735.1907 $[M+H]^+$.

mp (CH_2Cl_2) = 102-107 ^oC.

N-({1-[(2*R*,4*R*,5*R*)-3,3-Difluoro-4-hydroxy-5-(hydroxymethyl)oxolan-2-yl]-2,4-dioxo-1,2,3,4-tetrahydropyrimidin-5-yl}methyl)-5-(dimethylamino)naphthalene-1-sulfonamide 284

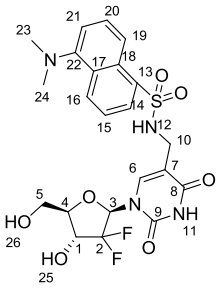

To solution of the dansylated nucleoside **283** (30 mg, 40 μmol) in MeOH (2.0 mL) at 0 ^oC was added 7.0 M NH_3 in MeOH (0.5 mL, 3.2 mmol) and the resulting solution warmed to room temperature and stirred for 16 hours. The solvents were removed *in vacuo* and the resultant residue purified using flash silica column chromatography (4% MeOH in CH_2Cl_2) to yield the product (16 mg, 76%) as a pale green fluorescent solid.

^{1}H-NMR (500MHz, MeOD-d$_4$): δ_H = 2.85 (s, 6H^{23+24}), 3.83 (m, 4H$^{4,5+10}$), 3.95-3.99 (m, 1H^5), 4.22 (td, 1H^1, $^3J_{H\text{-}F}$=12.1Hz, *J*=8.3Hz), 5.90 (m, 1H^3), 7.23 (dd, 1H-Ar, *J*=7.6Hz, *J*=0.7Hz), 7.53 (ddd, 2H-Ar, *J*=8.6Hz, *J*=7.5Hz, *J*=2.8Hz), 7.59 (s, 1H^6), 8.16 (dd, 1H-Ar, *J*=7.3Hz, *J*=1.2Hz), 8.21 (td, 1H-Ar, *J*=8.6Hz, *J*=0.8Hz), 8.50 (dt, 1H-Ar, *J*=8.6Hz, *J*=1.0Hz).

^{13}C-NMR (125 MHz, MeOD-d$_4$): δ_C = 40.6 (C-10), 45.8 (C23+24), 60.5 (C-5), 68.8-70.3 (m, C-1), 82.66 (d, C-4, $^3J_{C\text{-}F}$ =7.9Hz), 85.04 (dd, C-3, $^2J_{C\text{-}F}$ =39.2Hz, $^2J_{C\text{-}F}$ =25.5Hz), 111.2 (C-7), 116.4 (CH-Ar), 120.4 (CH-Ar), 123.76 (t, C-2, $J_{C\text{-}F}$ =252.8Hz) 124.6 (CH-Ar), 129.3 (CH-Ar), 130.6 (CH-Ar), 130.7 (C-Ar), 131.0 (C-Ar), 131.2 (CH-Ar), 137.3 (C-Ar), 139.2 (C-6), 151.3 (C-9), 153.1 (C-Ar), 164.2 (C-8).

IR v_{max} (neat) =3338, 1677 cm^{-1}

MS (ES+) m/z = 527 $[M+H]^+$.
HRMS (ES+) calculated 527.1412 for $C_{22}H_{25}N_4F_2O_7S$, observed 527.1408 $[M+H]^+$.

mp (MeOH-CH_2Cl_2) = 118-124 ^oC.

[(2*R*,3*R*)-3-(Benzoyloxy)-5-[5-({[({1-[(4*R*,5*R*)-4-(benzoyloxy)-5-[(benzoyloxy)methyl]-3,3-difluorooxolan-2-yl]-2,4-dioxo-1,2,3,4-tetrahydropyrimidin-5-yl}methyl)carbamoyl]amino}methyl)-2,4-dioxo-1,2,3,4-tetrahydropyrimidin-1-yl]-4,4-difluorooxolan-2-yl]methyl benzoate 285

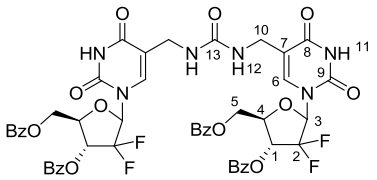

CDI (2.3 mg, 14 μmol) was added to a solution of amine **282** (15 mg, 28 μmol) in DMF (0.3 mL) and the resulting solution stirred at room temperature for 16 hours. The reaction mixture was concentrated *in vacuo* and the crude material purified using flash silica column chromatography (5-10% MeOH in CH_2Cl_2) to yield the product (12 mg, 80%) as a white solid.

^{1}H-NMR (500 MHz, THF-d_8): δ_H = 3.84-3.92 (m, 4H^{10}), 4.63-4.67 (m, 2H^4), 4.71-4.79 (m, 4H^5), 5.87 (m, 4H^{1+12}), 6.32 (br, s, 2H^3), 7.40-7.43 (m, 4H-Ar), 7.46-7.49 (m, 4H-Ar), 7.53 (tt, 2H-Ar, *J*=7.4, *J*=1.3Hz), 7.62 (tt, 2H-Ar, *J*=7.5, *J*=1.3Hz), 7.69 (s, 2H^6), 8.03-8.09 (m, 8H-Ar), 10.71 (s, 2H^{11}).

^{13}C-NMR (125 MHz, THF-d_8): δ_C = 37.3 (C-10), 64.1 (C-5), 72.6-73.0 (m, C-1), 78.0 (C-4), 85.6-86.1 (br, s, C-3), 114.0 (C-7), 122.64 (t, C-2, $J_{C\text{-}F}$=261.5Hz), 129.2 (CH-Ar), 129.3 (CH-Ar), 129.6 (C-Ar), 130.4 (CH-Ar), 130.6 (C-Ar), 130.6 (CH-Ar), 133.8 (CH-Ar), 134.5 (CH-Ar), 139.1 (C-6), 151.0 (C-9), 158.6 (C-13), 163.8 (C=O), 165.1 (C=O), 166.3 (C=O).

IR v_{max} (neat) = 1725, 1693 cm^{-1}

MS (ES+) m/z = 1029 $[M+H]^+$.

HRMS (ES+) calculated 1029.2566 for $C_{49}H_{41}F_4N_6O_{15}$, observed 1029.2566 $[M+H]^+$.

1,3-*bis*({1-[(4*R*,5*R*)-3,3-Difluoro-4-hydroxy-5-(hydroxymethyl)oxolan-2-yl]-2,4-dioxo-1,2,3,4-tetrahydropyrimidin-5-yl}methyl)urea 286

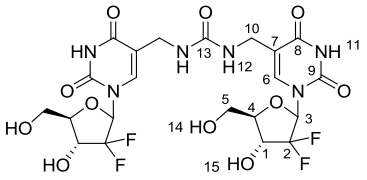

To a solution of dimeric nucleoside **285** (10 mg, 9.7 μmol) in MeOH (1.0 mL) at 0 ^oC was added 7.0 M NH_3 in MeOH (0.2 mL, 0.81 mmol) and the resulting solution warmed to room temperature and stirred for 16 hours. The reaction mixture was then concentrated *in vacuo* and partitioned between H_2O (5 mL) and EtOAc (5 mL). The organic layer was re-extracted with H_2O (5 mL) and the combined aqueous layers concentrated *in vacuo* to yield the crude product. Purification of the crude material using flash silica column chromatography (15% MeOH in CH_2Cl_2) gave the product (3 mg, 51%) as a white solid.

^{1}H-NMR (500 MHz, MeOD-d$_4$): δ_H = 3.79 (dd, 2H^5, *J*=12.6Hz, *J*=3.4Hz) 3.87-3.90 (m, 2H^4) 3.93-3.96 (m, 6H^{5+10}) 4.30 (td, 2H^1, $^3J_{H\text{-}F}$ =12.1Hz, *J*=8.3Hz) 6.11-6.13 (m, 2H^3) 7.80 (s, 2H^6).

^{13}C-NMR (125 MHz, MeOD-d$_4$): δ_C = 37.8 (C-10), 60.6 (C-5), 70.37 (dd, C-1, $^2J_{C\text{-}F}$=25.0Hz, $^2J_{C\text{-}F}$=20.8Hz), 82.70 (d, C-4, $^3J_{C\text{-}F}$ =7.1Hz), 85.34 (dd, C-3, $^2J_{C\text{-}F}$=36.3Hz, $^2J_{C\text{-}F}$=28.5Hz), 113.9 (C-7), 123.92 (t, C-2, $J_{C\text{-}F}$=252.5Hz), 138.9 (C-6), 151.9 (C-9), 160.5 (C-13), 165.1 (C-8).

IR ν_{max} (neat) = 3350, 1683 cm^{-1}

MS (ES-) m/z = 611 $[M-H]^-$.

HRMS (ES-) calculated 611.1361 for $C_{21}H_{23}F_4N_6O_{11}$, observed 611.1346 $[M-H]^-$.

But-3-ynyl-*p*-toluenesulfonate 280

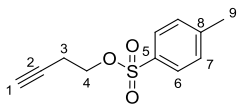

To a solution of 3-butyn-1-ol (0.22 mL, 2.85 mmol), NEt_3 (0.5 mL, 3.70 mmol) and 4-(dimethylamino)pyridine (34 mg, 0.28 mmol) in CH_2Cl_2 (11.5 mL) at 0 ^oC was added *p*-toluenesulfonyl chloride (598 mg, 3.14 mmol) and the resulting solution warmed to room temperature and stirred for 16 hours. 1.0 M NaOH (aq) (10 mL) was then added and the mixture stirred for a further 15 minutes. The phases were then separated and the organic layer diluted with CH_2Cl_2 (20 mL), washed sequentially with brine (20 mL) and H_2O (20 mL), then dried over $MgSO_4$ and concentrated *in vacuo*. The crude material was purified using flash silica column chromatography (30% EtOAc in 50-60 petroleum ether) to yield the product as a clear colourless oil (564 mg, 88%).
The data were in agreement with the published data.[251]

^{1}H-NMR (400 MHz, $CDCl_3$): δ_H = 1.97 (t, 1H^1, *J*=2.6Hz), 2.45 (s, 3H^9), 2.56 (td, 2H^3, *J*=7.1Hz, *J*=2.6Hz), 4.10 (t, 2H^4, *J*=7.1Hz), 7.35 (d, 2H^7, *J*=8.1Hz), 7.81 (d, 2H^6, *J*=8.2Hz).

^{13}C-NMR (100 MHz, $CDCl_3$): δ_C = 19.4 (C-3), 21.6 (C-9), 67.4 (C-4), 70.7 (C-1), 78.3 (C-2), 128.0 (C-6), 129.9 (C-7), 132.8 (C-8), 145.0 (C-5).

MS (CI+) m/z = 242 $[M+NH_4]^+$.
HRMS (CI+) calculated 242.0851 for $C_{11}H_{16}NSO_3$, observed 242.0850 $[M+NH_4]^+$.

(2*R*,3*R*,5*R*)-2-[(Benzoyloxy)methyl]-4,4-difluoro-5-(5-{[4-(2-{[(4-methylbenzene)sulfonyl]oxy}ethyl)-1H-1,2,3-triazol-1-yl]methyl}-2,4-dioxo-1,2,3,4-tetrahydropyrimidin-1-yl)oxolan-3-yl benzoate 281

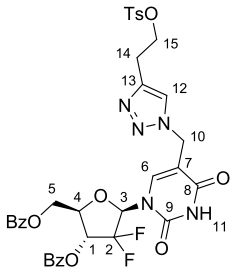

A solution of the azide **276** (90 mg, 0.17 mmol), ascorbic acid (30 mg, 0.17 mmol), $CuSO_4.5H_2O$ (21 mg, 90 μmol) and alkyne **280** (46 mg, 0.20 mmol) in DMF-H_2O (9:1, 3.7 mL) was stirred for 16 hours at room temperature. The reaction mixture was concentrated *in vacuo*, partitioned between CH_2Cl_2 (15 mL) and H_2O (15 mL), the organic layer dried over $MgSO_4$ and the solvent removed under reduced pressure. The crude product was purified using flash silica column chromatography (1-2% MeOH in CH_2Cl_2) to yield the product (85 mg, 67%) as a white solid.

^{1}H-NMR (400 MHz, $CDCl_3$): δ_H = 2.42 (s, 3H-Tos), 3.05 (t, 2H^{14}, *J*=6.8Hz), 4.27 (t, 2H^{15}, *J*=6.8Hz), 4.62 (dd, 1H^4, *J*=9.2Hz, *J*=4.6Hz), 4.75-4.83 (m, 2H^5), 5.00 (d, 1H^{10}, *J*=14.6Hz), 5.06 (d, 1H^{10}, *J*=14.6Hz), 5.66 (dd, 1H^1, $^3J_{H\text{-}F}$=16.3Hz, *J*=4.6Hz), 6.38 (dd, 1H^3, $^3J_{H\text{-}F}$=10.7Hz, $^3J_{H\text{-}F}$=7.1Hz), 7.32 (d, 2H-Ar, *J*=8.3Hz), 7.44-7.51 (m, 4H-Ar), 7.57-7.66 (m, 3H-Ar), 7.72 (s, 1H^{12}) 7.75 (d, 2H-Ar, *J*=8.3Hz), 8.06-8.09 (m, 4H-Ar), 9.70 (s, 1H^{11}).

^{13}C-NMR (100 MHz, $CDCl_3$): δ_C = 21.6 (CH_3-Tos), 25.8 (C-14), 46.0 (C-10), 62.6 (C-5), 68.9 (C-15), 71.5 (dd, C-1, $^2J_{C\text{-}F}$=34.4Hz, $^2J_{C\text{-}F}$=17.0Hz), 78.8 (C-4), 83.7 (br, s, C-3), 109.6 (C-7), 120.8 (dd, C-2, $J_{C\text{-}F}$=266.4Hz, $J_{C\text{-}F}$=260.0Hz), 123.1 (CH-Ar), 127.8 (C-Ar), 127.9 (CH-Ar), 128.7 (CH-Ar), 128.8 (CH-Ar), 129.1 (C-Ar), 129.7 (CH-Ar), 129.9 (CH-Ar), 130.1 (CH-Ar), 132.8 (C-Ar), 133.7 (CH-Ar), 134.3 (CH-Ar), 140.5 (CH-Ar), 142.7 (C-Ar), 144.9 (C-Ar), 149.5 (C-Ar), 162.0 (C=O), 162.6 (C=O), 164.7 (C=O), 166.0 (C=O).

IR ν_{max} (neat) = 3068, 1723, 1693 cm^{-1}

MS (ES+) m/z = 752 $[M+H]^+$, 774 $[M+Na]^+$.

HRMS (ES+) calculated 752.1838 for $C_{35}H_{32}N_2F_5O_{10}S$, observed 752.1846 $[M+H]^+$.

mp (CH_2Cl_2) = 162-167 ^oC.

(2*R*,3*R*,5*R*)-2-[(Benzoyloxy)methyl]-4,4-difluoro-5-(5-{[4-(2-hydroxyethyl)-1H-1,2,3-triazol-1-yl]methyl}-2,4-dioxo-1,2,3,4-tetrahydropyrimidin-1-yl)oxolan-3-yl benzoate 277

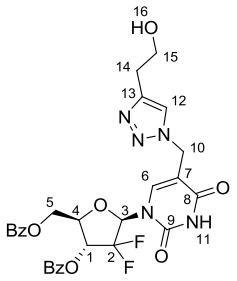

A solution of azide **276** (80 mg, 0.15 mmol), ascorbic acid (26 mg, 0.15 mmol), $CuSO_4.5H_2O$ (19 mg, 76 μmol) and 3-butyn-1-ol (13 μl, 0.17 mmol) in DMF-H_2O (9:1, 3.0 mL) was stirred for 16 hours at room temperature. The reaction mixture was then concentrated *in vacuo*, partitioned between CH_2Cl_2 (15 mL) and H_2O (15 mL), the organic layer dried over $MgSO_4$ and the solvent removed i*n vacuo*. The crude product was purified using flash silica column chromatography (5% MeOH in CH_2Cl_2) to yield the product (48 mg, 54%) as a white solid.

^{1}H-NMR (500 MHz, DMSO-d$_6$): δ_H = 2.73 (t, 2H^{14}, *J*=6.9Hz), 3.59 (td, 2H^{15}, *J*=6.9Hz, *J*=5.3Hz), 4.65 (t, 1H^{16}, *J*=5.3Hz), 4.64-4.82 (m, 3H^{4+5}), 5.07-5.13 (m, 2H^{10}), 5.79-5.88 (m, 1H^1), 6.40 (t, 1H^3, $^3J_{H\text{-}F}$=8.4Hz), 7.44 (m, 2H-Ar), 7.57 (m, 2H-Ar), 7.62 (m, 1H-Ar), 7.73 (m, 1H-Ar), 7.76 (s, 1H^6), 7.94 (m, 2H-Ar), 8.04 (m, 2H-Ar), 8.09 (s, 1H^{12}), 11.91 (s, 1H^{11}).

^{13}C-NMR (125 MHz, DMSO-d$_6$): δ_C = 29.2 (C-14), 45.7 (C-10), 60.4 (C-15), 63.5 (C-5), 71.4-71.8 (m, C-1), 75.8 (C-4), 83.9-85.2 (br, s, C-3), 109.0 (C-7), 121.7 (t, C-2, $J_{C\text{-}F}$=260.9Hz), 122.5 (C-12), 128.0 (C-Ar), 128.8 (CH-Ar), 129.0 (CH-Ar), 129.1 (C-Ar), 129.3 (CH-Ar), 129.8 (CH-Ar), 133.7 (CH-Ar), 134.4 (CH-Ar), 141.5 (C-6), 144.4 (C-13), 149.9 (C=O), 162.3 (C=O), 164.4 (C=O), 165.5 (C=O).

IR ν_{max} (neat) = 3281, 1728, 1676 cm^{-1}

MS (ES+) m/z = 598 $[M+H]^+$, 620 $[M+Na]^+$.

HRMS (ES+) calculated 598.1749 for $C_{28}H_{26}F_2N_5O_8$, observed 598.1731 $[M+H]^+$.

mp (THF-Hexane) = 173-178 ^oC.

(2*R*,3*R*,5*R*)-2-[(Benzoyloxy)methyl]-4,4-difluoro-5-(5-{[4-(2-fluoroethyl)-1H-1,2,3-triazol-1-yl]methyl}-2,4-dioxo-1,2,3,4-tetrahydropyrimidin-1-yl)oxolan-3-yl benzoate 278

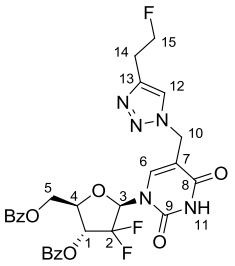

To a −78 ^oC solution of alcohol **277** (40 mg, 70 μmol) in THF (1.4 mL) was added diethylaminosulfur trifluoride (17 μl, 0.13 mmol) and stirring continued at this temperature for 30 minutes, before being warmed to room temperature and stirred for a further hour. Cold H_2O (5 mL) was then added to the reaction and the mixture extracted into CH_2Cl_2 (2 ×10 mL). The combined organic layers were then dried over $MgSO_4$ and concentrated *in vacuo* to yield the crude product. The crude material was purified using flash silica column chromatography (4% MeOH in CH_2Cl_2) to yield the product (9 mg, 21%) as a white solid.

^{1}H-NMR (500 MHz, THF-d$_8$): δ_H = 3.02 (dt, 2H^{14}, $^3J_{H\text{-}F}$=22.4Hz, *J*=6.6Hz), 4.61 (dt, 2H^{15}, $^2J_{H\text{-}F}$=47.2Hz, *J*=6.6Hz), 4.69-4.76 (m, 3H^{4+5}), 5.12 (s, 2H^{10}), 5.78-5.83 (m, 1H^1), 6.36 (t, 1H^3, $^3J_{H\text{-}F}$=7.6Hz), 7.44-7.52 (m, 4H-Ar), 7.54-7.57 (m, 1H-Ar), 7.63-7.67 (m, 1H-Ar), 7.71 (s, 1H$^{6/12}$), 7.87 (s, 1H$^{6/12}$), 8.05-8.10 (m, 4H-Ar), 11.00 (s, 1H^{11}).

^{13}C-NMR (125 MHz, THF-d$_8$): δ_C = 28.00 (d, C-14, $^2J_{C\text{-}F}$=21.8Hz), 46.5 (C-5), 63.9 (C-10), 72.5-72.9 (m, C-1), 78.4 (C-4), 83.11 (d, C-15, $J_{C\text{-}F}$=167.8Hz), 84.9-85.7 (br, s, C-3), 110.6 (C-7), 123.2 (C-12), 129.3 (CH-Ar), 129.4 (CH-Ar), 129.5 (C-Ar), 130.3 (CH-Ar), 130.5 (C-Ar), 130.6 (CH-Ar), 133.9 (CH-Ar), 134.6 (CH-Ar), 141.4 (C-6), 143.42 (d, C-13, $^3J_{C\text{-}F}$=7.5Hz), 150.7 (C-9), 163.0 (C=O), 165.1 (C=O), 166.3 (C=O).

Note: missing C-2 due to multiple overlapping signals.

IR ν_{max} (neat) = 2923, 1724, 1695 cm^{-1}

MS (ES+) m/z = 600 $[M+H]^+$.
HRMS (ES+) calculated 600.1706 for $C_{28}H_{25}F_3N_5O_7$, observed 600.1712 $[M+H]^+$.

mp (THF) = 168-172 ^oC.

1-[(2*R*,4*R*,5*R*)-3,3-Difluoro-4-hydroxy-5-(hydroxymethyl)oxolan-2-yl]-5-{[4-(2-fluoroethyl)-1H-1,2,3-triazol-1-yl]methyl}-1,2,3,4-tetrahydropyrimidine-2,4-dione 252

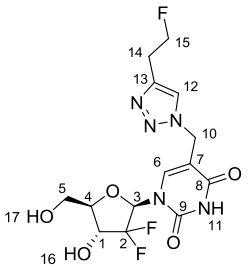

To a solution of the protected nucleoside **278** (9 mg, 15 μmol) in MeOH (1.5 mL) at 0 ^oC was added 7.0 M NH_3 in MeOH (0.2 mL, 1.2 mmol) and the resulting mixture warmed to room temperature and stirred for 16 hours. The reaction mixture was then concentrated *in vacuo* and purified using flash silica column chromatography (5% MeOH in CH_2Cl_2) to yield the product (2 mg, 34%) as a white solid.

^{1}H-NMR (400 MHz, MeOD-d$_4$): δ_H = 3.07 (dt, 2H^{14}, $^3J_{H\text{-}F}$=24.6Hz, *J*=6.1Hz), 3.79 (dd, 1H^5, *J*=12.6Hz, *J*=3.1Hz), 3.89-3.97 (m, 2H^{4+5}), 4.30 (td, 1H^1, $^3J_{H\text{-}F}$=12.2Hz, *J*=8.3Hz), 4.63 (dt, 1H^{15}, $^2J_{H\text{-}F}$=47.0Hz, *J*=6.2Hz), 5.20-5.28 (m, 2H^{10}), 6.14 (dd, 1H^3, $^3J_{H\text{-}F}$=9.1Hz, *J*=6.2Hz), 7.85 (s, 1H^6), 8.18 (s, 1H^{12}).

^{13}C-NMR (100 MHz, MeOD-d$_4$): δ_C = 28.0 (d, C-14, $^2J_{C\text{-}F}$=21.6Hz), 47.6 (C-10), 60.4 (C-5), 70.3 (dd, C-1, $^2J_{C\text{-}F}$ =26.6Hz, $^2J_{C\text{-}F}$=19.4Hz), 82.9 (d, C-4, $^3J_{C\text{-}F}$=8.3Hz), 83.3 (d, C-15, $J_{C\text{-}}$

$_F$=167.4Hz), 85.3 (dd, C-3, $^2J_{C\text{-}F}$=41.2Hz, $^2J_{C\text{-}F}$=24.7Hz), 110.0 (C-7), 124.6 (C-6), 125.17 (t, C-2, $J_{C\text{-}F}$=259.1Hz), 142.0 (C-12), 144.85 (d, C-13, $^3J_{C\text{-}F}$=5.6Hz), 151.7 (C-9), 164.3 (C-8).

IR ν_{max} (neat) = 3222, 2924, 1688 cm^{-1}

MS (ES+) m/z = 392 $[M+H]^+$.
HRMS (ES+) calculated 392.1182 for $C_{14}H_{17}N_5F_3O_5$, observed 392.1201 $[M+H]^+$.

2,3,4,6-Tetra-*O*-benzoyl-α-D-glucopyranosyl benzoate 287

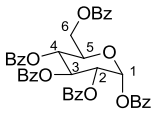

Benzoyl chloride (3.9 mL, 33.3 mmol) was added dropwise to a 0 ^oC solution of D-glucose (1.0 g, 5.6 mmol) and DMAP (136 mg, 1.11 mmol) in pyridine (28 mL) and the resulting solution allowed to warm to room temperature and stirred for 16 hours. Cold H_2O (50 mL) was then added to quench the reaction and the mixture extracted into EtOAc (2 × 100 mL). The combined organic layers were washed with 1.0 M HCl (aq) (2 × 100 mL), brine (50 mL), dried over $MgSO_4$ and concentrated *in vacuo* to give the crude product. The crude product was re-crystallised from EtOAc-Hexanes to yield the product (2.46 g, 63%) as a white solid.
The data were in agreement with the published data.[255]

^{1}H-NMR (400 MHz, $CDCl_3$): δ_H = 4.49-4.53 (m, 1H^6), 4.63-4.66 (m, 2H^{5+6}), 5.71 (dd, 1H^2, *J*=10.3Hz, *J*=3.6Hz), 5.89 (t, 1H^4, *J*=9.8Hz), 6.35 (t, 1H^3, *J*=10.0Hz), 6.88 (d, 1H^1, *J*=3.7Hz), 7.31-7.59 (m, 13H-Ar), 7.62-7.69 (m, 1H-Ar), 7.90-7.92 (m, 4H-Ar), 7.96-7.98 (m, 2H-Ar), 8.04-8.06 (m, 2H-Ar), 8.13-8.16 (m, 1H-Ar), 8.18-8.20 (m, 2H-Ar).

^{13}C-NMR (100 MHz, $CDCl_3$): δ_C = 62.5 (C-6), 68.8 (C-4), 70.4 (C-5), 70.4 (C-2), 70.5 (C-3), 90.0 (C-1), 128.4 (CH-Ar), 128.4 (CH-Ar), 128.7 (C-Ar), 128.8 (CH-Ar), 129.0 (C-Ar), 129.5 (C-Ar), 129.8 (CH-Ar), 129.8 (CH-Ar), 129.9 (CH-Ar), 129.9 (CH-Ar), 130.0 (CH-Ar), 130.2 (CH-Ar), 130.6 (C-Ar), 133.2 (CH-Ar), 133.4 (CH-Ar), 133.5 (CH-Ar), 133.6 (CH-Ar), 133.7 (CH-Ar), 134.0 (CH-Ar), 164.4 (C=O), 165.1 (C=O), 165.4 (C=O), 165.9 (C=O), 166.1 (C=O).

Note: missing 1 × C-Ar due overlapping peaks.

IR v_{max} (neat) =2959, 1719 cm^{-1}

MS (ES+) m/z = 723 $[M+Na]^+$, 764 $[M+Na+MeCN]^+$.
HRMS (ES+) calculated 764.2108 for $C_{43}H_{35}O_{11}NaN$, observed 764.2137 $[M+Na+MeCN]^+$.

2,3,4,6-Tetra-*O*-benzoyl-α/β-D-glucopyranose 289

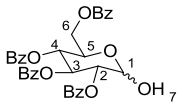

A solution of 2.0 M methylamine in THF (5.2 mL, 10.2 mmol) was added to a solution of the protected glucose **287** (1.3 g, 1.86 mmol) in THF:MeOH (5:1, 6 mL) and the mixture stirred for 6 hours at room temperature. The reaction mixture was concentrated *in vacuo* and the crude residue purified using flash silica column chromatography (30% EtOAc in 40-60 petroleum ether) to yield the product (0.76 g, 68%) as a colourless solid in a 4:1 mixture of α and β anomers.
The data were in agreement with the published data.[256]

^{1}H-NMR (400 MHz, $CDCl_3$): δ_H = 3.31 (dd, $1H^{7\alpha}$, *J*=3.9Hz, *J*=1.1Hz), 4.47 (dd, $1H^{6\alpha}$, *J*=12.4Hz, *J*=4.6Hz), 4.51-4.55 (m, $1H^{6\beta}$), 4.62-4.73 (m, $4H^{5+6,\ \alpha+\beta}$), 5.35 (ddd, $1H^{2\alpha}$, *J*=10.3Hz, *J*=3.6Hz, *J*=1.0Hz), 5.38-5.40 (m, $1H^{2\beta}$), 5.74-5.80 (m, $4H^{1+4,\ \alpha+\beta}$), 5.95-6.02 (m, $1H^{3\beta}$), 6.28 (t, $1H^{3\alpha}$, *J*=9.9Hz), 7.29-7.58 (m, 16H-Ar), 7.88-7.93 (m, 8H-Ar), 7.94-8.03 (m, 8H-Ar), 8.06-8.10 (m, 8H-Ar).

^{13}C-NMR (100 MHz, $CDCl_3$): δ_C = 62.8 (C-6), 67.9 (C-5), 69.4 (C-4), 70.1 (C-3), 72.2 (C-2), 90.5 (C-1), 128.3 (CH-Ar), 128.4 (CH-Ar), 128.5 (CH-Ar), 128.9 (CH-Ar), 128.9 (C-Ar), 129.0 (C-Ar), 129.2 (C-Ar), 129.2 (C-Ar), 129.7 (CH-Ar), 129.8 (CH-Ar), 129.9 (CH-Ar), 129.9 (CH-Ar), 130.0 (CH-Ar), 133.1 (CH-Ar), 133.4 (CH-Ar), 133.5 (CH-Ar)
165.3 (C=O), 165.5 (C=O), 165.5 (C=O), 166.3 (C=O).

Note: missing 1 × C-Ar due to overlapping peaks. ^{13}C data for α-anomer only.

IR ν_{max} (neat) = 3429, 2947, 1721 cm^{-1}

MS (ES-) m/z = 595 $[M-H]^-$.
HRMS (ES-) calculated 595.1604 for $C_{34}H_{27}O_{10}$, observed 595.1602 $[M-H]^-$.

***O*-(2,3,4,6-Tetra-*O*-benzoyl-α-D-glucopyranosyl) trichloroacetimidate 290**

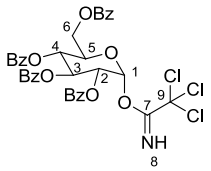

1,8-Diazabicyclo[5.4.0]undec-7-ene (38 µl, 0.25 mmol) was added to a 0 °C solution of the alcohol **289** (150 mg, 0.25 mmol) and trichloroacetontirile (0.25 mL, 2.5 mmol) in CH_2Cl_2 (1.25 mL) and the resulting solution warmed to room temperature and stirred for 1.5 hours. The reaction mixture was then concentrated *in vacuo* and the crude material purified using (20% EtOAc in 40-60 petroleum ether) to yield the product (136 mg, 73%) as a white foam.
The data were in agreement with the published data.[256]

^{1}H-NMR (400 MHz, $CDCl_3$): δ_H = 4.51 (dd, 1H^6, *J*=12.8Hz, *J*=5.4Hz), 4.64-4.69 (m, 2H^{5+6}), 5.65 (dd, 1H^2, *J*=10.1Hz, *J*=3.7Hz), 5.84 (t, 1H^4, *J*=9.8Hz), 6.30 (t, 1H^3, *J*=10.1Hz), 6.86 (d, 1H^1, *J*=3.7Hz), 7.46 (m, 12H-Ar), 7.89 (m, 2H-Ar), 7.98 (m, 4H-Ar), 8.07 (m, 2H-Ar), 8.66 (s, 1H^8).

^{13}C-NMR (100 MHz, $CDCl_3$): δ_C = 62.5 (C-6), 68.7 (C-4), 70.2 (C-3), 70.7 (C-5). 70.7 (C-2), 88.7 (C-9) 93.1 (C-1), 128.4 (CH-Ar), 128.4 (CH-Ar), 128.5 (CH-Ar), 128.5 (CH-Ar), 128.8 (CH-Ar), 128.9 (C-Ar), 129.6 (C-Ar), 129.7 (CH-Ar), 129.8 (CH-Ar), 129.9 (CH-Ar), 130.1 (C-Ar), 133.2 (CH-Ar), 133.3 (CH-Ar), 133.6 (CH-Ar), 160.5 (C-7), 165.2 (C=O), 165.4 (C=O), 165.7 (C=O), 166.1 (C=O).

Note: missing 1 × C-Ar and 1 × CH-Ar due to overlapping peaks.

IR ν_{max} (neat) = 2959, 1726, 1676 cm^{-1}

MS (ES+) m/z = 740 $[M+H]^+$.
HRMS (ES+) calculated 740.0857 for $C_{36}H_{29}Cl_3NO_{10}$, observed 740.0889 $[M+H]^+$.

2,3,4,6-Tetra-*O*-benzoyl-α-D-glucopyranosyl bromide 288

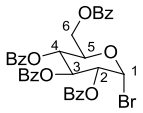

To a solution of protected glucose **287** (1.13 g, 1.6 mmol) in acetic anhydride-acetic acid (1.0:2.7, 18 mL) was added 33% HBr in AcOH (12.7 mL, 72.4 mmol) and the resulting solution heated to 50 ^oC and stirred for 4 hours. The reaction mixture was then cooled to room temperature, diluted with CH_2Cl_2 (150 mL), washed with H_2O (150 mL), brine (150 mL) and the organic layer dried over $MgSO_4$ and concentrated *in vacuo*. The crude product was purified using (20% EtOAc in 40-60 petroleum ether) to yield the product (0.81 g, 76%) as a white solid. The data were in agreement with the published data.[255]

^{1}H-NMR (400 MHz, $CDCl_3$): δ_H = 4.54 (dd, 1H^6, *J*=12.5Hz, *J*=4.5Hz), 4.70 (dd, 1H^6, *J*=12.5Hz, *J*=2.6Hz), 4.76 (ddd, 1H^5, *J*=10.2Hz, *J*=4.3Hz, *J*=2.7Hz), 5.36 (dd, 1H^2, *J*=10.0Hz, *J*=4.1Hz), 5.85 (t, 1H^4, *J*=10.0Hz), 6.29 (t, 1H^3, *J*=9.8Hz), 6.89 (d, 1H^1, *J*=4.0Hz), 7.31-7.60 (m, 12H), 7.88-7.92 (m, 2H), 7.98-8.04 (m, 4H), 8.08-8.11 (m, 2H).

^{13}C-NMR (100 MHz, $CDCl_3$): δ_C = 62.0 (C-6), 68.0 (C-5), 70.6 (C-4), 71.5 (C-3), 72.7 (C-2), 86.9 (C-1), 128.4 (CH-Ar), 128.5 (CH-Ar), 128.5 (CH-Ar), 128.6 (CH-Ar), 128.8 (C-Ar), 129.5 (C-Ar), 129.8 (CH-Ar), 129.8 (CH-Ar), 129.9 (CH-Ar), 130.1 (CH-Ar), 133.3 (CH-Ar), 133.4 (CH-Ar), 133.6 (CH-Ar), 133.8 (CH-Ar), 165.1 (C=O), 165.3 (C=O), 165.6 (C=O), 166.0 (C=O).

Note: missing 2 × C-Ar due to overlapping peaks.

IR ν_{max} (neat) = 2959, 1721 cm^{-1}

MS (ES+) m/z = 580 $[M-Br]^+$, 659 $[M+H]^+$.

HRMS (ES+) calculated 659.0917 for $C_{34}H_{28}BrO_9$, observed 659.0938 $[M+H]^+$.

4,5-Bis(benzoyloxy)-2-({1-[(2*R*,4*R*,5*R*)-4-(benzoyloxy)-5-[(benzoyloxy)methyl]-3,3-difluorooxolan-2-yl]-2,4-dioxo-1,2,3,4-tetrahydropyrimidin-5-yl}methoxy)-6-[(benzoyloxy)methyl]oxan-3-yl benzoate 291

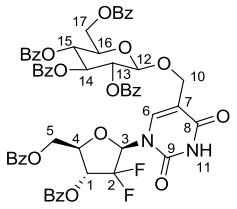

A solution of nucleoside **270β** (104 mg, 0.21 mmol) and glycosyl donor **290** (200 mg, 0.27 mmol) in MeCN (3 mL) was added to a flask containing 4Å molecular sieves and the suspension stirred for 15 minutes at room temperature, before being cooled to 0 ^oC and treated with TMSOTf (58μl, 0.27 mmol). The mixture was then warmed to room temperature and stirred for 16 hours. The reaction was quenched by addition of NEt_3 (0.1 mL), then filtered through a celite padded frit and concentrated *in vacuo* to give the crude product. The crude product was purified using flash silica column chromatography (40% EtOAc in 40-60 petroleum ether) to yield the product (125 mg, 55%) as a white solid.

^{1}H-NMR (400 MHz, $CDCl_3$): δ_H = 4.14 (ddd, 1H^{16}, *J*=9.8Hz, *J*=4.9Hz, *J*=3.3Hz), 4.38 (dd, 1H^5, *J*=13.1Hz, *J*=0.6Hz), 4.46-4.54 (m, 2H^{5+17}), 4.57-4.59 (m, 1H^4), 4.63 (dd, 1H^{17}, *J*=12.2Hz, *J*=3.2Hz), 4.76-4.79 (m, 2H^{10}), 4.97 (d, 1H^{12}, *J*=7.9Hz), 5.30 (dd, 1H^{13}, *J*=9.8Hz, *J*=7.9Hz), 5.59 (t, 1H^{15}, *J*=9.8Hz), 5.64-5.67 (m, 1H^1), 5.89 (t, 1H^{14}, *J*=9.7Hz), 6.25-6.29 (m, 1H^3), 7.29-7.65 (m, 19H-Ar), 7.81-7.83 (m, 2H-Ar), 7.89-7.92 (m, 4H-Ar), 8.01-8.03 (m, 2H-Ar), 8.06-8.09 (m, 4H-Ar), 8.70 (s, 1H^{11}).

^{13}C-NMR (100 MHz, $CDCl_3$): δ_C = 62.8 (C-10), 63.0 (C-17), 64.3 (C-5), 69.6 (C-15), 71.4-71.8 (m, C-1), 71.8 (C-13), 72.3 (C-16), 72.7 (C-14), 78.5 (C-4), 83.5-84.3 (br, s, C-3), 101.5 (C-12), 111.8 (C-7), 127.9 (C-Ar), 128.3 (CH-Ar), 128.3 (CH-Ar), 128.4 (CH-Ar), 128.7 (CH-Ar), 128.8

(C-Ar), 129.3 (C-Ar), 129.6 (C-Ar), 129.7 (CH-Ar), 129.8 (CH-Ar), 130.1 (CH-Ar), 133.2 (CH-Ar), 133.2 (CH-Ar), 133.2 (CH-Ar), 133.4 (CH-Ar), 133.6 (CH-Ar), 134.2 (CH-Ar), 138.0 (CH-Ar), 149.5 (C=O), 161.5 (C=O), 164.7 (C=O), 165.0 (C=O), 165.2 (C=O), 165.7 (C=O), 166.0 (C=O), 166.1 (C=O).

Note: missing 2 × C-Ar, 5 × CH-Ar and C-2 due to overlapping peaks.

IR ν_{max} (neat) = 3261, 1721 cm^{-1}

MS (ES+) m/z = 1103 $[M+Na]^+$, 1081 $[M+H]^+$.
HRMS (ES+) calculated 1080.2843 for $C_{58}H_{47}F_2N_2O_{17}$, observed 1081.2866 $[M+H]^+$.

1-[(2*R*,4*R*,5*R*)-3,3-difluoro-4-hydroxy-5-(hydroxymethyl)oxolan-2-yl]-5-({[3,4,5-trihydroxy-6-(hydroxymethyl)oxan-2-yl]oxy}methyl)-1,2,3,4-tetrahydropyrimidine-2,4-dione 253

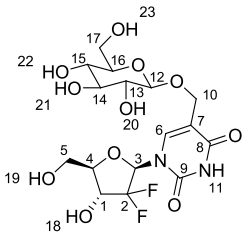

Protected nucleoside **291** (53 mg, 0.05 mmol) was dissolved in 7.0 M NH_3 in MeOH (3.3 mL) and allowed to stir for 16 hours at room temperature. The reaction mixture was then concentrated *in vacuo* and partitioned between EtOAc (10 mL) and H_2O (10 mL), the organic layer extracted with H_2O (10 mL) and the combined organic layers concentrated *in vacuo*. The crude material was triturated using MeOH-CH_2Cl_2 to yield the product (15 mg, 66%) as an amorphous white solid.

^{1}H-NMR (500 MHz, D_2O): δ_H = 3.20 (dd, $1H^{13}$, *J*=9.3Hz, *J*=8.0Hz), 3.28-3.36 (m, $2H^{15+16}$), 3.40 (t, $1H^{14}$, *J*=9.0Hz), 3.64 (dd, $1H^{17}$, *J*=12.3Hz, J=5.5Hz), 3.81 (dd, $1H^5$, *J*=13.1Hz, *J*=4.1Hz), 3.82 (dd, $1H^{17}$, *J*=12.3Hz, *J*=3.3Hz), 3.95 (dd, $1H^5$, *J*=13.2Hz, J=2.3Hz), 4.01 (ddd, $1H^4$, *J*=8.4Hz, *J*=4.0Hz, *J*=2.6Hz), 4.33 (td, $1H^1$, $^2J_{H\text{-}F}$=11.8Hz, J=8.5Hz), 4.43 (d, $1H^{12}$, *J*=8.0Hz), 4.45 (d, $1H^{10}$, *J*=12.7Hz), 4.55 (d, $1H^{10}$, *J*=12.7Hz), 6.14-6.17 (m, $1H^3$), 7.88 (s, $1H^6$).

^{13}C-NMR (125 MHz, D_2O): δ_C = 59.2 (C-5), 60.7 (C-17), 64.0 (C-10), 69.1 (dd, C-1, $^2J_{C-F}$=24.6Hz, $^2J_{C-F}$=21.7Hz), 69.5 (C-14/15/16), 72.9 (C-13), 75.7 (C-14/15/16), 76.0 (C-14/15/16), 80.5 (d, C-4, $^3J_{C-F}$ =7.2Hz), 84.1 (dd, C-3, $^2J_{C-F}$ =25.3Hz, $^2J_{C-F}$ =38.5Hz), 101.4 (C-12), 110.9 (C-7), 122.1 (dd, C-2, J_{C-F}=259.7Hz, J_{C-F} =258.6Hz), 140.7 (C-6), 151.5 (C-9), 165.0 (C-8).

IR v_{max} (neat) =3356, 1678 cm^{-1}

MS (ES-) m/z = 595 $[M+CO_2H]^-$.

HRMS (ES-) calculated 501.1168 for $C_{17}H_{23}F_2N_2O_{13}$, observed 501.1187 $[M+CO_2H]^-$.

RADIOCHEMISTRY

Experimental Radiochemistry

Radiosynthesis was performed on a GE TRACERlab FXc® synthesis module at the Wolfson Brain Imaging Centre (WBIC), University of Cambridge under the supervision of Dr Patrick Riss. Set-up of the synthesis module was performed by Dr Patrick Riss and Dr Valentina Ferrari.

Analytical radio-HPLC was performed on an Agilent 1100 series HPLC system (Agilent Technologies UK Ltd, Wokingham, UK), consisting of a G1312 A gradient pump and a G1314 variable wavelength UV detector. A Bioscan (Bioscan Inc., Washington DC, USA) thallium doped sodium iodide NaI(Tl) detector with Flow Count B FC 4000 analogue/digital interface were used for radioactivity detection. Lablogic Laura 4 software (LablogicSystems Ltd, Sheffield, UK) was used for data analysis and acquisition. For quality control a Chromolith RP-18e endcapped column (5 μm, 100 mm × 4.6 mm, Merck KGaA, Darmstadt, Germany) was used. The column was eluted at a flow rate of 1 mL/min using 6% EtOH in H_2O (v/v) as the mobile phase.

Semi-preparative radio-HPLC was performed using a Sykam S1122 isocratic pump, a UV detector (K2001, Knauer) and a radiodetector (built-in TRACERlab FXc®). A Phenomenex Luna RP18(2) column (10 μm, 250 mm × 10 mm), was fitted to the module. The column was eluted at a flow rate of 4.5 mL/min using 6% EtOH in H_2O (v/v) as the mobile phase. UV and radioactive traces were monitored with the TRACERlab (GE Medical Systems) software.

5-[Methyl-^{11}C]- 2'-deoxy-2',2'-difluorothymidine 90*

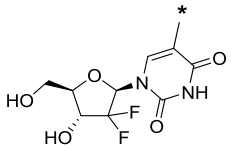

[^{11}C] CO_2 was produced by the $^{14}N(p,\alpha)^{11}C$ nuclear reaction on an aluminium target filled with [^{14}N] N_2 containing 2% oxygen, using a GE PETtrace cyclotron. Proton energy was 13 MeV with a beam current of 40 μA and the duration of irradiation was 15-30 minutes. At EOB, the target gas was delivered and trapped in the GE MeI Microlab synthesiser (*Figure 22 Section 3.2.1*). [^{11}C] CH_3I was released into the reaction vessel under a stream of helium.

A mixture of $Pd_2(dba)_3$ (0.6 mg, 0.6 μmol), tri(*o*-tolyl)phosphine (0.7 mg, 2.4 μmol) and stannane **224** (0.5 mg, 1.2 μmol) in DMF (0.17 mL) was prepared in an oven-dried, septum-equipped-vial at room temperature. The solution was purged with helium gas for 10 minutes and [^{11}C] CH_3I trapped in the solution at room temperature. The resulting mixture was heated at 130 ^{o}C for 5 minutes then cooled to room temperature and diluted with H_2O (250 μL). The mixture was filtered (13 mm, 0.22 μm PTFE filter) and injected onto the HPLC with a semi-preparative column. At a flow rate of 4.5 mL/min using 6% EtOH in H_2O (v/v) as the mobile phase a fraction corresponding to radiolabelled **90** was eluted at 19.5 minutes in a decay-corrected radiochemical yield of 5% (*n*=3).

The product was assayed for radiochemical purity by analytical HPLC. The column was eluted at 1 mL/min using 6% EtOH in H_2O (v/v), the retention time for **90** was 4.5 minutes with a radiochemical purity of 97%.

Supporting Data: NOESY Spectrum for 270β

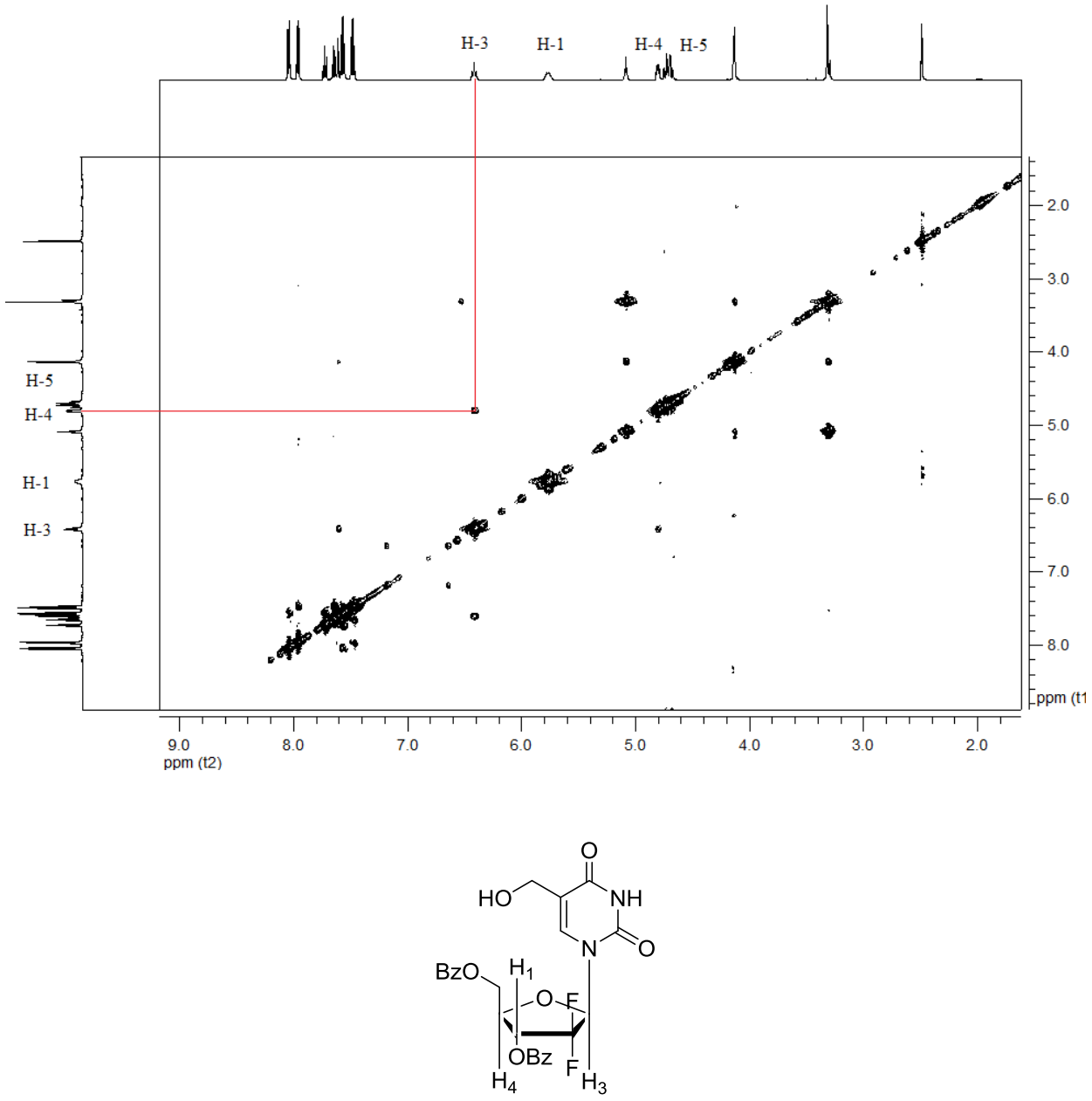

Figure 32- Nucleoside **270β**. Bond lengths exaggerated for clarity. H-5 corresponds to CH_2 next to benzoyl protected alcohol.

A key correlation between protons H-3 and H-4 indicates both protons occupy the same face of the molecule confirming assignment as the β-anomer. Furthermore there is no correlation apparent between protons H-3 and H-1, which would be expected in the α-anomer.

REFERENCES

[1] Campbell, N. A.; Reece, J. B. *Biology*, **2003**, Pearson Education International.

[2] American Cancer Society. *Cancer Facts & Figures 2013*. Atlanta: American Cancer Society, **2013**.

[3] International Agency for Research on Cancer and Cancer Research UK. *World Cancer Factsheet*, Cancer Research UK: London, **2012**.

[4] Sinclair, D. A. *Science* **2003**, *301*, 1859−1860.

[5] Bray, F.; Jemal, A.; Grey, N.; Ferlay, J.; Forman, D. *Lancet Oncol*. **2012**, *13*, 790–801.

[6] Hanahan, D.; Weinberg, R. A. *Cell* **2000**, *100*, 57−70.

[7] Hanahan, D.; Weinberg, R. A. *Cell* **2011**, *144*, 646−674.

[8] Weinberg, R. A. *Sci*. *Am.* **1996**, *275*, 62−70.

[9] Fedi, P.; Tronick, S. R.; Aaronson, S. A. *Cancer Medicine,* Williams and Wilkins, Baltimore, **1997**, 41−64.

[10] Hayflick, L. *Biochemistry* **1997**, *62*, 1180−1190.

[11] Bryan, T. M.; Cech, T. R. *Curr*. *Opin*. *Cell Biol.* **1999**, *11*, 318−324.

[12] Evan, G.; Littlewood, T. *Science* **1998**, *281*, 1317−1322.

[13] Hollstein, M.; Sidransky, D.; Vogelstein, B.; Harris, C. C. *Science* **1991**, *253*, 49–53.

[14] Talmadge, J. E.; Fidler, I. J.; *Cancer Res.* **2010**, *70*, 5649−5669.

[15] Christofori, G.; Semb, H. *Trends. Biochem. Sci.* **1999**, *24*, 73−76.

[16] Singh, R. K.; Gutman, M.; Bucana, C. D.; Sanchez, R.; Llansa, N.; Fidler, I. J.; *Proc. Natl. Acad. Sci.* **1995**, *92*, 4562−4566.

[17] Warburg, O. *Science* **1956**, *123*, 309–314.

[18] Vajdic, C.M.; Van Leeuwen, M.T. *Int*. *J. Cancer* **2009**, *125*, 1747–1754.

[19] Teng, M.W.L.; Swann, J. B.; Koebel, C. M.; Schreiber, R. D.; Smyth, M. J. *J*. *Leukoc*. *Biol*. **2008**, *84*, 988–993.

[20] Kim, R.; Emi, M.; Tanabe, K. *Immunology* **2007**, *121*, 1–14.

[21] Fass, L. *Mol. Oncol.* **2008**, 2, 115−152.

[22] Rudin, M.; Weissleder, R. *Nauret. Rev. Drug Discov*. **2003**, *2*, 123−131.

[23] Yan, G. P.; Robinson, L.; Hogg, P. *Radiography* **2007**, *13*, 5−19.

[24] Amrami, K. K. *J. Am. Soc. For Surgery of the Hand* **2005**, 5, 81−86.

[25] Runge, V. M.; Dean, B.; Lee, C.; Carolan, F.; Heard, G. *J. MRI* **1991**, *1*, 47−56.

[26] Aldrich, J. E. *Crit. Care. Med.* **2007**, *35*, 131−137.

[27] Rickes, S.; Wermke, W. *J. Gastroenterol. Hepatol*, **2004**, *19*, 761−766.

[28] Simpson, G. *Aust. Prescr.* **2009**, *32*, 105–7.

[29] Ginsberg, S. M.; Akin, O.; Berger, D. M.; Zakowski, M. F.; Panicek, D. M. *Am. J. Roentgenology* **2004**, *183*, 293−296.

[30] Weissleder, R; Ntziachristos, V. *Nature Med*. **2003**, *9*, 123−128.

[31] Groch, M. W.; Erwin, W. D. *J. Nucl. Med. Technol*. **2000**, *28*, 233–244.

[32] Phelps, M. E. *PET: Molecular Imaging and Its Biological Applications*, **2004**, Springer-Verlag.

[33] Loch'h, C.; Mazièré, B.; Comar, D. *J. Nucl. Med*. **1980**, *21*, 171−173.

[34] Åberg, O. *Design and Synthesis of ^{11}C-Labelled Compound Libraries for the Molecular Imaging of EGFr, VEGFr-2, AT_1 and AT_2 Receptors*, Ph.D.Thesis, Uppsala Universitet, Uppsala, **2009**.

[35] Ollinger, J. M.; Fessler *IEEE. Signal. Proc. Mag.* **1997**, *14*, 43−55.

[36] Phelps, M. E. *PNAS* **2000**, *97*, 9226−9233.

[37] Shöker, H.; Noy, A.; Gonen, M.; Weng, L.; Green, D.; Erdi, Y. E.; Larson, S. M.; Yeung, H. W. D. *J. Clin. Oncol.* **2005**, *23,* 4643−4651.

[38] Lucignani, G.; Paganelli, G.; Bombardieri, E. *Nucl. Med. Comm.* **2004**, *25*, 651−656.

[39] Wechalekar, K.; Sharma, B.; Cook, G. *Clin. Radiol*. **2005**, *60*, 1143−1155.

[40] Serdons, K.; Verbruggen. A.; Bormans, G. M. *Methods* **2009**, *48*, 104–111.

[41] Miller, W. P.; Long, N. J.; Vilar, R.; Gee, A. D. *Angew. Chem. Int. Ed*. **2008**, *47*, 8998–9033.

[42] Laurell, M.; Siilfstein, M.; Huag, Y. *Mol. Imaging. Biol*. **2003**, *5*, 363–375.

[43] Patel, S.; Gibson, R. *Nucl. Med. Biol*. **2008**, *35*, 805–815.

[44] Vallabhajosula, S. *Molecular Imaging: Radiopharmaceuticals for PET and SPECT*, **2009**, Springer-Verlag.

[45] D. R. Casey, S. C. Sebai, G. C. Shearman, O. Ces, R. V. Law, R. H. Templer, A. D. Gee, *Ind. Eng. Chem. Res*. **2008**, *47*, 650−655.

[46] Van Grieken, R.; De Bruin, M. *Pure & App/. Chem.* **1994**, *66*, 2513−2526.

[47] Pike, V. W. *Trends. Pharmacol. Sci*. **2009**, *30*, 431–440.

[48] Elizarov, A. M. *Lab. Chip* **2009**, *9*, 1326–1333.

[49] Passchier, J. Q. *J. Nucl. Med. Mol. Imaging* **2009**, *53*, 411−416.

[50] Sun, H.; DiMagno, S. G. *Chem. Commun*. **2007**, 528−529.

[51] Beuthien-Baumann, B.; Hamacher, K.; Oberdorfer, F.; Steinbach, J. *Carbohyd. Res*. **2000**, *327*, 107−118.

[52] Shen, B.; Löffler, D.; Zeller, K-P.; Übele, M.; Reischl, G.; Machulla, H-J.; *J. Fluorine Chem*. **2007**, *128*, 1461−1468.

[53] Bormans, G.; Kilbourn, M. R. *J. Labelled Compd. Rad.* **1995**, *2*, 103−110.

[54] Glaser, M.; Årstad, E. *Bioconjugate Chem*. **2007**, *18*, 989−993.

[55] Smith, G.; Glaser, M.; Perumal, M.; Nguyen, Q-D.; Shan, B.; Årstad, E.; Aboagye, E. O. *J. Med. Chem.* **2008**, *51*, 8057–8067.

[56] Chirakal, R.; Adams, R. M.; Firnau, G.; Schrobilgen, G. J.; Coates, G.; Garnett. *Nucl. Med. Biol*. **1995**, *2*, 111−116.

[57] Stöcklin, G.; Pike, V. W. *Radiopharmaceuticals for Positron Emission Tomography- Methodological Aspects*, **1993**, Kulwer Academic Publishers.

[58] Teare, H.; Robins, E. G.; Kirjavainen, A.; Forsback, S.; Sandfors, G.; Solin, O.; Luthra, S.K.; Gouverneur, V. *Angew. Chem. Int. Ed*. **2010**, *49*, 6821–6824.

[59] Alauddin, M. M. *Am. J. Nucl. Med. Mol. Imaging* **2012**, *2*, 55−76.

[60] Visser, G. W. M.; Gorree, G. C. M.; Braakhuis, B. J. M.; Hercheid, J. D. M. *Eur. J. Nucl. Med*. **1989**, *15*, 225−229.

[61] Forsback, S.; Eskola, O.; Haaparanta-Solin, M.; Bergman, J.; Solin, O. *Radiochim. Acta* **2008**, *96*, 845−848.

[62] Bergman, J.; Solin, O. *Nucl. Med. Biol*. **1997**, *24*, 677−683.

[63] Eunsung, L.; Ritter, T. et al. *Science* **2011**, *334*, 639

[64] Samuelsson, L.; Långström, B. *J. Labelled Compd. Rad*. **2003**, *46*, 263–272.

[65] Scott, P. J. H. *Angew. Chem. Int. Ed*. **2009**, *48*, 6001−6004.

[66] Långström, B.; Antoni, G.; Gullberg, P.; Halldin, C.; Malmborg, P.; Nagren, K.; Rimland, A.; Svard, H. *J. Nucl. Med*. **1987**, *28*, 1037−1040.

[67] Larsen, P.; Ulin, J.; Dahlstrom, K. Jensen, M. *Appl. Radiat. Isotopes* **1997**, *48*, 153−157.

[68] Jacobson, O.; Mishani, E. *Appl. Radiat. Isotopes* **2008**, *66*, 188−193.

[69] J. M. Hooker, M. Schönberger, H. Schieferstein, J. S. Fowler. *Angew. Chem. Int. Ed*. **2008**, *47*, 5989−5992.

[70] Hostetler, E. D.; Terry, G. E.; Burns H. D. *J. Labelled Compd. Rad.* **2005**, *48*, 629−634.

[71] Maclean, D.; Zhu, J.; Chen, M. Y.; Hale, R.; Satymurthy, N.;Barrio, J. R. *J. Am. Chem. Soc.* **2003**, *125*, 10168−10169.

[72] Wilson, A, A.; Garcia, A.; Jin, L.; Houle, S. *Nucl. Med. Biol.* **2000**, *27*, 529−532.

[73] Långström, B.; Itsenko, O.; Rahman, O. *J. Labelled Compd. Rad.* **2007**, *50*, 794–810.

[74] "Methods and Apparatus for Production and Use of [11C]Carbon Monoxide in labelling Synthesis": International patent application, Kihlberg, T.; Långström, B.; Ferm, T.; Eriksson, J. PCT/IB2005/001939, **2005**.

[75] Rahman, O.; Kihlberg, T.; Långström, B. *Eur. J. Org. Chem.* **2004**, 474–478.

[76] Karimi, F.; Barletta, J. Långström, B. *Eur. J. Org. Chem.* **2005**, 2374–2378.

[77] Kihlberg, T.; Långström, B. *J. Org. Chem.* **1999**, *64*, 9201–9205.

[78] Itsenko, O.; Långström, B. *Org. Lett.* **2005**, *7*, 4661−4664.

[79] Itsenko, O.; Kihlberg, T.; Långström, B. *J. Org. Chem.* **2004**, *69*, 4356−4360.

[80] McCarron, J. A.; Turton, D. R.; Pike, V. W.; Poole, K. G. *J. Labelled Compd. Rad.* **1996**, *38*, 941−953.

[81] Soloviev, D.; Tamburella, C. *Appl. Radiat. Isotopes* **2006**, *64*, 995−1000.

[82] Iwata, R.; Ido, T.; Takahashi, T.; Nakanishi, H.; Iida, S. *Appl. Radiat. Isotopes* **1987**, *38*, 97−102.

[83] Andersson, Y.; Långström, B. *J. Chem. Soc. Perkin Trans. 1.* **1994**, 1395−1400.

[84] Ponchant, M.; Hinnen, F.; Demphel, S.; Crouzel, C. *Appl. Radiat. Isotopes* **1997**, *48*, 755−762.

[85] Dence, C. S.; Napolitano, E.; Katzenellenbogen, J. A.; Welch, M. *J. Nucl. Med. Biol.* **1996**, *23*, 491−496.

[86] Mulholland, K. G.; Kilbourn, M. R.; Moskwa, J. J. *Appl. Radiat. Isotopes* **1990**, *41*, 1193−1199.

[87] Raichle, M. E. *Sci. Am.* **1994**, *270*, 58−64.

[88] Suzuki, K.; Yoshida, Y.; Shikano, N.; Kubodera, A. *Appl. Radiat. Isotopes* **1999**, *50*, 1033−1038.

[89] Holschbach, M.; Hamkens, W.; Steinbach, A.; Hamacher, K.; Stöcklin, G. *Appl. Radiat. lsotopes.* **1997**, *48*, 739−744.

[90] Fowler, J. S.; Ido, T. *Semin. Nucl. Med.* **2002**, *32*, 6−12.

[91] Kim, J.; Dang, C. V. *Cancer Res.* **2006**, *66*, 8927−8930.

[92] Jones, R. G.; Thompson, G. B. *Genes Dev.* **2009**, *23*, 537−548.

[93] Chen, W.; Cloughesy, T.; Kamdar, N.; Satyamurthy, N.; Bergsneider, M.; Liau, L.; Mischel, P.; Czernin, J.; Phelps, M.E.; Silverman, D. H. S. *J. Nucl. Med.* **2005**, *46*, 945−952.

[94] Yap, C. S.; Czernin, J.; Fishbein, M. C.; Cameron, R. B.; Schiepers, C.; Phelps, M. E.; Weber, W. A. *Chest*, **2006**, *129*, 393−401.

[95] Suehiro, M.; Vallabhajosula, S.; Goldsmith, S. J.; Ballon, D. J. *Appl. Radiat. Isotopes* **2007**, *65*, 1350−1358.

[96] Van Rompay, R.; Johansson, M.; Karlsson, A. *Pharmacol. Therapeut*. **2003**, *100*, 119−139.

[97] Krohn, K. A.; Mankoff, D. A.; Muzi, M.; Link, J. M.; Spence, A. M. *Nucl. Med. Biol*. **2005**, *32*, 663−671.

[98] Barthel, H.; Cleij, M. C.; Collingridge, D. R.; Hutchinson, O. C.; Osman, S.; He, Q.; Luthra, S. K.; Brady, F.; Price, P. M.; Aboagye, E. O. *Cancer Res*. **2003**, *63*, 3791−3798.

[99] Schöder, H.; Ong, S. C. *Semin. Nucl. Med*. **2008**, *38*, 119−128.

[100] Alauddin, M. M.; Ravert, H. T.; Musachio, J. L.; Matthews, W. B.; Dannals, R. F.; Conti, P. S. *Nucl. Med. Biol*. **1995**, *22*, 791−794.

[101] Steel, C. J.; Brady, F.; Luthra, S .K.; Brown, G.; Khan, I.; Poole, K. G.; Sergis, A.; Jones, T.; Price, P. M. *Appl. Radiat. lsotopes* **1999**, *51*, 377−388.

[102] Toyohara, J.; Fujibayashib, Y. *Nucl. Med. Biol*. **2003**, *30*, 681−685.

[103] Grierson, J. R.; Schwartz, J. L.; Muzi, M.; Jordan, R.; Krohn, K. A. *Nucl. Med. Biol*. **2004**, 31, 829−837.

[104] Toyohara, J.; Okada, M.; Toramatsu, C.; Suzuki, K.; Irie, T. *Nucl. Med. Biol*. **2008**, *35*, 67−74.

[105] Toyohara, J.; Kumata, K.; Fukushi, K.; Irie, T.; Suzuki, K. *J. Nucl. Med*. **2006**, *47*, 17–22.

[106] Radu, C. G.; Shu, C. J.; Nair-Gill, E.; Shelly, S. M.; Barrio, J. R.; Satyamurthy, M.; Phelps, M. E.; Witte, O. N. *Nature Med*. **2008**, *14*, 783−788.

[107] Paolillo, V.; Riese, S.; Gelovani, J. G.; Alauddin, M. M. *J. Labelled Compd. Rad*. **2009**, *52*, 553–558.

[108] Shu, C. J.; Campbell, D. O.; Lee, J. T.; Tran, A. Q.; Wengood, J. C.; Witte, O. N.; Phelps, M. E.; Satyamurthy, N.; Czernin, J.; Radu, C. G. *J. Nucl. Med*. **2010**, *51*, 1092−1098.

[109] Galmarini, C. M.; Mackey, J.R.; Dumontet, C. *Leukemia* **2001**, *15*, 875–890.

[110] Sabini, E.; Ort, S.; Monnerjahn, C.; Konrad, M.; Lavie, A. *Nat. Struct. Biol.* **2003**, *10*, 513−519.

[111] Sun, H.; Sloan, A.; Mangner, T. J.; Vaishampayan, U.; Muzik, O.; Collins, J. M.; Douglas, K.; Shields, A. F. *Eur. J. Nucl. Med. Mol. Imaging* **2005**, *32*, 15–22.

[112] Conti, P. S.; Bading, J. R.; Mouton, P. P.; Links, J. M.; Alauddin, M. M.; Fissekis, J. D.; Ravert, H. T.; Hilton, J.; Wong, D. F.; Anderson, J. H. *Nucl. Med. Biol*. **2008**, *35*, 131−141.

[113] Clayden, J.; Greeves, N.; Warren, S.; Wothers, P. *Organic Chemistry,* **2005**, Oxford University Press.

[114] Olofson, R. A.; Vander Meer, R. K.; Hoskin, D. H..; Bernheim, M. Y.; Stournas, S.; Morrison, D. S. *J. Org. Chem.* **1984**, *49*, 3367−3372.

[115] Arbuzov, B. A.; Zoboya, N. N. *Dokl. Akad. Nauk. SSSR* **1967**, *172*, 845−848.

[116] Arbuzov, B. A.; Zobova, N. N.; Balabanova, F. B *B*. *Acad*. *Sci*. *USSR CH*+ **1970**, *19*, 1479−1482.

[117] Arbuzov, B. A.; Zobova, N. N.; Balabanova, F. B. *B*. *Acad*. *Sci*. *USSR CH*+ **1971**, *20*, 510−513.

[118] Lattrell, R. *Justus Liebigs*. *Ann. Chem.* **1969**, *722*, 142−145.

[119] Dehmlow, E. V. *Z. Naturforsch* **1975**, *30*, 822−823.

[120] Pericás, M. A.; Serratosa, F.; Valenti, E. *Chem*. *Soc*. *Perkin*. *Trans*. *II*. **1986**, 961−967.

[121] Kappe, C. O.; Kollenz, G.; Netsch, K.-P.; Leung-Toung, R.; Wentrup, C. *J. Chem. Soc., Chem. Commun*. **1992**, 488−490.

[122] Dai, W-M.; Cheung, Y. K.; Tang, W. K.; Choi, P. Y.; Chung, S. L. *Tetrahedron* **1995**, *51*, 12,263−12,276.

[123] Karimi, F.; Långström, B. *Org.Biomol. Chem.* **2003**, *1*, 541−546.

[124] Kappe, T.; Zadeh, R. K. *Synthesis* **1975**, 247−249.

[125] Kato, H.; Wakao, K.; Yamada, A.; Mutoh, Y. *J*. *Chem*. *Soc*. *Perkin*. *Trans*. *I*. **1988**, 189−192.

[126] Micetich, R. G.; Maiti, S. N.; Tanaka, M.; Yamazaki, T.; Ogawa, K. *J. Org. Chem.* **1986**, *51*, 853−858.

[127] Alajarin, M.; Vidal, A.; Sanxhez-Andrada, P.; Tovar, F.; Ochoa, G. *Org. Lett.* **2000**, *2*, 965−968.

[128] Alajarin, M.; Sanxhez-Andrada, P. *J. Org. Chem.* **2001,** *66,* 8470−8477.

[129] Emerson, D.; Craig, A.; Potts, I. *J. Org. Chem.*, **1967**, *32*, 102−105.

[130] Chou, S. P.; Chiu, H.; Hung, C. *Tetrahedron Lett*. **2003**, *44*, 4653−4655.

[131] Chou, S. P.; Hung, C. C. *Synthesis* **2001**, *16*, 2450–2462.

[132] Dollé, F.; Martarello, L.; Bramaoullé, Y.; Bottlaender, M.; Gee, A. D. *J. Labelled Compd. Rad*. **2005**, *48*, 501–513.

[133] Crouzel, C.; Hinnen, F.; Maitre, E. *Appl*. *Radiat*. *Isotopes* **1995**, *46*, 167−170.

[134] Brown, G. D.; Henderson, D.; Steel, C.; Luthra, S.; Price, P. M.; Brady, F. *Nucl. Med. Biol*. **2001**, *28*, 991−998.

[135] Brown, G. D.; Lutrhra, S. K.; Brock, C. S.; Stevens, M. F. G.; Price, P. M.; Brady, F. *J. Med. Chem.* **2002**, *45,* 5448−5457.

[136] Långström, B.; Barletta, J.; Doi, H.; Suzuki, M.; Noyori, R.; Watanabe, Y.; Farhad, K.et al. *Methods For Carbon Isotope Labelling Synthesis By Transition Metal- Promoted Carbonylation Via Isocyanate Using Azides and Carbonisotope Monoxide.* PCT Int Appl, Vol. WO 2006100563, **2006**.

[137] Doi, H.; Barletta, J.; Suzuki, M.; Noyori, R.; Watanabe, Y.; Långström, B. *Org. Biomol. Chem*. **2004**, *2*, 3063−3066.

[138] Van Tilburg, E. W.; Windhorst, A. D.; Van der Mey, M.; Herscheid, J. D. M.; *J. Labelled Compd. Rad.* **2006**, *49*, 321–330.

[139] Wilson, A. A.; Garcia, A.; Houle, S.; Sadovski, O.; Vasdev, N. *Chem*. *Eur. J*. **2011**, *17*, 259–264.

[140] Urbach, A.; Muccioli, G. G.; Stern, E.; Lambert, D. M.; Marchand-Brynaert, J. *Bioorgan. Med. Chem. Lett*. **2008**, *18*, 4163–4167.

[141] Kano, S.; Ebato, T.; Yusa, Y.; Shibuya, S. *Heterocycles* **1980**, *14*, 167−172.

[142] Williams, D. R.; Donnell, A. F.; Kammler, D. C. *Heterocycles* **2004**, *64*, 167−172.

[143] Miller, J. M. *Acc*. *Chem*. *Res*. **1986**, *19*, 49−56.

[144] Karimi, B.; Zareyee, D. *J. Iran. Chem. Soc.* **2008***, 5*, 103−107.

[145] Varma, R. S.; Saini, R. K.; Meshram, H. M. *Tetrahedron Lett.* **1997**, *38*, 6525−6528.

[146] Kakarla, R.; Dulina, R. G.; Hatzenbuhler, N. T.; Sofia, M. G. *J. Org. Chem.* **1996**, *61*, 8347−8349

[147] Easton, C. J.; Love. S. G.; Wang, P. *J. Chem. Soc. Perkin Trans. 1*, **1990**, 277−282.

[148] Moghaddam. F. M.; Ghaffarzadeh, M. *Tetrahedron Lett.* **1996**, *37*, 1855−1858.

[149] Sharpless, K. B.; Lauer, R. F.; Teranishi, A. Y. *J. Am. Chem. Soc.* **1973**, *95*, 6137−6139.

[150] Freeman, D.B.; Holubec, A. A.; Weiss, M. W.; Dixon, J. A.; Kakefuda, A.; Ohtsuka, M.; Inoue, M.; Vasawani, R. G.; Ohki, H.; Doan, B. D.; Reisman, S. E.; Stoltz, B. M.; Day, J. J.; Tao, R. N.; Dieterich, N. A.; Wood, J. L. *Tetrahedron*, **2010**, *66*, 6647−6655.

[151] Sharpless, K. B.; Young, M.W.; Lauer, RF. *Tetrahedron Lett.* **1973**, *22*, 1979−1982.

[152] Procter, D. J.; Rayner, C. M. *Tetrahedron. Lett.* **1996**, *35*, 1449−1452.

[153] Nangia, A.; Biradha, K.; Desiraju, G.R. *J. Chem. Soc. Perkin. Trans. 2.* **1996**, *5*, 943–953.

[154] Bannister, T.; Celatka, C.; Chandrkumar, N. S.; Deng, H.; Guo, Z.; Jin, L.; Lazarova, T.; Lin, J.; Moe, S. T.; Nagafuji, P.; Navia, M.; Ripka, A.; Rynkiewicz, M. J.; Spear, K. L.; Strickler, J. E. Substituted Azetidinones. WIPO. WO 2006/108039 A2 Oct 12, **2005**.

[155] Cobb, A. J. A.; Shaw, D. M.; Longbottom, D. A.; Gold, J. B.; Ley, S. V. *Org. Biomol. Chem.* **2005**, *3*, 84−96.

[156] Alcaide, B.; Aly, M. F.; Rodriguez, C.; Rodriguez-Vicente, A. *J. Org. Chem.* **2000**, *65,* 3453−3459.

[157] Hart, D. J.; Ha, D-C. *Tetrahedron Lett*. **1985**, *26*, 5493–5496.

[158] Alcaide, B.; Martin-Cantalejo, Y.; Perez-Castells, J.; Rodriguez-Lopez, J.; Sierra, M. A. *J. Org. Chem.* **1992**, *57*, 5921−5931.

[159] Buckley, B. R.; Neary, S. P. *Tetrahedron* **2010**, *66*, 7988−7994.

[160] Kemp, J. E. G. 6-Perhaloalkylsulfonyloxypenicillanic Acids and Derivatives Thereof. U.S. Patent. 4, 356,122 A1 Oct 26, **1982**.

[161] Claudio, P.; Aizpurua, J. M.; Garcia, J. M.; Galarza, R.; Legido, M.; Roman, P.; Luque, A.; Server-Carrio, J.; Linden, A. *J. Org. Chem.* **1997**, *62*, 2070−2079.

[162] Annunziata, R.; Benaglia, M.; Cinquini, M.; Cozzi, F.; Ponzini, F. *J. Org. Chem*. **1993**, *58*, 4746−4748.

[163] Lovric, M.; Cepanec, I.; Litvic, M.; Bartolincic, A.; Vinkovic, V. *Croat. Chem. Acta* **2007**, *80*, 109−115.

[164] Finet, L.; Dakir, M.; Castellote, I.; Kaoudi, T.; Toupet, L.; Arseniyadis. S. *Eur. J. Org. Chem.* **2007**, 335–341.

[165] Zhou, C.; Birney, D. M. *J. Org. Chem*. **2004**, *69*, 86-94.

[166] Baggaley, K. H.; Elson, S. W.; Nicholson, N. H.; Sime, J. T. *J. Chem. Soc., Perkin. Trans. 1.* **1990**, 1513−1520.

[167] Barili, P. L.; Berti, G.; Catelani, G.; Cini, C.; D'Andrea, F.; Mastrorilli, E. *Carbohyd. Res.* **1995**, *278*, 43−57.

[168] Tanabe, G.; Yoshikai, K.; Hatanake, T.; Yamamoto, M.; Shao, Y.; Minematsu, T.; Muraoka, O.; Wang, T.; Matsuda, H.; Yoshikawa, M. *Bioorgan. Med. Chem.* **2007**, *15*, 3926−3937.

[169] Subba Rao, G. S. R.; Kondaiah, P.; Singh, S. K.; Ravanan, P.; Sporn, M. B. *Tetrahedron* **2008**, *64,* 11,541–11,548.

[170] Anderson, N. G.; Lust, D. A.; Colapret, K. A.; Simpson, J. H.; Malley, M. F.; Gougoutas, J. Z. *J. Org. Chem.* **1996**, *61*, 7955−7958.

[171] Helmbolt, H.; Hiersemann, M. *J. Org. Chem.* **2009**, *74*, 1698−1708.

[172] Jauch, J. *Eur. J. Org. Chem.* **2001**, 473−476.

[173] Chakraborty,T. K.; Ghosh, S.; Jayaprakash, S.; Sharma, J. A. R. P.; Ravikanth, V.; Diwan, P.V.; Nagaraj, R.; Kunwar, A. C. *J. Org. Chem.* **2000**, *65,* 6441−6457.

[174] Chikashita, H.; Nikaya T.; Uemurea, H.; Itoh, K.. *Bull. Chem. Soc. Jpn*. **1989**, *62*, 2121−2123.

[175] Blajet, M. Z.; Kuckarska, M.; Scarzewski, J. *Synthesis* **2006**, *7*, 1176−1182.

[176] Uenishi, J.; Hamada, M.; Takagi, T.; Yonumitsu, O. *Heterocycles* **2001**, *54*, 735−746.

[177] Williams, A. M.; Rapoport, H. *J. Org. Chem.* **1994**, *59*, 3616−3625.

[178] Romanelli, M. N.; Bartolini, A.; Bertucci, C.; Dei, S.; Ghelardini, C.; Giovannini, M. G.; Gualtieri, F.; Pepeu, G.; Scapecchi, S.; Teodori, E. *Chirality* **1996**, *8*, 579−584.

[179] Fleming, F.F.; Liu, W. *Eur. J. Org. Chem.* **2009**, 699−708.

[180] Chadwick, S.; Englich, U.; Ruhlandt-Senge, K. *Organometallics* **1997**, *16*, 5792−5803.

[181] Kuznik, N.; Krompiec, S.; Bieg, S.; Baj, S.; Skutil, K.; Chrobok, A. *J. Organomet. Chem.* **2003**, *665*, 167−175.

[182] Masquelin, T.; Obrecht, D. *Tetrahedron Lett*. **1994**, *35*, 9387−9390.

[183] Hashimoto, H.; Masayuki, I. *Chem. Lett.* **1992**, *21*, 25−28.

[184] Brouwer, A. J.; Bunschote, A.; Liskamp, R. M. *Bioorg. Med. Chem.* **2007**, *15*, 6985−6993.

[185] Simiand, C.; Samian, E.; Martin, O. R.; Driguez, H. *Carbohyd. Res.* **1995**, *26*, 1−15.

[186] Zaidi, J. H.; Naeem, F.; Khan, K. M.; Iqbal, R.; Ullah, Z. *Synthetic Comm.* **2011**, *34*, 2641−2653.

[187] Willis, M. C.; Taylor, D.; Gillmore, A. T. *Tetrahedron* **2006**, *62*, 11,513–11,520.

[188] Bradford, R. F.; Schuster, G. B. *J. Org. Chem.* **2003**, *68*, 1075−1080.

[189] Washburne, S. S.; Peterson, W. R.; Berman, D. A. *J. Org. Chem.* **1972**, *37*, 1738 – 1742.

[190] Akssira, M.; Dandouh, A.; Kasmi, H.; Boumzebra, M. *Tetrahedron* **1993**, *49*, 1985−1992.

[191] Chwang, T. L.; Wood, W. F.; Parkhurst, J. R.; Nesnow, S.; Danenberg, P. V.; Heidelberger, C. *J. Med. Chem.* **1976**, *19,* 643−647.

[192] Bobek, M.; Bloch, A. *Tetrahedron Lett*. **1973**, *36*, 3493–3496.

[193] Otter, G. P.; Elzagheid, M. I.; Jones, G. D.; MacCulloch, A. C.; Walker, R. T.; Oivanen, M.; Klika, K. D. *J. Chem. Soc*., *Perkin Trans. 2*, **1998**, 2343–2349

[194] Chou, T. S.; Heath, P. C.; Patterson, L. E.; Poteet, L. M.; Lakin, R. E.; Hunt, A. H. *Synthesis* **1992**, *6*, 565−570.

[195] Alvarenga, E. S.; Carneiro, V. M. T.; Silverio, F. O.; Saliba, W. M. *J. Chil. Chem. Soc.* **2006***, 51*, 986−988.

[196] Zhong, Y.; Shing, T. K. M. *J. Org. Chem.* **1997**, *62*, 2622−2624.

[197] Schmid, C. R.; Bryant, J. D. *Org. Synth. Coll*. **1998**, *9*, 450.

[198] Hertel, L. W.; Kroin, J. S.; Misner, J. W.; Tustin, J. M. *J. Org. Chem.* **1988***, 53*, 2406−2409.

[199] Awl, R. A.; Pryde, E. H. *J. Am. Oil. Chem. Soc*. **1966**, *1*, 35−37.

[200] Palmieri, A.; Petrini. *J. Org. Chem.* **1997**, *72,* 1863−1866.

[201] Robins, M. J.; Barr, P. J.; Giziewicz, J. *Can. J. Chem*. **1982**, *60*, 554−557.

[202] Asakura, J.; Robins, M. J. *J. Org. Chem.* **1990**, *55*, 4928−4933.

[203] Ukai, T.; Kawazura, H.; Ishii, Y. *J. Organomet. Chem*. **1974**, 65, 253−266.

[204] GE Medical Systems PETtrace MeI Microlab Service Manual.

[205] Sandell, J.; Langer, O.; Larsen, P.; Dolle, F.; Vaufrey, F.; Demphel, S.; Crouzel, C.; Halldin, C. *J. Labelled Compd. Rad.* **2000**, *43*, 331–338.

[206] Miller, P. W. *J. Chem. Technol. Biotechnol.* **2009**, *84*, 309–315.

[207] Audrain, H. *Angew. Chem. Int. Ed.* **2007**, *46*, 1772–1775.

[208] Halldin, C.; Farde, L.; Höberg, T.; Håkan, H.; Ström, P.; Ohlberger, A.; Solin, O. *Nucl. Med. Biol.* **1991**, *18*, 871−881.

[209] Toyohara, J.; Hayashi, A.; Sato, M.; Tanka, H.; Haraguchi, K.; Yoshimura, Y.; Yonekura, Y.; Fujibayashi, Y. *J. Nucl. Med.* 2002, *43*, 1218–1226.

[210] Albers, P.; Pietsch, J.; Parker, S. F. *J. Mol. Catal. A-Chem,* **2001**, *173*, 275–286.

[211] Reddington, M. V.; Cunninghan-Bryant, D. *Tetrahedron. Lett.* **2011**, *52*, 181–183.

[212] Matulic-Adamic, J.; Daniher, A. T.; Karpeisky, A.; Haeberli, P.; Sweedler, D.; Biegelman, L. *Bioorgan. Med. Chem.* **2000**, *10*, 1299−1302.

[213] Paolini, L.; Petricci, E.; Corelli, F.; Botta, M. *Synthesis* **2003**, *7*, 1039−1042.

[214] Bobek, M.; Kavai, L.; Sharma, R. A.; Grill, S.; Dutschman, G.; Cheng, Y. C. *J. Org. Chem.* **1987**, *30*, 2154−2157.

[215] Naimi, E.; Zhou, A.; Khalili, P.; Wiebe, L. I.; Balzarini, J.; De Clerq, E.; Knaus, E. E. *J. Med. Chem.* **2003**, *46,* 995−1004.

[216] Beigelman, L.; Blatt, L.; Wang, G. Substituted Nucleoside and Nucleotide Analogues Patent. WIPO. WO 2010/108140 A1 Sep 23, **2010**.

[217] Cline, R. E.; Fink, R. M.; Fink, K. *J. Am. Chem. Soc.* **1959**, *81*, 2521−2527.

[218] Gavriliu, D.; Fossey, C.; Fontaine, G.; Benzaria, S.; Ciurea, A.; Delbederi, Z.; Lelong, B.; Laduree, D.; Aubertin, A. M.; Kirn, A.; *Nucleos. Nucleot. Nucl.* **2000**, *19*, 1017−1031.

[219] Chung, R.; Anderson, K. S. *Tetrahedron. Lett* **2006**, *47*, 8361–8363.

[220] Hudson, R .H. E; Liu, Y.; Wojciechowski, F. *Can. J. Chem.* **2007**, *85*, 302−312.

[221] Dai, Q.; Song, C-X.; Pan, T.; He, C. *J. Org. Chem.* **2011**, *76*, 4182–4188.

[222] Border, S. *Antivir. Res.* **2010**, *85*, 1−18.

[223] Mitsuya, H.; Weinhold, K. J.; Furman, P. A.; St. Clair, M. H.; Lehrman, S. N.; Gallo, R. C.; Bolognesi, D.; Barry, D. W.; Broder, S. *Proc. Nati. Acad. Sci. USA* **1985**, *83*, 8333−8337.

[224] Masereeuw, R.; Jaehde, U.; Langemeijer, M. W. E.; De Boer, A. G.; Breimer, D. D.; *Pharm. Res.* **1994**, *11*, 324−330.

[225] Seio, K.; Wada, T.; Sakamoto, K.; Yokoyama, S.; Sekine, M. *J. Org. Chem.* **1998**, *63,* 1429−1443.

[226] Smith, G.; Sala, R.; Carroll, L.; Behan, K.; Glaser, M.; Robins, E.; Nguyen, Q-D.; Aboagye, E. O. *Nucl. Med. Biol.* **2012**, *39*, 652−665.

[227] Velázquez, S.; Tuñón, V.; Jimeno, M. L.; Chamorro, C.; De Clerq, E.; Balzarini, J.; Camarasa, M. J. *J. Med. Chem.* **1999**, *42,* 5188−5196.

[228] Noll, D. M.; Mason, T. M.; Miller, P. S. *Chem*. *Rev*. **2006**, *106*, 277−301.

[229] Wu, X.; Cooperman, B. S. *Bioorg. Med. Chem. Lett*. **2000**, *10*, 2387–2389.

[230] Wysocki, L. M.; Lavis, L. D. *Curr*. *Opin*. *Chem*. *Biol*. **2011**, *15*, 752–759.

[231] Borst, P.; Sabatini, R. *Annu*. *Rev*. *Microbiol*. **2008**, *62*, 235–251.

[232] De Kort, M.; Ebrahimi, E.; Wijsman, E. R.; Van der Marel, G. A.; Van Boom, J. H. *Eur. J. Org. Chem.* **1999**, 2337−2344.

[233] Abdel-Rahman, A.A-H.; El Ashry, E-S. H. *Synlett*. **2002**, *12*, 2043−2044.

[234] Finet, L.; Dakir, M.; Castellote, I.; Kaoudi, T.; Toupet, T.; Arseniyadis, S. *Eur. J. Org. Chem.* **2007**, 335–341.

[235] Chung, R.; Anderson, K. S. *Tetrahedron Lett*. **2006**, *47*, 8361–8363.

[236] Sheikh, K. D.; Banerjee, P. P.; Jagadeesh, S.; Grindrod, S. C.; Zhang, Li.; Paige, M.; Brown, M. L. *J. Med*. *Chem*. **2010**, *53*, 2376–2382.

[237] Han, J. H.; Kwon, Y. E.; Sohn, J.; Ryu, D. H. *Tetrahedron* **2010**, *66*, 1673–1677.

[238] Kishuku, H.; Shindo, M.; Shishido, K. *Chem*. *Commun*. **2003**, 350−351.

[239] Adamczyk, M.; Akireddy, S. R.; Mattingly, P. G.; Reddy, R. E. *Tetrahedron* **2003**, *59*, 5749–5761.

[240] Shiau, G. T.; Schinazi, R. F.; Chen, M. S.; Prusoff, W. H. *J. Med. Chem.* **2010**, *23*, 127−133.

[241] Brulíková, L.; Džubák, P.; Hajdúch, M.; Hlaváč, J. *Carbohyd*. *Res*. **2011**, *346*, 2136−2144.

[242] Uchida, K.; Kato, K.; Yamaguchi, K.; Akita, H. *Heterocycles* **2001**, *53*, 2253−2259.

[243]Zhang, D.; Xu, L.; Wei, X.; Li, Y.; He, J.; Liu, K. *Nucleos. Nucleot. Nucl*. **2009**, *28,*924–942.

[244] Gupta, V. S.; Bubbar, G. L. *Can. J. Chemistry*. **1971**, *49*, 719−724.

[245] Solladié, G.; Adamy, M.; Colobert, F. *J. Org. Chem*. **1996**, *61*, 4369–4373.

[246] Hogrefe, R. I.; M^{c}Caffrey, A. P.; Borozdina, L. U.; M^{c}Campbell, E. S.; Vaghefi, M. M. *Nucleic*. *Acids. Res*. **1993**, *21*, 4739−4741.

[247] Baggett, N.; Samara, A. K.; Smithson, A. *Carbohyd*. *Res*. **1983**, *124*, 63−74.

[248] Straatmann, M. G.; Welch, M. J. *J. Nucl*. *Med*. **1977**, *18*, 151−158.

[249] Matulic-Adamic, J.; Takahashi, K.; Chou, T-C.; Gadler, H.; Price, R. W.; Reddy, A. R. V.; Kalman, T. I.; Watanabe, K. A. *J. Med. Chem.* **1988**, *31*, 1642−1647.

[250] Turner, J. J.; Meeuwenoord, M. J.; Rood, A.; Borst, P.; Van der Marel, G. A.; Van Boom, J. H. *Eur. J. Org. Chem.* **2003**, 3832−3839.

[251] Bélanger, G.; Dupuis, M.; Larouche-Gauthier, R. *J. Org. Chem.* **2012**, *77*, 3215−3221.

[252] Seio, K.; Wada, T.; Sekine, M. *Helv. Chim. Acta*. **2000**, *83*, 162−180.

[253] König, C. M.; Björn, G.; Schleth, C.; Dauber, M.; Koert, U. *Org. Lett*. **2009**, *11*, 2728−2731.

[254] Staab, H. A. *Angew. Chem. Int. Ed.* **1961**, *1*, 351−367.

[255] Sjölin, P.; Kihlberg, J.; *J. Org. Chem.* **2001,** *66,* 2957−2965.

[256] Egusa, K.; Kusumoto, S.; Fukase, K. *Eur. J. Org. Chem.* **2003**, 3435−3445.

[257] Ihara, M.; Haga, Y.; Yonekura, M.; Ohsawa, T.; Fukumoto, K.; Kametani, T. *J. Am. Chem. Soc.* **1983**, *105*, 7345−7352.

[258] Kasagami, T.; Kim, I-H.; Tsai, H-J.; Nishi, K.; Hammock, B. D.; Morisseau, C. *Bioorg. Med. Chem. Lett*. **2009**, *19*, 1784–1789.